TECHNISCHE UNIVERSITÄT WIEN

DISSERTATION

Topological asymptotic expansion of shape functionals via adjoint based methods and nonsmooth analysis in structural optimisation

ausgeführt zum Zwecke der Erlangung des akademischen Grades eines Doktors der technischen Wissenschaften unter der Leitung von

Associate Prof. Dipl.-Math. Dr.rer.nat. Kevin Sturm
E101 – Institut für Analysis und Scientific Computing, TU Wien

eingereicht an der Technischen Universität Wien
Fakultät für Mathematik und Geoinformation

von

Dipl. Ing. Phillip Baumann
[redacted]

Diese Dissertation haben begutachtet:

1. **Associate Prof. Dr. Kevin Sturm**
   Institut für Analysis und Scientific Computing, TU Wien, Austria
2. **Prof. Dr. Samuel Amstutz**
   Department of Mathematics, Avignon University, France
1. **Prof. Dr. Antonio André Novotny**
   National Laboratory of Scientific Computing, Brazil

Wien, am 13. Mai 2024

Kurzfassung

Designoptimierung befasst sich mit der Minimierung (Maximierung) einer gegebenen Formfunktion, die Teilmengen von $\mathbf{R}^d$ auf reelle Zahlen abbildet, in Bezug auf die Designvariable. Dabei unterscheidet man zwischen den Begriffen *Formoptimierung*, die sich mit glatten Verformungen eines gegebenen Designs befasst, und *Topologieoptimierung*, die topologische Veränderungen anspricht. Im Kontext des Ingenieurwesens bezeichnen wir beide Themen als *Strukturoptimierung*. Fortschritte in der Fertigungstechnik haben eine Vielzahl von Gestaltungsmöglichkeiten hervorgebracht. Folglich hat die Nachfrage nach optimalen Designs und geeigneten Optimierungsmethoden signifikant zugenommen.

Zunächst folgen wir dem Ansatz der klassischen Formoptimierung. Wir wenden die etablierte Theorie rund um die Formableitung auf ein Modellproblem im Rahmen der linearen Elastizität mit punktweisen Spannungseinschränkungen an. Diese Einschränkungen werden dann kompakt formuliert durch die Maximumnorm, was zu einem nichtglatten Optimierungsproblem führt. Wir verwenden Methoden der nichtglatten Analysis, um Optimalitätsbedingungen herzuleiten und eine Verbindung zum Clarke-Subgradienten herzustellen. Zusätzlich betrachten wir drei einfache Geometrien, um die numerische Anwendbarkeit unserer Methodik zu erörtern.

Als Nächstes untersuchen wir topologische Sensitivitäten im Rahmen der Topologieoptimierung. Wir vergleichen drei verschiedene adjungierte Methoden, um die erste und zweite Topologieableitung herzuleiten. Wir wenden diese Methoden auf ein durch partielle Differentialgleichungen beschränktes Problem im Rahmen der linearen Elastizität an und heben die Unterschiede hinsichtlich Anwendbarkeit und Effizienz hervor.

Basierend auf unseren Beobachtungen verwenden wir dann die gemittelte adjungierten Methode, um die vollständige topologische asymptotische Entwicklung für ein durch partielle Differentialgleichungen beschränktes Modellproblem zu berechnen; einschließlich des Laplace-Operators und einer Störung auf der rechten Seite. Wir stellen fest, dass die asymptotische Analyse der adjungierten Variablen je nach Zielfunktion komplizierter sein kann. Tatsächlich erfordert eine Kostenfunktion vom L_2-Trackingtyp die Einführung der Fundamentallösung der biharmonischen Gleichung.

Schließlich nutzen wir den Begriff der topologischen Zustandsableitungen, um numerische Verfahren im Kontext der Topologieoptimierung zu untersuchen. Wir approximieren einen modernen Level-Set-Algorithmus und führen ein steilstes-Abstiegs Verfahren im Rahmen von One-Shot-Typ Methoden ein.

Abstract

Design optimisation deals with the minimisation (maximisation) of a given shape functional, which maps subsets of $\mathbf{R}^d$ to the real numbers, with respect to the design variable. Therein, one distinguishes between the terminology *shape optimisation*, which is concerned with smooth deformations of a given shape and *topology optimisation*, which addresses topological changes. Put into the context of mechanical engineering, we refer to both topics as *structural optimisation*. Recent advances in the manufacturing process gave rise to a large variety of design possibilities. Consequently, the demand for optimal designs and appropriate optimisation methodologies has increased significantly.

We first follow the approach of classical shape optimisation. We apply the well established theory revolving around the shape derivative to a model problem in the framework of linear elasticity with pointwise stress constraints. These constraints are then compactly formulated by the maximum norm, which results in a nonsmooth optimisation problem. We employ methods from nonsmooth analysis to derive optimality conditions and draw a connection to the Clarke subgradient. Additionally, we consider three simple geometries to address the numerical applicability of our methodology.

Next, we investigate topological sensitivities in the framework of topology optimisation. We compare three different adjoint based methods to derive the first and second order topological derivative. We apply these methods to a PDE constrained problem in the framework of linear elasticity and highlight the differences in view of applicability and efficiency.

Based on our observations, we then employ the averaged adjoint method to compute the complete topological asymptotic expansion for a PDE constrained model problem including the Laplacian and a perturbation of the right hand side. We observe that, depending on the objective functional, the asymptotic analysis of the adjoint variable can be more involved. In fact, a L_2 tracking-type cost functional requires the introduction of the fundamental solution of the biharmonic equation.

Finally, we utilise the notion of topological state derivatives to investigate numerical schemes in the context of topology optimisation. We approximate a state of the art level-set algorithm and introduce a steepest descend scheme in the context of one-shot type methods.

Danksagung

An dieser Stelle möchte ich mich bei all jenen bedanken, die mich auf die eine oder andere Weise beim Verfassen meiner Arbeit unterstützt haben. Allen voran gilt mein Dank meinem Betreuer Kevin Sturm, der mir erst dieses spannende und faszinierende Themengebiet näher gebracht hat. Er stand mir stets mit Rat zur Seite, wenn ich einmal nicht weiter wusste. Insbesondere dann, wenn die Algorithmen mal wieder nicht machen wollten, was sie sollten. Ich hätte mir keine bessere Betreuung wünschen können.
Ebenso möchte ich mich bei Prof. Dr. Amstutz und Prof. Dr. Novotny bedanken, die sich bereit erklärt haben diese Arbeit zu begutachten.
Weiters möchte ich mich beim Österreichischen Wissenschaftsfond (FWF) bedanken, dass dieser meine Arbeit durch das Projekt P32911 finanziell unterstützt hat. Bei der Gelegenheit möchte ich mich ebenso bei Peter Gangl bedanken, der das Projekt gemeinsam mit Kevin Sturm ins Leben gerufen hat. Meine Besuche in Graz, und später in Linz, haben mich tiefer in die Materie eintauchen lassen und für diverse Denkanstöße gesorgt.
Außerdem möchte ich mich bei meinen Freunden bedanken, die immerzu für Ablenkung gesorgt haben, wenn es mal schwierig wurde. So auch bei "Fisch" für die beinahe wöchentlichen Kaffeetreffen.
Ein großer Dank gilt meiner Familie. Meiner Schwester Alexandra und Chris, die durch gemeinsame Aktivitäten und Spieleabende für einen Ausgleich in meinem mathematischen Alltag gesorgt haben. Meinen Eltern, Andreas und Ulrike, die mich seit jeher unterstützt haben. Sie haben es mir ermöglicht meine Ziele zu verfolgen und mich stets aufgepäppelt, wenn es mal nicht so gut lief. Ohne euch wäre das nicht möglich gewesen.
Besonders erwähnen möchte ich auch meine Freundin Theresa. Einerseits hat sie sich akribisch durch die Vielzahl an Seiten gearbeitet und so maßgeblich dazu beigetragen die Fehleranzahl zu reduzieren. Sie war der Gradient in meinem Tippfehler-Such-Algorithmus. Andererseits war sie stets für mich da, wenn ich sie gebraucht habe. Oft war es ihr positiver Zuspruch, der mich erst weiter angetrieben hat. Vielen Dank für die vielseite Unterstützung - und ich freue mich schon auf zahlreiche weitere Abendspaziergänge!

FWF Der Wissenschaftsfonds.

TU WIEN TECHNISCHE UNIVERSITÄT WIEN

Eidesstattliche Erklärung

Ich erkläre an Eides statt, dass ich die vorliegende Dissertation selbstständig und ohne fremde Hilfe verfasst habe, andere als die angegebenen Quellen und Hilfsmittel nicht benutzt bzw. die wörtlich oder sinngemäß entnommenen Stellen als solche kenntlich gemacht habe.

Wien, am 13. Mai 2024

Phillip Baumann

Contents

1 Introduction

Design optimisation deals with the minimisation (maximisation) of a given shape functional with respect to a design variable. In this context, the shape functional (or objective functional) denotes a map $\mathcal{J} : \mathcal{U}_{ad} \to \mathbf{R}$, where $\mathcal{U}_{ad}$, a subset of the powerset of $\mathbf{R}^d$, contains the admissible design variables (shapes). Depending on the composition of the set $\mathcal{U}_{ad}$, the wide topic of design optimisation ranges from parameter optimisation, where the design is described by a parameter of an object, to shape optimisation, where the optimal design is searched inside a set of homeomorphic sets, to topology optimisation, where topological changes are considered as well. While the notion of parameter optimisation allows to carry over a linear structure to the set of design variables, the set of admissible shapes in the framework of shape and topology optimisation cannot directly be endowed with a vector space structure.
Recent advances in manufacturing technologies gave rise to a great variety of design possibilities and thus the demand for design optimisation algorithms increased significantly. This introduction aims at providing a general overview of various state of the art methodologies and their applications in the framework of shape and topology optimisation. More specific literature revolving around the contributions of this thesis can be found in the introductions of the according parts.

1.1 Shape optimisation

The terminology "shape optimisation" often combines two branches: parametric shape optimisation and non-parametric shape optimisation. Parametric shape optimisation refers to the previously mentioned parameter optimisation, where the design is described by a finite dimensional variable. Whilst classical examples of this type are the thickness or the height of an object, this notion can be extended to capture irregular shapes. That is, optimising a shape in terms of its boundary, which consists of splines with a finite number of control points, can be classified as parametric shape optimisation as well. More insights on this topic can be found in [37].
On the contrary, in non-parametric shape optimisation one is interested in more general design options. The main ingredient of this branch is the notion of “shape derivative”, which measures the sensitivity of the shape functional with respect to smooth boundary variations of the shape. This method circumvents the lack of vector space structure from shapes by starting from an initial shape and inherits the required structure by considering deformations of the initial shape in terms of vector fields. To formalise this idea let

$$\mathcal{J} : \mathcal{U}_{ad} \to \mathbf{R}, \tag{1.1}$$

be a shape functional and $\Omega \in \mathcal{U}_{ad}$ an admissible shape. The shape derivative is defined as the limit

$$D\mathcal{J}(\Omega)(X) := \lim_{t \searrow 0} \frac{\mathcal{J}(\Omega_t) - \mathcal{J}(\Omega)}{t}. \tag{1.2}$$

Here, $\Omega_t = F_t(\Omega)$ denotes the transformation of Ω with respect to the flow F_t defined by the vector field $X : \mathbf{R}^d \to \mathbf{R}^d$. Of course, one needs to assume that the transformations are compatible with the admissible set, i.e. $F_t(\Omega) \in \mathcal{U}_{\text{ad}}$. There are two commonly used approaches in this context. The first one, the so-called **velocity method** introduced in [100], considers for each Lipschitz vector field $X \in W^{1,\infty}(\mathbf{R}^d)^d$

and $x_0 \in \mathbf{R}^d$ the flow $t \mapsto \theta_X(t, x_0)$ solution of

$$\frac{\partial \theta_X}{\partial t}(t, x_0) = X(\theta_X(t, x_0)), \qquad \theta(0, x_0) = x_0. \tag{1.3}$$

By the Picard-Lindelöf theorem (1.3) admits a unique solution and thus one defines the deformation of an initial set Ω_0 in direction X by

$$\Omega_t = \theta_X(t, \Omega_0). \tag{1.4}$$

A second approach is the so-called **perturbation of the identity method** introduced in [98]. It is based on the idea to construct the deformation of an initial shape Ω_0 as the sum of the identity map and an additional vector field $X \in W^{1,\infty}(\mathbf{R}^d)^d$ with a small weighting factor. To be precise, one considers the deformation in direction X

$$\Omega_t = (\mathrm{Id} + tX)(\Omega_0). \tag{1.5}$$

While these approaches coincide in terms of the first order shape derivative, differences occur in the case of the second order shape derivative, which is a natural extension of (1.2) [44]. It has been found that Lipschitz vector fields are the most general choice of such deformation fields, which allow a rigorous sensitivity analysis. For more details on this topic we refer to [69]. This framework has been employed intensely in the literature and found various applications, many including optimisation problems constrained by partial differential equations (PDEs).

One key property of the shape sensitivity analysis is the possibility to reformulate the governing equations on a fixed domain Ω for sufficiently small transformations F_t. While the perturbation of the identity method suffices in this aspect in many applications, some problem settings require different techniques. In [62] the authors studied the optimisation of a viscous incompressible fluid governed by Stokes equation. Special care had to be taken of the vector field transformations in order to preserve the divergence-free property of the solution space. This has been achieved by introducing the Piola transformation. A similar issue occurred in [72], where the authors investigated the inverse problem occurring in magnetic induction tomography, which describes the reconstruction of the conductivity given a sample of reference measurements.

It is notable that in some cases not only the final shape needs to be optimised. In fact, sometimes also the manufacturing process should be taken into consideration. In [2, 3] the authors applied the method of shape optimisation to a compliance minimisation problem in the context of linear elastic materials. Additionally, they incorporated the manufacturability of the object via an additive manufacturing process as a penalty term into the optimisation problem. In this context, additive manufacturing labels a variety of different manufacturing methodologies that share the common scheme of layer-by-layer construction. Examples of these are material extrusion methods and powder bed fusion strategies [2, Figure 2]. Previous works detect overhangs, the main issue in additive manufacturing, by means of geometric constraints involving the surface normal of the domain (see e.g. [40]). In contrast, the authors of [2, 3] mimicked the layer-by-layer production and introduced the self-weight manufacturing compliance as a penalty.

The works previously mentioned can be classified as smooth shape optimisation. That is, the objective functional, combined with a possible constraint, admits a one-sided derivative that is linear with respect to the vector field. Of course, there is also a large variety of works on nonsmooth shape optimisation in the literature. In [54] the authors considered the shape optimisation of an obstacle type problem. This naturally led to an variational inequality (VI) as a constraint. In order to apply the well established optimisation techniques for smooth shape optimisation, the authors incorporated the VI as an equality using

the nonsmooth maximum function and regularised the term to obtain differentiability.
In contrast, in [104] the author studied the pointwise maximum of a smooth function depending on the state variable, the solution to a quasilinear elliptic PDE. Here, the author resorted to a Danskin type theorem to deal with the nonsmooth objective functional and used results from nonsmooth analysis to characterise the resulting “differential” as well as optimality criteria.
The notion of "shape derivative" naturally gives rise to gradient based optimisation algorithms. Identifying a descend direction, i.e. a vector field X such that $D\mathscr{J}(\Omega)(X)$ is negative, one can use this information implicitly to guide a levelset function [7] or explicitly to deform control points; e.g. mesh nodes [61].
In this context, there is also literature targeting the numerical aspects of shape optimisation. In [49] the authors modelled an air foil as a star-shaped domain and optimised the shape with respect to a given pressure distribution. They computed first and second order shape derivatives and used significant parts of the shape Hessian to increase the convergence rate of the gradient based optimisation algorithm. The contribution [66] aims at controlling the numerical error introduced during the computation of the shape gradient. In the context of an inverse problem occurring in electrical impedance tomography (EIT) the authors introduced an a posteriori error estimator to guarantee a decrease of the objective functional along the direction of the approximated shape gradient. Furthermore, the shape sensitivity encoded in the first and second order shape derivative can be used in Newton-type methods. For an example of this idea we refer to [103].

1.2 Topology optimisation

In contrast to smooth deformations considered before, topology optimisation allows topological changes during the optimisation process. There is a great variety of methodologies to tackle this task analytically and numerically. In the following we are going to introduce some of these. We start with a sensitivity based method, that is comparable to the shape sensitivity in some aspects. Since Part II and Part III employ this methodology, we are going to address this approach in more detail.

Topological sensitivity analysis This method is based on the notion of the topological derivative, which measures the sensitivity of a given objective functional with respect to the inclusion of a small hole. Similarly to (1.2) the first order topological derivative of a shape functional

$$\mathscr{J} : \mathscr{U}_{ad} \to \mathbf{R}, \tag{1.6}$$

denotes the limit

$$d\mathscr{J}(\Omega,\omega)(x_0) := \lim_{\varepsilon \searrow 0} \frac{\mathscr{J}(\Omega_\varepsilon) - \mathscr{J}(\Omega)}{\ell(\varepsilon)}, \tag{1.7}$$

where $\ell : \mathbf{R}^+ \to \mathbf{R}^+$ is function vanishing at 0 that encodes the asymptotic order. Contrary to (1.2) however, Ω_ε denotes a singularly perturbed set Ω at x_0 with the perturbation shape ω. Again, we have to assume that $\Omega_\varepsilon \in \mathscr{U}_{\text{ad}}$ to obtain a well-defined expression. This quantity is able to capture a variety of physical interpretations such as the removal or addition of material, the replacement of different materials or the placement of a rivet, to name a few. The topological derivative was first introduced in [50] and later mathematically justified in [63] in the context of linear elasticity. Since then, the asymptotic expansion with respect to singular perturbations has been derived for various PDE constraint design optimisation problems.

In [32] the authors used the elastostatic Green's tensor to derive a fourth order asymptotic expansion regarding the inclusion of a small inhomogeneity in an elastic material. A fourth order differential operator has been considered in [18], where the authors computed the topological derivative for a Kirchhoff plate bending problem.
Semilinear problems have been discussed in [105] via the averaged adjoint equation and in [14] in a different adjoint framework. In the latter work, the author considered a general class of semilinear equations and prescribed Dirichlet boundary conditions on the inclusion boundary. Instead of poking a hole, this can be interpreted as the addition of a rivet at a particular position. Topological asymptotics of semilinear problems were also addressed in [87, Section 10]. Further works covering the derivation of topological sensitivities for semilinear problems are [29, 75].
Additional complications arise when nonlinearities of the operator occur. In [58] the authors addressed a quasilinear transmission problem. They used a projection trick to circumvent the absence of a fundamental solution, which is often required to derive an asymptotic expansion.
There are various ways to incorporate the local information given by the topological derivative into a numerical optimisation scheme. In [70] the authors investigated the EIT problem with constant conductivities. They used the topological derivative in a one-shot type approach to find an initial set and used the shape derivative as well as sensitivity with respect to the conductivities to further optimise the result. In [71] the authors extended the idea of [70] by deriving a higher order topological expansion, which increased the accuracy of the initialisation.
Another approach was introduced in [17], where the optimality criteria of the topological gradient is used to guide the evolution of a level-set. This idea was further investigated in [15] and extended to capture multi-material problems in [56]. In [31] the authors interpreted the optimality criteria of the topological gradient in a different way. Their observations gave rise to quasi-Newton methods for PDE constrained topology optimisation problems.

Homogenisation method The homogenisation method is based on the idea to fill the domain with periodic cells attaining a microstructure, which depend on a number of parameter. These cells are assumed to consist of two different regions; material and void. Now, the goal is to find an optimal alignment of these cells in terms of a cost function. This leads to a large number of degrees of freedom. By construction, the resulting optimum consists of a microstructure and thus is not very feasible in real life applications. A remedy to get rid of these can be the introduction of a threshold for solid material. Therefore, one fills cells that surpass a given threshold in terms of their microstructure with material, and sets the remaining cells to void. A more subtle approach, called *dehomogenisation*, was introduced in [91].
Applications of the homogenisation method in structural optimisation can be found in [28]. For more details regarding this approach we refer to [1].

Density methods The distribution of material in a domain can be associated with a characteristic function. That is, regions where material is present correlate to the value 1, and void is marked by 0. The idea of density methods is the relaxation of the discrete value set $\{0, 1\}$ to the continuous interval $[0, 1]$. That is, one allows intermediate values, which do not relate to physical interpretations. Thus, the design variable in this context is a density function ρ. Additionally, one enforces a black and white solution by penalisation. This is usually achieved in combination with a volume constraint. For more insights on this topic we refer to [27]. Applications of this method will be given in the introduction of Part I in the context of stress-constrained optimisation.

Phase-Field method Phase-field methods or *diffuse interface methods* stem from physics and can be classified as density based methods as well. Similarly to the previous methodology, the structural domain is identified with a density function ρ. The difference lies in the method to get rid of intermediate densities. In this method, the density is driven towards the value set $\{0,1\}$ with the help of the Van der Waals free energy functional [4]

$$F_\varepsilon(\rho) = \int_D \left(\varepsilon^2|\nabla\rho|^2 + \varepsilon^{-2}W(\rho)\right)\, dx.$$

Here, $W : \mathbf{R} \to \mathbf{R}$ is a double well functional with minima $W(0) = W(1) = 0$ and positive values elsewhere. Thus, the second term encourages a black and white behaviour as $\varepsilon \searrow 0$, while the first term becomes less oppressive and thus allows jumps. This functional is then incorporated as a penalty term into the problem formulation. For an application of this methodology we refer to [30] and references in the introduction of the upcoming parts.

1.3 Existence theory

In the previous discussion we focussed our attention on methods that are capable to guide numerical optimisation algorithms. A more detailed overview of such methods can be found in the work [4]. Of course there is also a wide theoretical framework targeting the existence and regularity of optimal shapes. The foundation is built by the notion of shape continuity, which allows to construct a topology on the set of admissible shapes. With the addition of an appropriate compactness result, which suits the underlying notion of continuity, one can formulate existence results for general design optimisation problems. Further details including concrete techniques to introduce the notion of shape continuity and existence results for optimal shapes can be found in the exhaustive manuscripts [44, 100].

1.4 Outline of the thesis

This thesis is concerned with the sensitivity analysis in the context of shape- and topology optimisation. Our main contributions are the following:

- The incorporation of pointwise stress constraints into the objective functional in a nonsmooth way.
- We perform the sensitivity analysis for the material derivative in the context of shape optimisation in a generalised way and compute the first order semi shape derivative for the nonsmooth objective functional. We further connect the object to the Clarke subgradient.
- We compare three different adjoint based methods to perform topological sensitivity analysis. We highlight the differences in view of applicability and efficiency for various objective functionals in dimension two and three.
- We incorporate the fundamental solution of the biharmonic equation to compute the complete topological asymptotic expansion for a tracking-type objective functional constrained by Poisson's equation.
- We introduce a steepest descend approach to combine topological- and shape-sensitivities on a numerical level.

Structure of the thesis The rest of this thesis is structured as follows: in Part I we investigate the minimisation of peak stresses in the context of shape optimisation. Therein we derive a nonsmooth methodology in the analytical setting, which we then apply to three model problems in a numerical scheme. The results of this part stem from the article [26]. Part II is concerned with topology optimisation in the framework of linear elasticity. Based on the article [25], we compare three adjoint based methods to compute topological sensitivities up to order two and compare these methods in terms of their applicability and efficiency. In Part III we employ a suitable adjoint approach to investigate topological derivatives of arbitrary order for certain objective functionals subject to a PDE constraint in terms of Poisson's equation. Based on the results of [23], we observe that the asymptotic analysis of the adjoint variable necessitates the fundamental solution of the biharmonic equation. Finally, in Part IV we address the numerical treatment of the topological derivative. We therefore introduce the topological state derivative based on the article [24] and utilise this generalised notion to construct two numerical schemes.

List of symbols

Notation	Description
Operators	
Id	identity map on a given set
I_d	d-dimensional identity matrix on $\mathbf{R}^d$
$\mathbf{A}$	tensor, i.e. linear map $\mathbf{R}^{d\times d} \to \mathbf{R}^{d\times d}$
$A^\top$	transpose of a matrix A
A^{-1}	inverse of a quadratic matrix A
$a \cdot b$	Euclidean scalar product of two vectors $a, b \in \mathbf{R}^d$
$\lvert a\rvert$	Euclidean norm of a vector $a \in \mathbf{R}^d$
$A : B$	Frobenius scalar product of two matrices $A, B \in \mathbf{R}^{d\times d}$
$\mathrm{tr}(A)$	trace of a quadratic matrix $A \in \mathbf{R}^{d\times d}$
$(v', v)_{\mathscr{X}'\times\mathscr{X}}$	duality product on $\mathscr{X}' \times \mathscr{X}$
$\langle u, v\rangle_{\mathscr{H}}$	inner product on a Hilbert space $\mathscr{H}$
$\lVert\cdot\rVert_{\mathscr{H}}$	canonical norm on a Hilbert space $\mathscr{H}$, i.e. $\lVert u\rVert^2_{\mathscr{H}} = \langle u, u\rangle_{\mathscr{H}}$
$u_k \to u$	strong convergence
$u_k \rightharpoonup u$	weak convergence
$f \circ g$	composition of two functions
f^{-1}	inverse of a function
$\partial\varphi$	Jacobian or associated weak derivative of a function $\varphi : \mathbf{R}^d \to \mathbf{R}^m$
∂_γ	partial derivative with respect to the vector $\gamma = (\gamma_1, ..., \gamma_d)^\top$, i.e. $\partial_\gamma f = \frac{\partial^{\lvert\gamma\rvert} f}{\partial^{\gamma_1} x_1 \cdots \partial^{\gamma_d} x_d}$, with $\lvert\gamma\rvert = \gamma_1 + \cdots + \gamma_d$
∂_ν	normal derivative of a function $f : \Omega \to \mathbf{R}$, i.e. $\partial_\nu f = \nabla f \cdot n$
$\nabla\varphi$	gradient or associated weak derivative of a function $\varphi : \mathbf{R}^d \to \mathbf{R}$
$\epsilon(\varphi)$	symmetrised gradient of a function $\varphi : \mathbf{R}^d \to \mathbf{R}^d$, i.e. $\epsilon(\varphi) = \frac{1}{2}\left(\partial\varphi + (\partial\varphi)^\top\right)$
$\mathrm{div}(X)$	divergence of a vector field $X \in C^1(\mathrm{D})^d$
$\Delta\varphi$	divergence of a function, i.e. $\Delta\varphi = \mathrm{div}((\nabla\varphi))$
$\mathrm{supp}(\varphi)$	support of a function φ on $\mathbf{R}^d$, i.e. $\overline{\{x \in \mathbf{R}^d \mid \varphi(x) \neq 0\}}$
$\mathrm{tr}_\Gamma(\varphi)$	trace of a function φ on Ω with respect to $\Gamma \subset \partial\Omega$
$\varphi\vert_K$	restriction of a function φ to the set K
$\varphi\vert_\Gamma$	formal abbreviation for $\mathrm{tr}_\Gamma(\varphi)$

Notation	Description
Function spaces	
$C(\Omega)$	space of continuous functions from Ω into $\mathbf{R}$
$C^k(\Omega)$	space of k-times differentiable functions from Ω into $\mathbf{R}$
$C_c^k(\Omega)$	space of functions $f \in C^k(\Omega)$ such that $\text{supp}(f) \subset \Omega$
$L_p(\Omega)$	space of p-integrable functions from Ω into $\mathbf{R}$ for $1 \leq p < \infty$
$W^{k,p}(\Omega)$	Sobolev space of k-times weakly differentiable functions from Ω into $\mathbf{R}$ with derivatives in $L_p(\Omega)$ for $1 \leq p < \infty$, $0 \leq k < \infty$
$H^k(\Omega)$	Sobolev space $W^{k,2}(\Omega)$
$H^1_\Gamma(\Omega)$	$\{\varphi \in H^1(\Omega) \mid \varphi\|_\Gamma = 0\}$ for $\Gamma \subset \partial\Omega$
$H^1_0(\Omega)$	abbreviation for $H^1_{\partial\Omega}(\Omega)$
$\\|\cdot\\|_{C(\bar{\Omega})}$	supremum norm defined by $\\|\varphi\\|_{C(\bar{\Omega})} = \sup_{x\in\Omega} \|\varphi(x)\|$
$\\|\cdot\\|_{C^k(\bar{\Omega})}$	supremum norm defined by $\\|\varphi\\|_{C^k(\bar{\Omega})} = \sum_{j=0}^k \sup_{\|\gamma\|=k} \sup_{x\in\Omega} \left\|\partial_\gamma \varphi(x)\right\|$
$\\|\cdot\\|_{L_p(\Omega)}$	L_p norm defined by $\\|\varphi\\|_{L_p(\Omega)} = \left(\int_\Omega \|\varphi\|^p \, dx\right)^{\frac{1}{p}}$, $1 \leq p < \infty$
$\\|\cdot\\|_{L_\infty(\Omega)}$	essential supremum norm $\\|\varphi\\|_{L_\infty(\Omega)} = \text{ess} \sup_{x\in\Omega} \|f(x)\|$
$\\|\cdot\\|_{W^{k,p}(\Omega)}$	standard Sobolev norm, i.e. $\\|\varphi\\|_{W^{k,p}(\Omega)} = \left(\sum_{\|\gamma\|\leq k} \\|\partial_\gamma \varphi\\|^p_{L_p(\Omega)}\right)^{\frac{1}{p}}$, for $1 \leq p < \infty$
$\\|\cdot\\|_{W^{k,\infty}(\Omega)}$	Sobolev norm defined by $\\|\varphi\\|_{W^{k,\infty}(\Omega)} = \sum_{\|\gamma\|\leq k} \\|\partial_\gamma \varphi\\|_{L_\infty(\Omega)}$
$\|\cdot\|_{H^{\frac{1}{2}}(\Omega)}$	Sobolev-Slobodeckij seminorm defined for a bounded set $\Omega \subset \mathbf{R}^d$ by $\|\varphi\|_{H^{\frac{1}{2}}(\Omega)} = \left(\int_\Omega \int_\Omega \frac{\|\varphi(x)-\varphi(y)\|^2}{\|x-y\|^{d+1}} \, dx dy\right)^{\frac{1}{2}}$
$C^k(\bar{\Omega})$	functions $\varphi \in C^k(\Omega)$ such that $\\|\varphi\\|_{C^k(\bar{\Omega})}$ is finite

Remark 1.1. We denote the vector valued counterparts of $C^k(\Omega)$, $L_p(\Omega)$, $W^{k,p}(\Omega)$,... by $C^k(\Omega)^d$, $L_p(\Omega)^d$, $W^{k,p}(\Omega)^d$,... . Similarly, we proceed with matrix valued function spaces and the according norms.

Part I

Nonsmooth shape optimisation with an application to minimise peak stresses

The content of this part stems from the following article, which is submitted for publication:

[26] P. Baumann and K. Sturm. Minimsation of peak stresses with the shape derivative. 2024. arXiv:2402.12978.

2 Introduction to stress-constrained shape optimisation

Stress describes the internal force present during deformation of an elastic medium. By their nature stresses are a great measure for longevity and stability of a device. Thus, considering stresses in the design process has become to play a crucial part in structural optimisation. A common failure criterion in this context is the maximum distortion energy criterion or von Mises yield criterion. It predicts yielding of a material when the von Mises stress, a scalar quantity depending on the Cauchy stress tensor, exceeds a critical value [77]. The yield point on the strain-stress curve indicates the point where the linear behaviour governed by Hooke's law switches to nonlinear behaviour. Stresses below this point cause an elastic deformation of the material and are therefore reversible. In contrast, stresses that exceed the yield point cause a plastic deformation. This property underlines the importance of stress constraints in the context of structural optimisation. For this reason, various methods to include stresses into the optimisation process have been developed and a great variety of tools in the framework of design optimisation has been used to tackle these problems.

One possibility revolves around density based methods, where the shape dependence of the underlying problem is first identified with a characteristic function and then relaxed to a density function with values in the interval $[0, 1]$. In [95] the authors used the solid isotropic material with penalisation (SIMP) approach to minimise the volume of a material subject to pointwise constraints on the von Mises stress. First, they reformulated the pointwise constraint as a single constraint on the maximum of the von Mises stress. Then the authors included the constraint into the optimisation formulation as a smooth penalty term by approximating the maximal von Mises stress in terms of a regularised ramp function.

In [34] the authors addressed a similar problem in the framework of phase field methods. Contrary to [95] the authors considered a constraint on the total stress but clarified that the same method can be applied to von Mises stress constraints. In their work they lifted the pointwise constraint on the stress tensor in terms of characteristic functions and relaxed the problem by allowing intermediate densities. They further introduced the Cahn-Hillard term to penalise intermediate densities and encourage a "black and white" representation of the optimal domain. Additionally, the authors derived qualification constraints and first order optimality conditions for a discrete finite element formulation of their problem.

The SIMP approach has been further employed in [78], where the authors considered localised stress measure as well as a global stress measure in terms of the p-norm. They further introduced an iterative normalization to approximate the maximum stress. Other works highlighting the usefulness of the SIMP approach in the context of stress optimisation are [33, 74, 107, 108], to name only a few.

As an alternative to the density based SIMP approach, the authors of [6] addressed stress optimisation in the context of the homogenisation method. Their objective functional consists of the L_2 norm of the stress tensor with an additional weight factor, which is able to capture global as well as localised stress constraints.

Even though the previously mentioned approaches have been proven promising, we are going to follow a different route. That is, we are going to utilise the shape gradient in this work. This approach falls into the class of gradient methods based on topological and shape sensitivities, which has been employed in various studies revolving around structural optimisation with stress constraints.

Focusing on topological sensitivites, the authors of [19] employed the topological derivative to address von Mises stress constraints in the framework of linear elasticity. They introduced a smooth regularisation of the maximum function to capture peak stresses. Furthermore, they extended their method in [20] to target constraints on the Drucker-Prager stress. In a similar fashion, [106] employs the topological

derivative as well.
In [5] the authors addressed an objective functional similar to [6] with an additional volume term to regularise the problem. They computed both, the topological and shape gradient, and used these to guide a level-set function in a numerical scheme. This enabled the flexibility to alternate between smooth boundary variations and the nucleation of holes, which leads to topological changes.
As shown in [47], the choice of the method to deal with stress constraints is not black and white. The authors combined the previously described branches to improve their optimisation process. First, they employed the density based SIMP approach to find an initial design. Next, they performed smooth boundary variations to further optimise their shape. Contrary to [5], they computed shape sensitivities on a discrete level based on the position of nodes describing the boundary.
Aside from the choice of shape presentation and identification, the integration of the stress constraint into the optimisation problem plays a crucial role. The physical interpretation of elastic deformation usually calls for a pointwise constraint on the stress on the whole body to guarantee that failure does not occur. Included as a penalty term into the optimisation process, this translates to the maximum norm. Since this generally describes a nonsmooth functional, a common strategy is to regularise this problem and deal with a smooth approximation. A well established approach in this context is the so-called p-norm approach, which replaces the maximum norm with the L_p norm. Indeed this method is reasonable, as the L_p norm mimics the maximum norm for sufficiently large p. This method was employed in [92], where the p-norm approach is used to capture peak von Mises stresses. The authors first discretised both, the underlying PDEs built of the equations of linear elasticity as well as the stress constraints. Next, they computed sensitivities in the context of shape optimisation on the discrete level. They further used these to guide a level-set function describing their design variable. The interchangeable nature of the problem formulation with a penalty term allowed them to consider stress constraints as well as stress minimisation in their numerical examples. The authors extended their work in [93] to cover stress constraints in subregions of the domain as well.
A similar approach was investigated in [84], where the authors used hexahedral meshes to increase the accuracy of stress estimations and shape sensitivities near the boundary. They first introduced their method in [83], where the authors employed hexahedral meshes to improve the level-set approach for a compliance minimisation problem in the context of shape optimisation.
In this part of the thesis we discuss stress and volume control of a physical material governed by the equations of linear elasticity. Contrary to the previously mentioned works, we follow a direct route and consider the maximum norm of the von Mises stress in our problem formulation. This naturally leads to a nonsmooth optimisation problem. We tackle this problem with techniques derived in [104] to compute shape sensitivities. Opposed to [92], we derive these results on a continuous level. Due to the nature of the maximum norm, the resulting derivative is in general nonlinear with respect to deformation vector fields. We therefore take a short detour to the notion of generalised derivatives introduced by Clarke [39] and connect our resulting object to the Clarke subgradient. Finally, we employ our results in a numerical setting to tackle three model problems. We therefore utilise the moving mesh approach guided by shape gradients. We compare our approach to the usual p-norm regularisation and highlight the differences in terms of stress values as well as designs. The content of this part stems from the article [26] in collaboration with Kevin Sturm.

Problem formulation

We consider the following model problem. Let $\mathsf{D} \subset \mathbf{R}^d$, an open and bounded Lipschitz domain, denote the hold-all domain and $\Gamma \subset \mathsf{D}$ be a smooth $d-1$ dimensional Lipschitz manifold with $|\Gamma| > 0$. We introduce the set of admissible shapes by

$$\mathscr{U}_{ad} := \{\Omega \subset \mathsf{D} | \ \Omega \text{ is open, Lipschitz and } \Gamma \subset \partial\Omega\}. \tag{2.1}$$

The elastic body is clamped at Γ. Additionally, we seek an elastic body with target volume $V > 0$. Thus, we introduce the shape functional

$$\mathscr{J}_{\text{vol}}(\Omega) := (|\Omega| - V)^2. \tag{2.2}$$

The global minimum 0 of (2.2) is attained for $|\Omega| = V$. Hence, such Ω are feasible designs for the elastic body. Furthermore, we consider a constraint on the von Mises stress

$$\sigma_M^2(u_\Omega) \le \delta \quad \text{ in } \overline{\Omega \setminus \omega}, \tag{2.3}$$

where $u_\Omega \in H^1_\Gamma(\Omega)^d$ is the unique solution of the equation of linear elasticity on Ω, that is

$$\int_\Omega \mathbf{A}\epsilon(u_\Omega) : \epsilon(\varphi)\, dx = \int_\Omega f \cdot \varphi \, dx + \int_{\Gamma^N} g \cdot \varphi \, dS \quad \text{ for all } \varphi \in H^1_\Gamma(\Omega)^d. \tag{2.4}$$

Here, $H^1_\Gamma(\Omega)^d := \{u \in H^1(\Omega)^d | \ u|_\Gamma = 0\}$, $\Gamma^N := \partial\Omega \setminus \Gamma$, $\omega \subset \mathsf{D}$ open such that $\Gamma \subset \omega$, $f \in H^1(\mathsf{D})^d$, $g \in H^2(\mathsf{D})^d$, $\delta > 0$ is a given stress threshold and $\epsilon(u)$ denotes the symmetrised gradient, i.e.

$$\epsilon(v) := \frac{1}{2}\left(\partial v + \partial v^\top\right) \quad \text{ for all } v \in H^1(\mathsf{D})^d. \tag{2.5}$$

Additionally, we define the elasticity tensor $\mathbf{A}$ in terms of Lamé coefficients $\lambda, \mu > 0$ by

$$\mathbf{A}M := 2\mu M + \lambda \text{tr}(M) I_d \quad \text{ for all } M \in \mathbf{R}^{d\times d}, \tag{2.6}$$

where I_d denotes the identity matrix and the squared von Mises stress is given by

$$\sigma_M^2(u) := \mathbf{B}\epsilon(u) : \epsilon(u), \tag{2.7}$$

with the constant tensor

$$\mathbf{B}(M) := 6\mu M + (\lambda - 2\mu)\text{tr}(M) I_d \quad \text{ for all } M \in \mathbf{R}^{d\times d}. \tag{2.8}$$

We include this pointwise constraint on the von Mises stress as a penalty to the objective functional $\mathscr{J}_{\text{vol}}$. Therefore, we introduce the cost functional

$$\mathscr{J}_\sigma(\Omega) := \max\{ \max_{x \in \overline{\Omega \setminus \omega}} \sigma_M^2(u_\Omega)(x) - \delta, 0\}, \tag{2.9}$$

where $u_\Omega \in H^1_\Gamma(\Omega)^d$ solves (2.4). One readily checks that the global minimum $\mathscr{J}_\sigma(\Omega) = 0$ is attained if and only if $\sigma_M^2(u_\Omega) \le \delta$, in $\overline{\Omega \setminus \omega}$. These observations lead to the introduction of the cost functional

$$\mathscr{J}(\Omega) := \mathscr{J}_{\text{vol}}(\Omega) + \alpha \mathscr{J}_\sigma(\Omega), \tag{2.10}$$

for a penalty parameter $\alpha > 0$. Note that we omitted a factor $\frac{1}{2}$ in our definition of the von Mises tensor (2.8), which is no restriction for the upcoming work. In the following we study the shape derivative of the function $\mathscr{J}$, i.e. the limit

$$\lim_{t \searrow 0} \frac{\mathscr{J}(\Omega_t) - \mathscr{J}(\Omega)}{t},$$

where Ω_t is a smooth deformation of the initial set that tends to Ω for $t \searrow 0$. We are going to introduce such deformations in the next section and give a rigorous definition of the shape derivative in Section 4.

Remark 2.1. We want to emphasize that our problem formulation and upcoming analysis focuses on the integration of stress constraints into a shape optimisation problem. Naturally, a similar methodology could be employed to tackle more involved problem settings. In this context we want to mention an important application of stress constraints; that is an electric motor. The two dimensional cross-section of an electric motor D can be modelled by three mutually disjoint subdomains: an inner part $\mathsf{D}^{\mathrm{rot}}$denoting the rotor, an outer part $\mathsf{D}^{\mathrm{stat}}$ denoting the stator and an intermediate gap $\mathsf{D}^{\mathrm{gap}}$. The motor is built of different materials, these are a ferromagnetic material Ω_{Fe}, permanent magnets Ω_{PM}, copper coils Ω_{CU} and air Ω_{air}. The interaction of different parts is governed by a system of partial differential equations. These are the equation of magnetoquasistatics, the heat equation, and the previously introduced equation of linear elasticity. Since each material is endowed with a different set of material parameter, one could generally address the design optimisation of various parts of the electric motor, as long as each physical requirement is met. A typical example is depicted in Figure 1, where the interface between the ferromagnetic material and the air subdomain is subject to optimisation.
Possible objectives in this context can be the tracking of a target torque or the minimisation of electromagnetic losses. Nonetheless, one should keep in mind that thermal expansion of the material, as well as the rotation of the rotor can lead to high stresses in specific regions of the motor. In order to keep the involved stresses below a certain failure-related threshold, a constraint is desirable. This underlines the importance of our upcoming methodology.

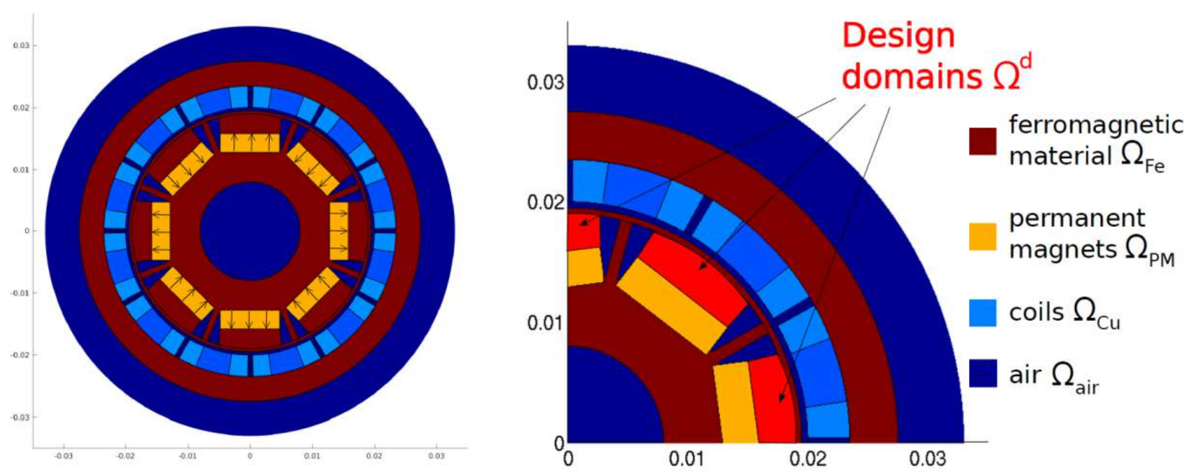

Figure 1: Visualisation of the cross-section of an electric motor [55].

3 Shape sensitivity analysis of the state variable

As we have mentioned in the introduction, the general method of computing sensitivities with respect to deformations of the boundary is based on the idea to identify such deformations with vector fields and inherit a vector field structure that way. In what follows we are going to employ the **perturbation of the identity** approach (cf. Section 1.1). We are going to add an additional perturbation to the deformation map, which allows us to perform differentiation in the context of Clarke in Section 6. It should be noted that this is a generalisation of the usual setting and thus won't result in any problems during the classical shape sensitivity analysis. Even though it has been shown that Lipschitz vector fields are the most general ones to perform the upcoming analysis in a rigorous way, we are going to use smooth vector fields for the sake of simplicity.
Recall the notations introduced in the problem setting. That is, let $\mathsf{D} \subset \mathbf{R}^d$ be open, bounded and Lipschitz, $\Omega \in \mathscr{U}_{ad}$ be an initial shape with boundary $\partial\Omega = \Gamma \cup \Gamma^N$ and fix an open set $\omega \subset \mathsf{D}$ such that $\Gamma \subset \omega$. In order to deduce a derivative consistent with our problem formulation, i.e. compatible with (2.9), we consider deformation vector fields $X \in C^1(\bar{\mathsf{D}})^d$ with $\operatorname{supp}(X) \subset (\mathsf{D} \setminus \bar{\omega})$. On the one hand, this ensures that the region ω remains fixed. By our assumption this includes the portion of the boundary Γ, which denotes the part where the material is clamped. Hence, this is a feasible assumption. Additionally, this choice allows us to avoid the region of low regularity, that is the intersection of both boundary parts. This is crucial to obtain sufficient regularity of the state variable u_Ω in view of the point evaluation of the gradient in (2.9). We will elaborate on this matter further in a later part of this section.
In the following we are going to study the shape sensitivity of the state variable u_Ω. Therefore, we fix a vector field $X \in C^1(\bar{\mathsf{D}})^d$ with $\operatorname{supp}(X) \subset (\mathsf{D} \setminus \bar{\omega})$. Furthermore, we introduce the generalised transformation $F_{Y,t} := \mathrm{Id} + Y + tX$, for $t \geq 0$ and $Y \in C^1(\bar{\mathsf{D}})^d$ with $\operatorname{supp}(Y) \subset (\mathsf{D} \setminus \bar{\omega})$. This transformation gives rise to the definitions $\Omega_{Y,t} := F_{Y,t}(\Omega)$ and $\Gamma^N_{Y,t} := F_{Y,t}(\Gamma^N)$. For $t = 0$ we introduce the abbreviations $F_Y := F_{Y,0}$, $\Omega_Y := \Omega_{Y,0}$ and $\Gamma^N_Y := \Gamma^N_{Y,0}$.

Remark 3.1. We observe that $F_{Y,t}$ coincides with the transformation defined in (1.5) in the special case $Y \equiv 0$. This simplification is sufficient to allow a rigorous computation of the shape derivative. In fact, we are going to recall the special case throughout the next section, where the shape derivative is computed. Nonetheless, we require the more general case and the associated sensitivity results to deal with the derivative in terms of the Clarke subgradient [39].

First, we introduce the perturbed state variable $u_{Y,t} \in H^1_\Gamma(\Omega_{Y,t})^d$ as the unique solution to the perturbed state equation (i.e. the state equation formulated on the deformed domain)

$$\int_{\Omega_{Y,t}} \mathbf{A}\epsilon(u_{Y,t}) : \epsilon(\varphi)\,dx = \int_{\Omega_{Y,t}} f \cdot \varphi\,dx + \int_{\Gamma^N_{Y,t}} g \cdot \varphi\,dS \quad \text{for all } \varphi \in H^1_\Gamma(\Omega_{Y,t})^d, \tag{3.1}$$

and similarly for $t = 0$ we obtain the unperturbed state variable $u_Y \in H^1_\Gamma(\Omega_Y)^d$ as the unique solution to the unperturbed state equation

$$\int_{\Omega_Y} \mathbf{A}\epsilon(u_Y) : \epsilon(\varphi)\,dx = \int_{\Omega_Y} f \cdot \varphi\,dx + \int_{\Gamma^N_Y} g \cdot \varphi\,dS \quad \text{for all } \varphi \in H^1_\Gamma(\Omega_Y)^d. \tag{3.2}$$

Remark 3.2. Note that we defined u_Y as the unperturbed state variable even though a perturbation Y is present. This is reasonable, because the perturbation does not play an important role in terms of the derivation of the shape derivative.

One key property of the transformation is the following: for sufficient small $t > 0$ and Y sufficiently close to 0, i.e. $\|Y\|_{C^1(\bar{D})^d}$ sufficiently small, $F_{Y,t}$ is a bi-Lipschitz transformation field on $\mathbf{R}^d$. According to [110, Theorem 2.2.2] there holds

$$\varphi \in H^1_\Gamma(\Omega)^d \quad \text{iff} \quad \varphi \circ F_{Y,t} \in H^1_\Gamma(F^{-1}_{Y,t}(\Omega))^d.$$

This property allows us to reformulate the perturbed (and unperturbed) state variable on the fixed domain Ω. Indeed, a change of variables entails that $u^{Y,t} := u_{Y,t} \circ F_{Y,t} \in H^1_\Gamma(\Omega)^d$ satisfies

$$\int_\Omega \xi_{Y,t} \mathbf{A} \epsilon_{Y,t}(u^{Y,t}) : \epsilon_{Y,t}(\varphi)\, dx = \int_\Omega \xi_{Y,t} f \circ F_{Y,t} \cdot \varphi\, dx + \int_{\Gamma^N} \nu_{Y,t}\, g \circ F_{Y,t} \cdot \varphi\, dS \quad \text{for all } \varphi \in H^1_\Gamma(\Omega)^d, \tag{3.3}$$

where $\xi_{Y,t} := \det(\partial F_{Y,t})$, $\nu_{Y,t} := \det(\partial F_{Y,t})|(\partial F_{Y,t})^{-\top} n|$ and $\epsilon_{Y,t}(\varphi) := \frac{1}{2}\left(\partial \varphi (\partial F_{Y,t})^{-1} + (\partial F_{Y,t})^{-\top} \partial \varphi^\top\right)$. In this context n denotes the normal vector on Γ^N. Similarly, we deduce that $u^Y := u_Y \circ F_Y \in H^1_\Gamma(\Omega)^d$ satisfies

$$\int_\Omega \xi_Y \mathbf{A} \epsilon_Y(u^Y) : \epsilon_Y(\varphi)\, dx = \int_\Omega \xi_Y f \circ F_Y \cdot \varphi\, dx + \int_{\Gamma^N} \nu_Y\, g \circ F_Y \cdot \varphi\, dS \quad \text{for all } \varphi \in H^1_\Gamma(\Omega)^d, \tag{3.4}$$

where $\xi_Y := \det(\partial F_Y)$, $\nu_Y := \det(\partial F_Y)|(\partial F_Y)^{-\top} n|$ and $\epsilon_Y(\varphi) := \frac{1}{2}\left(\partial \varphi (\partial F_Y)^{-1} + (\partial F_Y)^{-\top} \partial \varphi^\top\right)$. One readily checks that (3.4) coincides with (2.4), if $Y \equiv 0$. Since this equation admits a unique solution, this further entails $u^Y = u$ in this case. In the following we are interested in the limit

$$\lim_{\substack{Y \to 0 \\ t \searrow 0}} \frac{u^{Y,t} - u^Y}{t}, \tag{3.5}$$

where here, and throughout the rest of Part I the notation $Y \to 0$ is understood with respect to the norm on $C^1(\bar{D})^d$, that is $\|Y\|_{C^1(\bar{D})^d} \to 0$. Before we focus on the limit in (3.5), we state the following auxiliary results. For the sake of brevity we introduce the notations

$$f^{Y,t} := f \circ F_{Y,t}, \quad g^{Y,t} := g \circ F_{Y,t}, \quad f^Y := f \circ F_Y, \quad g^Y := g \circ F_Y, \tag{3.6}$$

which we are going to use throughout the rest of this part.

Lemma 3.3. Let $\Omega \in \mathcal{U}_{ad}$ be a Lipschitz domain. Furthermore, let $f \in H^1(D)^d$, $g \in H^2(D)^d$ and the deformation vector field $X \in C^1(\bar{D})^d$ with $\operatorname{supp}(X) \subset (D \setminus \bar{\omega})$. Then there holds

(i) $\lim\limits_{\substack{Y \to 0 \\ t \searrow 0}} \left\| f^{Y,t} - f^Y \right\|_{L_2(D)^d} = 0,$

(ii) $\lim\limits_{\substack{Y \to 0 \\ t \searrow 0}} \left\| \frac{f^{Y,t} - f^Y}{t} - \partial f X \right\|_{L_2(D)^d} = 0,$

(iii) $\lim\limits_{\substack{Y \to 0 \\ t \searrow 0}} \left\| g^{Y,t} - g^Y \right\|_{L_2(\partial\Omega)^d} = 0,$

(iv) $\lim\limits_{\substack{Y \to 0 \\ t \searrow 0}} \left\| \frac{g^{Y,t} - g^Y}{t} - \partial g X \right\|_{L_2(\partial\Omega)^d} = 0.$

Proof. ad (i): First, note that for $\varphi \in C^\infty(\mathsf{D})^d$ there holds

$$\varphi \circ F_{Y,t}(x) - \varphi \circ F_Y(x) = t \int_0^1 \partial\varphi(x + Y(x) + stX(x))X(x)\, ds. \tag{3.7}$$

Since the integrand is bounded, we observe $|\varphi \circ F_{Y,t}(x) - \varphi \circ F_Y(x)| \le Ct$ and thus further

$$\|\varphi^{Y,t} - \varphi^Y\|_{L_2(\mathsf{D})^d} \le Ct, \tag{3.8}$$

where here and throughout the rest of the proof $C \in \mathbf{R}$ denotes a constant independent of t and Y. Next, we consider $f \in H^1(\mathsf{D})^d$ and choose a smooth approximation. That is, for each $\varepsilon > 0$ we choose a smooth function $f_\varepsilon \in C^\infty(\mathsf{D})^d$ such that $\|f_\varepsilon - f\|_{H^1(\mathsf{D})^d} \le \varepsilon$. An application of the triangle inequality yields

$$\|f^{Y,t} - f^Y\|_{L_2(\mathsf{D})^d} \le \|f^{Y,t} - f_\varepsilon^{Y,t}\|_{L_2(\mathsf{D})^d} + \|f_\varepsilon^{Y,t} - f_\varepsilon^Y\|_{L_2(\mathsf{D})^d} + \|f_\varepsilon^Y - f^Y\|_{L_2(\mathsf{D})^d}. \tag{3.9}$$

A change of variables now shows that

$$\|f^{Y,t} - f_\varepsilon^{Y,t}\|^2_{L_2(\mathsf{D})^d} = \int_{\mathsf{D}} |f^{Y,t} - f_\varepsilon^{Y,t}|^2\, dx = \int_{\mathsf{D}} \det(I + \partial Y + t\partial X)^{-1} |f - f_\varepsilon|^2\, dx. \tag{3.10}$$

Since $\det(I + \partial Y + t\partial X) \to 1$ as $Y \to 0$ in $C^1(\bar{\mathsf{D}})^d$ and $t \searrow 0$, there holds $\det(I + \partial Y + t\partial X)^{-1} \le C$ for $t > 0$ and $\|Y\|_{C^1(\bar{\mathsf{D}})^d}$ sufficiently small. The same argument can be applied to the third term on the right hand side of (3.9). Thus, choosing $\varepsilon = t$ and inserting (3.8) with $\varphi = f_\varepsilon$ into (3.9), we conclude

$$\|f^{Y,t} - f^Y\|_{L_2(\mathsf{D})^d} \le Ct, \tag{3.11}$$

which shows (i).
ad (ii): We start again with a smooth function $\varphi \in C^\infty(\mathsf{D})^d$. Using Lebesgue's dominated convergence theorem, we deduce from equation (3.7) that

$$\frac{\varphi^{Y,t}(x) - \varphi^Y(x)}{t} \to \partial\varphi(x)X(x) \quad \text{for all } x \in \mathsf{D}. \tag{3.12}$$

Since X has compact support, there further holds $|\frac{\varphi^{Y,t}(x) - \varphi^Y(x)}{t}| \le C$ for all $x \in \mathsf{D}$. Now, as D has finite measure, we can employ dominated convergence to extend the convergence (3.12) to L_2. That is,

$$\|\frac{\varphi^{Y,t} - \varphi^Y}{t} - \partial\varphi X\|_{L_2(\mathsf{D})^d} \to 0. \tag{3.13}$$

For $f \in H^1(\mathsf{D})^d$ we use a smooth approximation, i.e. for each $\varepsilon > 0$ let $f_\varepsilon \in C^\infty(\mathsf{D})^d$ such that

$$\|f_\varepsilon - f\|_{H^1(\mathsf{D})^d} \le \varepsilon.$$

Now a splitting similar to the previous proof entails

$$\begin{aligned}\|\frac{f^{Y,t} - f^Y}{t} - \partial f X\|_{L_2(\mathsf{D})^d} \le & \frac{1}{t}\|f^{Y,t} - f_\varepsilon^{Y,t}\|_{L_2(\mathsf{D})^d} + \frac{1}{t}\|f^Y - f_\varepsilon^Y\|_{L_2(\mathsf{D})^d} \\ & + \|(f_\varepsilon^{Y,t} - f_\varepsilon^Y)/t - \partial f_\varepsilon X\|_{L_2(\mathsf{D})^d} + \|\partial f_\varepsilon X - \partial f X\|_{L_2(\mathsf{D})^d}.\end{aligned} \tag{3.14}$$

Hence, choosing $\varepsilon = t^2$ and using the same arguments as in the proof of item (i) to estimate the first, second and fourth term gives

$$\|\frac{f^{Y,t} - f^Y}{t} - \partial f X\|_{L_2(\mathsf{D})^d} \leq Ct + \|\frac{f_\varepsilon^{Y,t} - f_\varepsilon^Y}{t} - \partial f_\varepsilon X\|_{L_2(\mathsf{D})^d}. \tag{3.15}$$

Finally, equation (3.13) applied to $\varphi = f_\varepsilon$ shows (ii).
The proof of item (iii) and (iv) follows from similar arguments, employing the continuity of the trace operator $\|\varphi\|_{L_2(\partial\Omega)^d} \leq C\|\varphi\|_{H^1(\mathsf{D})^d}$, for all $\varphi \in H^1(\mathsf{D})^d$. The higher regularity is used to approximate ∂g in the H^1 norm. □

In addition to the asymptotic behaviour with respect to the transformation of the forces, we also need to study the sensitivity associated with the transformation of the differentials $\xi_{Y,t}, \boldsymbol{\epsilon}_{Y,t}, \nu_{Y,t}$. This topic is addressed in the following auxiliary lemma. Note that we split the symmetrised gradient $\boldsymbol{\epsilon}_{Y,t}$ therein and rather investigate the Jacobian $(\partial F_{Y,t})^{-1}$. This is sufficient due to the underlying linear structure.

Lemma 3.4. Let $\Omega \in \mathscr{U}_{ad}$ and $X \in C^1(\bar{\mathsf{D}})^d$ with $\operatorname{supp}(X) \subset (\mathsf{D} \setminus \bar{\omega})$. Furthermore, for $Y \in C^1(\bar{\mathsf{D}})^d$ with $\operatorname{supp}(Y) \subset (\mathsf{D} \setminus \bar{\omega})$ and $\|Y\|_{C^1(\bar{\mathsf{D}})^d}$, $t > 0$ sufficient small recall the notations $\xi_{Y,t} := \det(\partial F_{Y,t})$, $\xi_Y := \det(\partial F_Y)$, $\nu_{Y,t} := \det(\partial F_{Y,t})|(\partial F_{Y,t})^{-\top} n|$, $\nu_Y := \det(\partial F_Y)|(\partial F_Y)^{-\top} n|$. Additionally we introduce the perturbed and unperturbed Jacobian $\alpha_{Y,t} := (\partial F_{Y,t})^{-1}$, $\alpha_Y := (\partial F_Y)^{-1}$. Then the following limits hold.

(i) $\displaystyle\lim_{\substack{Y\to 0\\ t\searrow 0}} \frac{\xi_{Y,t} - \xi_Y}{t} = \operatorname{div}(X) \quad \text{in } C^0(\mathsf{D}),$

(ii) $\displaystyle\lim_{\substack{Y\to 0\\ t\searrow 0}} \frac{\alpha_{Y,t} - \alpha_Y}{t} = -\partial X \quad \text{in } C^0(\mathsf{D})^{d\times d},$

(iii) $\displaystyle\lim_{\substack{Y\to 0\\ t\searrow 0}} \frac{\nu_{Y,t} - \nu_Y}{t} = \operatorname{div}(X) - (\partial X n)\cdot n \quad \text{in } C^0(\partial\Omega).$

Proof. ad (i): Employing an asymptotic expansion of $\det(I + \partial Y + t\partial X)$ with respect to the parameter t yields

$$\det(I + \partial Y + t\partial X) = \det(I + \partial Y) + t\det(I + \partial Y)\operatorname{tr}((I + \partial Y)^{-1}\partial X) + \mathscr{O}(t^2; \partial X; \partial Y), \tag{3.16}$$

where the remainder satisfies $\displaystyle\lim_{\substack{Y\to 0\\ t\searrow 0}} \frac{\mathscr{O}(t^2;\partial X;\partial Y)}{t} \to 0$ uniformly in D. Hence, we conclude that

$$\lim_{\substack{Y\to 0\\ t\searrow 0}} \frac{\xi_{Y,t} - \xi_Y}{t} = \lim_{\substack{Y\to 0\\ t\searrow 0}} \det(I + \partial Y)\operatorname{tr}((I + \partial Y)^{-1}\partial X) + \frac{\mathscr{O}(t^2;\partial X;\partial Y)}{t} = \operatorname{tr}(\partial X) = \operatorname{div}(X), \tag{3.17}$$

holds uniformly in D, which shows (i).
ad (ii): First, we expand the terms in a Neumann series: for sufficiently small $\|Y\|_{C^1(\bar{\mathsf{D}})^d}$ and $t > 0$ there holds

$$(I + \partial Y)^{-1} = \sum_{\ell=0}^{\infty} (-1)^\ell (\partial Y)^\ell, \tag{3.18}$$

and

$$(I + \partial Y + t\partial X)^{-1} = \sum_{\ell=0}^{\infty}(-1)^{\ell}(\partial Y + t\partial X)^{\ell} = \sum_{\ell=0}^{\infty}(-1)^{\ell}\sum_{k=0}^{\ell}(\partial Y)^{k}t^{\ell-k}(\partial X)^{\ell-k}. \tag{3.19}$$

Hence, we observe

$$\begin{aligned}
\frac{\alpha_{Y,t}-\alpha_Y}{t} &= \sum_{\ell=0}^{\infty}(-1)^{\ell}\sum_{k=0}^{\ell-1}(\partial Y)^{k}t^{\ell-k-1}(\partial X)^{\ell-k} \\
&= (-\partial X) + \sum_{\ell=2}^{\infty}(-1)^{\ell}\sum_{k=0}^{\ell-2}(\partial Y)^{k}t^{\ell-k-1}(\partial X)^{\ell-k} + \sum_{\ell=2}^{\infty}(-1)^{\ell}(\partial Y)^{\ell-1} \\
&= (-\partial X) + t\sum_{\ell=2}^{\infty}(-1)^{\ell}\sum_{k=0}^{\ell-2}(\partial Y)^{k}t^{\ell-k-2}(\partial X)^{\ell-k} + (\partial Y)\sum_{\ell=0}^{\infty}(-1)^{\ell}(\partial Y)^{\ell}.
\end{aligned}$$

Since both series on the right hand side converge uniformly in D, passing to the limit $Y \to 0$ in $C^1(\bar{\mathsf{D}})^d$, $t \searrow 0$ shows

$$\lim_{\substack{Y\to 0\\ t\searrow 0}} \frac{\alpha_{Y,t}-\alpha_Y}{t} = -\partial X \quad \text{in } C^0(\mathsf{D})^{d\times d}, \tag{3.20}$$

which shows (ii).
ad (iii): Expanding the difference yields

$$\frac{\nu_{Y,t}-\nu_Y}{t} = \frac{\det(\partial F_{Y,t})-\det(\partial F_Y)}{t}|\partial F_{Y,t}n| + \det(\partial F_Y)\frac{|\partial F_{Y,t}n|-|\partial F_Y n|}{t}. \tag{3.21}$$

Employing item (i) and taking into account $|n| = 1$, we can pass to the limit in the first term on the right hand side of (3.21). This shows

$$\lim_{\substack{Y\to 0\\ t\searrow 0}} \frac{\det(\partial F_{Y,t})-\det(\partial F_Y)}{t}|\partial F_{Y,t}n| = \operatorname{div}(X), \tag{3.22}$$

uniformly on $\partial\Omega$. Regarding the limit of the remaining term we observe

$$\begin{aligned}
\det(\partial F_Y)\frac{|\partial F_{Y,t}n|-|\partial F_Y n|}{t} &= \det(\partial F_Y)\frac{|\partial F_{Y,t}n|^2-|\partial F_Y n|^2}{t}\big(|\partial F_{Y,t}n|+|\partial F_Y n|\big)^{-1} \\
&= \det(\partial F_Y)\frac{(\partial F_{Y,t}n-\partial F_Y n)\cdot(\partial F_{Y,t}n+\partial F_Y n)}{t}\big(|\partial F_{Y,t}n|+|\partial F_Y n|\big)^{-1} \\
&= \det(\partial F_Y)\left(\frac{\partial F_{Y,t}-\partial F_Y}{t}n\right)\cdot(\partial F_{Y,t}n+\partial F_Y n)\big(|\partial F_{Y,t}n|+|\partial F_Y n|\big)^{-1}.
\end{aligned}$$

Now, item (ii) yields the uniform limit

$$\lim_{\substack{Y\to 0\\ t\searrow 0}} \det(\partial F_Y)\frac{|\partial F_{Y,t}n|-|\partial F_Y n|}{t} = (-\partial X n)\cdot n, \tag{3.23}$$

on $\partial\Omega$. □

We have thus gathered all necessary tools to investigate the material derivative, i.e. the limit (3.5). We are going to tackle this limit in several steps.

Lemma 3.5. Let $\Omega \in \mathcal{U}_{ad}$ and $X \in C^1(\bar{\mathsf{D}})^d$ with $\operatorname{supp}(X) \subset (\mathsf{D} \setminus \bar{\omega})$. Furthermore, for $Y \in C^1(\bar{\mathsf{D}})^d$ with $\operatorname{supp}(Y) \subset (\mathsf{D} \setminus \bar{\omega})$ and $\|Y\|_{C^1(\bar{\mathsf{D}})^d}$, $t > 0$ sufficient small let $u^{Y,t} \in H^1_\Gamma(\Omega)^d$ be defined in (3.3). Then there is a constant $C \in \mathbf{R}$ independent of t and Y such that

$$\|u^{Y,t}\|_{H^1(\Omega)^d} \leq C.$$

Proof. Testing (3.3) with $\varphi = u^{Y,t}$ yields

$$\int_\Omega \xi_{Y,t} \mathbf{A} \epsilon_{Y,t}(u^{Y,t}) : \epsilon_{Y,t}(u^{Y,t})\, dx = \int_\Omega \xi_{Y,t} f^{Y,t} \cdot u^{Y,t}\, dx + \int_{\Gamma^N} \nu_{Y,t} g^{Y,t} \cdot u^{Y,t}\, dS.$$

Thus, due to the differentiability results of Lemma 3.3, Lemma 3.4 and Hölder's inequality, we deduce

$$\|\epsilon(u^{Y,t})\|^2_{L_2(\Omega)^d} \leq C \|u^{Y,t}\|_{H^1(\Omega)^d}.$$

Now the result follows from Korn's inequality (cf. [88]). □

Lemma 3.6. With the assumptions of Lemma 3.5 let $u^{Y,t}$ and u^Y be defined in (3.3) and (3.4), respectively. Then there is a constant $C \in \mathbf{R}$ independent of Y and t such that

$$\|u^{Y,t} - u^Y\|_{H^1(\Omega)^d} \leq Ct. \tag{3.24}$$

Proof. Subtracting equations (3.3) and (3.4) yields

$$\begin{aligned}
\int_\Omega \xi_Y \mathbf{A} \epsilon_Y(u^{Y,t} - u^Y) : \epsilon_Y(\varphi)\, dx = &\int_\Omega \xi_{Y,t} \mathbf{A}[\epsilon_Y(u^{Y,t}) - \epsilon_{Y,t}(u^{Y,t})] : \epsilon_Y(\varphi)\, dx \\
&+ \int_\Omega [\xi_Y - \xi_{Y,t}] \mathbf{A} \epsilon_Y(u^{Y,t}) : \epsilon_Y(\varphi)\, dx \\
&+ \int_\Omega \xi_{Y,t} \mathbf{A} \epsilon_{Y,t}(u^{Y,t}) : [\epsilon_Y(\varphi) - \epsilon_{Y,t}(\varphi)]\, dx \\
&+ \int_\Omega (\xi_{Y,t} - \xi_Y) f^{Y,t} \cdot \varphi\, dx + \int_\Omega \xi_Y (f^{Y,t} - f^Y) \cdot \varphi\, dx \\
&+ \int_{\Gamma^N} (\nu_{Y,t} - \nu_Y) g^{Y,t} \cdot \varphi\, dS + \int_{\Gamma^N} \nu_Y (g^{Y,t} - g^Y) \cdot \varphi\, dS,
\end{aligned} \tag{3.25}$$

for all $\varphi \in H^1_\Gamma(\Omega)^d$. Now testing with $\varphi = u^{Y,t} - u^Y \in H^1_\Gamma(\Omega)^d$ and using similar arguments as in the proof of Lemma 3.5 shows (3.24). □

Theorem 3.7. With the assumptions of the previous lemma there holds

$$\lim_{\substack{Y \to 0 \\ t \searrow 0}} \left\| \frac{u^{Y,t} - u^Y}{t} - \dot{u} \right\|_{H^1(\Omega)^d} = 0, \tag{3.26}$$

where $\dot{u} \in H^1_\Gamma(\Omega)^d$ is the unique solution to

$$\begin{aligned}\int_\Omega \mathbf{A}\epsilon(\dot{u}) : \epsilon(\varphi)\, dx =& \frac{1}{2}\int_\Omega \mathbf{A}[\partial u \partial X + \partial X^\top \partial u^\top] : \epsilon(\varphi)\, dx \\ &- \int_\Omega \operatorname{div}(X)\mathbf{A}\epsilon(u) : \epsilon(\varphi)\, dx \\ &+ \frac{1}{2}\int_\Omega \mathbf{A}\epsilon(u) : [\partial \varphi \partial X + \partial X^\top \partial \varphi^\top]\, dx \\ &+ \int_\Omega \operatorname{div}(X) f \cdot \varphi\, dx + \int_\Omega \partial f X \cdot \varphi\, dx \\ &+ \int_{\Gamma^N} (\operatorname{div}(X) - (\partial X n)\cdot n) g \cdot \varphi\, dS + \int_{\Gamma^N} \partial g X \cdot \varphi\, dS,\end{aligned} \tag{3.27}$$

for all $\varphi \in H^1_\Gamma(\Omega)^d$.

Proof. First, consider sequences $t_n \searrow 0$ and $Y_n \in C^1(\bar{\mathrm{D}})^d$ with $\operatorname{supp}(Y_n) \subset (\mathrm{D} \setminus \bar{\omega})$, $Y_n \to 0$ in $C^1(\bar{\mathrm{D}})^d$ starting sufficiently close to 0. From Lemma 3.6 we know that $V^{Y_n,t_n} := \frac{u^{Y_n,t_n} - u^{Y_n}}{t_n}$ is bounded in $H^1(\Omega)^d$. Hence, there exists $V \in H^1_\Gamma(\Omega)^d$ such that, up to a subsequence denoted the same, $V^{Y_n,t_n} \rightharpoonup V$ in $H^1(\Omega)^d$. Now, dividing (3.25) by t_n, using an arbitrary testfunction $\varphi \in H^1_\Gamma(\Omega)^d$ and passing to the limit according to Lemma 3.4 and Lemma 3.3, entails that V satisfies

$$\begin{aligned}\int_\Omega \mathbf{A}\epsilon(V) : \epsilon(\varphi)\, dx =& \frac{1}{2}\int_\Omega \mathbf{A}[\partial u \partial X + \partial X^\top \partial u^\top] : \epsilon(\varphi)\, dx \\ &- \int_\Omega \operatorname{div}(X)\mathbf{A}\epsilon(u) : \epsilon(\varphi)\, dx \\ &+ \frac{1}{2}\int_\Omega \mathbf{A}\epsilon(u) : [\partial \varphi \partial X + \partial X^\top \partial \varphi^\top]\, dx \\ &+ \int_\Omega \operatorname{div}(X) f \cdot \varphi\, dx + \int_\Omega \partial f X \cdot \varphi\, dx \\ &+ \int_{\Gamma^N} (\operatorname{div}(X) - (\partial X n)\cdot n) g \cdot \varphi\, dS + \int_{\Gamma^N} \partial g X \cdot \varphi\, dS,\end{aligned} \tag{3.28}$$

for all $\varphi \in H^1_\Gamma(\Omega)^d$. By uniqueness we conclude that $V = \dot{u}$ and thus also that $\frac{u^{Y,t} - u^Y}{t} \rightharpoonup \dot{u}$ in $H^1(\Omega)^d$. In order to deduce strong convergence in H^1, we work with the underlying PDEs and use the same arguments as in the proof of Lemma 3.6. Subtracting (3.25) divided by t and (3.27) yields

$$
\begin{aligned}
\int_\Omega \xi_Y A\epsilon_Y(V^{Y,t}-\ddot{u}) : \epsilon_Y(\varphi)\,dx = &\int_\Omega (1-\xi_Y)A\epsilon_Y(\ddot{u}) : \epsilon_Y(\varphi)\,dx \\
&+\int_\Omega A[\epsilon-\epsilon_Y](\ddot{u}) : \epsilon_Y(\varphi)\,dx + \int_\Omega A\epsilon(\ddot{u}) : [\epsilon-\epsilon_Y](\varphi)\,dx \\
&+\int_\Omega A\left(\frac{\epsilon_{Y,t}(u^{Y,t})-\epsilon_Y(u^{Y,t})}{t} - \frac{1}{2}[\partial u^{Y,t}\partial X + \partial X^\top(\partial u^{Y,t})^\top]\right) : \epsilon_Y(\varphi)\,dx \\
&+\int_\Omega \xi_{Y,t} A\frac{1}{2}[\partial(u^{Y,t}-u)\partial X + \partial X^\top(\partial(u^{Y,t}-u))^\top] : \epsilon_Y(\varphi)\,dx \\
&+\int_\Omega (\xi_{Y,t}-1)A\frac{1}{2}[\partial u\partial X + \partial X^\top(\partial u)^\top] : \epsilon_Y(\varphi)\,dx \\
&+\int_\Omega A\frac{1}{2}[\partial u\partial X + \partial X^\top(\partial u)^\top] : [\epsilon_Y(\varphi)-\epsilon(\varphi)]\,dx \\
&+\int_\Omega \left(\frac{\xi_Y-\xi_{Y,t}}{t} + \operatorname{div}(X)\right)A\epsilon_y(u^{Y,t}) : \epsilon_Y(\varphi)\,dx \\
&+\int_\Omega \operatorname{div}(X)A\epsilon_Y(u^{Y,t}) : [\epsilon(\varphi)-\epsilon_Y(\varphi)]\,dx \\
&+\int_\Omega \operatorname{div}(X)A\epsilon_Y(u-u^{Y,t}) : \epsilon(\varphi)\,dx + \int_\Omega \operatorname{div}(X)A[\epsilon(u)-\epsilon_Y(u)] : \epsilon(\varphi)\,dx \\
&+\int_\Omega \xi_{Y,t}A\epsilon_{Y,t}(u^{Y,t}) : \left(\frac{\epsilon_{Y,t}(\varphi)-\epsilon_Y(\varphi)}{t} - \frac{1}{2}[\partial\varphi\partial X + \partial X^\top\partial\varphi^\top]\right)dx \\
&+\int_\Omega (\xi_{Y,t}-1)A\epsilon_{Y,t}(u^{Y,t}) : \left(\frac{1}{2}[\partial\varphi\partial X + \partial X^\top\partial\varphi^\top]\right)dx \\
&+\int_\Omega A\epsilon_{Y,t}(u^{Y,t}-u) : \left(\frac{1}{2}[\partial\varphi\partial X + \partial X^\top\partial\varphi^\top]\right)dx \\
&+\int_\Omega A[\epsilon_{Y,t}(u)-\epsilon(u)] : \left(\frac{1}{2}[\partial\varphi\partial X + \partial X^\top\partial\varphi^\top]\right)dx \\
&+\int_\Omega \left(\frac{\xi_{Y,t}-\xi_Y}{t} - \operatorname{div}(X)\right)f\cdot\varphi\,dx \\
&+\int_\Omega \xi_Y\left(\frac{f^{Y,t}-f^Y}{t} - \partial f X\right)\cdot\varphi\,dx + \int_\Omega (\xi_Y-1)\partial f X\cdot\varphi\,dx \\
&+\int_{\Gamma^N} \left(\frac{\nu_{Y,t}-\nu_Y}{t} - (\operatorname{div}(X)-(\partial X n)\cdot n)\right)g\cdot\varphi\,dS \\
&+\int_{\Gamma^N} \nu_Y\left(\frac{g^{Y,t}-g^Y}{t} - \partial g X\right)\cdot\varphi\,dS + \int_{\Gamma^N} (\nu_Y-1)\partial g X\cdot\varphi\,dS,
\end{aligned}
$$

for all $\varphi \in H^1_\Gamma(\Omega)^d$, where $V^{Y,t} = \frac{u^{Y,t}-u^Y}{t}$. Note that the lengthy expression is a consequence of the differing coefficients in terms of perturbations. Now, we can apply Hölder's inequality to each integral on the right hand side to isolate $\|\varphi\|_{H^1(\Omega)^d}$. Similarly to the proof of Lemma 3.6, Lemma 3.3, Lemma 3.4 as well as the bounds on $u^{Y,t}$ entail

$$\|V^{Y,t} - \dot{u}\|_{H^1(\Omega)^d} \leq c_{Y,t}, \quad \lim_{\substack{Y \to 0 \\ t \searrow 0}} c_{Y,t} = 0.$$

This concludes the proof. □

Remark 3.8. Due to the symmetry properties of the elasticity tensor **A** we can simplify equation (3.27) as follows

$$\begin{aligned}\int_\Omega \mathbf{A}\epsilon(\dot{u}) : \epsilon(\varphi)\, dx = &\int_\Omega \mathbf{A}[\partial u \partial X] : \epsilon(\varphi)\, dx \\ &- \int_\Omega \operatorname{div}(X)\mathbf{A}\epsilon(u) : \epsilon(\varphi)\, dx \\ &+ \int_\Omega \mathbf{A}\epsilon(u) : [\partial \varphi \partial X]\, dx \\ &+ \int_\Omega \operatorname{div}(X) f \cdot \varphi\, dx + \int_\Omega \partial f X \cdot \varphi\, dx \\ &+ \int_{\Gamma^N} (\operatorname{div}(X) - (\partial X n) \cdot n) g \cdot \varphi\, dS + \int_{\Gamma^N} \partial g X \cdot \varphi\, dS,\end{aligned} \tag{3.29}$$

for all $\varphi \in H^1_\Gamma(\mathrm{D})^d$. This simplification will be advantageous for numerical implementations of the expression, as it appears in an adjoint formulation for certain cost functionals.

Assumption A. There hold the stronger results $u^{Y,t} \in C^1(K)^d$,

$$\lim_{\substack{Y \to 0 \\ t \searrow 0}} \|u^{Y,t} - u\|_{C^1(K)^d} = 0, \tag{3.30}$$

as well as

$$\lim_{\substack{Y \to 0 \\ t \searrow 0}} \left\|\frac{u^{Y,t} - u^Y}{t} - \dot{u}\right\|_{C^1(K)^d} = 0, \tag{3.31}$$

where $K := \overline{\Omega \setminus \omega}$.

Remark 3.9. In this remark we want to elaborate on Assumption A. We would like to highlight that this assumption is of reasonable nature, since the results obtained in [38] and further literature mentioned therein ensure that similar estimates can be obtained in terms of the stronger convergence $W^{2,p}(\Omega)^d$, $p > d$ which continuously embeds into $C^1(\bar{\Omega})^d$ (cf. [82]). Unfortunately, this only holds true for pure traction or pure Dirichlet problems, where the involved data satisfies sufficient regularity assumptions. It is well known that the intersection of different boundary conditions lacks regularity. Since we are interested in a mixed boundary problem, the strong regularity result obtained in [38] cannot directly be recast on our problem. Nonetheless, the set ω ensures that the region of low regularity, i.e. the vicinity of $\Gamma \cap \Gamma^N$, is not considered. Since the results obtained in Lemma 3.5, Lemma 3.6 and Theorem 3.7 rely on a priori estimates in $H^1(\Omega)^d$, it is reasonable that these can be recast in $W^{2,p}(\tilde{\Omega})^d$, $p > d$ for $\tilde{\Omega} \subset \Omega$, if the problematic region is avoided.

4 Shape derivative

In this section we compute the first order shape derivative of $\mathcal{J}$. In view of the different properties of the smooth volume term $\mathcal{J}_{\text{vol}}$ and the nonsmooth penalty term $\mathcal{J}_\sigma$ we split the cost functional accordingly and address each part separately. We are now going to give a precise meaning to the term *shape derivative*. Let $X \in C^1(\bar{\mathrm{D}})^d$ with $\mathrm{supp}(X) \subset (\mathrm{D} \setminus \bar{\omega})$ denote a deformation vector field and $t > 0$ sufficiently small. In analogy to Section 3 we define the perturbed identity $F_t := \mathrm{Id} + tX$ (cf. (1.5)) and let $\Omega_t := F_t(\Omega)$.

Definition 4.1. With the previous notation we define the first order shape derivative of the functional $\mathcal{J} : \mathcal{U}_{ad} \to \mathbf{R}$ at $\Omega \in \mathcal{U}_{ad}$ in direction $X \in C_c^1(\mathrm{D})^d$ by

$$D\mathcal{J}(\Omega)(X) := \lim_{t \searrow 0} \frac{\mathcal{J}(\Omega_t) - \mathcal{J}(\Omega)}{t}. \tag{4.1}$$

Even though we only need to consider deformations X that vanish on ω in this section, we defined the shape derivative for more general deformation fields X. This allows us to return to this definition in the last part of this thesis.

Remark 4.2. Note that the notion of *shape derivative* and the corresponding limit in Definition 4.1 is not uniquely used throughout the literature. Usually, this quantity is required to be both, linear and continuous with respect to the deformation vector field X. Whilst these are desirable properties to deduce further results, such as the identification of a gradient with respect to a Hilbert space (cf. Section 5), we do not want to prescribe them. This allows us to use a unified terminology throughout this section. Additionally, we want to mention the notion of *Eulerian semiderivative* (cf. [43, Definition 3.1]), which usually refers to the analogous quantity defined in Definition 4.1 following the velocity method (1.3).

For the sake of simplicity, we introduce the notion of perturbed and unperturbed state variables for $Y \equiv 0$. That is, let $u_t := u_{0,t}$ and $u := u_0$, where $u_{0,t}$ and u_0 are defined by (3.1) and (3.2), respectively. Similarly, we denote the lifted perturbed state variable $u^t := u_t \circ F_t$. We first address the volume term of the cost functional.

Lemma 4.3. Let $\mathcal{J}_{\text{vol}} : \mathcal{U}_{ad} \to \mathbf{R}$ be defined in (2.2) and $X \in C^1(\bar{\mathrm{D}})^d$ with $\mathrm{supp}(X) \subset (\mathrm{D} \setminus \bar{\omega})$ and $\Omega \in \mathcal{U}_{ad}$. Then there holds

$$D\mathcal{J}_{\text{vol}}(\Omega)(X) = 2\,(|\Omega| - V) \int_\Omega \mathrm{div}(X)\, dx. \tag{4.2}$$

Proof. Let $t > 0$ small. By definition we have to investigate the term

$$\frac{\mathcal{J}_{\text{vol}}(\Omega_t) - \mathcal{J}_{\text{vol}}(\Omega)}{t}. \tag{4.3}$$

Expanding the nominator yields

$$\mathcal{J}_{\text{vol}}(\Omega_t) - \mathcal{J}_{\text{vol}}(\Omega) = (|\Omega_t| - V)^2 - (|\Omega| - V)^2 = (|\Omega_t| - |\Omega|)\,(|\Omega_t| + |\Omega| - 2V). \tag{4.4}$$

Taking into account

$$|\Omega_t| = \int_{\Omega_t} dx = \int_\Omega \det(\mathrm{Id} + t\partial X)\, dx, \tag{4.5}$$

we can employ Lemma 3.4 item (i) with $Y \equiv 0$ to deduce

$$\begin{aligned} D\mathscr{J}_{\text{vol}}(\Omega)(X) &= \lim_{t\searrow 0} \frac{\mathscr{J}_{\text{vol}}(\Omega_t) - \mathscr{J}_{\text{vol}}(\Omega)}{t} \\ &= \lim_{t\searrow 0} \frac{|\Omega_t| - |\Omega|}{t} (|\Omega_t| + |\Omega| - 2V) \\ &= 2(|\Omega| - V) \int_\Omega \operatorname{div}(X)\, dx, \end{aligned} \tag{4.6}$$

which finishes the proof. □

We observe that the shape derivative of $\mathscr{J}_{\text{vol}}$ is linear and continuous with respect to the deformation field X. Next we address the second part of the cost functional, that is $\mathscr{J}_\sigma$. The derivation of an analogous result for the penalty term strongly relies on the following Danskin type result (cf. [104]).

Lemma 4.4. Let $K \subset \mathbf{R}^d$ be compact, $\tau > 0$ and $g : [0,\tau] \times K \to \mathbf{R}$ some function. Additionally, define for $t \in [0,\tau]$ the set $R^t := \{z \in K | \max_{x\in K} g(t,x) = g(t,z)\}$ with the convention $R := R^0$. Further assume that

(A1) for all $x \in R$ the partial derivative $\partial_t g(0^+, x)$ exists,

(A2) for all $t \in [0,\tau]$ the function $x \mapsto g(t,x)$ is upper semicontinuous,

(A3) for all real nullsequences (t_n), $t_n \searrow 0$ and all sequences (y_{t_n}) converging to some $y \in R$ we have

$$\lim_{n\to\infty} \frac{g(t_n, y_{t_n}) - g(0, y_{t_n})}{t_n} = \partial_t g(0^+, y). \tag{4.7}$$

Then

$$\frac{\partial}{\partial t}\left(\max_{x\in K} g(t,x)\right)_{t=0} = \max_{x\in R} \partial_t g(0^+, x). \tag{4.8}$$

Proof. For a proof we refer to [104, Lemma 2.19]. □

Next, we investigate the interior part of the penalty term, which refers to the function $g(t,x)$ in Lemma 4.4. In view of the stronger regularity assumption (cf. Assumption A) we can treat this functional in a similar fashion to $\mathscr{J}_{\text{vol}}$.

Lemma 4.5. Let the compact set K be defined in Assumption A. For $x \in K$ and $t \geq 0$ let

$$\mathscr{J}_\sigma^x(\Omega_t) := \sigma_M^2(u_t)(x_t) - \delta, \tag{4.9}$$

where $x_t := F_t(x)$ and $\delta \in \mathbf{R}$ denotes the stress threshold. Additionally, fix a deformation vector field $X \in C^1(\bar{\mathrm{D}})^d$ with $\operatorname{supp}(X) \subset (\mathrm{D} \setminus \bar{\omega})$ and $\Omega \in \mathscr{U}_{ad}$. Then there holds

$$D\mathscr{J}_\sigma^x(\Omega)(X) = 2\mathbf{B}\epsilon(u)(x) : \epsilon(\dot{u})(x) - \mathbf{B}[\partial u \partial X + (\partial X)^\top (\partial u)^\top](x) : \epsilon(u)(x), \tag{4.10}$$

with the constant tensor $\mathbf{B}$ defined in (2.8) and $\dot{u}$ solving (3.27).

Proof. We first perform a change of variables to obtain

$$\mathscr{J}_\sigma^x(\Omega_t) = \mathbf{B}\epsilon_t(u^t)(x) : \epsilon_t(u^t)(x) - \delta. \tag{4.11}$$

Next, we can expand the quotient

$$\begin{aligned}\frac{\mathscr{J}_\sigma^x(\Omega_t) - \mathscr{J}_\sigma^x(\Omega)}{t} =& \mathbf{B}\frac{\epsilon_t(u^t)(x) - \epsilon(u^t)(x)}{t} : \epsilon_t(u^t)(x)\\ &+ \mathbf{B}\epsilon(\frac{u^t - u}{t})(x) : \epsilon_t(u^t)(x)\\ &+ \mathbf{B}\epsilon(u)(x) : \frac{\epsilon_t(u^t)(x) - \epsilon(u^t)(x)}{t}\\ &+ \mathbf{B}\epsilon(u)(x) : \epsilon(\frac{u^t - u}{t})(x).\end{aligned} \tag{4.12}$$

Due to Assumption A we are able to pass to the limit and deduce

$$\begin{aligned}D\mathscr{J}_\sigma^x(\Omega)(X) =& -\frac{1}{2}\mathbf{B}[\partial u \partial X + (\partial X)^\top(\partial u)^\top] : \epsilon(u)(x) + \mathbf{B}\epsilon(\dot{u})(x) : \epsilon(u)(x)\\ &- \mathbf{B}\epsilon(u)(x) : \frac{1}{2}[\partial u \partial X + (\partial X)^\top(\partial u)^\top] + \mathbf{B}\epsilon(u)(x) : \epsilon(\dot{u})(x).\end{aligned} \tag{4.13}$$

By symmetry of the inner product we conclude (4.10). □

Again, we want to highlight that the shape derivative of the interior part is a continuous and linear functional with respect to the deformation field X.

Remark 4.6. The symmetric tensor $\mathbf{B}$ allows the simplified expression

$$D\mathscr{J}_\sigma^x(\Omega)(X) = 2\mathbf{B}\left(\epsilon(\dot{u})(x) - [\partial u \partial X](x)\right) : \epsilon(u)(x). \tag{4.14}$$

Now, we are able to prove the main result regarding the derivative of the penalty term. We will proceed in two steps.

Lemma 4.7. Let $\tilde{\mathscr{J}}_\sigma : \mathscr{U}_{ad} \to \mathbf{R}$ be defined as

$$\tilde{\mathscr{J}}_\sigma(\Omega) := \max_{x \in K} \mathscr{J}_\sigma^x(\Omega), \tag{4.15}$$

where $X \in C^1(\bar{\mathsf{D}})^d$ with $\operatorname{supp}(X) \subset (\mathsf{D} \setminus \bar{\omega})$ and $\Omega \in \mathscr{U}_{ad}$. Then there holds

$$D\tilde{\mathscr{J}}_\sigma(\Omega)(X) = \max_{x \in A(u)} 2\mathbf{B}\epsilon(u)(x) : \epsilon(\dot{u})(x) - \mathbf{B}[\partial u \partial X + (\partial X)^\top(\partial u)^\top](x) : \epsilon(u)(x), \tag{4.16}$$

where $A(u) := \{z \in K \mid \sigma_M^2(u)(z) = \max_{x \in K} \sigma_M^2(u)(x)\}$.

Proof. First note that we can rewrite the functional as

$$\tilde{\mathscr{J}}_\sigma(\Omega_t) = \max_{x \in K} \mathscr{J}_\sigma^x(\Omega_t). \tag{4.17}$$

Now our goal is to apply Lemma 4.4 to

$$g : [0,\tau] \times K \to \mathbf{R}, \quad (t,x) \mapsto \mathscr{J}_\sigma^x(\Omega_t), \tag{4.18}$$

where $\tau > 0$ is a sufficiently small constant. In order to apply the lemma, we need to check assumptions (A1)-(A3). Since $R = A(u) \subset K$, Lemma 4.5 shows that (A1) is satisfied. To show (A2), note that due to Assumption A, $u^t \in C^1(K)^d$ and thus the mapping $x \mapsto g(t,x)$ is continuous for $t \in [0,\tau]$. The proof of (A3) follows the lines of Lemma 4.5, where we further use the uniform convergence $\frac{u^t - u}{t} \to \dot{u}$ in $C^1(K)^d$. □

Theorem 4.8. Let $\mathscr{J}_\sigma : \mathscr{U}_{ad} \to \mathbf{R}$ be defined as in (2.9), $X \in C^1(\bar{\mathrm{D}})^d$ with $\mathrm{supp}(X) \subset (\mathrm{D} \backslash \bar{\omega})$ and $\Omega \in \mathscr{U}_{ad}$. Then there holds:

$$D\mathscr{J}_\sigma(\Omega)(X) = \begin{cases} \max_{x \in A(u)} \Phi(x) & \text{if } \sigma_M^2(u)|_{A(u)} > \delta, \\ \max\{\max_{x \in A(u)} \Phi(x), 0\} & \text{if } \sigma_M^2(u)|_{A(u)} = \delta, \\ 0 & \text{if } \sigma_M^2(u)|_{A(u)} < \delta, \end{cases} \tag{4.19}$$

where $A(u) := \{z \in K |\, \sigma_M^2(u)(z) = \max_{x \in K} \sigma_M^2(u)(x)\}$ and

$$\Phi(x) := 2\mathbf{B}\epsilon(u)(x) : \epsilon(\dot{u})(x) - \mathbf{B}[\partial u \partial X + (\partial X)^\top (\partial u)^\top](x) : \epsilon(u)(x). \tag{4.20}$$

Proof. The proof is another application of Theorem 4.4. Let the compact set K denote a two valued index set. That is, $K = \{1,2\}$ and

$$g(t,x) = \begin{cases} \tilde{\mathscr{J}}_\sigma(\Omega_t) & \text{if } x = 1, \\ 0 & \text{if } x = 2. \end{cases} \tag{4.21}$$

Now the result follows similarly to the previous lemma, where we note that the active set R of the two valued set correlates to the three cases as follows:

$$\begin{cases} R = \{1\} & \text{if } \sigma_M^2(u)|_{A(u)} > \delta, \\ R = \{1,2\} & \text{if } \sigma_M^2(u)|_{A(u)} = \delta, \\ R = \{2\} & \text{if } \sigma_M^2(u)|_{A(u)} < \delta. \end{cases} \tag{4.22}$$

□

5 Hilbert space setting

In this section we study optimality conditions and steepest descent directions for the penalised objective functional $\mathscr{J}_{\mathrm{vol}} + \alpha \mathscr{J}_\sigma$. We therefore formulate the results of the previous section in a Hilbert space setting. This allows us to recast some well-known results of nonsmooth analysis (cf. [45]). The key observation in this context is the following: Let $\mathscr{H}$ be a Hilbert space such that

$$\mathscr{H} \subset \{X \in C^1(\bar{\mathrm{D}})^d |\, \mathrm{supp}(X) \subset (\mathrm{D} \setminus \bar{\omega})\},$$

and point evaluation of the gradient is continuous. A possible approach to construct such a Hilbert space involves the notion of reproducing kernel Hilbert spaces. More details on this topic can be found in the article [48]. For now we just assume such a Hilbert space exists. Since the mappings $X \mapsto D\mathscr{J}_{\text{vol}}(\Omega)(X)$ and $X \mapsto D\mathscr{J}_\sigma^x(\Omega)(X)$, for $x \in A(u)$ are linear and by our assumption also continuous, the Riesz representation theorem entails that there are elements$\nabla\mathscr{J}_{\text{vol}} \in \mathscr{H}$ and $\nabla\mathscr{J}_\sigma^x \in \mathscr{H}$, such that

$$D\mathscr{J}_{\text{vol}}(\Omega)(X) = \langle \nabla\mathscr{J}_{\text{vol}}, X\rangle_{\mathscr{H}}, \qquad D\mathscr{J}_\sigma^x(\Omega)(X) = \langle \nabla\mathscr{J}_\sigma^x, X\rangle_{\mathscr{H}}, \tag{5.1}$$

for all $x \in A(u)$ and $X \in \mathscr{H}$. Utilising these Riesz representatives allows us to formulate the statement of Theorem 4.8 as follows:

$$D\mathscr{J}(\Omega)(X) = \begin{cases} \max_{x\in A(u)}\langle \nabla\mathscr{J}_{\text{vol}} + \alpha\nabla\mathscr{J}_\sigma^x, X\rangle_{\mathscr{H}} & \text{if } \sigma_M^2(u)|_{A(u)} > \delta, \\ \max\{\max_{x\in A(u)}\langle \nabla\mathscr{J}_{\text{vol}} + \alpha\nabla\mathscr{J}_\sigma^x, X\rangle_{\mathscr{H}}, \langle \nabla\mathscr{J}_{\text{vol}}, X\rangle_{\mathscr{H}}\} & \text{if } \sigma_M^2(u)|_{A(u)} = \delta, \\ \langle \nabla\mathscr{J}_{\text{vol}}, X\rangle_{\mathscr{H}} & \text{if } \sigma_M^2(u)|_{A(u)} < \delta. \end{cases} \tag{5.2}$$

Introducing the set

$$\mathscr{Z} := \begin{cases} \{\nabla\mathscr{J}_{\text{vol}} + \alpha\nabla\mathscr{J}_\sigma^x \mid x \in A(u)\} & \text{if } \sigma_M^2(u)|_{A(u)} > \delta, \\ \{\nabla\mathscr{J}_{\text{vol}} + \alpha\nabla\mathscr{J}_\sigma^x \mid x \in A(u)\} \cup \{\nabla\mathscr{J}_{\text{vol}}\} & \text{if } \sigma_M^2(u)|_{A(u)} = \delta, \\ \{\nabla\mathscr{J}_{\text{vol}}\} & \text{if } \sigma_M^2(u)|_{A(u)} < \delta, \end{cases} \tag{5.3}$$

this further simplifies to

$$D\mathscr{J}(\Omega)(X) = \max_{L\in\mathscr{Z}}\langle L, X\rangle_{\mathscr{H}}. \tag{5.4}$$

The following lemma are classical results in the context of nonsmooth analysis. For the sake of completeness, we are going to add the proof nonetheless. First, we show that one can extend (5.4) to the closed convex hull of $\mathscr{Z}$.

Lemma 5.1. Let $\mathscr{L} := \overline{\text{conv}(\mathscr{Z})}$. Then there holds

$$D\mathscr{J}(\Omega)(X) = \max_{L\in\mathscr{L}}\langle L, X\rangle_{\mathscr{H}}, \tag{5.5}$$

for all $X \in \mathscr{H}$.

Proof. Fix $X \in \mathscr{H}$. Since $\mathscr{Z} \subset \mathscr{L}$, it readily follows that

$$\max_{L\in\mathscr{Z}}\langle L, X\rangle_{\mathscr{H}} \leq \max_{L\in\mathscr{L}}\langle L, X\rangle_{\mathscr{H}}. \tag{5.6}$$

For the converse let $L \in \mathscr{L}$. Thus, there exist $Z_n = \sum_{k=0}^{N_n} \lambda_k^n A_k^n$ such that $A_k^n \in \mathscr{Z}$, $\sum_{k=0}^{N_n} \lambda_k^n = 1$ for $n \in \mathbf{N}$ and $k \in \{0, .., N_n\}$ and $Z_n \to L$ in $\mathscr{H}$. Next we observe that

$$\langle Z_n, X\rangle_{\mathscr{H}} = \langle \sum_{k=0}^{N_n} \lambda_k^n A_k^n, X\rangle_{\mathscr{H}} = \sum_{k=0}^{N_n} \lambda_k^n \langle A_k^n, X\rangle_{\mathscr{H}} \leq \sum_{k=0}^{N_n} \lambda_k^n D\mathscr{J}(\Omega)(X) = D\mathscr{J}(\Omega)(X). \tag{5.7}$$

Hence, passing to the limit yields $\langle L, X\rangle_{\mathscr{H}} \leq D\mathscr{J}(\Omega)(X)$ and thus the result follows. □

With this result we are able to characterise steepest descend directions (cf. [45, Lemma 3.3])

Lemma 5.2. Assume $0 \notin \mathscr{L}$. Then there holds

$$\min_{\|X\|_{\mathscr{H}}=1} D\mathscr{J}(\Omega)(X) = -\|X^*\|_{\mathscr{H}}, \tag{5.8}$$

where $X^* = -\frac{Z^*}{\|Z^*\|_{\mathscr{H}}}$ and $Z^* = \operatorname{argmin}_{Z\in\mathscr{L}} \|Z\|_{\mathscr{H}}$.

Proof. First note that $Z^* = P_{\mathscr{L}}(0)$, where $P_{\mathscr{L}}$ denotes the projection onto the closed and convex set $\mathscr{L}$. Thus, we deduce by the properties of the projection map (cf. [64, Theorem 2.18])

$$\langle P_{\mathscr{L}}(0) - 0, Z - P_{\mathscr{L}}(0)\rangle_{\mathscr{H}} \geq 0 \quad \text{for all } Z \in \mathscr{L}, \tag{5.9}$$

which is equivalent to

$$\langle Z^*, Z^*\rangle_{\mathscr{H}} \leq \langle Z, Z^*\rangle_{\mathscr{H}} \quad \text{for all } Z \in \mathscr{L}. \tag{5.10}$$

Next we observe that for each $Z \in \mathscr{L}$ there holds

$$\langle Z, X^*\rangle_{\mathscr{H}} = -\frac{1}{\|Z^*\|_{\mathscr{H}}}\langle Z, Z^*\rangle_{\mathscr{H}} \leq -\frac{1}{\|Z^*\|_{\mathscr{H}}}\langle Z^*, Z^*\rangle_{\mathscr{H}}. \tag{5.11}$$

Hence, taking the maximum yields

$$D\mathscr{J}(\Omega)(X^*) = \max_{Z\in\mathscr{L}}\langle Z, X^*\rangle_{\mathscr{H}} = -\frac{1}{\|Z^*\|_{\mathscr{H}}}\langle Z^*, Z^*\rangle_{\mathscr{H}} = -\|Z^*\|_{\mathscr{H}}. \tag{5.12}$$

Additionally, for each $X \in \mathscr{H}$, $\|X\|_{\mathscr{H}} = 1$ there holds by the Cauchy-Schwarz inequality

$$-\|Z^*\|_{\mathscr{H}} \leq \langle Z^*, X\rangle_{\mathscr{H}} \leq \max_{Z\in\mathscr{L}}\langle Z, X\rangle_{\mathscr{H}} = D\mathscr{J}(\Omega)(X). \tag{5.13}$$

Thus we conclude

$$D\mathscr{J}(\Omega)(X^*) = \min_{\|X\|_{\mathscr{H}}=1} D\mathscr{J}(\Omega)(X), \tag{5.14}$$

which finishes the proof. □

The previous lemma entails the following optimality condition.

Corollary 5.3. The set $\Omega \in \mathscr{U}_{ad}$ is a local minimiser of the penalised objective functional $\mathscr{J}$ if and only if $0 \in \mathscr{L}$. In this context Ω is said to be a local minimum of $\mathscr{J}$ if there is a constant $\rho > 0$ such that $\mathscr{J}(\Omega) \leq \mathscr{J}((\mathrm{Id} + X)(\Omega))$ for all $X \in \mathscr{H}$, $\|X\|_{\mathscr{H}} < \rho$.

Proof. From Lemma 5.2 we know that $D\mathscr{J}(\Omega)(X^*) < 0$ if $0 \notin \mathscr{L}$. Hence a descend in direction X^* is possible for a sufficiently small step size. In contrast, if $0 \in \mathscr{L}$ there holds $D\mathscr{J}(\Omega)(X) \geq \langle 0, X\rangle_{\mathscr{H}} = 0$ for all $X \in \mathscr{H}$. □

Remark 5.4. In view of the definition of $\mathscr{Z}$ in (5.3), the optimality conditions read as follows: if the stress constraint is strictly not violated, i.e. if $\sigma_M^2(u)(x) < \delta$ for all $x \in K$, then $\mathscr{L} = \{\nabla\mathscr{J}_{\text{vol}}\}$ and thus the optimality condition reads $\nabla\mathscr{J}_{\text{vol}} = 0$. Furthermore, if the stress threshold is surpassed, i.e. if there is $x \in K$ such that $\sigma_M^2(u)(x) > \delta$, the optimality condition entails $0 \in \overline{\operatorname{conv}(\mathscr{Z})}$. Finally, if the stress constraint is active, i.e. if there is $x \in A(u)$ such that $\sigma_M^2(u)(x) = \delta$, the optimality condition reads $0 \in \overline{\operatorname{conv}(\mathscr{Z})}$. By definition this includes the previous case $\nabla\mathscr{J}_{\text{vol}} = 0$ as well as the second case.

6 Clarke subgradient

In this section we are going to take a short detour to the framework of Clarke differentiation. Our goal is to connect the set $\mathscr{L}$ defined in Lemma 5.1 to the Clarke subgradient [39]. This section strongly relies on the generalised approach of the perturbation of the identity introduced in Section 3. We begin with the following central definition.

Definition 6.1. Let $(\mathscr{X}, \|\cdot\|)$ be a Banach space and $f : \mathscr{X} \to \mathbf{R}$ a function. The generalised directional derivative of f at $x \in \mathscr{X}$ in direction $v \in \mathscr{X}$ is defined as

$$D^\circ f(x;v) := \limsup_{\substack{y \to x \\ t \searrow 0}} \frac{f(y+tv) - f(y)}{t}. \tag{6.1}$$

Furthermore, the Clarke subgradient (generalised gradient) at $x_0 \in \mathscr{X}$ is defined as the set

$$\partial^\circ f(x_0) := \{x' \in \mathscr{X}' \,|\, D^\circ f(x_0;v) \geq x'(v), \text{ for all } v \in \mathscr{X}\}. \tag{6.2}$$

Remark 6.2. In the pioneering work [39] F. H. Clarke introduced the notation $f^\circ(x;v)$ for the generalised directional derivative. It has been shown in [39, Proposition 2.1.1] that, given a locally Lipschitz function f, the function $v \mapsto D^\circ f(x;v)$ is finite, subadditive, positively homogeneous and Lipschitz on $\mathscr{X}$. Furthermore, the author has shown [39, Proposition 2.1.2] that locally Lipschitz functions admit a nonempty, convex and weak*-compact Clarke subgradient.

For the sake of completeness we recall the notion of a directional derivative at this point.

Definition 6.3. Let $\mathscr{X}$ be a vector space and $f : \mathscr{X} \to \mathbf{R}$ a function. The directional derivative of f at $x \in \mathscr{X}$ in direction $v \in \mathscr{X}$ is defined as

$$D^+ f(x;v) := \lim_{t \searrow 0} \frac{f(y+tv) - f(y)}{t}. \tag{6.3}$$

In general, this limit does not have to exist. Yet, it is well known that convex functions entail sufficient properties to make sense of this definition (cf. [64]). In order to fit into the Clarke framework, we redefine the objective functional $\mathscr{J}$ as follows.

Definition 6.4. Let $\Omega \in \mathscr{U}_{ad}$ fix and $\mathscr{H}$ denote the Hilbert space introduced in the previous section. Furthermore, let $\rho > 0$ be sufficiently small. The function $G : B_\rho(0) \to \mathbf{R}$ is defined as

$$G(X) := \mathscr{J}((\mathrm{Id} + X)(\Omega)) \quad \text{for all } X \in B_\rho(0), \tag{6.4}$$

where $B_\rho(0)$ denotes the ball of radius ρ centered at 0 with respect to the norm $\|\cdot\|_{\mathscr{H}}$. Additionally, we define for $x \in K$ the pointwise function $G^x : B_\rho(0) \to \mathbf{R}$ by

$$G^x(X) := \mathscr{J}_{\mathrm{vol}}((\mathrm{Id} + X)(\Omega)) + \alpha \mathscr{J}_\sigma^x((\mathrm{Id} + X)(\Omega)) \quad \text{for all } X \in B_\rho(0), \tag{6.5}$$

where $\alpha > 0$ denotes the penalty parameter.

Remark 6.5. Note that the functions are indeed well defined for $\|X\|_{\mathscr{H}}$ sufficiently small. Furthermore, there holds

$$D^+G(0;X) = D\mathscr{J}(\Omega)(X) = \max_{L\in\mathscr{L}}\langle L,X\rangle_{\mathscr{H}}, \tag{6.6}$$

where $D^+G(0;X)$ denotes the directional derivative of G at $0\in\mathscr{H}$ in direction $X\in\mathscr{H}$. Similarly, we observe that

$$D^+G^x(0;X) = \langle\nabla\mathscr{J}_{\text{vol}} + \alpha\nabla\mathscr{J}_\sigma^x, X\rangle_{\mathscr{H}}. \tag{6.7}$$

In contrast to [39], our definition of the generalised directional derivative does not require G to be locally Lipschitz. The next lemma shows that the quotient is finite nonetheless. This further entails that the generalised directional derivative is well-defined.

Lemma 6.6. Let $Y\in\mathscr{H}$ sufficiently close to $0\in\mathscr{H}$ and $t>0$ small. Then there exists $C\in\mathbf{R}$ independent of Y and t such that

$$\left|\frac{G(Y+tX)-G(Y)}{t}\right| \le C. \tag{6.8}$$

Proof. Let $x^{Y,t}\in A(u^{Y,t})$. Then there holds by the maximising property of the set $A(u^{Y,t})$

$$\begin{aligned}
\frac{G(Y+tX)-G(Y)}{t} \le& \frac{G^{x^{Y,t}}(Y+tX)-G^{x^{Y,t}}(Y)}{t}\\
=&\frac{\mathbf{B}\epsilon_{Y,t}(u^{Y,t})(x^{Y,t}) : \epsilon_{Y,t}(u^{Y,t})(x^{Y,t}) - \mathbf{B}\epsilon_Y(u^Y)(x^{Y,t}) : \epsilon_Y(u^Y)(x^{Y,t})}{t}\\
=&\mathbf{B}[\frac{\epsilon_{Y,t}-\epsilon_Y}{t}](u^{Y,t})(x^{Y,t}) : \epsilon_{Y,t}(u^{Y,t})(x^{Y,t})\\
&+\mathbf{B}\epsilon_Y(\frac{u^{Y,t}-u^Y}{t})(x^{Y,t}) : \epsilon_{Y,t}(u^{Y,t})(x^{Y,t})\\
&+\mathbf{B}\epsilon_Y(u^Y)(x^{Y,t}) : [\frac{\epsilon_{Y,t}-\epsilon_Y}{t}](u^{Y,t})(x^{Y,t})\\
&+\mathbf{B}\epsilon_Y(u^Y)(x^{Y,t}) : \epsilon_Y(\frac{u^{Y,t}-u^Y}{t})(x^{Y,t}).
\end{aligned} \tag{6.9}$$

Assumption A entails $\frac{u^{Y,t}-u^Y}{t}\to\dot{u}$, $u^{Y,t}\to u$ and $u^Y\to u$ in $C^1(K)$. Furthermore, Lemma 3.4 item (ii) yields the uniform convergences of $\frac{\alpha_{Y,t}-\alpha_Y}{t}$, $\alpha_{Y,t}$ and α_Y. Thus, we conclude that for sufficiently small $Y\in\mathscr{H}$ and $t>0$ the right-hand side of equation (6.9) remains bounded. Using $x^Y\in A(u^Y)$ in a similar way shows that

$$\frac{G(Y)-G(Y+tX)}{t} \le C. \tag{6.10}$$

This concludes the proof. □

The next lemma constitutes the central result of this section. It states that for our objective function under consideration, both notions of directional derivative coincide.

Lemma 6.7. Let $X\in\mathscr{H}$. Then there holds

$$D^+G(0;X) = D^\circ G(0;X). \tag{6.11}$$

Proof. We show this result in two steps. For the inequality "≤" note that by the definition of the generalised directional derivative there holds

$$D^+G(0;X) = \lim_{t\searrow 0} \frac{G(tX)-G(0)}{t} \leq \limsup_{\substack{Y\to 0\\ t\searrow 0}} \frac{G(Y+tX)-G(Y)}{t} = D^\circ G(0;X). \tag{6.12}$$

For the converse note that by Lemma 6.6 the quotient appearing in the generalised direction derivative remains bounded. Hence, there are $Y_k \in \mathscr{H}$, $t_k > 0$ such that $Y_k \to 0$, $t_k \searrow 0$ for $k \to \infty$ and

$$D^\circ G(0;X) = \limsup_{\substack{Y\to 0\\ t\searrow 0}} \frac{G(Y+tX)-G(Y)}{t} = \lim_{k\to\infty} \frac{G(Y_k+t_kX)-G(Y_k)}{t_k}. \tag{6.13}$$

Next we pick for each $k \in \mathbf{N}$ a point $x^k \in A(u^{Y_k,t_k}) \subset K$. Since K is compact, there exists a subsequence, which we denote the same, and $x \in K$ such that $x_k \to x$. This yields

$$D^\circ G(0;X) = \lim_{k\to\infty} \frac{G(Y_k+t_kX)-G(Y_k)}{t_k} \leq \lim_{k\to\infty} \frac{G^{x_k}(Y_k+t_kX)-G^{x_k}(Y_k)}{t_k}. \tag{6.14}$$

Now expanding the right-hand side as in (6.9) and using the same arguments to pass to the limit, shows

$$D^\circ G(0;X) \leq \lim_{k\to\infty} \frac{G^{x_k}(Y_k+t_kX)-G^{x_k}(Y_k)}{t_k} = D^+G^x(0;X). \tag{6.15}$$

Next we note that for each $y \in K$ there holds $G^y(Y_k + t_kX) \leq G^{x_k}(Y_k + t_kX)$. Hence, passing to the limit $k \to \infty$ yields

$$G^y(0) \leq G^x(0), \tag{6.16}$$

i.e. $x \in A(u)$. Hence, putting our observations together yields

$$D^\circ G(0;X) \leq D^+G^x(0;X) \leq \max_{z\in A(u)} D^+G^z(0,X) = D^+G(0;X), \tag{6.17}$$

which concludes the proof. □

As a result we obtain the desired characterisation of $\mathscr{L}$.

Theorem 6.8. Let $\mathscr{L}$ be defined in Lemma 5.1 and $\partial^\circ G(0)$ denote the Clarke subgradient of G at $0 \in \mathscr{H}$. Then there holds

$$\mathscr{L} = \partial^\circ G(0). \tag{6.18}$$

Proof. First note that by the definition of the generalised directional derivative and Lemma 6.7 there holds for every $X \in \mathscr{H}$

$$\langle L,X\rangle_{\mathscr{H}} \leq \max_{L\in\mathscr{L}} \langle L,X\rangle_{\mathscr{H}} = D^+G(0;X) = D^\circ G(0;X) \quad \text{for all } L \in \mathscr{L}. \tag{6.19}$$

Thus, we conclude $\mathscr{L} \subset \partial^\circ G(0)$. For the converse let $Z \in \mathscr{L}^c$. By the Hahn-Banach separation theorem there exists a linear continuous functional μ and a constant $c \in \mathbf{R}$ such that $\mu(Z) > c > \mu(L)$ for all $L \in \mathscr{L}$. By the Riesz-representation we can identify μ with an element $\bar{X} \in \mathscr{H}$. Hence, it follows

$$\langle Z,\bar{X}\rangle_{\mathscr{H}} > c > \langle L,\bar{X}\rangle_{\mathscr{H}} \quad \text{for all } L \in \mathscr{L}. \tag{6.20}$$

Taking the maximum over $L \in \mathscr{L}$ now shows

$$\langle Z, \bar{X} \rangle_{\mathscr{H}} > D^{\circ} G(0; \bar{X}), \tag{6.21}$$

where we used again that the directional derivative and the generalised directional derivative coincide. Hence, we deduce $Z \notin \partial^{\circ} G(0)$, which concludes the proof. □

7 Numerical implementation

In this section we address the application of the previously derived results in a numerical scheme. Therefore, we extend the initial problem formulation by adding a weighting factor to the volume term $\mathscr{J}_{\text{vol}}$. On the one hand this enables a more sensitive numerical treatment of both parts of the cost functional. On the other hand, scaling this factor allows to treat $\mathscr{J}_{\text{vol}}$ as a penalty term and thus interpret the given task as a stress minimisation problem with a volume constraint. Before we specify the formulation of our model problem, we describe the general methodology.

Shape derivative and shape gradient In Section 5 we have seen that a Riesz-representation can be used to identify linear and continuous shape derivatives with gradients in a given Hilbert space $\mathscr{H}$. In the numerical scheme we obtain such gradients by solving a sub-problem. To specify, given a linear and continuous shape derivative $D\tilde{\mathscr{J}}(\Omega)(\cdot)$ we define $\nabla \tilde{\mathscr{J}} \in H^1_{\Gamma \cup \Gamma^N}(\Omega)^d$ as the unique solution of

$$\int_{\Omega} \epsilon(\nabla \tilde{\mathscr{J}}) : \epsilon(X) + B\nabla \tilde{\mathscr{J}} \cdot BX + \rho_{\text{low}} \nabla \tilde{\mathscr{J}} \cdot X \, dx = D\tilde{\mathscr{J}}(\Omega)(X) \quad \text{for all } X \in H^1_{\Gamma \cup \Gamma^N}(\Omega)^d. \tag{7.1}$$

Here, $\rho_{\text{low}} > 0$ is a constant and the term

$$B = \begin{pmatrix} -\partial_x & \partial_y \\ \partial_y & \partial_x \end{pmatrix}, \tag{7.2}$$

incorporates the Cauchy-Riemann equations and thus encourages the solution to be a conformal mapping, which accounts for a good mesh quality. It is noteworthy that due to this approach $\nabla \tilde{\mathscr{J}}$ is merely in $H^1_{\Gamma \cup \Gamma^N}(\Omega)^d$. This is a definite conflict to the analytic setting, where higher regularity of the deformation fields is necessary to compute the shape derivatives. Nevertheless, this does not cause any problems in the numerical realm.

Remark 7.1. Recall that the derivative of the maximum norm is by its nature nonlinear. Nonetheless, we can utilise this approach to identify gradients ∇J^x_{σ} for $x \in A(u)$, since the interior functionals (cf. Lemma 4.5) satisfy sufficient properties. These gradients can further be used according to Section 5.

Moving mesh method and mesh quality We realise deformations of the shape Ω following the "moving mesh" approach. That is, in each iteration we move the mesh according to a vector field. This underlines the importance of the Cauchy-Riemann term. Nonetheless, it is still possible that the mesh quality declines after a certain number of iterations. We therefore introduce the quantity

$$\min_{E \in \mathrm{El}(\Omega)} \frac{r_i^E}{r_o^E},$$

where $\mathrm{El}(\Omega)$ denotes the set of triangular elements constituting the finite element space on Ω and r_i^E, r_o^E denote the inner radius and outer radius of each element E, respectively. Whenever this quantity falls below a certain threshold, i.e. when some elements are too thin, a remeshing is performed.

Differences to the analytic setting To conclude our general methodology, we want to highlight some simplifications we impose in the numerical setting. Contrary to the initial problem formulation, we do not consider the subset ω for the numerical implementation. Recall that the main purpose of this set was the avoidance of the low regularity area. This can be justified, since we are working in a finite dimensional finite element space. Additionally, we only consider deformation vector fields that vanish on the boundary Γ^N, where the force is applied, as well. This ensures, that the algorithm behaves appropriately. In fact, without this assumption the algorithm would try to shrink the boundary part Γ^N, since this leads to a decrease of the applied force and thus also minimises the present stresses. This behaviour would be further reinforced, since we do not consider a volume force for the numerical implementation. Nonetheless, we would like to point out that we consider an additional free boundary. Therefore, the assumption $X \equiv 0$ on $\Gamma \cup \Gamma^N$ does not fix the whole body. Finally, we want to mention that, in contrast to the initial problem formulation, the domains occurring in the upcoming numerical examples include corners on the boundary and thus lack some regularity that is required in the analytical setting.

7.1 max-norm approach

Our goal is to minimise the functional

$$\mathscr{J}(\Omega) := \gamma_1 (|\Omega| - V)^2 + \gamma_2 \max\{\max_{x\in\bar{\Omega}} \sigma_M^2(u_\Omega) - \delta, 0\}, \tag{7.3}$$

where $\Omega \in \mathscr{U}_{ad}$, $u_\Omega \in H^1_\Gamma(\Omega)^2$ solves (2.4), $\gamma_1, \gamma_2 \in \mathbf{R}^+$ are given weights and $\delta = 0$ denotes the stress threshold. Here, $|\Omega|$ denotes the volume of Ω and the constant $V \in \mathbf{R}$ is a given target volume. In view of an efficient numerical implementation it is feasible to have access to the associated adjoint variable. Since the state variable u_Ω solely appears in the stress term, we only need to investigate the penalty term $\mathscr{J}_\sigma$. In view of Lemma 4.5 we seek adjoint variables q^x, $x \in A(u)$ such that

$$\int_\Omega \mathbf{A}\epsilon(\varphi) : \epsilon(q^x)\, dx = 2\mathbf{B}\epsilon(u)(x) : \epsilon(\varphi)(x) \quad \text{for all } \varphi \in H^1_\Gamma(\mathrm{D})^d. \tag{7.4}$$

Unfortunately, equation (7.4) is not well defined, since point evaluation of the gradient is generally not possible in H^1. As a remedy, we introduce for given $r > 0$ the approximation $q^{x,r} \in H^1_\Gamma(\mathrm{D})^d$ as the unique solution of

$$\int_\Omega \mathbf{A}\epsilon(\varphi) : \epsilon(q^{x,r})\, dx = \frac{2}{|B_r(x)|} \int_{B_r(x)} \mathbf{B}\epsilon(u) : \epsilon(\varphi)\, dx \quad \text{for all } \varphi \in H^1_\Gamma(\mathrm{D})^d. \tag{7.5}$$

Here, $B_r(x)$ denotes the ball centered at x with radius r. A possible workaround could be the introduction of so-called very-weak solutions. In our setting however, the formulation is not straightforward and thus requires further research. Nonetheless, we want to point out that a thorough study of the numerical treatment of this adjoint equation could improve the efficiency of our approach.

Remark 7.2. At this point, we require the adjoint variable to enable an efficient numerical treatment of the state-dependent derivative. In Part II of this thesis we elaborate further on various adjoint equations in the context of sensitivity analysis.

We observe that for each $x \in A(u)$ and $r > 0$, employing the approximated adjoint variable $q^{x,r}$ yields

$$
\begin{aligned}
D\mathscr{J}_\sigma^x(\Omega)(X) \approx & -\mathbf{B}[\partial u \partial X + (\partial X)^\top (\partial u)^\top] : \epsilon(u)(x) \\
& + \frac{1}{2}\int_\Omega \mathbf{A}[\partial u \partial X + \partial X^\top \partial u^\top] : \epsilon(q^{x,r})\, dx - \int_\Omega \operatorname{div}(X) \mathbf{A}\epsilon(u) : \epsilon(q^{x,r})\, dx \\
& + \frac{1}{2}\int_\Omega \mathbf{A}\epsilon(u) : [\partial q^{x,r} \partial X + \partial X^\top (\partial q^{x,r})^\top]\, dx \\
& + \int_\Omega \operatorname{div}(X) f \cdot q^{x,r}\, dx + \int_\Omega \partial f X \cdot q^{x,r}\, dx \\
& + \int_{\Gamma^N} (\operatorname{div}(X) - (\partial X n) \cdot n) g \cdot q^{x,r}\, dS + \int_{\Gamma^N} \partial g X \cdot q^{x,r}\, dS.
\end{aligned}
\tag{7.6}
$$

In the numerical scheme we realise the point evaluation on the right hand side of (7.6) in the same fashion utilising an averaging. Keeping minor notational conflicts in mind, we continue to use the notation $u_n := u_{\Omega_n}$ for the sake of brevity. With this, we introduce the steepest descend approach (Algorithm 1) that builds on the results of Section 5.

Remark 7.3. Note that there are various alternatives to tackle nonsmooth optimisation problems numerically. In this context we would like to mention subgradient methods, cutting plane methods and bundle methods, which rely on the set $\mathscr{L}$ (or a generalisation, c.f. [64, Section 6.6]) as well. For more details on this topic we refer to [64].

Remark 7.4. In order to identify the active set $A(u_n)$, we iterate over all mesh vertices and choose nodes that maximise the von Mises stress up to a given tolerance $\varepsilon > 0$. This tolerance captures the numerical error of the exact value due to the representation of floats in python. Hence, the active set $A(u_n)$ is finite in each iteration. Nonetheless, a high computational effort is possible, since we have to compute adjoint variables $q^{x,r}$ and gradients $\nabla \mathscr{J}_\sigma^x$ for each active point. This can necessitate to solve a large number of sub problems in each iteration. Fortunately, we observed in our algorithm that $A(u_n)$ is a singleton throughout the majority of iterations, which entails a feasible runtime.

Algorithm 1 Steepest descend algorithm - max-norm approach

Require: initial shape $\Omega_0 \subset \mathbf{R}^2$, $N_{max} \in \mathbf{N}$
  while $n \leq N_{max}$ **do**
    choose Hilbert space $\mathscr{H}_n = H^1_{\Gamma \cup \Gamma^N}(\Omega_n)^2$.
    check mesh quality and remesh if required.
    compute state u_n by solving state equation (2.4) on Ω_n.
    compute active set $A(u_n) = \{x_1, ..., x_k\}$
    compute adjoint states $q_n^{x_i,r}$ (7.5), $i \in \{1, ..., k\}$ on domain Ω_n with state u_n.
    compute gradients $\nabla \mathscr{J}_{\text{vol}}, \nabla \mathscr{J}_2^{x_i} \in \mathscr{H}_n$, for $x_i \in A(u_n)$.
    assemble $A \in \mathbf{R}^{k \times k}$ with $a_{ij} := (\gamma_1 \nabla \mathscr{J}_{\text{vol}} + \gamma_2 \nabla \mathscr{J}_\sigma^{x_i}, \gamma_1 \nabla \mathscr{J}_{\text{vol}} + \gamma_2 \nabla \mathscr{J}_\sigma^{x_j})_{\mathscr{H}_n}$ for $i, j \in \{1, \ldots, k\}$.
    solve $\min_{\alpha \in \mathbf{R}^k} A\alpha \cdot \alpha$ subject to $\sum_{i=1}^k \alpha_i = 1$.
    $Z_n := \sum_{i=1}^k \alpha_i v_i$, where $v_i = \gamma_1 \nabla \mathscr{J}_{\text{vol}} + \gamma_2 \nabla \mathscr{J}_\sigma^{x_i}$.
    descent direction $X_n := -Z_n$.
    choose step size $s_n > 0$.
    if $\mathscr{J}((\mathsf{Id} + s_n X_n)(\Omega_n)) > \mathscr{J}(\Omega_n)$ and no remeshing occurred in the previous step **then**
      remesh.
    else
      deform shape $\Omega_{n+1} := (\mathsf{Id} + s_n X_n)(\Omega_n)$.
    end if
    iterate $n+ = 1$.
  end while

7.2 *p*-norm approach

In order to validate our method we compare our results to the following p-norm approach, which includes a smooth regularisation of the stress term:

$$\mathscr{J}(\Omega) := \gamma_1 (|\Omega| - V)^2 + \gamma_2 \left(\int_\Omega |\sigma_M(u_\Omega)|^p \, dx \right)^{\frac{1}{p}}, \tag{7.7}$$

for $p \geq 2$. The shape derivative of $\mathscr{J}_p(\Omega) := \left(\int_\Omega |\sigma_M(u_\Omega)|^p \, dx\right)^{\frac{1}{p}}$, for $2 \leq p < \infty$ can be computed by various techniques as reported in [102]. We are omitting the proof here and only state the derivative. For

$X \in C^1(\bar{\mathsf{D}})^d$ with $\mathrm{supp}(X) \subset (\mathsf{D} \setminus \bar{\omega})$ we have

$$\begin{aligned} D\mathscr{J}_p(\Omega)(X) =& c_\Omega \int_\Omega \mathrm{div}(X)|\sigma_M(u_\Omega)|^p \, dx + \int_\Omega \mathrm{div}(X) f \cdot q \, dx + \int_\Omega \partial f X \cdot q \, dx \\ & - c_\Omega \frac{p}{2} (\mathbf{B}\epsilon(u) : \epsilon(u))^{\frac{p}{2}-1} \mathbf{B}[\partial u \partial X + (\partial X)^\top (\partial u)^\top] : \epsilon(u) \, dx \\ & + \frac{1}{2} \int_\Omega \mathbf{A}[\partial u \partial X + \partial X^\top \partial u^\top] : \epsilon(q) \, dx - \int_\Omega \mathrm{div}(X) \mathbf{A}\epsilon(u) : \epsilon(q) \, dx \\ & + \frac{1}{2} \int_\Omega \mathbf{A}\epsilon(u) : [\partial q \partial X + \partial X^\top (\partial q)^\top] \, dx \\ & + \int_{\Gamma^N} (\mathrm{div}(X) - (\partial X n) \cdot n) g \cdot q \, dS + \int_{\Gamma^N} \partial g X \cdot q \, dS, \end{aligned} \tag{7.8}$$

where $c_\Omega = \frac{1}{p} \left(\int_\Omega |\sigma_M(u_\Omega)|^p \, dx \right)^{\frac{1-p}{p}}$ and $q \in H^1_\Gamma(\Omega)^d$ solves

$$\int_\Omega \mathbf{A}\epsilon(\varphi) : \epsilon(q) \, dx = c_\Omega p \, (\mathbf{B}\epsilon(u) : \epsilon(u))^{\frac{p}{2}-1} \mathbf{B}\epsilon(u) : \epsilon(\varphi) \, dx \quad \text{for all } \varphi \in H^1_\Gamma(\Omega)^d. \tag{7.9}$$

Remark 7.5. Note that the previous result incorporates the adjoint variable q. In contrast to the nonsmooth approach, the adjoint equation associated with the regularised cost functional $\mathscr{J}_p$ is well-defined and does not require additional treatment. Furthermore, we want to mention that the functional $\mathscr{J}_p$ approximates the maximal von Mises stress. Contrary, $\mathscr{J}_\sigma$ captures the squared von Mises stress. Nonetheless, we are able to compare these methods, since both lead to a decrease of the von Mises stress. Additionally, we would like to point out that we omitted the stress threshold δ in the regularised approach. This is reasonable, since we are going to address the special case $\delta = 0$ in our numerical examples.

Algorithm 2 Basic gradient algorithm - p-norm approach

Require: initial shape $\Omega_0 \subset \mathbf{R}^2$, $N_{max} \in \mathbf{N}$
- **while** $n \le N_{max}$ **do**
  - choose Hilbert space $\mathscr{H}_n = H^1_{\Gamma \cup \Gamma^N}(\Omega_n)^2$.
  - check mesh quality and remesh if required.
  - compute state u_n by solving state equation (2.4) on Ω_n.
  - compute adjoint state q_n by solving adjoint state equation (7.9) on Ω_n with state u_n.
  - compute gradients $\nabla \mathscr{J}_{\mathrm{vol}}, \nabla \mathscr{J}_p \in \mathscr{H}_n$.
  - descent direction $X_n := -\left(\gamma_1 \nabla \mathscr{J}_{\mathrm{vol}} + \gamma_2 \nabla \mathscr{J}_p\right)$.
  - choose step size $s_n > 0$.
  - **if** $\mathscr{J}((\mathsf{Id} + s_n X_n)(\Omega_n)) > \mathscr{J}(\Omega_n)$ and no remeshing occurred in the previous step **then**
    - remesh.
  - **else**
    - deform shape $\Omega_{n+1} := (\mathsf{Id} + s_n X_n)(\Omega_n)$.
  - **end if**
  - iterate $n+ = 1$.
- **end while**

7.3 Numerical results

We implemented both algorithms in the software NGSolve [96]. In order to achieve comparable results, we normalised the respective stress gradients in each iteration and moved a fixed step size. Throughout our numerical experiments we chose the material parameter as follows: the Poisson ratio $\nu = 0.3$ and the Young modulus $E = 1$. These in turn yield the Lamé coefficients

$$\lambda = \frac{\nu E}{(1+\nu)(1-2\nu)}, \qquad \mu = \frac{E}{2(1+\nu)}. \tag{7.10}$$

Additionally we consider the absence of a volume force, i.e. $f \equiv 0$, which allows a simplified representation of the involved terms and neglect the stress threshold, i.e. $\delta = 0$.

7.3.1 L-bracket

For the first example we considered the L-bracket problem. Here, the initial set is given as

$$\Omega = (0,100) \times (0,100) \setminus [40,100] \times [40,100]. \tag{7.11}$$

The bracket is fixed on the upper part of the boundary $\Gamma = [0,40] \times \{100\}$ and the boundary force $g = (0,-3)^\top$ is applied at the corner of the rightmost boundary part, i.e.

$$\Gamma^N = \{100\} \times [35,40] \cup [95,100] \times \{40\}. \tag{7.12}$$

Furthermore, the target volume was fixed as 70% of the initial volume. The setting is depicted in Figure 2. The remaining unknowns were chosen as follows: $p = 6$, $\gamma_1 = 10^{-4}$, $\gamma_2 = 1$, $\rho_{\text{low}} = 10^{-2}$, $r = 100$, the initial mesh size $h = 5$ and finite elements of order 3.

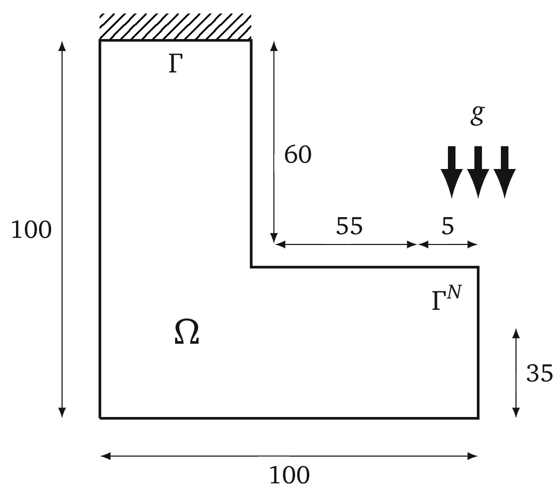

Figure 2: Visualisation of the L-bracket [26].

The resulting deformations of the shape are visualised in Figure 3 and the corresponding evolution of the cost functionals is given in Figure 4.

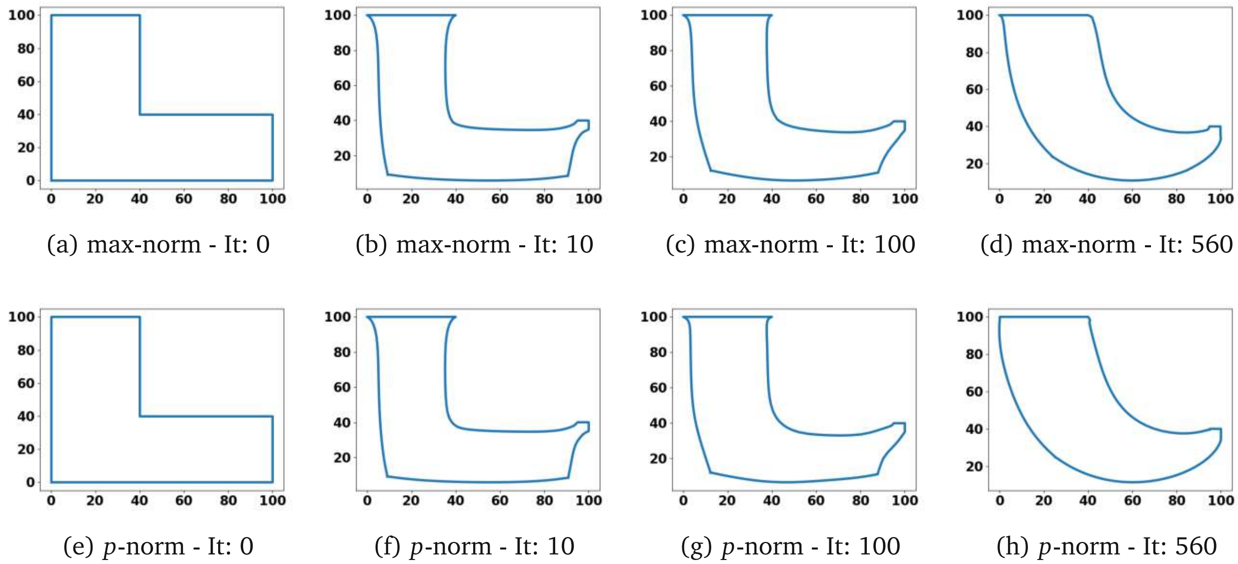

(a) max-norm - It: 0 (b) max-norm - It: 10 (c) max-norm - It: 100 (d) max-norm - It: 560

(e) p-norm - It: 0 (f) p-norm - It: 10 (g) p-norm - It: 100 (h) p-norm - It: 560

Figure 3: Deformation of the L-bracket [26].

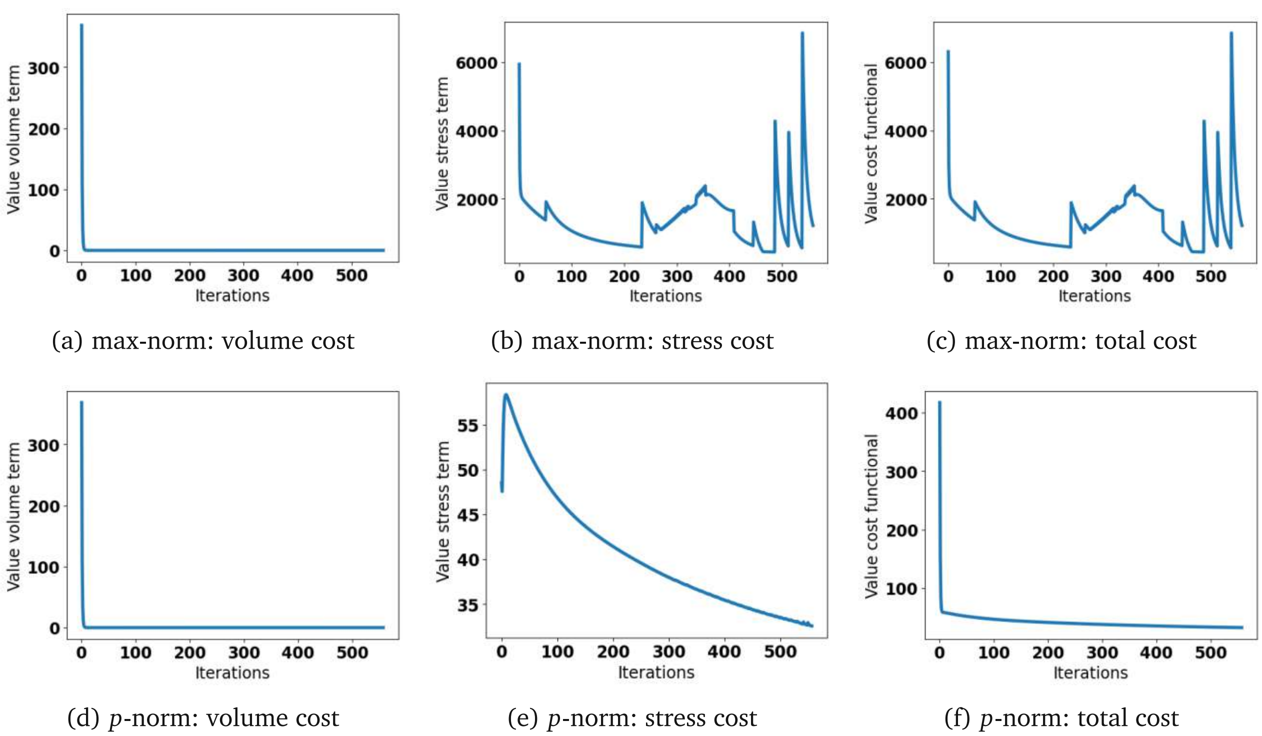

(a) max-norm: volume cost (b) max-norm: stress cost (c) max-norm: total cost

(d) p-norm: volume cost (e) p-norm: stress cost (f) p-norm: total cost

Figure 4: Cost evolution for the L-bracket problem [26].

To compare both methods in terms of the pointwise stress optimisation, we deduced the minimal mesh sizes $h^{\min}_{p\text{-norm}}$, $h^{\min}_{\text{max-norm}}$ of both algorithms after a given number of iterations. We then chose the minimum $h^{\min} = \min\{h^{\min}_{p\text{-norm}}, h^{\min}_{\text{max-norm}}\}$ and remeshed both final shapes with the minimal mesh size $h^{\min}$. Finally, we solved the PDE on both domains and compared the resulting maximum von Mises stress. This uniform mesh size is necessary, since the maximum stress highly depends on the underlying mesh size. The results for some iterations are listed in Table 1.

	max-norm approach	p-norm approach
10 iterations	1258	1466
30 iterations	691	771
50 iterations	464	615
100 iterations	384	391
140 iterations	262	330

Table 1: Comparison of the maximal von Mises stress σ_M^2 [26].

Comparing the final results (Figure 3d, Figure 3h) we observe that visually both algorithms yield similar results. These in fact coincide with the results obtained in [92], where the p-norm problem formulation was investigated with a different numerical approach. While both approaches approximate the target volume within a few iterations (Figure 4a, Figure 4d), the stress-cost evolves differently. In the p-norm approach, the value of the stress functional shows a steady decrease until the deformation causes some minor artificial fluctuations towards the end (see Figure 4e). In contrast, the maximum stress curve in the max-norm approach (see Figure 4b) shows a number of peaks. These are linked to the occurrence of remeshes, as the refined mesh yields higher stress values. Finally, Table 1 shows that both algorithms yield a decrease of the maximal von Mises stress, yet the max-norm approach seems to perform slightly better in this regard.

7.3.2 Bridge

For the second example we consider a bridge with vertical load placed in the center of the upper boundary. To be precise, the initial set is given as

$$\Omega = (0,5) \times (0,5) \setminus [1,4] \times [0,2]. \tag{7.13}$$

The bridge is fixed at the bottom boundary $\Gamma = ([0,1] \times \{0\}) \cup ([4,5] \times \{0\})$ and the force $g = (0,-3)^\top$ is applied on $\Gamma^N = [2,3] \times \{5\}$. Again, the target volume was fixed as 70% of the initial volume. A schematic of the setting can be seen in Figure 5. For this example we chose the regularisation $p = 2$. Furthermore, the remaining parameter were set $\gamma_1 = 10^{-2}$, $\gamma_2 = 1$, $\rho_{\text{low}} = 10$, $r = 7.5$, the initial meshsize $h = 0.5$ and finite elements of order 3.

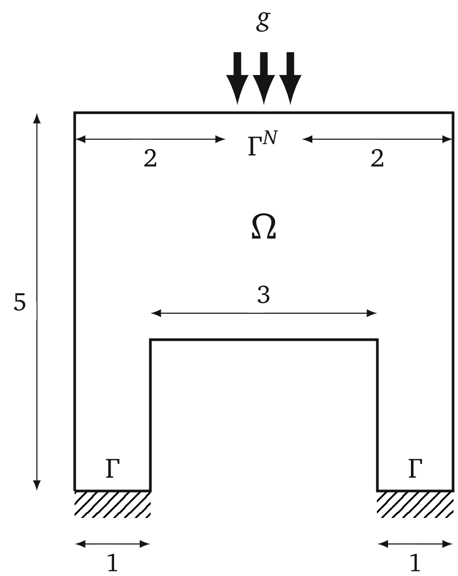

Figure 5: Visualisation of the bridge [26].

The resulting deformations of the shape are visualised in Figure 6 and the corresponding evolution of the cost functionals is given in Figure 7.

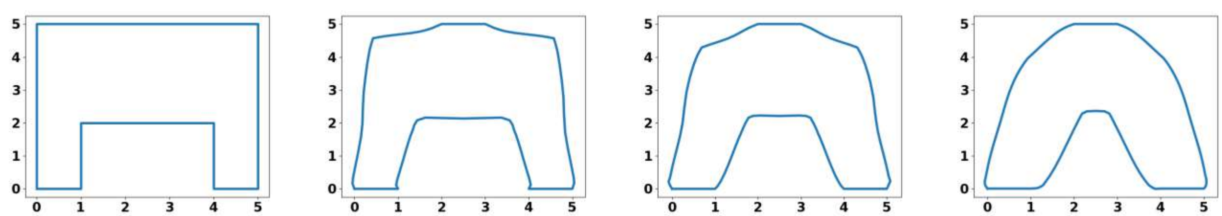

(a) max-norm - It: 0 (b) max-norm - It: 20 (c) max-norm - It: 40 (d) max-norm - It: 80

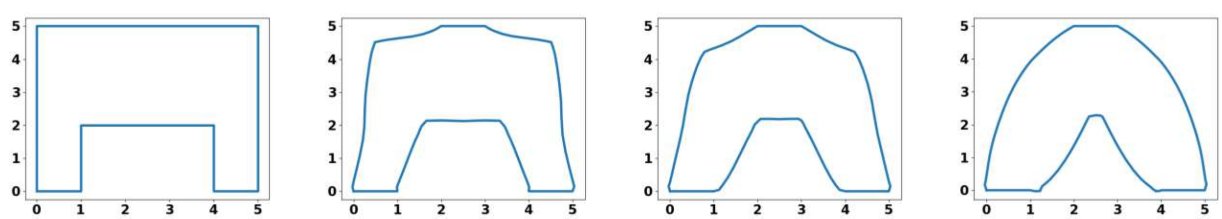

(e) p-norm - It: 0 (f) p-norm - It: 20 (g) p-norm - It: 40 (h) p-norm - It: 80

Figure 6: Deformation of the bridge [26].

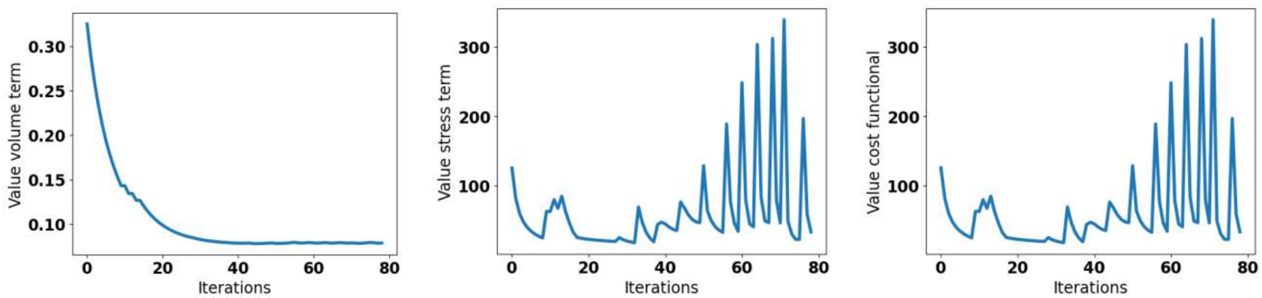

(a) max-norm: volume cost (b) max-norm: stress cost (c) max-norm: total cost

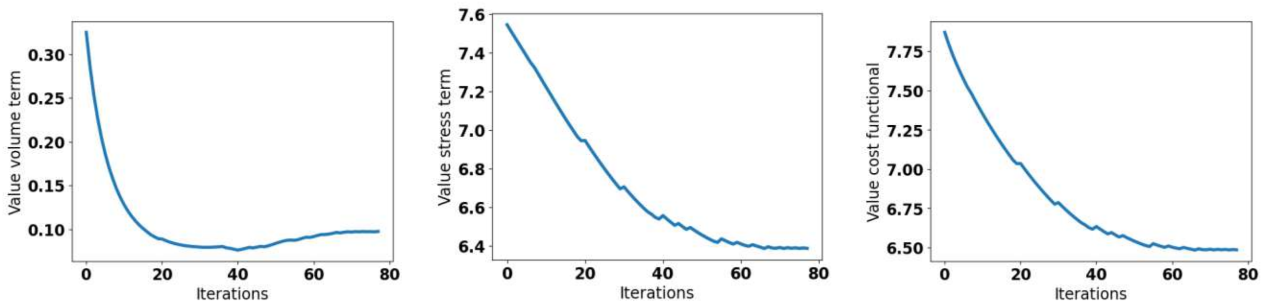

(d) p-norm: volume cost (e) p-norm: stress cost (f) p-norm: total cost

Figure 7: Cost evolution for the bridge problem [26].

Again, we solved the PDE on the deformed domains after a fixed number of iterations with the identical mesh size $h^{\min} = \min\{h^{\min}_{p\text{-norm}}, h^{\min}_{\text{max-norm}}\}$ and computed the maximal von Mises stress. The results for some iterations are listed in Table 2.

	max-norm approach	p-norm approach
10 iterations	92	86
20 iterations	52	76
40 iterations	214	593
80 iterations	964	1417

Table 2: Comparison of the maximal von Mises stress σ_M^2 [26].

In this example we are able to observe different behaviours of our approaches. While the p-norm approach yields a steady decline of the stress cost (Figure 7e), the max-norm cost functional is vulnerable to remeshes and thus the associated curve shows some peaks (Figure 7b). Furthermore, we observe that the volume cost in the max-norm approach is monotone decreasing until it reaches a steady behaviour at approximately 40 iterations (Figure 7a). Contrary, the p-norm approach shows a slightly faster decrease of the volume cost during the first few iterations (Figure 7d). Yet, the minimisation of the stress functional causes a minor increase of the volume cost. This can also be seen in the final shapes (Figure 6h, Figure 6d), where the p-norm approach yields slightly wider bridge piers. Furthermore, the corners of the Dirichlet boundaries, i.e. the corners of the lower part of the bridge piers, attain a smoother appearance in the max-norm approach. This is also reflected by the last entry of Table 2, which shows a decrease of the maximal von Mises stress of 32%. In addition the averaging parameter p had to be reduced compared to the previous example, since the p-norm approach did not manage to smoothen the interior corners for larger p.

7.3.3 L-bracket with hole

For the third example we considered the L-bracket problem from the first example with an additional square shaped hole. Hence, the initial set is given as

$$\Omega = (0,100) \times (0,100) \setminus \big([40,100] \times [40,100] \cup [15,25] \times [70,80]\big). \tag{7.14}$$

The bracket is fixed on the upper part of the boundary $\Gamma = [0,40] \times \{100\}$ and the boundary force $g = (0,-3)^\top$ is applied at the corner of the rightmost boundary part, i.e.

$$\Gamma^N = \{100\} \times [35,40] \cup [95,100] \times \{40\}. \tag{7.15}$$

Again, the target volume was fixed as 70% of the initial volume. The setting is depicted in Figure 8. The remaining unknowns were chosen as follows: $p = 4$, $\gamma_1 = 10^{-4}$, $\gamma_2 = 1$, $\rho_{\text{low}} = 10^{-2}$, $r = 100$, the initial mesh size $h = 5$ and finite elements of order 3.

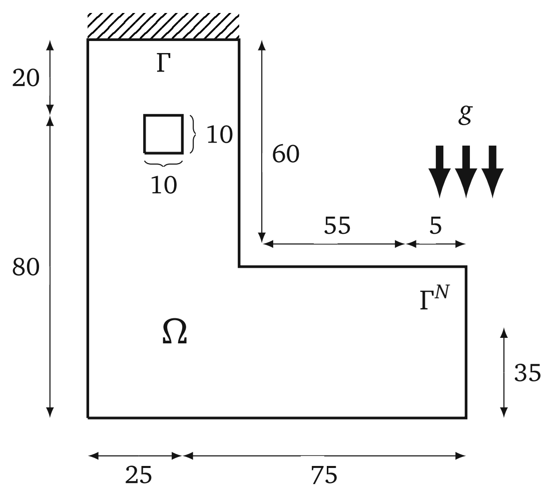

Figure 8: Visualisation of the L-bracket with hole.

The resulting deformations of the shape are visualised in Figure 9 and the corresponding evolution of the cost functionals is given in Figure 10.

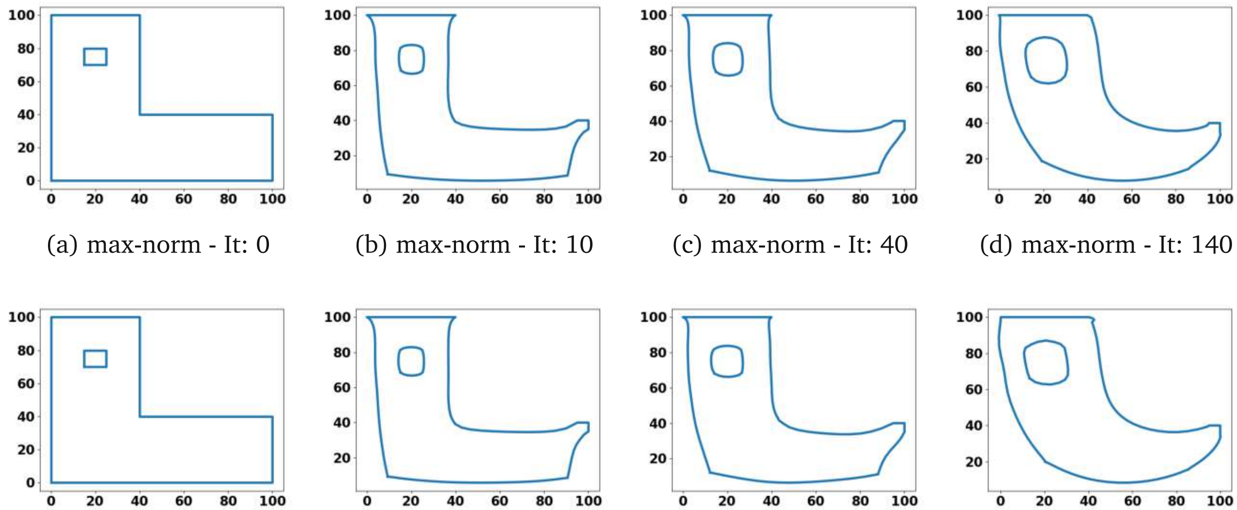

(a) max-norm - It: 0 (b) max-norm - It: 10 (c) max-norm - It: 40 (d) max-norm - It: 140

(e) p-norm - It: 0 (f) p-norm - It: 10 (g) p-norm - It: 40 (h) p-norm - It: 140

Figure 9: Deformation of the L-bracket with hole.

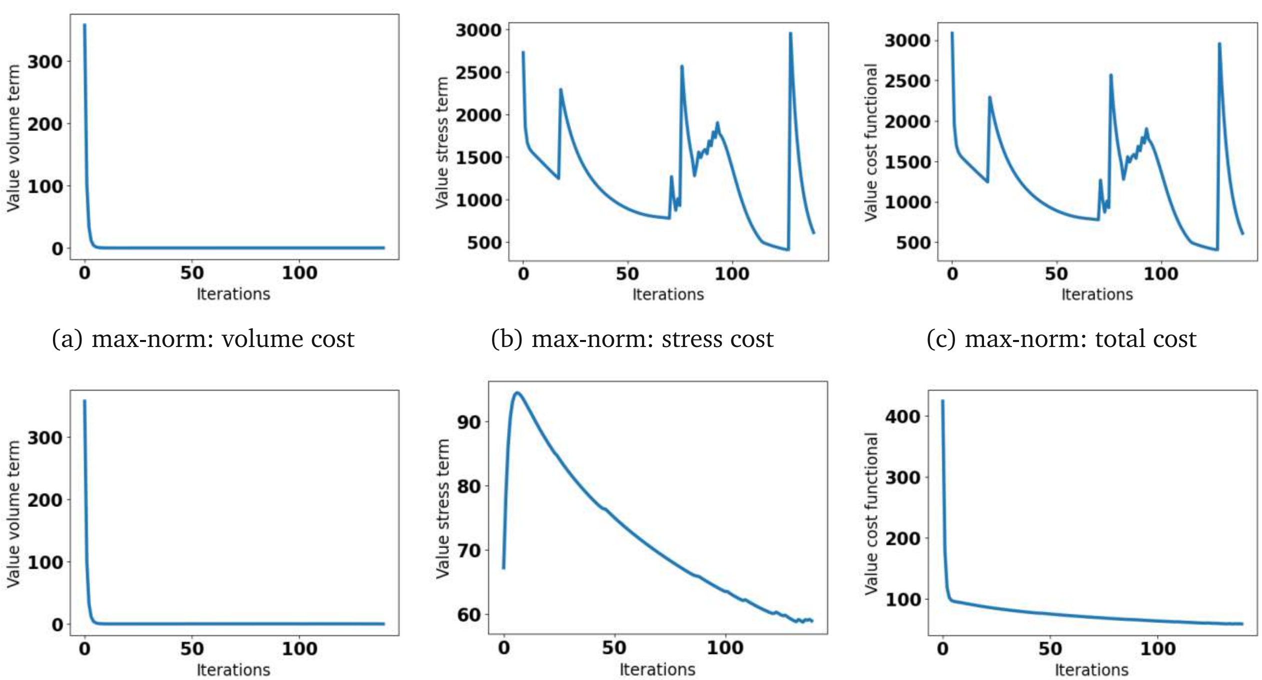

(a) max-norm: volume cost (b) max-norm: stress cost (c) max-norm: total cost

(d) p-norm: volume cost (e) p-norm: stress cost (f) p-norm: total cost

Figure 10: Cost evolution for the L-bracket with hole problem.

Similarly to the first two examples, we solved the PDE on the deformed domains after a fixed number of iterations with the identical mesh size $h^{\min} = \min\{h^{\min}_{p\text{-norm}}, h^{\min}_{\text{max-norm}}\}$ and computed the maximal von Mises stress. The results for some iterations are listed in Table 3.

	max-norm approach	p-norm approach
10 iterations	697	753
40 iterations	397	332
100 iterations	3839	4799
140 iterations	8064	33952

Table 3: Comparison of the maximal von Mises stress σ_M^2.

At a first glimpse, the deformations obtained during this experiment resemble the ones obtained in the first exercise. That is, both methods deform the outer boundary of the L-bracket into a smooth hook-like shape. Additionally, the interior sharp corners of the hole are smoothened during this deformation. In fact, the max-norm approach seems to slightly outperform the p-norm approach in this context, since the hole in Figure 9d has a smoother and more symmetric appearance compared to Figure 9h. Furthermore, we observe that the p-norm approach introduces an artificial wave-like structure of the boundary in the vicinity of the top-right corner, which causes higher stresses. This problem does not occur during the max-norm approach. This also reflects in the direct comparison of the von Mises stress values in Table 3, where the maximal stress of the p-norm approach increases significantly towards the last iterations.
The cost functionals in turn show the typical, previously described behaviour. While the target volume is attained after the first few steps in both approaches likewise (see Figure 10a, Figure 10d), the stress terms behave differently. The stress functional of the p-norm approach shows a steady decline until some minor fluctuations occur towards the end (see Figure 10e). In contrast, the stress functional of the max-norm approach is characterised by some intermediate peaks (see Figure 10b). These are a consequence of the lack of stability with respect to remeshes.

8 Conclusion and outlook

In this part of the thesis we investigated the shape sensitivity of a nonsmooth objective functional in the framework of linear elasticity. We computed the first order term and put the object into the context of Clarke subgradients. Lending tools from nonsmooth analysis, we further derived optimality conditions as well as steepest descend directions. These gave rise to a nonsmooth methodology to address the minimisation of peak stresses. Our numerical implementations suggest that the nonsmooth approach entails a faster minimisation of the maximal von Mises stress compared to the regularised p-norm approach. This heavily relied on the fact that for our model problems, the active set was small. Otherwise high computational efforts are to be expected.
For future research it would be interesting to study the adjoint variable corresponding to the low regularity functional $\mathscr{J}_\sigma^x$, $x \in A(u)$ on an analytic level as well as in the numerical setting. Whilst very-weak solutions could entail an appropriate adjoint formulation corresponding to the problematic point evaluation of the gradient, an efficient numerical treatment of these is not known yet.

Part II

Adjoint based methods to compute topological derivatives

The content of this part stems from the article:

[25] P. Baumann and K. Sturm. Adjoint based methods for the computation of higher order topological derivatives with an application to linear elasticity. *Engineering Computations*, 39(1), 2021.

9 Introduction to adjoint based topological sensitivity analysis

In this part of the thesis we are going to dive into the framework of topology optimisation employing the notion of topological derivatives. The main idea of the topological derivative is to introduce a singular perturbation to the design variable and study the sensitivity of the shape functional with respect to the size of the perturbation. Thus, the topological derivative encodes information about the optimal topology of the design variable. This information can be used in a numerical scheme via one-shot type methods [70, 99] or to guide the evolution of a level-set function in an iterative process [17].
A large variety of design optimisation problems stemming from applications can be classified as state constrained optimisation problems, where the state variable is governed by a partial differential equation. It is well known from shape optimisation and optimal control (see e.g. [73, 76]) that adjoint variables constitute an efficient approach to the numerical treatment of these problems. In fact, for the special case when the governing PDEs are linear and the inclusions are ball-shaped, the first order topological derivative can be expressed solely in terms of the state and adjoint state variable [99]. Higher order topological derivatives usually require additional corrector terms, solutions to exterior partial differential equations. Even though in general these correctors give rise to numerical expenses, in some cases they can be explicitly computed [70]. Aside from the numerical advantages, adjoint variables have been proven to be an useful tool to compute the topological derivative for state constraint design optimisation problems.
One well established method in this context is the method of Amstutz [12]. It is based on the sensitivity analysis of an adjoint state that only depends on the unperturbed state variable. This method has been proven versatile and thus found application in various works such as [13, 14, 68, 79] to only mention a few. It is advantageous over the direct computation of the topological derivative via a Taylors' expansion as it simplifies the analysis significantly.
Another adjoint based method to compute topological derivatives we want to highlight relies on the averaged adjoint state [101]. In contrast to Amstutz' approach, the adjoint variable in this setting additionally depends on the perturbed state variable. This entails some difficulties towards the study of the asymptotics for the adjoint state and thus results in a more challenging analysis. Yet, once the asymptotic expansion of the averaged adjoint state is known, the computation of the topological derivative is straight forward and can easily be extended to compute higher order topological derivatives. For applications of the averaged adjoint approach we refer to [58, 105].
A third method we want to mention in this context was introduced in [41]. Contrary to the previous approaches, this method only depends on the unperturbed adjoint state and therefore does not necessitate a sensitivity analysis of the adjoint state variable. This results in a faster computation of the topological derivative, but unfortunately seems to come with the shortcoming that this method is not applicable to specific cost functionals [58].
In the following we study a model problem in the framework of linear elasticity, where we consider perturbations of the material coefficients as well as perturbations of the applied volume forces. We apply these three adjoint based methods to compute the first and second order topological derivative for a versatile cost functional and compare them in view of applicability and efficiency.
Before we introduce the problem formulation we would like to mention that the computation of topological derivatives for state constrained design optimisation problems does not solely rely on the introduction of adjoint variables. In [85] the authors used the singular limit of a shape derivative to compute the topological derivative. Even though this method is not always applicable, it provides an efficient scheme to compute even higher order topological derivatives [97].

In this part of the thesis our focus lies on the differences between adjoint based methods to perform sensitivity analysis and to compute the topological derivative. We thoroughly study and review the first three methods mentioned and apply them to the model problem of linear elasticity. We first exam the asymptotic behaviour of the underlying state variable up to order two and then study the asymptotic behaviour of Amstutz' perturbed adjoint variable and the averaged adjoint variable. We then employ the three methods to compute first and second order topological derivatives for three types of cost functions, the compliance, a boundary tracking-type cost function and a tracking-type cost function of the gradient. The content of this part stems from the article [25] in collaboration with Kevin Sturm.
Before we introduce the concrete setting for our model problem, we specify the notion of "topological derivative" (cf. Section 1.2) in the following definition. Note that this quantity plays a central role in the remainder of this thesis.

Definition 9.1. Let $\mathsf{D} \subset \mathbf{R}^d$ be a bounded, smooth domain and $\Omega \subset \mathsf{D}$ open and Lipschitz. Furthermore, let $\omega \subset \mathbf{R}^d$ be an open, bounded and connected set with C^1 boundary containing the origin. We define for $x_0 \in \mathsf{D} \setminus \partial\Omega$ and $\varepsilon > 0$ sufficiently small the perturbed set

$$\Omega_\varepsilon := \begin{cases} \Omega \setminus \omega_\varepsilon & \text{if } x_0 \in \Omega, \\ \Omega \cup \omega_\varepsilon & \text{else,} \end{cases} \tag{9.1}$$

where $\omega_\varepsilon := \{x_0 + \varepsilon z \,|\, z \in \omega\}$. Furthermore, consider a shape functional

$$\mathscr{J} : \mathscr{U}_{ad} \to \mathbf{R}, \tag{9.2}$$

where $\mathscr{U}_{ad}$, a subset of the powerset of D, denotes the admissible shapes. With the assumption that $\Omega \in \mathscr{U}_{ad}$ and $\Omega_\varepsilon \in \mathscr{U}_{ad}$ for $\varepsilon > 0$ sufficiently small we define the first order topological derivative of $\mathscr{J}$ at x_0 as

$$d\mathscr{J}(\Omega,\omega)(x_0) := \lim_{\varepsilon \searrow 0} \frac{\mathscr{J}(\Omega_\varepsilon) - \mathscr{J}(\Omega)}{\ell_1(\varepsilon)}, \tag{9.3}$$

where $\ell_1 : \mathbf{R}^+ \to \mathbf{R}^+$ is a continuous function vanishing at 0. Furthermore, given a sequence of continuous functions $\ell_k : \mathbf{R}^+ \to \mathbf{R}^+$, $k \geq 1$ vanishing at 0 such that

$$\lim_{\varepsilon \searrow 0} \frac{\ell_{k+1}(\varepsilon)}{\ell_k(\varepsilon)} = 0 \quad \text{for } k \geq 1, \tag{9.4}$$

we define the n—th order topological derivative for $n \geq 2$ iteratively by

$$d^n\mathscr{J}(\Omega,\omega)(x_0) := \lim_{\varepsilon \searrow 0} \frac{\mathscr{J}(\Omega_\varepsilon) - \mathscr{J}(\Omega) - \sum_{k=1}^{n-1} \ell_k(\varepsilon) d^k \mathscr{J}(\Omega,\omega)(x_0)}{\ell_n(\varepsilon)}. \tag{9.5}$$

Remark 9.2. Note that the topological derivative depends on a large variety of parameters. In the context of directional derivatives, Ω and x_0 can bee seen as the evaluation point, while the inclusion shape ω resembles a given direction. Yet, we avoid the use of a semicolon to emphasise that the topological derivative is no directional derivative according to Definition 6.3. Furthermore, we would like to highlight the dependence on the sequences ℓ_k. Even though this dependence is not directly visible in the notation of the topological derivative, it is of great importance nonetheless, as it gives rise to the question "when a topological derivative vanishes". To specify, one could always introduce a "slower" decreasing function ℓ to a given formulation leading to a vanishing topological derivative.

Problem formulation

Let $\mathsf{D} \subset \mathbf{R}^d$, $d \in \{2,3\}$ be a bounded and smooth domain. Our goal is to compute the topological derivative of the cost functional

$$\mathscr{J}(\Omega) = \gamma_f \int_{\mathsf{D}} f_\Omega \cdot u_\Omega \, dx + \gamma_g \int_{\mathsf{D}} |\partial u_\Omega - \partial u_d|^2 \, dx + \gamma_m \int_{\Gamma^m} |u_\Omega - u_m|^2 \, dS, \tag{9.6}$$

where $\gamma_f, \gamma_g, \gamma_m \in \mathbf{R}$, $u_d \in H^1(\mathsf{D})^d$, $u_m \in L_2(\Gamma^m)^d$ subject to a design region $\Omega \subset \mathsf{D}$. Here, the displacement field $u_\Omega \in H^1(\mathsf{D})^d$ solves the equation of linear elasticity (cf. (2.4))

$$\int_{\mathsf{D}} \mathbf{A}_\Omega \epsilon(u_\Omega) : \epsilon(\varphi) \, dx = \int_{\mathsf{D}} f_\Omega \cdot \varphi \, dx + \int_{\Gamma^N} g_N \cdot \varphi \, dS \quad \text{for all } \varphi \in H^1_\Gamma(\mathsf{D})^d, \tag{9.7}$$

$$u_\Omega = g_D \quad \text{on } \Gamma. \tag{9.8}$$

where $\Gamma \subset \partial\mathsf{D}$, $|\Gamma| > 0$, $\Gamma_N := \partial\mathsf{D} \setminus \Gamma$, $H^1_\Gamma(\mathsf{D})^d := \{\varphi \in H^1(\mathsf{D})^d : \varphi = 0 \text{ on } \Gamma\}$, $g_D \in L_2(\Gamma)^d$, $g_N \in L_2(\Gamma^N)^d$ and

$$\mathbf{A}_\Omega = \mathbf{A}_1 \chi_\Omega + \mathbf{A}_2 \chi_{\mathsf{D}\setminus\overline{\Omega}}, \quad f_\Omega = f_1 \chi_\Omega + f_2 \chi_{\mathsf{D}\setminus\overline{\Omega}}. \tag{9.9}$$

Here, $\chi_\Omega, \chi_{\mathsf{D}\setminus\overline{\Omega}}$ denote characteristic functions on their respective sets, $\mathbf{A}_1, \mathbf{A}_2 : \mathbf{R}^{d\times d} \to \mathbf{R}^{d\times d}$ are symmetric stress tensors given in terms of characteristic material parameters (cf. Lamé coefficients in (2.6)), $f_1, f_2 \in H^1(\mathsf{D})^d \cap C^2(B_\delta(x_0))^d$ for a given $\delta > 0$ and $\epsilon(u)$ denotes the symmetrised gradient of u, that is, $\epsilon(u) = \frac{1}{2}(\partial u + \partial u^\top)$.

Remark 9.3. In some parts of this work we require the assumption $\gamma_g = 0$ in dimension $d = 2$. We will elaborate further on this detail in the course of this work.

In contrast to the model problem in Part I we assume that the whole domain D is filled with two different materials as well as two different volume forces acting on these, respectively. We are thus interested in the optimal distribution of these materials within the hold-all domain D in terms of the versatile objective functional (9.6). In what follows, we are only going to discuss the topological derivative of a singularly perturbed domain by adding material 1 and force 1, respectively. That is, we are interested in perturbations $\Omega_\varepsilon = \Omega \cup \omega_\varepsilon$ with $\omega_\varepsilon \subset \bar{\Omega}^c$ (cf. Definition 9.1). The remaining case $\Omega_\varepsilon = \Omega \setminus \omega_\varepsilon$, $\omega_\varepsilon \subset \Omega$ can be treated identically and merely leads to a change of sign in the final formula. Additionally, for the sake of simplicity, we are going to restrict ourselves to the special case $\Omega = \emptyset$. The general setting can be treated in a similar fashion and we will highlight the passages in the upcoming sensitivity analysis, where special care has to be taken in this case.

10 Lagrangian techniques to compute the topological derivative

Before we dive into the sensitivity analysis, we want to give an overview of the three methods mentioned in the introduction. We therefore reformulate these approaches in a general Lagrangian setting. While it is well-established in optimisation algorithms to compute derivatives of PDE constrained problems with the help of Lagrangians, it seems rather new to the topology optimisation community.

10.1 Abstract setting

Let $\mathscr{X}$ be a real Hilbert space, $\mathscr{W} \subset \mathscr{X}$ a subspace and $\bar{u} \in \mathscr{X}$ a fixed element. We further define the affine space $\mathscr{V} := \bar{u} + \mathscr{W}$. For all parameter $\varepsilon \geq 0$ small consider a function $u_\varepsilon \in \mathscr{V}$ solving the variational problem of the form

$$a_\varepsilon(u_\varepsilon, v) = f_\varepsilon(v) \quad \text{for all } v \in \mathscr{W}, \tag{10.1}$$

where a_ε is a bilinear form on $\mathscr{X} \times \mathscr{W}$ and f_ε is a linear form on $\mathscr{W}$, respectively. Throughout we assume that this abstract state equation admits a unique solution $u_\varepsilon \in \mathscr{V}$ for all $\varepsilon \geq 0$. Consider now a cost function

$$j(\varepsilon) = J_\varepsilon(u_\varepsilon), \tag{10.2}$$

where for all $\varepsilon \geq 0$ the functional $J_\varepsilon : \mathscr{V} \to \mathbf{R}$ is differentiable at u_0. In the following sections we review methods how to obtain an asymptotic expansion of $j(\varepsilon)$ at $\varepsilon = 0$. For this purpose we introduce the Lagrangian function

$$\mathscr{L}(\varepsilon, u, v) = J_\varepsilon(u) + a_\varepsilon(u, v) - f_\varepsilon(v) \quad \text{for all } u \in \mathscr{V},\ v \in \mathscr{W}. \tag{10.3}$$

We observe that we can indeed use this Lagrangian to express the quantity of interest

$$j(\varepsilon) = \mathscr{L}(\varepsilon, u_\varepsilon, v) \quad \text{for all } v \in \mathscr{W}. \tag{10.4}$$

Additionally, we would like to mention that the rather uncommon choice of $\mathscr{V}$ as an affine space is a direct consequence of our problem formulation. To specify, the inhomogeneous Dirichlet boundary condition (9.8) necessitates the use of an affine space instead of a Hilbert space.

10.2 Amstutz' method

We first review the approach of Amstutz [12] (cf. [13, Proposition 2.1]). This approach has been applied to various problems and thus has been proven to be a versatile method. For instance in [13] a linear transmission problem was examined and its first order topological derivative was computed. In [21] the topological derivative of elliptic differential equations including a differential operator of order $2m$ was derived. In [14] the topological derivative for a class of certain nonlinear equations has been studied. The following proposition states the central result of Amstutz' method:

Proposition 10.1 ([13, Proposition 2.1]). Assume the following hypotheses hold.

(1) There exist numbers $\delta a^{(1)}$ and $\delta f^{(1)}$ and a function $\ell_1 : \mathbf{R}^+ \to \mathbf{R}^+$ with $\lim_{\varepsilon \searrow 0} \ell_1(\varepsilon) = 0$, such that

$$(a_\varepsilon - a_0)(u_0, p_\varepsilon) = \ell_1(\varepsilon)\delta a^{(1)} + o(\ell_1(\varepsilon)), \tag{10.5}$$
$$(f_\varepsilon - f_0)(p_\varepsilon) = \ell_1(\varepsilon)\delta f^{(1)} + o(\ell_1(\varepsilon)), \tag{10.6}$$

where $p_\varepsilon \in \mathscr{W}$ is the adjoint state satisfying

$$a_\varepsilon(\varphi, p_\varepsilon) = -\partial J_\varepsilon(u_0)(\varphi) \quad \text{for all } \varphi \in \mathscr{V}. \tag{10.7}$$

(2) There exist two numbers $\delta J_1^{(1)}$ and $\delta J_2^{(1)}$, such that

$$J_\varepsilon(u_\varepsilon) = J_\varepsilon(u_0) + \partial J_\varepsilon(u_0)(u_\varepsilon - u_0) + \ell_1(\varepsilon)\delta J_1^{(1)} + o(\ell_1(\varepsilon)), \tag{10.8}$$

$$J_\varepsilon(u_0) = J_0(u_0) + \ell_1(\varepsilon)\delta J_2^{(1)} + o(\ell_1(\varepsilon)). \tag{10.9}$$

Then the following expansion holds

$$j(\varepsilon) = j(0) + \ell_1(\varepsilon)(\delta a - \delta f^{(1)} + \delta J_1^{(1)} + \delta J_2^{(1)}) + o(\ell_1(\varepsilon)). \tag{10.10}$$

Next, we reformulate and generalise the previous result in terms of a Lagrangian function $\mathscr{L}(\varepsilon, u, v)$. Additionally, we state an analogous extension addressing the second order derivative.

Proposition 10.2. Let $\ell_1, \ell_2 : \mathbf{R}^+ \to \mathbf{R}^+$ be functions with

$$\lim_{\varepsilon \searrow 0} \ell_1(\varepsilon) = 0, \quad \text{and} \quad \lim_{\varepsilon \searrow 0} \frac{\ell_2(\varepsilon)}{\ell_1(\varepsilon)} = 0. \tag{10.11}$$

(i) Assume that the limits

$$\mathscr{R}^{(1)}(u_0, p_0) := \lim_{\varepsilon \searrow 0} \frac{\mathscr{L}(\varepsilon, u_\varepsilon, p_\varepsilon) - \mathscr{L}(\varepsilon, u_0, p_\varepsilon)}{\ell_1(\varepsilon)}, \tag{10.12}$$

$$\partial_\ell^{(1)} \mathscr{L}(0, u_0, p_0) := \lim_{\varepsilon \searrow 0} \frac{\mathscr{L}(\varepsilon, u_0, p_\varepsilon) - \mathscr{L}(0, u_0, p_\varepsilon)}{\ell_1(\varepsilon)}, \tag{10.13}$$

exist. Then we have the following expansion:

$$j(\varepsilon) = j(0) + \ell_1(\varepsilon)(\mathscr{R}^{(1)}(u_0, p_0) + \partial_\ell^{(1)} \mathscr{L}(0, u_0, p_0)) + o(\ell_1(\varepsilon)). \tag{10.14}$$

In particular

$$\mathscr{R}^{(1)}(u_0, p_0) + \partial_\ell^{(1)} \mathscr{L}(0, u_0, p_0) = \delta a^{(1)} - \delta f^{(1)} + \delta J_1^{(1)} + \delta J_2^{(1)},$$

where $\delta a^{(1)}, \delta f^{(1)}, \delta J_1^{(1)}, \delta J_2^{(1)}$ are as in Proposition 10.1.

(ii) Assume that the assumptions under (i) hold and that the limits

$$\mathscr{R}^{(2)}(u_0, p_0) := \lim_{\varepsilon \searrow 0} \frac{\mathscr{L}(\varepsilon, u_\varepsilon, p_\varepsilon) - \mathscr{L}(\varepsilon, u_0, p_\varepsilon) - \ell_1(\varepsilon)\mathscr{R}^{(1)}(u_0, p_0)}{\ell_2(\varepsilon)}, \tag{10.15}$$

$$\partial_\ell^{(2)} \mathscr{L}(0, u_0, p_0) := \lim_{\varepsilon \searrow 0} \frac{\mathscr{L}(\varepsilon, u_0, p_\varepsilon) - \mathscr{L}(0, u_0, p_\varepsilon) - \ell_1(\varepsilon)\partial_\ell^{(1)} \mathscr{L}(0, u_0, p_0)}{\ell_2(\varepsilon)}, \tag{10.16}$$

exist. Then we have the following expansion

$$\begin{aligned} j(\varepsilon) = j(0) &+ \ell_1(\varepsilon)(\mathscr{R}^{(1)}(u_0, p_0) + \partial_\ell^{(1)} \mathscr{L}(0, u_0, p_0)) \\ &+ \ell_2(\varepsilon)(\mathscr{R}^{(2)}(u_0, p_0) + \partial_\ell^{(2)} \mathscr{L}(0, u_0, p_0)) + o(\ell_2(\varepsilon)). \end{aligned}$$

Proof. ad (i): since $\mathscr{L}(\varepsilon,u_\varepsilon,0)=\mathscr{L}(\varepsilon,u_\varepsilon,p_\varepsilon)$ and $\mathscr{L}(0,u_0,p_\varepsilon)=\mathscr{L}(0,u_0,0)$, we get

$$\begin{aligned} j(\varepsilon)-j(0) =& \mathscr{L}(\varepsilon,u_\varepsilon,0)-\mathscr{L}(0,u_0,0) && (10.17)\\ =& \mathscr{L}(\varepsilon,u_\varepsilon,p_\varepsilon)-\mathscr{L}(\varepsilon,u_0,p_\varepsilon) && (10.18)\\ &+\mathscr{L}(\varepsilon,u_0,p_\varepsilon)-\mathscr{L}(0,u_0,p_\varepsilon). && (10.19)\end{aligned}$$

Dividing by $\ell_1(\varepsilon)$ for $\varepsilon>0$ and passing to the limit yields

$$\lim_{\varepsilon\searrow 0}\frac{j(\varepsilon)-j(0)}{\ell_1(\varepsilon)}=\mathscr{R}^{(1)}(u_0,p_0)+\partial_\ell^{(1)}\mathscr{L}(0,u_0,p_0), \tag{10.20}$$

in view of our assumptions. Hence, (10.20) entails

$$\begin{aligned} &j(\varepsilon)-j(0)-\ell_1(\varepsilon)\Big(\mathscr{R}^{(1)}(u_0,p_0)+\partial_\ell^{(1)}\mathscr{L}(0,u_0,p_0)\Big)\\ &\quad=\ell_1(\varepsilon)\left(\frac{j(\varepsilon)-j(0)}{\ell_1(\varepsilon)}-\mathscr{R}^{(1)}(u_0,p_0)-\partial_\ell^{(1)}\mathscr{L}(0,u_0,p_0)\right) \qquad (10.21)\\ &\quad=o(\ell_1(\varepsilon)),\end{aligned}$$

which shows (i).
ad (ii): the same arguments yield

$$\lim_{\varepsilon\searrow 0}\frac{j(\varepsilon)-j(0)-\ell_1(\varepsilon)\Big(\mathscr{R}^{(1)}(u_0,p_0)+\partial_\ell^{(1)}\mathscr{L}(0,u_0,p_0)\Big)}{\ell_2(\varepsilon)}=\mathscr{R}^{(2)}(u_0,p_0)+\partial_\ell^{(2)}\mathscr{L}(0,u_0,p_0). \tag{10.22}$$

Now the result follows from

$$\begin{aligned} &j(\varepsilon)-j(0)-\ell_1(\varepsilon)\Big(\mathscr{R}^{(1)}(u_0,p_0)+\partial_\ell^{(1)}\mathscr{L}(0,u_0,p_0)\Big)-\ell_2(\varepsilon)\Big(\mathscr{R}^{(2)}(u_0,p_0)+\partial_\ell^{(2)}\mathscr{L}(0,u_0,p_0)\Big)\\ &=\ell_2(\varepsilon)\left(\frac{j(\varepsilon)-j(0)-\ell_1(\varepsilon)\Big(\mathscr{R}^{(1)}(u_0,p_0)+\partial_\ell^{(1)}\mathscr{L}(0,u_0,p_0)\Big)}{\ell_2(\varepsilon)}-\mathscr{R}^{(2)}(u_0,p_0)-\partial_\ell^{(2)}\mathscr{L}(0,u_0,p_0)\right)\\ &=o(\ell_2(\varepsilon)),\end{aligned}$$

in view of (10.22). □

In order to compare this approach to the upcoming methods, we want to formulate the adjoint variable in the Lagrangian framework as well. Therefore, it is readily checked that (10.7) reads

$$\text{find } p_\varepsilon\in\mathscr{W}\quad\text{such that}\quad \partial_u\mathscr{L}(\varepsilon,u_0,p_\varepsilon)(\varphi)=0\quad\text{for all }\varphi\in\mathscr{W}. \tag{10.23}$$

Remark 10.3. Checking the expansions (10.13),(10.16) in applications usually requires some regularity of the state u_0 and knowledge of the asymptotics of the adjoint state p_ε on a small domain of size ε. This limit additionally necessitates higher regularity of the volume force (we assumed that f_1,f_2 admit C^2 regularity in the vicinity of the perturbation).
The computation of the asymptotic expansions (10.12),(10.15) requires the study of the asymptotic behaviour of u_ε on the whole domain D. This often causes problems, especially in dimension two. The reader will find an application of this method in Section 14.1.

10.3 Averaged adjoint method

Another approach to compute topological derivatives was proposed in [105], applied to nonlinear problems in [58, 60, 105] and used for the optimisation on surfaces in [59]. Recall the Lagrangian function

$$\mathscr{L}(\varepsilon,u,v)=J_\varepsilon(u)+a_\varepsilon(u,v)-f_\varepsilon(v) \quad \text{for all } u\in\mathscr{V},\ v\in\mathscr{W}. \tag{10.24}$$

We henceforth assume that for all $(\varphi,q)\in\mathscr{V}\times\mathscr{W}$ and $\varepsilon\geq 0$ the function

$$s\mapsto \partial_u\mathscr{L}(\varepsilon,su_\varepsilon+(1-s)u_0,q)(\varphi), \tag{10.25}$$

is continuously differentiable on $[0,1]$. Note that this function is indeed well defined since convex combinations remain in the affine space, i.e. $su_\varepsilon+(1-s)u_0\in\mathscr{V}$ for $s\in[0,1]$. With the Lagrangian we are able to define the averaged adjoint equation associated with state variables u_ε (solution of (10.1) for $\varepsilon>0$) and u_0 (solution of (10.1) for $\varepsilon=0$): find $q_\varepsilon\in\mathscr{W}$, such that

$$\int_0^1 \partial_u\mathscr{L}(\varepsilon,su_\varepsilon+(1-s)u_0,q_\varepsilon)(\varphi)\,ds=0 \quad \text{for all } \varphi\in\mathscr{W}. \tag{10.26}$$

It is noteworthy that the affine setting again restricts us to only use derivatives in direction $\mathscr{W}$. These details might seem irritating in this general setting, but we will see that they resolve naturally in the applied formulation later on. Testing (10.26) with $\varphi=u_\varepsilon-u_0\in\mathscr{W}$ and employing the fundamental theorem of calculus yields

$$\mathscr{L}(\varepsilon,u_\varepsilon,q_\varepsilon)=\mathscr{L}(\varepsilon,u_0,q_\varepsilon) \quad \text{for } \varepsilon\geq 0, \tag{10.27}$$

for the averaged adjoint variable $q_\varepsilon\in\mathscr{W}$. This is the central property of this approach and will be used in the following proposition. We henceforth assume that the averaged adjoint equation admits a unique solution.

Proposition 10.4. Let $\ell_1,\ell_2:\mathbf{R}^+\to\mathbf{R}^+$ be functions with

$$\lim_{\varepsilon\searrow 0}\ell_1(\varepsilon)=0, \quad \text{and} \quad \lim_{\varepsilon\searrow 0}\frac{\ell_2(\varepsilon)}{\ell_1(\varepsilon)}=0. \tag{10.28}$$

(i) Assume that the limits

$$\mathscr{R}^{(1)}(u_0,q_0):=\lim_{\varepsilon\searrow 0}\frac{\mathscr{L}(\varepsilon,u_0,q_\varepsilon)-\mathscr{L}(\varepsilon,u_0,q_0)}{\ell_1(\varepsilon)}, \tag{10.29}$$

$$\partial_\ell^{(1)}\mathscr{L}(0,u_0,q_0):=\lim_{\varepsilon\searrow 0}\frac{\mathscr{L}(\varepsilon,u_0,q_0)-\mathscr{L}(0,u_0,q_0)}{\ell_1(\varepsilon)}, \tag{10.30}$$

exist. Then we have the following expansion

$$j(\varepsilon)=j(0)+\ell_1(\varepsilon)(\mathscr{R}^{(1)}(u_0,q_0)+\partial_\ell^{(1)}\mathscr{L}(0,u_0,q_0))+o(\ell_1(\varepsilon)). \tag{10.31}$$

(ii) Assume that the assumption under (i) holds and the limits

$$\mathscr{R}^{(2)}(u_0,q_0):=\lim_{\varepsilon\searrow 0}\frac{\mathscr{L}(\varepsilon,u_0,q_\varepsilon)-\mathscr{L}(\varepsilon,u_0,q_0)-\ell_1(\varepsilon)\mathscr{R}^{(1)}(u_0,q_0)}{\ell_2(\varepsilon)}, \tag{10.32}$$

$$\partial_\ell^{(2)}\mathscr{L}(0,u_0,q_0):=\lim_{\varepsilon\searrow 0}\frac{\mathscr{L}(\varepsilon,u_0,q_0)-\mathscr{L}(0,u_0,q_0)-\ell_1(\varepsilon)\partial_\ell^{(1)}\mathscr{L}(0,u_0,q_0)}{\ell_2(\varepsilon)}, \tag{10.33}$$

exist. Then we have the following expansion

$$j(\varepsilon) = j(0) + \ell_1(\varepsilon)(\mathscr{R}^{(1)}(u_0, q_0) + \partial_\ell^{(1)} \mathscr{L}(0, u_0, q_0)) \\ + \ell_2(\varepsilon)(\mathscr{R}^{(2)}(u_0, q_0) + \partial_\ell^{(2)} \mathscr{L}(0, u_0, q_0)) + o(\ell_2(\varepsilon)).$$

Proof. ad (i): employing property (10.27), we deduce

$$\begin{aligned} j(\varepsilon) - j(0) &= \mathscr{L}(\varepsilon, u_\varepsilon, 0) - \mathscr{L}(0, u_0, 0) \\ &= \mathscr{L}(\varepsilon, u_0, q_\varepsilon) - \mathscr{L}(0, u_0, q_0) \\ &= \mathscr{L}(\varepsilon, u_0, q_\varepsilon) - \mathscr{L}(\varepsilon, u_0, q_0) + \mathscr{L}(\varepsilon, u_0, q_0) - \mathscr{L}(0, u_0, q_0). \end{aligned}$$

Hence, we observe

$$\lim_{\varepsilon \searrow 0} \frac{j(\varepsilon) - j(0)}{\ell_1(\varepsilon)} = \mathscr{R}^{(1)}(u_0, q_0) + \partial_\ell^{(1)} \mathscr{L}(0, u_0, q_0), \tag{10.34}$$

in view of our assumptions. This in turn yields

$$\begin{aligned} j(\varepsilon) - j(0) - \ell_1(\varepsilon)&\left(\mathscr{R}^{(1)}(u_0, q_0) + \partial_\ell^{(1)} \mathscr{L}(0, u_0, q_0)\right) \\ &= \ell_1(\varepsilon)\left(\frac{j(\varepsilon) - j(0)}{\ell_1(\varepsilon)} - \mathscr{R}^{(1)}(u_0, q_0) - \partial_\ell^{(1)} \mathscr{L}(0, u_0, q_0)\right) \\ &= o(\ell_1(\varepsilon)), \end{aligned} \tag{10.35}$$

which shows (i).
ad (ii): the proof follows the same lines as Proposition 10.1 item (ii). □

The previous result can readily be generalised to compute the n-th order topological derivative (cf. Definition 9.1). We will employ this generalisation in the last part of this thesis, where we tackle higher order topological derivatives. However, instead of stating an abstract result, we are going to employ an analogous splitting directly in the asymptotic analysis (cf. Theorem 19.2, Theorem 21.1).

Remark 10.5. Similarly to Amstutz' method, checking the expansions (10.30),(10.33) in applications usually requires some regularity of the state u_0, adjoint state q_0 and forces f_1, f_2 in the vicinity of the perturbation. However, the computation of this expansion is a straight forward application of Taylor's formula. An application is given in Section 14.2.
The computation of the asymptotic expansions (10.29),(10.32) requires the study of the asymptotic behaviour of q_ε and therefore also of u_ε. This is the most difficult part and can be done by the compound layer expansion involving corrector equations (see for instance [81], [80]) as is presented in Section 13.2.

10.4 Delfour's method

In this section we discuss a method proposed by M.C. Delfour in [41, Theorem 3.3]. The definite advantage is that it uses the unperturbed adjoint equation and thus only requires the asymptotic analysis of the state equation. Yet, it seems to come with the shortcoming that it is only applicable to certain cost functions; see [58]. As before we let $\mathscr{L}$ be a Lagrangian function and denote by $u_\varepsilon \in \mathscr{V}$ the perturbed state variable (solution to (10.1) for $\varepsilon \geq 0$) and $p_0 \in \mathscr{W}$ the unperturbed adjoint variable (solution to (10.7) for $\varepsilon = 0$). Using these variables, Delfour proposed the following result for computing the first topological derivative, where we also incorporated the second order topological derivative.

Proposition 10.6 ([41]). Let $\ell_1, \ell_2 : \mathbf{R}^+ \to \mathbf{R}^+$ be functions with

$$\lim_{\varepsilon \searrow 0} \ell_1(\varepsilon) = 0, \quad \text{and} \quad \lim_{\varepsilon \searrow 0} \frac{\ell_2(\varepsilon)}{\ell_1(\varepsilon)} = 0. \tag{10.36}$$

(i) Assume that the limits

$$\mathscr{R}_1^{(1)}(u_0, p_0) := \lim_{\varepsilon \searrow 0} \frac{1}{\ell_1(\varepsilon)} [\mathscr{L}(\varepsilon, u_\varepsilon, p_0) - \mathscr{L}(\varepsilon, u_0, p_0) - \partial_u \mathscr{L}(\varepsilon, u_0, p_0)(u_\varepsilon - u_0)], \tag{10.37}$$

$$\mathscr{R}_2^{(1)}(u_0, p_0) := \lim_{\varepsilon \searrow 0} \frac{1}{\ell_1(\varepsilon)} (\partial_u \mathscr{L}(\varepsilon, u_0, p_0) - \partial_u \mathscr{L}(0, u_0, p_0))(u_\varepsilon - u_0), \tag{10.38}$$

$$\partial_\ell^{(1)} \mathscr{L}(0, u_0, p_0) := \lim_{\varepsilon \searrow 0} \frac{1}{\ell_1(\varepsilon)} (\mathscr{L}(\varepsilon, u_0, p_0) - \mathscr{L}(0, u_0, p_0)), \tag{10.39}$$

exist. Then the following expansion holds:

$$j(\varepsilon) = j(0) + \ell_1(\varepsilon)((\mathscr{R}_1^{(1)}(u_0, p_0) + \mathscr{R}_2^{(1)}(u_0, p_0) + \partial_\ell^{(1)} \mathscr{L}(0, u_0, p_0)) + o(\ell_1(\varepsilon)). \tag{10.40}$$

(ii) Assume that the assumptions under (i) hold and that the limits

$$\mathscr{R}_1^{(2)}(u_0, p_0) := \lim_{\varepsilon \searrow 0} \frac{1}{\ell_2(\varepsilon)} \Big[\mathscr{L}(\varepsilon, u_\varepsilon, p_0) - \mathscr{L}(\varepsilon, u_0, p_0) - \partial_u \mathscr{L}(\varepsilon, u_0, p_0))(u_\varepsilon - u_0) - \ell_1(\varepsilon) \mathscr{R}_1^{(1)}(u_0, p_0) \Big], \tag{10.41}$$

$$\mathscr{R}_2^{(2)}(u_0, p_0) := \lim_{\varepsilon \searrow 0} \frac{1}{\ell_2(\varepsilon)} \Big[(\partial_u \mathscr{L}(\varepsilon, u_0, p_0) - \partial_u \mathscr{L}(0, u_0, p_0))(u_\varepsilon - u_0) - \ell_1(\varepsilon) \mathscr{R}_2^{(1)}(u_0, p_0) \Big], \tag{10.42}$$

$$\partial_\ell^{(2)} \mathscr{L}(0, u_0, p_0) := \lim_{\varepsilon \searrow 0} \frac{1}{\ell_2(\varepsilon)} \Big[\mathscr{L}(\varepsilon, u_0, p_0) - \mathscr{L}(0, u_0, p_0) - \ell_1(\varepsilon) \partial_\ell^{(1)} \mathscr{L}(0, u_0, p_0) \Big], \tag{10.43}$$

exist. Then we have the following expansion:

$$\begin{aligned} j(\varepsilon) = j(0) &+ \ell_1(\varepsilon)(\mathscr{R}_1^{(1)}(u_0, p_0) + \mathscr{R}_2^{(1)}(u_0, p_0) + \partial_\ell^{(1)} \mathscr{L}(0, u_0, p_0)) \\ &+ \ell_2(\varepsilon)(\mathscr{R}_1^{(2)}(u_0, p_0) + \mathscr{R}_2^{(2)}(u_0, p_0) + \partial_\ell^{(2)} \mathscr{L}(0, u_0, p_0)) + o(\ell_2(\varepsilon)). \end{aligned} \tag{10.44}$$

Proof. ad (i): firstly note that by definition the unperturbed adjoint state p_0 satisfies

$$\partial_u \mathscr{L}(0, u_0, p_0)(\varphi) = 0 \quad \text{for all } \varphi \in \mathscr{W}.$$

Thus, we can rewrite $j(\varepsilon) - j(0)$ in the following way:

$$\begin{aligned} j(\varepsilon) - j(0) =& \mathscr{L}(\varepsilon, u_\varepsilon, 0) - \mathscr{L}(0, u_0, 0) \\ =& \mathscr{L}(\varepsilon, u_\varepsilon, p_0) - \mathscr{L}(0, u_0, p_0) \\ =& \mathscr{L}(\varepsilon, u_\varepsilon, p_0) - \mathscr{L}(\varepsilon, u_0, p_0) - \partial_u \mathscr{L}(\varepsilon, u_0, p_0)(u_\varepsilon - u_0) \\ &+ \partial_u \mathscr{L}(\varepsilon, u_0, p_0)(u_\varepsilon - u_0) - \partial_u \mathscr{L}(0, u_0, p_0)(u_\varepsilon - u_0) \\ &+ \mathscr{L}(\varepsilon, u_0, p_0) - \mathscr{L}(0, u_0, p_0). \end{aligned} \tag{10.45}$$

Dividing by $\ell_1(\varepsilon)$, $\varepsilon > 0$ and passing to the limit yields

$$\lim_{\varepsilon \searrow 0} \frac{j(\varepsilon) - j(0)}{\ell_1(\varepsilon)} = \mathscr{R}_1^{(1)}(u_0, p_0) + \mathscr{R}_2^{(1)}(u_0, p_0) + \partial_\ell^{(1)} \mathscr{L}(0, u_0, p_0). \tag{10.46}$$

Thus we deduce

$$\begin{aligned} j(\varepsilon) - j(0) - \ell_1(\varepsilon) &\left(\mathscr{R}_1^{(1)}(u_0, p_0) + \mathscr{R}_2^{(1)}(u_0, p_0) + \partial_\ell^{(1)} \mathscr{L}(0, u_0, p_0) \right) \\ &= \ell_1(\varepsilon) \left(\frac{j(\varepsilon) - j(0)}{\ell_1(\varepsilon)} - \mathscr{R}_1^{(1)}(u_0, p_0) - \mathscr{R}_2^{(1)}(u_0, p_0) - \partial_\ell^{(1)} \mathscr{L}(0, u_0, p_0) \right) \\ &= o(\ell_1(\varepsilon)), \end{aligned} \tag{10.47}$$

which shows (i).
ad (ii): the proof follows the same lines as Proposition 10.1 item (ii). □

Remark 10.7. Similarly to Amstutz' method and the averaged adjoint method, Delfour's method requires the asymptotic behaviour of u_ε on the whole domain to compute (10.37),(10.41). This may be challenging in the analysis in dimension two for some cost functionals. Additionally, (10.38),(10.42) can be checked by smoothness assumptions on p_0 and u_0 and the knowledge of the asymptotics of u_ε on a small subset of size ε. The remaining terms (10.39),(10.43) usually are computed making use of a Taylor's expansion of u_0, p_0 and f_1, f_2, respectively.

Overview of the adjoint equations To conclude the abstract setting we give a short overview of the employed adjoint variables. In total, we can detect three different adjoint equations governing the adjoint variables within the previous section.

- The method of Amstutz [13] uses an adjoint equation which depends on the unperturbed state variable:

$$\text{find } p_\varepsilon \in \mathscr{W} \quad \text{such that} \quad \partial_u \mathscr{L}(\varepsilon, u_0, p_\varepsilon)(\varphi) = 0 \quad \text{for all } \varphi \in \mathscr{W}. \tag{10.48}$$

- The averaged adjoint method employs the averaged adjoint equation:

$$\text{find } q_\varepsilon \in \mathscr{W} \quad \text{such that} \quad \int_0^1 \partial_u \mathscr{L}(\varepsilon, s u_\varepsilon + (1-s) u_0, q_\varepsilon)(\varphi)\, ds = 0 \quad \text{for all } \varphi \in \mathscr{W}. \tag{10.49}$$

- Finally, Delfour's method is based on the usual adjoint equation

$$\text{find } v_\varepsilon \in \mathscr{W} \quad \text{such that} \quad \partial_u \mathscr{L}(\varepsilon, u_\varepsilon, v_\varepsilon)(\varphi) = 0 \quad \text{for all } \varphi \in \mathscr{W}. \tag{10.50}$$

It should be noted though that in the unperturbed setting, i.e. $\varepsilon = 0$, all three adjoint variables coincide. That is,

$$p_0 = q_0 = v_0. \tag{10.51}$$

We use this equality in Defour's method, which is only based on the unperturbed adjoint variable, to justify the notational choice p_0 instead of v_0 within this subsection. Hidden within the assumptions of the according propositions, we see that the asymptotic expansions of the state and adjoint variables play a central role in the computation of the derivatives.

11 Auxiliary results

Before we dive into the analysis of the state and adjoint variables, we formulate some auxiliary results that are necessary for a rigorous derivation. Their function in the upcoming analysis compares to the role of Lemma 3.4 and Lemma 3.3 within the derivation of the material derivative in the previous part. Since we need these results in the last part of this thesis as well, we devote a whole section to it. Throughout this section we fix a point $x_0 \in \mathsf{D}$.

11.1 Scaling of inequalities

In this section, we discuss the influence of a parametrised affine transformation $T_\varepsilon : \mathbf{R}^d \to \mathbf{R}^d$ onto norms and the scaling behaviour of some well-known inequalities with respect to that parameter. To specify, we consider the following set of transformations:

Definition 11.1. Let $\mathsf{D} \subset \mathbf{R}^d$ be an open and bounded Lipschitz domain and $\varepsilon > 0$. We define the affine transformation

$$T_\varepsilon : \mathbf{R}^d \to \mathbf{R}^d, \quad x \mapsto x_0 + \varepsilon x. \tag{11.1}$$

Since T_ε is a bi-Lipschitz continuous map, there holds

$$\varphi \in H^1_\Gamma(\mathsf{D})^d \quad \text{if and only if} \quad \varphi \circ T_\varepsilon \in H^1_{T_\varepsilon^{-1}(\Gamma)}(T_\varepsilon^{-1}(\mathsf{D}))^d,$$

see [110, p.52, Theorem 2.2.2]. For the sake of readability, we introduce the following notation:

Notational convention Let $\mathsf{D} \subset \mathbf{R}^d$ be an open and bounded Lipschitz domain, $\Gamma \subset \partial\mathsf{D}$ and $\Gamma^N = \partial\mathsf{D} \setminus \Gamma$. Then we denote, for $\varepsilon > 0$ sufficiently small, the scaled quantities

- $\mathsf{D}_\varepsilon := T_\varepsilon^{-1}(\mathsf{D})$,
- $\Gamma_\varepsilon := T_\varepsilon^{-1}(\Gamma)$,
- $\Gamma_\varepsilon^N := T_\varepsilon^{-1}(\Gamma^N)$,

where T_ε is defined in Definition 11.1.

The action of the transformation T_ε^{-1} on D is depicted in Figure 11. While the domain D_ε is inflated as $\varepsilon \to 0$, the small inclusion ω_ε is scaled to unit size ω and centered around the origin. Furthermore, the inflated initial shape, denoted Ω^ε, is pushed towards the boundary of D_ε. The scaled H^1 norm will occur throughout the rest of this thesis. This motivates the next definition.

Definition 11.2. Let $\mathsf{D} \subset \mathbf{R}^d$ be an open and bounded Lipschitz domain and $\varepsilon > 0$. For $\varphi \in H^1(\mathsf{D}_\varepsilon)^d$ we define

$$\|\varphi\|_\varepsilon := \varepsilon\|\varphi\|_{L_2(\mathsf{D}_\varepsilon)^d} + \|\partial\varphi\|_{L_2(\mathsf{D}_\varepsilon)^{d\times d}}. \tag{11.2}$$

Remark 11.3. Even though the fixed point x_0 might get lost in the previous definitions, as it is not highlighted in the notation we are using, it plays a prominent role in the analytic setting. In fact, x_0 denotes the point, where a singular perturbation is performed. It will appear explicitly again in the asymptotic analysis of the state and adjoint state as well as in the final formulas of the topological derivatives.

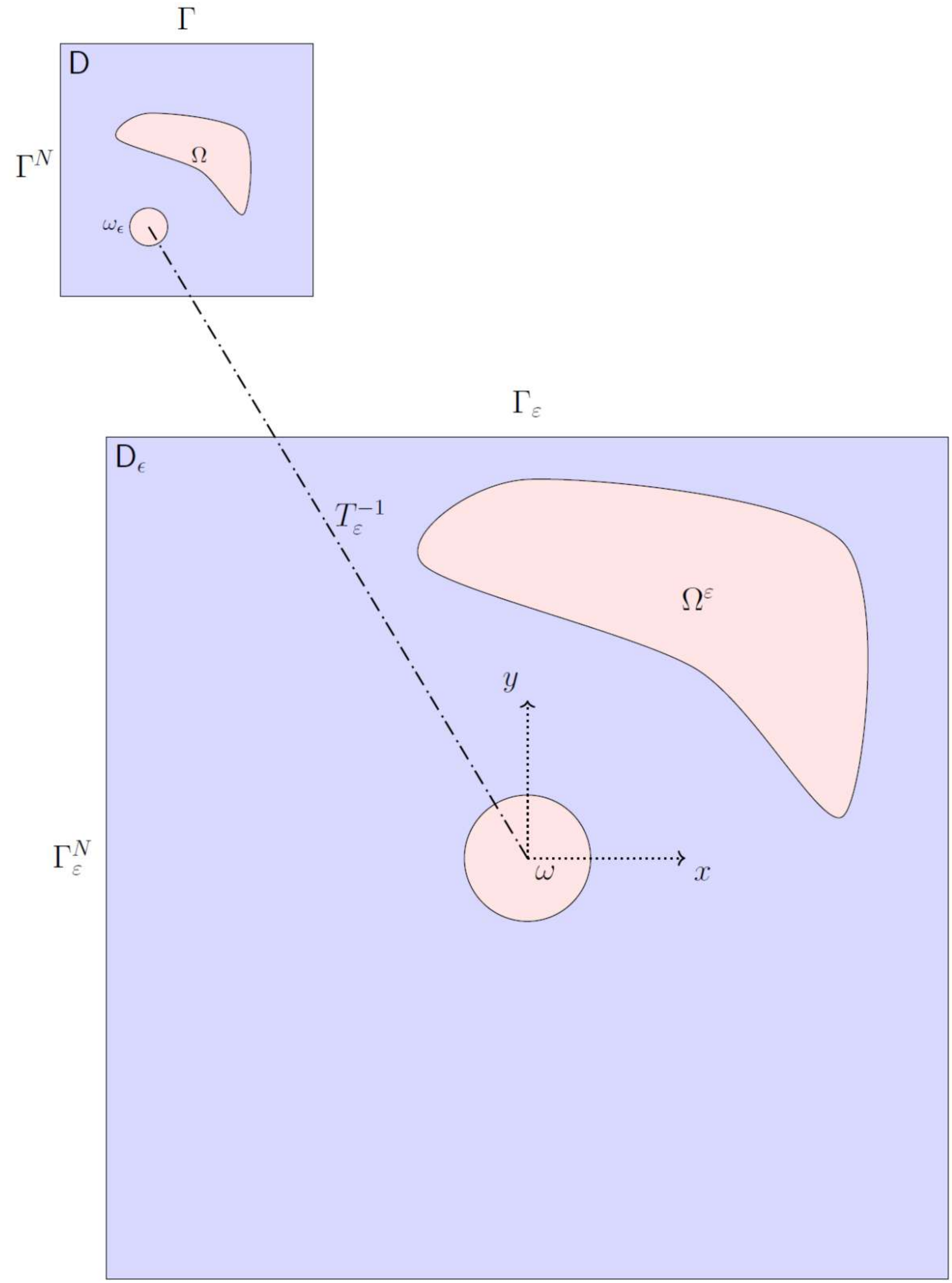

Figure 11: Visualisation of the transformation $D \to D_\varepsilon$ (cf. [105, Figure 1]).

Lemma 11.4. Let $\mathsf{D} \subset \mathbf{R}^d$ be an open and bounded Lipschitz domain and let $\varepsilon > 0$ sufficiently small.

(i) For $1 \leq p < \infty$ and $\varphi \in L_p(\mathsf{D}_\varepsilon)^d$ there holds

$$\varepsilon^{\frac{d}{p}} \|\varphi\|_{L_p(\mathsf{D}_\varepsilon)^d} = \|\varphi \circ T_\varepsilon^{-1}\|_{L_p(\mathsf{D})^d}. \tag{11.3}$$

(ii) For $1 \leq p < \infty$ and $\varphi \in W_p^1(\mathsf{D}_\varepsilon)^d$ there holds

$$\varepsilon^{\frac{d}{p}-1} \|\partial\varphi\|_{L_p(\mathsf{D}_\varepsilon)^{d\times d}} = \|\partial(\varphi \circ T_\varepsilon^{-1})\|_{L_p(\mathsf{D})^{d\times d}}. \tag{11.4}$$

(iii) For $\varphi \in H^1(\mathsf{D}_\varepsilon)^d$ there holds

$$\|\varphi \circ T_\varepsilon^{-1}\|_{H^1(\mathsf{D})^d} = \varepsilon^{\frac{d}{2}-1} \|\varphi\|_\varepsilon. \tag{11.5}$$

Proof. (i) A change of variables yields

$$\|\varphi\|^p_{L_p(\mathsf{D}_\varepsilon)^d} = \varepsilon^{-d} \int_{\mathsf{D}} |\varphi \circ T_\varepsilon^{-1}|^p \, dx = \varepsilon^{-d} \|\varphi \circ T_\varepsilon^{-1}\|^p_{L_p(\mathsf{D})^d}, \tag{11.6}$$

where we used $|\det(\partial T_\varepsilon^{-1})| = \varepsilon^{-d}$.

(i) Taking into account that by the chain rule $\partial(\varphi \circ T_\varepsilon^{-1}) = \varepsilon^{-1}\partial\varphi \circ T_\varepsilon^{-1}$, a change of variables yields

$$\begin{aligned} \|\partial\varphi\|^p_{L_p(\mathsf{D}_\varepsilon)^{d\times d}} &= \varepsilon^{-d} \int_{\mathsf{D}} |\partial\varphi \circ T_\varepsilon^{-1}|^p \, dx \\ &= \varepsilon^{-d}\varepsilon^p \int_{\mathsf{D}} |\partial(\varphi \circ T_\varepsilon^{-1})|^p \, dx = \varepsilon^{p-d} \|\partial(\varphi \circ T_\varepsilon^{-1})\|^p_{L_p(\mathsf{D})^{d\times d}}. \end{aligned} \tag{11.7}$$

(iii) This follows from item (i) and (ii).

□

Lemma 11.5. Let $\mathsf{D} \subset \mathbf{R}^d$ be an open and bounded Lipschitz domain, $\Gamma \subset \partial\mathsf{D}$, with $|\Gamma| > 0$ and let $\varepsilon > 0$. Then the following results hold:

(i) For $d \geq 2$ and $1 \leq p \leq q < \infty$ there is a constant $C > 0$ independent of ε such that

$$\|\varphi\|_{L_p(\mathsf{D}_\varepsilon)^d} \leq C\varepsilon^{\frac{d}{q}-\frac{d}{p}} \|\varphi\|_{L_q(\mathsf{D}_\varepsilon)^d} \quad \text{for all } \varphi \in L_q(\mathsf{D}_\varepsilon)^d. \tag{11.8}$$

(ii) Let $d \geq 3$ and 2^* denote the Sobolev conjugate of 2. There is a constant $C > 0$ independent of ε such that

$$\|\varphi\|_{L_{2^*}(\mathsf{D}_\varepsilon)^d} \leq C\|\varphi\|_\varepsilon \quad \text{for all } \varphi \in H^1(\mathsf{D}_\varepsilon)^d. \tag{11.9}$$

(iii) Let $d = 2$ and $\alpha > 0$ small. There is a constant $C > 0$ independent of ε and $\delta > 0$ small such that

$$\|\varphi\|_{L_{(2-\delta)^*}(\mathsf{D}_\varepsilon)^d} \leq C\varepsilon^{-\alpha} \|\varphi\|_\varepsilon \quad \text{for all } \varphi \in H^1(\mathsf{D}_\varepsilon)^d. \tag{11.10}$$

(iv) There is a constant $C > 0$ independent of ε such that

$$\|\varphi\|_{L_2(\Gamma_\varepsilon)^d} \leq C\varepsilon^{-\frac{1}{2}}\|\varphi\|_\varepsilon \quad \text{for all } \varphi \in H^1(\mathsf{D}_\varepsilon)^d. \tag{11.11}$$

(v) Given a smooth, connected part of a Lipschitz boundary $\Gamma \subset \partial\mathsf{D}$ with positive measure, there is a continuous extension operator $Z_{\Gamma_\varepsilon} : H^{\frac{1}{2}}(\Gamma_\varepsilon)^d \to H^1(\mathsf{D}_\varepsilon)^d$, such that

$$\|Z_{\Gamma_\varepsilon}(\varphi)\|_\varepsilon \leq C(\varepsilon^{\frac{1}{2}}\|\varphi\|_{L_2(\Gamma_\varepsilon)^d} + |\varphi|_{H^{\frac{1}{2}}(\Gamma_\varepsilon)^d}) \quad \text{for all } \varphi \in H^{\frac{1}{2}}(\Gamma_\varepsilon)^d, \tag{11.12}$$

where $C > 0$ is independent of ε.

(vi) There is a constant $C > 0$ independent of ε such that

$$\|\varphi\|_{L_2(\mathsf{D}_\varepsilon)^d} \leq C\varepsilon^{-1}\|\partial\varphi\|_{L_2(\mathsf{D}_\varepsilon)^{d\times d}} \quad \text{for all } \varphi \in H^1_{\Gamma_\varepsilon}(\mathsf{D}_\varepsilon)^d. \tag{11.13}$$

Proof. (i) Let $\varphi \in L_q(\mathsf{D}_\varepsilon)^d$. By the inclusion of L_p-spaces we observe $\varphi \in L_p(\mathsf{D}_\varepsilon)^d$, for $p \leq q$. Now Lemma 11.4 item (i) yields

$$\|\varphi\|_{L_p(\mathsf{D}_\varepsilon)^d} = \varepsilon^{-\frac{d}{p}}\|\varphi\|_{L_p(\mathsf{D})^d} \leq C\varepsilon^{-\frac{d}{p}}\|\varphi\|_{L_q(\mathsf{D})^d} = C\varepsilon^{\frac{d}{q}-\frac{d}{p}}\|\varphi\|_{L_q(\mathsf{D}_\varepsilon)^d}, \tag{11.14}$$

where the constant C solely depends on the domain D and p, q.

(ii) We use Lemma 11.4 item (i) and (ii), and apply the Gagliardo-Nirenberg inequality [51, p. 279, Theorem 2] to the bounded domain D to obtain

$$\begin{aligned}
\|\varphi\|_{L_{2^*}(\mathsf{D}_\varepsilon)^d} &= \varepsilon^{-\frac{d}{2^*}}\|\varphi\circ T_\varepsilon^{-1}\|_{L_{2^*}(\mathsf{D})^d} \\
&\leq C\varepsilon^{-\frac{d}{2^*}}\|\varphi\circ T_\varepsilon^{-1}\|_{H^1(\mathsf{D})^d} \\
&= C\varepsilon^{\frac{d}{2}-\frac{d}{2^*}-1}\|\varphi\|_\varepsilon.
\end{aligned} \tag{11.15}$$

Since the Sobolev conjugate is given by

$$2^* := \frac{2d}{d-2}, \tag{11.16}$$

there holds $\frac{d}{2} - \frac{d}{2^*} = 1$. Hence, the result follows.

(iii) We apply the Gagliardo-Nirenberg inequality with respect to $p := 2-\delta < 2$ and use the continuous embedding $L_2(\mathsf{D})^d \hookrightarrow L_{2-\delta}(\mathsf{D})^d$ on the bounded domain D:

$$\begin{aligned}
\|\varphi\|_{L_{(2-\delta)^*}(\mathsf{D}_\varepsilon)^d} &= \varepsilon^{-\frac{2}{(2-\delta)^*}}\|\varphi\circ T_\varepsilon^{-1}\|_{L_{(2-\delta)^*}(\mathsf{D})^d} \\
&\leq C\varepsilon^{-\frac{2}{(2-\delta)^*}}(\|\varphi\circ T_\varepsilon^{-1}\|_{L_{(2-\delta)}(\mathsf{D})^d} + \|\partial(\varphi\circ T_\varepsilon^{-1})\|_{L_{(2-\delta)}(\mathsf{D})^{d\times d}}) \\
&\leq C\varepsilon^{-\frac{2}{(2-\delta)^*}}(\|\varphi\circ T_\varepsilon^{-1}\|_{L_2(\mathsf{D})^d} + \|\partial(\varphi\circ T_\varepsilon^{-1})\|_{L_2(\mathsf{D})^{d\times d}}) \\
&= C\varepsilon^{-\frac{2}{(2-\delta)^*}}\|\varphi\|_\varepsilon.
\end{aligned} \tag{11.17}$$

Now the asymptotic behaviour

$$\lim_{\delta\searrow 0}(2-\delta)^* = \lim_{\delta\searrow 0}\frac{(2-\delta)2}{\delta} = \infty, \tag{11.18}$$

shows (iii).

(iv) A change of variables (cf. Lemma 11.4) and the continuity of the trace operator entail

$$\begin{aligned}\|\varphi\|_{L_2(\Gamma_\varepsilon)^d} &= \varepsilon^{-\frac{d-1}{2}}\|\varphi\circ T_\varepsilon^{-1}\|_{L_2(\Gamma)^d} \\ &\le C\varepsilon^{-\frac{d-1}{2}}\|\varphi\circ T_\varepsilon^{-1}\|_{H^1(\mathrm{D})^d} \\ &= C\varepsilon^{-\frac{1}{2}}\|\varphi\|_\varepsilon,\end{aligned} \tag{11.19}$$

for all $\varphi\in H^1(\mathrm{D}_\varepsilon)^d$. This shows (iv).

(v) From [109, p. 129, Theorem 8.8] we know there exists a continuous extension operator $Z_\Gamma : H^{\frac{1}{2}}(\Gamma)^d \to H^1(\mathrm{D})^d$. Thus, a scaling argument similar to the previous one yields the result.

(vi) An application of Friedrich's inequality combined with Lemma 11.4 item (i) and (ii) yields the result.

□

11.2 Remainder estimates

This section is dedicated to the estimation of remainders on the boundary of an inflated domain D_ε. We will use them to extract an asymptotic behaviour of layer potentials.

Lemma 11.6. Let $V:\mathbf{R}^d\to\mathbf{R}^d\in H^1_{loc}(\mathbf{R}^d)^d$ satisfy

$$|V(x)| = c_1|x|^{-m}+\mathcal{O}(|x|^{-m-1}),\quad |\partial V(x)| = c_2|x|^{-m-1}+\mathcal{O}(|x|^{-m-2}), \tag{11.20}$$

for $x\in B_\rho(0)^c$ as $|x|\to\infty$, where $\rho>0$ is fixed, $m\in\mathbf{R}$ and $c_1,c_2>0$ are constants. Furthermore, let $\mathrm{D}\subset\mathbf{R}^d$ be an open and bounded Lipschitz domain. Then there is a constant $C>0$ independent of ε, such that for $\Gamma\subset\partial\mathrm{D}$, $|\partial\mathrm{D}|>0$ and $\varepsilon>0$ sufficiently small the following estimates hold:

(i) $\|V\|_{L_2(\Gamma_\varepsilon)^d}\le C\varepsilon^{\frac{2m+1-d}{2}}$,

(ii) $|V|_{H^{\frac{1}{2}}(\Gamma_\varepsilon)^d}\le C\varepsilon^{\frac{2m+2-d}{2}}$,

(iii) $\|\partial V\|_{L_2(\Gamma_\varepsilon)^{d\times d}}\le C\varepsilon^{\frac{2m+3-d}{2}}$,

(iv) $\|\partial V\|_{L_2(\mathbf{R}^d\setminus\mathrm{D}_\varepsilon)^{d\times d}}\le C\varepsilon^{\frac{2m+2-d}{2}}$, if $m>\frac{d}{2}-1$.

Proof. (i) Let $M:=\inf_{x\in\Gamma}|x-x_0|>0$ and $\varepsilon>0$ sufficiently small, such that the leading term of V dominates the remainder for $x\in\Gamma_\varepsilon$. This is possible, since $x_0\notin\Gamma$ and therefore the inflated boundary Γ_ε tends to infinity for $\varepsilon\searrow 0$. We thus conclude

$$\|V\|^2_{L_2(\Gamma_\varepsilon)^d} = \int_{\Gamma_\varepsilon}|V|^2\,dS \le |\Gamma_\varepsilon|(\varepsilon^{-1}M)^{-2m}\le C\varepsilon^{1-d+2m}. \tag{11.21}$$

Now taking the square root shows the result.

(ii) Let $0 < r_1 < r_2$ such that $\partial D \subset S$, where $S := B_{r_2}(x_0) \setminus B_{r_1}(x_0)$. Additionally, let $\varepsilon > 0$ sufficiently small, such that $\rho < \varepsilon^{-1} r_1$. Now we apply a change of variables to integrate over the fixed domain and split the norm into two terms, which are treated separately. Therefore, fix some $\delta > 0$ sufficiently small. Then

$$
\begin{aligned}
|V|^2_{H^{\frac{1}{2}}(\partial \mathrm{D}_\varepsilon)^d} &= \int_{\partial \mathrm{D}_\varepsilon} \int_{\partial \mathrm{D}_\varepsilon} \frac{|V(x) - V(y)|^2}{|x-y|^d} \, dS_y dS_x \\
&= \varepsilon^{2-2d} \int_{\partial D} \int_{\partial D} \frac{|V(T_\varepsilon^{-1}(x)) - V(T_\varepsilon^{-1}(y))|^2}{|T_\varepsilon^{-1}(x) - T_\varepsilon^{-1}(y)|^d} \, dS_y dS_x \\
&= \varepsilon^{2-d} \int_{\partial D} \int_{\partial D} \frac{|V(T_\varepsilon^{-1}(x)) - V(T_\varepsilon^{-1}(y))|^2}{|x-y|^d} \, dS_y dS_x \\
&= \varepsilon^{2-d} \int_{\partial D} \int_{\partial D \setminus B_\delta(x)} \frac{|V(T_\varepsilon^{-1}(x)) - V(T_\varepsilon^{-1}(y))|^2}{|x-y|^d} \, dS_y dS_x \qquad (11.22) \\
&\quad + \varepsilon^{2-d} \int_{\partial D} \int_{\partial D \cap B_\delta(x)} \frac{|V(T_\varepsilon^{-1}(x)) - V(T_\varepsilon^{-1}(y))|^2}{|x-y|^d} \, dS_y dS_x. \qquad (11.23)
\end{aligned}
$$

In order to compute the first term (11.22), we consider for each pair $(x, y) \in \partial \mathrm{D} \times \partial \mathrm{D}$ a smooth path $\varphi_{x,y} : [0,1] \to S$ satisfying $\varphi_{x,y}(0) = x$ and $\varphi_{x,y}(1) = y$. Since V is smooth in $T_\varepsilon^{-1}(S)$, we can apply the mean value theorem to the function $F(t) := V(T_\varepsilon^{-1}(\varphi_{x,y}(t)))$. Taking into account $\partial(T_\varepsilon^{-1}) = \varepsilon^{-1} I_d$ entails

$$
V(T_\varepsilon^{-1}(y)) - V(T_\varepsilon^{-1}(x)) = \int_0^1 \varepsilon^{-1} \partial V(T_\varepsilon^{-1}(\varphi_{x,y}(s))) \varphi'_{x,y}(s) \, ds. \tag{11.24}
$$

Thus, by Hölder's inequality we conclude

$$
|V(T_\varepsilon^{-1}(y)) - V(T_\varepsilon^{-1}(x))| \leq \varepsilon^{-1} \|\partial V(T_\varepsilon^{-1}(\varphi_{x,y}(\cdot)))\|_{L^\infty(0,1)^{d\times d}} \|\varphi'_{x,y}\|_{L^1(0,1)^d}. \tag{11.25}
$$

Since this inequality holds for every smooth path $\varphi_{x,y}$ connecting x and y, the estimate holds for $d_S(x,y) := \inf_{\varphi_{x,y}[0,1]\to S} \|\varphi'_{x,y}\|_{L^1(0,1)^d}$. Furthermore, since S is bounded and path connected, the following estimate holds (see [44, Theorem 5.8]):

$$
d_S(x,y) \leq C|x-y| \quad \text{for } x, y \in \bar{S}, \tag{11.26}
$$

for some constant $C > 0$ that only depends on S. Additionally, considering the representation formula of V, we have $|\partial V(x)| = c_2|x|^{-m-1} + \mathcal{O}(|x|^{-m-2})$. Hence, choosing $\varepsilon > 0$ small enough, such that the leading term dominates the remainder, we get

$$
\|\partial V(T_\varepsilon^{-1}(\varphi_{x,y}(s)))\|_{L^\infty(0,1)^{d\times d}} \leq \max_{z\in\bar{S}} |\partial V(T_\varepsilon^{-1}(z))| \leq C\varepsilon^{m+1}. \tag{11.27}
$$

As a result, we conclude

$$\begin{aligned}
&\varepsilon^{2-d} \int_{\partial D} \int_{\partial D \setminus B_\delta(x)} \frac{|V(T_\varepsilon^{-1}(y)) - V(T_\varepsilon^{-1}(x))|^2}{|x-y|^d} \, dS_y dS_x \\
&\leq \varepsilon^{-d} \int_{\partial D} \int_{\partial D \setminus B_\delta(x)} \frac{C\varepsilon^{2m+2}|x-y|^2}{|x-y|^d} \, dS_y dS_x \\
&\leq \varepsilon^{-d} \int_{\partial D} \int_{\partial D \setminus B_\delta(x)} \frac{C\varepsilon^{2m+2}}{\delta^{d-2}} \, dS_y dS_x \\
&\leq C\varepsilon^{2m+2-d}.
\end{aligned} \tag{11.28}$$

The key here was to choose the set S such that $T_\varepsilon^{-1} \circ \varphi_{x,y}([0,1]) \subset B_\rho(0)^c$ for every path $\varphi_{x,y}$. The second term (11.23) can be estimated using a straight line, which connects $x \in \partial D$ and $y \in \partial D$. Therefore, let $\varphi_{x,y}(t) := x + t(y-x)$, for $t \in [0,1]$. Since we only need to consider $(x,y) \in \partial D \times \partial D$ such that $|x-y| < \delta$, $T_\varepsilon^{-1} \circ \varphi_{x,y}([0,1]) \subset B_\rho(0)^c$ can be guaranteed by choosing δ sufficiently small. Again, an application of the mean value theorem yields

$$|V(T_\varepsilon^{-1}(x)) - V(T_\varepsilon^{-1}(y))|^2 \leq \varepsilon^{-2} \max_{z \in \bar{S_\delta}} |\partial V(T_\varepsilon^{-1}(z))|^2 |x-y|^2, \tag{11.29}$$

where $S_\delta := \bigcup_{x \in \partial D} B_\delta(x)$. Furthermore, an estimate similar to (11.27) yields

$$\max_{z \in \bar{S_\delta}} |\partial V(T_\varepsilon^{-1}(z))|^2 \leq C\varepsilon^{2m+2}. \tag{11.30}$$

Plugging this estimate into (11.23) yields

$$\begin{aligned}
&\varepsilon^{2-d} \int_{\partial D} \int_{\partial D \cap B_\delta(x)} \frac{|V(T_\varepsilon^{-1}(x)) - V(T_\varepsilon^{-1}(y))|^2}{|x-y|^d} \, dS_y dS_x \\
&\leq \varepsilon^{-d} \int_{\partial D} \int_{\partial D \cap B_\delta(x)} \frac{\max_{z \in \bar{S_\delta}} |\partial V(T_\varepsilon^{-1}(z))|^2}{|x-y|^{d-2}} \, dS_y dS_x \\
&\leq C\varepsilon^{2m+2-d} \int_{\partial D} \int_{\partial D \cap B_\delta(x)} \frac{1}{|x-y|^{d-2}} \, dy dx.
\end{aligned} \tag{11.31}$$

To finish our proof, we need to show that the integral on the right hand side is finite. Therefore, let $A_j(x) := B_{2^{(1-j)}\delta}(x) \setminus B_{2^{-j}\delta}(x)$, for $j \in \mathbf{N}$. Hence,

$$B_\delta(x) = \bigcup_{j \geq 1} A_j(x).$$

Now we can split the inner integral into layers according to these sets:

$$\begin{aligned}\int_{\partial \mathrm{D}\cap B_\delta(x)} \frac{1}{|x-y|^{d-2}}\,dy &= \sum_{j\geq 1}\int_{\partial \mathrm{D}\cap A_j(x)} \frac{1}{|x-y|^{d-2}}\,dy\\ &\leq \sum_{j\geq 1}\int_{\partial \mathrm{D}\cap A_j(x)} \frac{1}{[2^{-j}\delta]^{d-2}}\,dy\\ &\leq \sum_{j\geq 1} 2^{jd-2j}\delta^{2-d}|A_j(x)| \\ &= \delta^{2-d}\sum_{j\geq 1} 2^{jd-2j}[C(2^{(1-j)d}\delta^d - 2^{-jd}\delta^d)]\\ &= \delta^2 C\sum_{j\geq 1} 2^{jd-2j-jd}[2-1] = C\sum_{i\geq 1}\left(\frac{1}{4}\right)^j < \infty.\end{aligned} \tag{11.32}$$

Hence, combining (11.28) and (11.31) and using monotonicity of the seminorm, i.e.

$$A\subset B \Rightarrow |V|^2_{H^{\frac{1}{2}}(A)^d} \leq |V|^2_{H^{\frac{1}{2}}(B)^d}, \tag{11.33}$$

the result follows.

(iii) Similarly to (i), let $M := \inf_{x\in\Gamma}|x-x_0| > 0$ and $\varepsilon > 0$ sufficiently small, such that the leading term of ∂V dominates the remainder for $x\in\Gamma_\varepsilon$. This yields

$$\|\partial V\|^2_{L_2(\Gamma_\varepsilon)^{d\times d}} = \int_{\Gamma_\varepsilon} |\partial V|^2\,dS \leq |\Gamma_\varepsilon|(\varepsilon^{-1}M)^{-2m-2} \leq C\varepsilon^{1-d+2m+2}. \tag{11.34}$$

Hence, we conclude (iii).

(iv) For $\varepsilon > 0$ sufficiently small we have

$$\int_{\mathbf{R}^d\setminus \mathrm{D}_\varepsilon} |\partial V|^2\,dx \leq \int_{\mathbf{R}^d\setminus B_{\varepsilon^{-1}r}(0)} |\partial V|^2\,dx \leq C\int_{\varepsilon^{-1}R}^\infty r^{d-2m-2}\,dr = \varepsilon^{2m+2-d}, \tag{11.35}$$

where $R>0$ is a fixed radius such that $B_{\varepsilon^{-1}r}(0)\subset \mathrm{D}_\varepsilon$. This shows (iv) and thus finishes the proof. □

12 Analysis of the perturbed state equation

In this section we derive an asymptotic expansion of the state variable. Therefore, recall the setting:

- $\mathrm{D}\subset\mathbf{R}^d$ is an open and bounded Lipschitz domain,
- $\Gamma\subset\mathbf{R}^d$ with $|\Gamma|>0$,
- $\omega\subset\mathbf{R}^d$ open, bounded and connected, with C^1 boundary contains the origin,

- $\Omega = \emptyset$,
- $x_0 \in \mathsf{D}$,
- for $\varepsilon > 0$ sufficiently small $T_\varepsilon(x) = x_0 + \varepsilon x$ for all $x \in \mathbf{R}^d$.

With these notations, the perturbed set (cf. (9.1)) is given as

$$\Omega_\varepsilon = \omega_\varepsilon := T_\varepsilon(\omega). \tag{12.1}$$

We denote the perturbed state variable $u_\varepsilon \in H^1(\mathsf{D})^d$ as the unique solution to (9.7) with $\Omega = \omega_\varepsilon$, i.e.

$$\begin{aligned} \int_{\mathsf{D}} \mathbf{A}_{\omega_\varepsilon} \epsilon(u_\varepsilon) : \epsilon(\varphi)\, dx = & \int_{\mathsf{D}} f_{\omega_\varepsilon} \cdot \varphi \, dx + \int_{\Gamma^N} g_N \cdot \varphi \, dS \quad \text{for all } \varphi \in H^1_\Gamma(\mathsf{D})^d, \\ u_\varepsilon = & g_D \quad \text{on } \Gamma. \end{aligned} \tag{12.2}$$

Similarly, we denote the unperturbed state variable $u_0 \in H^1(\mathsf{D})^d$ as the unique solution to (9.7) with $\Omega = \emptyset$, i.e.

$$\begin{aligned} \int_{\mathsf{D}} \mathbf{A}_2 \epsilon(u_0) : \epsilon(\varphi)\, dx = & \int_{\mathsf{D}} f_2 \cdot \varphi \, dx + \int_{\Gamma^N} g_N \cdot \varphi \, dS \quad \text{for all } \varphi \in H^1_\Gamma(\mathsf{D})^d, \\ u_0 = & g_D \quad \text{on } \Gamma. \end{aligned} \tag{12.3}$$

Assumption B. We henceforth assume that $u_0 \in C^3(B_\delta(x_0))^d$ for a small radius $\delta > 0$.

Note that this can be achieved by assuming enough regularity on the data. In what follows, we are going to derive the asymptotic expansion of u_ε using the **compound layer method**; see [81], [80]. We note that this expansion has already been computed in [32] by means of a Green's function and earlier in [11] for $f_\Omega = 0$.
The compound layer method is based on the strategy to approximate the perturbed variable u_ε by u_0 and introduce a sequence of corrector variables; **boundary layer correctors** and **regular correctors**. While boundary layer correctors aim to approximate the error in the vicinity of the perturbation x_0, they introduce an error on the boundary. This error in turn is corrected by regular correctors, which are homogeneous solutions to the underlying PDE. Hence an alternating interplay between both corrector types will increase the accuracy of the approximation.
While regular correctors are solutions to PDEs on the fixed domain D, boundary layer correctors solve exterior problems on the whole domain $\mathbf{R}^d$. In order to guarantee solvability of these equations we need to introduce an appropriate function space:

Definition 12.1. For $d \geq 1$ and $1 < p < \infty$ we define

$$BL_p(\mathbf{R}^d)^d := \{v \in W^{1,p}_{\text{loc}}(\mathbf{R}^d)^d \,|\, \partial v \in L_p(\mathbf{R}^d)^{d\times d}\}. \tag{12.4}$$

The Beppo-Levi space $\left(\dot{BL}_p(\mathbf{R}^d)^d, \|\cdot\|_{BL_p}\right)$ is defined by

$$\dot{BL}_p(\mathbf{R}^d)^d := BL_p(\mathbf{R}^d)^d \setminus \mathbf{R}^d, \tag{12.5}$$

$$\|v\|_{BL_p} := \|\partial v\|_{L_2(\mathbf{R}^d)^{d\times d}} \quad \text{for all } v \in \dot{BL}_p(\mathbf{R}^d)^d. \tag{12.6}$$

Here, $\backslash\mathbf{R}^d$ indicates that we quotient out the constant functions. It can be shown that for $p = 2$ the Beppo-Levi space is a Hilbert space and $C_c^\infty(\mathbf{R}^d)^d \setminus \mathbf{R}^d$ is dense in $\dot{BL}_p(\mathbf{R}^d)^d$ (cf. [22, 46, 89]). An alternative to tackle the exterior problem are weighted Sobolev spaces. For more details we refer to [105]. With these introductory notes we are now able to move on to the asymptotic analysis.

Lemma 12.2. Let u_ε, u_0 be defined in (12.2) and (12.3), respectively. Then there is a constant $C > 0$ independent of ε, such that for $\varepsilon > 0$ sufficiently small there holds

$$\|u_\varepsilon - u_0\|_{H^1(\mathsf{D})^d} \leq C\varepsilon^{\frac{d}{2}}. \tag{12.7}$$

Proof. Subtracting (12.2) for $\varepsilon > 0$ and (12.3) yields

$$\begin{aligned}\int_{\mathsf{D}} \mathbf{A}_{\omega_\varepsilon}\boldsymbol{\epsilon}(u_\varepsilon - u_0) : \boldsymbol{\epsilon}(\varphi)\,dx = &\int_{\omega_\varepsilon} (\mathbf{A}_2 - \mathbf{A}_1)\boldsymbol{\epsilon}(u_0) : \boldsymbol{\epsilon}(\varphi)\,dx \\ &+ \int_{\omega_\varepsilon} (f_1 - f_2)\cdot\varphi\,dx \quad \text{for all } \varphi \in H^1_\Gamma(\mathsf{D})^d.\end{aligned} \tag{12.8}$$

Therefore, testing with $\varphi := u_\varepsilon - u_0 \in H^1_\Gamma(\mathsf{D})^d$, applying Korn's inequality to the gradient term on the left hand side followed by Friedrich's inequality and using Hölder's inequality to estimate the right hand side, leads to

$$\|u_\varepsilon - u_0\|^2_{H^1(\mathsf{D})^d} \leq C\left(\|(\mathbf{A}_2 - \mathbf{A}_1)\boldsymbol{\epsilon}(u_0)\|_{L_2(\omega_\varepsilon)^{d\times d}} + \|f_1 - f_2\|_{L_2(\omega_\varepsilon)^d}\right)\|u_\varepsilon - u_0\|_{H^1(\mathsf{D})^d}, \tag{12.9}$$

for a positive constant $C > 0$. In view of Assumption B, we have $u_0 \in C^3(B_\delta(x_0))$ for $\delta > 0$ small enough and thus (12.9) can be further estimated to obtain

$$\|u_\varepsilon - u_0\|_{H^1(\mathsf{D})^d} \leq C\sqrt{\omega_\varepsilon}(\|(\mathbf{A}_2 - \mathbf{A}_1)\boldsymbol{\epsilon}(u_0)\|_{C(\omega_\varepsilon)^{d\times d}} + \|f_1 - f_2\|_{C(\omega_\varepsilon)^d}). \tag{12.10}$$

Now, the result follows from $\sqrt{|\omega_\varepsilon|} = \sqrt{|\omega|}\varepsilon^{\frac{d}{2}}$. □

Definition 12.3. For almost every $x \in \mathsf{D}$ and $\varepsilon > 0$ small we define the first variation of the state u_ε by

$$U_\varepsilon^{(1)}(x) := \left(\frac{u_\varepsilon - u_0}{\varepsilon}\right) \circ T_\varepsilon(x). \tag{12.11}$$

The second variation of u_ε is defined by

$$U_\varepsilon^{(2)}(x) := \frac{U_\varepsilon^{(1)}(x) - U^{(1)}(x) - \varepsilon^{d-1}u^{(1)} \circ T_\varepsilon}{\varepsilon} \quad \text{for } \varepsilon > 0. \tag{12.12}$$

More generally, we define the $(i+1)$-th variation of u_ε for $i \geq 2$ by

$$U_\varepsilon^{(i+1)}(x) := \frac{U_\varepsilon^{(i)}(x) - U^{(i)}(x) - \varepsilon^{d-2}u^{(i)} \circ T_\varepsilon}{\varepsilon} \quad \text{for } \varepsilon > 0. \tag{12.13}$$

Here, $U^{(i)} : \mathbf{R}^d \to \mathbf{R}^d$ are the previously mentioned boundary layer correctors and $u^{(i)} : \mathsf{D} \to \mathbf{R}^d$ are regular correctors. Extending u_ε and u_0 outside of D by a continuous extension operator $E : H^1(\mathsf{D})^d \to H^1(\mathbf{R}^d)^d$, one can view $U_\varepsilon^{(1)}$ as an element of the Beppo-Levi space $BL_2(\mathbf{R}^d)^d$. This is a consequence of the estimate

$$\|\partial U_\varepsilon^{(1)}\|_{L_2(\mathbf{R}^d)^{d\times d}} \leq \|\partial U_\varepsilon^{(1)}\|_{L_2(\mathsf{D}_\varepsilon)^{d\times d}} \leq \|U_\varepsilon^{(1)}\|_\varepsilon \leq C, \tag{12.14}$$

which is based on Lemma 12.2 and the continuity of the extension operator. Here, as well as in the upcoming analysis we omit the extension operator E to allow a clearer notation. Note that in the special case $\Gamma = \partial \mathsf{D}$, an extension of $U_\varepsilon^{(1)}$ by 0 outside of D is sufficient.
In the following, we show that the first variation of the state converges to a function $U \in BL_2(\mathbf{R}^d)^d$ and determine an equation satisfied by this limit. The next Lemma helps us to handle the inhomogeneous Dirichlet boundary condition on Γ_ε.

Lemma 12.4. Let $\mathbf{A} : \mathbf{R}^{d\times d} \to \mathbf{R}^{d\times d}$ be uniformly positive definite, $F_\varepsilon : H^1_{\Gamma_\varepsilon}(\mathsf{D}_\varepsilon)^d \to \mathbf{R}$ be a linear and continuous functional with respect to $\|\cdot\|_\varepsilon$ and $g_\varepsilon \in H^{\frac{1}{2}}(\Gamma_\varepsilon)^d$. Then there exists a unique $V_\varepsilon \in H^1(\mathsf{D}_\varepsilon)^d$, such that

$$\int_{\mathsf{D}_\varepsilon} \mathbf{A}\epsilon(V_\varepsilon) : \epsilon(\varphi)\, dx = F_\varepsilon(\varphi) \quad \text{for all } \varphi \in H^1_{\Gamma_\varepsilon}(\mathsf{D}_\varepsilon)^d, \tag{12.15}$$

$$V_\varepsilon|_{\Gamma_\varepsilon} = g_\varepsilon. \tag{12.16}$$

Furthermore, there exists a constant $C > 0$ such that

$$\|V_\varepsilon\|_\varepsilon \leq C(\|F_\varepsilon\| + \varepsilon^{\frac{1}{2}}\|g_\varepsilon\|_{L_2(\Gamma_\varepsilon)^d} + |g_\varepsilon|_{H^{\frac{1}{2}}(\Gamma_\varepsilon)^d}). \tag{12.17}$$

Proof. Let $a_\varepsilon(u,v) := \int_{\mathsf{D}_\varepsilon} \mathbf{A}\epsilon(u) : \epsilon(v)\, dx$, for $u, v \in H^1(\mathsf{D}_\varepsilon)^d$. Thanks to our assumption, $\mathbf{A}$ is uniformly positive definite and thus one readily checks that a_ε is an elliptic and continuous bilinear form on $H^1_{\Gamma_\varepsilon}(\mathsf{D}_\varepsilon)^d$ endowed with the scaled norm $\|\cdot\|_\varepsilon$. Furthermore, let Z_{Γ_ε} denote the right-inverse extension operator of the trace operator T_{Γ_ε} and define $G_\varepsilon := Z_{\Gamma_\varepsilon}(g_\varepsilon) \in H^1(\mathsf{D}_\varepsilon)^d$. Now consider $\tilde{F}_\varepsilon(\varphi) := F_\varepsilon(\varphi) - a_\varepsilon(G_\varepsilon, \varphi)$. Since

$$\begin{aligned} |\tilde{F}_\varepsilon(\varphi)| &\leq |F_\varepsilon(\varphi)| + |a_\varepsilon(G_\varepsilon, \varphi)| \\ &\leq C\|F_\varepsilon\|\|\varphi\|_\varepsilon + C\|G_\varepsilon\|_\varepsilon\|\varphi\|_\varepsilon \leq C\|\varphi\|_\varepsilon \quad \text{for all } \varphi \in H^1_{\Gamma_\varepsilon}(\mathsf{D}_\varepsilon)^d, \end{aligned} \tag{12.18}$$

for a constant $C > 0$, $\tilde{F}_\varepsilon$ is continuous with respect to $\|\cdot\|_\varepsilon$. Thus, by the Lax-Milgram theorem, there exists a unique $u_\varepsilon \in H^1_{\Gamma_\varepsilon}(\mathsf{D}_\varepsilon)^d$, such that

$$a_\varepsilon(u_\varepsilon, \varphi) = \tilde{F}_\varepsilon(\varphi) \quad \text{for all } \varphi \in H^1_{\Gamma_\varepsilon}(\mathsf{D}_\varepsilon)^d. \tag{12.19}$$

Hence, we conclude that $V_\varepsilon := u_\varepsilon + G_\varepsilon$ satisfies (12.15) and (12.16). Uniqueness is guaranteed by the ellipticity of a_ε. Applying the triangle inequality and using the continuity of Z_{Γ_ε} to estimate $\|G_\varepsilon\|_\varepsilon$ yields

$$\begin{aligned} \|V_\varepsilon\|_\varepsilon &\leq \|u_\varepsilon\|_\varepsilon + \|G_\varepsilon\|_\varepsilon \leq C(\|\tilde{F}_\varepsilon\| + \|G_\varepsilon\|_\varepsilon) \leq C(\|F_\varepsilon\| + \|G_\varepsilon\|_\varepsilon) \\ &\leq C(\|F_\varepsilon\| + \varepsilon^{\frac{1}{2}}\|g_\varepsilon\|_{L_2(\Gamma_\varepsilon)^d} + |g_\varepsilon|_{H^{\frac{1}{2}}(\Gamma_\varepsilon)^d}), \end{aligned}$$

which shows (12.17) and thus finishes the proof. □

The subsequent analysis heavily relies on the knowledge of the fundamental solution $\Gamma_{\gamma,\mu}$ of the Lamé system. We thus recall that $\Gamma_{\gamma,\mu}$ admits the following representation [8], [9, Lemma 3.3.2]

$$\Gamma_{\gamma,\mu}(x)_{ij} = \begin{cases} \frac{\gamma+3\mu}{4\pi\mu(\gamma+2\mu)}\left(-\log|x|\delta_{ij} + \frac{\gamma+\mu}{\gamma+3\mu}\frac{x_i x_j}{|x|^2}\right) & \text{for } d=2, \\ \frac{\gamma+3\mu}{8\pi\mu(\gamma+2\mu)}\left(\frac{1}{|x|}\delta_{ij} + \frac{\gamma+\mu}{\gamma+3\mu}\frac{x_i x_j}{|x|^3}\right) & \text{for } d=3. \end{cases} \tag{12.20}$$

Lemma 12.5. There exists a unique solution $[U] \in \dot{BL}_2(\mathbf{R}^d)^d$ to

$$\int_{\mathbf{R}^d} \mathbf{A}_\omega \epsilon([U]) : \epsilon(\varphi)\, dx = \int_\omega (\mathbf{A}_2 - \mathbf{A}_1)\epsilon(u_0)(x_0) : \epsilon(\varphi)\, dx \quad \text{for all } \varphi \in \dot{BL}_2(\mathbf{R}^d)^d. \tag{12.21}$$

Moreover, there exists a representative $U^{(1)} \in [U]$, which satisfies pointwise for $|x| \to \infty$:

$$U^{(1)}(x) = R^{(1)}(x) + \mathcal{O}(|x|^{-d}), \tag{12.22}$$

where $R^{(1)} : \mathbf{R}^d \to \mathbf{R}^d$ satisfies

$$|R^{(1)}(x)| = \begin{cases} b_2|x|^{-1} & \text{for } d=2, \\ b_3|x|^{-2} & \text{for } d=3, \end{cases} \tag{12.23}$$

for some constants $b_2, b_3 \in \mathbf{R}$.

Proof. Since the domain of integration is bounded, the right hand side of (12.21) is continuous with respect to $\|\cdot\|_{\dot{BL}_2}$. Hence, unique solvability follows from the Lemma of Lax-Milgram. The only thing left to show is the asymptotic behaviour (12.22) of $U^{(1)}$. Therefore, we first note that $U^{(1)}$ can be characterised by the following set of equations:

$$\begin{aligned} -\operatorname{div}(\mathbf{A}_1\epsilon(U^{(1)})) &= 0 && \text{in } \omega, && (12.24)\\ -\operatorname{div}(\mathbf{A}_2\epsilon(U^{(1)})) &= 0 && \text{in } \bar{\omega}^c, && (12.25)\\ [U^{(1)}]^+ &= [U^{(1)}]^- && \text{on } \partial\omega, && (12.26)\\ [\mathbf{A}_1\epsilon(U^{(1)})n]^+ - [\mathbf{A}_2\epsilon(U^{(1)})n]^- &= (\mathbf{A}_2 - \mathbf{A}_1)\epsilon(U^{(1)})(x_0)n && \text{on } \partial\omega, && (12.27) \end{aligned}$$

where n denotes the normal vector on $\partial\omega$. In [9, p.76, Theorem 3.3.8] it is shown that there are $f, g \in L_2(\partial\omega)^d$ such that

$$\begin{aligned} [\mathcal{S}^1_\omega f]^+ - [\mathcal{S}^2_\omega g]^- &= 0 \quad \text{on } \partial\omega, \\ [\mathbf{A}_1\epsilon(\mathcal{S}^1_\omega f)n]^+ - [\mathbf{A}_2\epsilon(\mathcal{S}^2_\omega g)n]^- &= (\mathbf{A}_2 - \mathbf{A}_1)\epsilon(U^{(1)})(x_0)n \quad \text{on } \partial\omega, \end{aligned} \tag{12.28}$$

where $\mathcal{S}^i_\omega f$ denotes the single layer potential on $\partial\omega$ with respect to the fundamental solution Γ_i, i.e.

$$\mathcal{S}^i_\omega h(x) := \int_{\partial\omega} \Gamma_i(x-y)h(y)\, dS(y), \tag{12.29}$$

for $i \in \{1,2\}$ and a function $h \in L_2(\partial\omega)^d$. Additionally, since $\int_{\partial\omega}(\mathbf{A}_2 - \mathbf{A}_1)\epsilon(U^{(1)})(x_0)n\, dS = 0$, it follows that $\int_{\partial\omega} g\, dS = 0$ (cf. [9, p.76, Theorem 3.3.8]). Thus,

$$U^{(1)} := \begin{cases} \mathcal{S}^1_\omega f & \text{in } \omega, \\ \mathcal{S}^2_\omega g & \text{in } \bar{\omega}^c, \end{cases}$$

satisfies (12.24)-(12.27). Furthermore, considering $\int_{\partial\omega} g \, dS = 0$ and the asymptotic behaviour of the fundamental solution Γ_2, a Taylor expansion of $\Gamma_2(x-y)$ in $y=0$ yields the desired asymptotic behaviour (12.22). □

The next result covers the first order asymptotic expansion of the state variable.

Theorem 12.6. Let $U_\varepsilon^{(1)}$ be as in Definition 12.3 and $\alpha \in (0,1)$. There exists a constant $C>0$ independent of ε such that

$$\|U_\varepsilon^{(1)} - U^{(1)}\|_\varepsilon \leq \begin{cases} C\varepsilon^{1-\alpha} & \text{for } d=2, \\ C\varepsilon & \text{for } d=3, \end{cases} \tag{12.30}$$

for $\varepsilon > 0$ sufficiently small.

Proof. We start by deriving an equation for $U_\varepsilon^{(1)}$. For this purpose, we change variables in (12.8) to obtain

$$\begin{aligned} \int_{\mathsf{D}_\varepsilon} \mathbf{A}_\omega \epsilon(U_\varepsilon^{(1)}) : \epsilon(\varphi)\, dx = & \int_\omega (\mathbf{A}_2 - \mathbf{A}_1)\epsilon(u_0)\circ T_\varepsilon : \epsilon(\varphi)\, dx \\ & + \varepsilon \int_\omega (f_1 - f_2)\circ T_\varepsilon \cdot \varphi \, dx \quad \text{ for all } \varphi \in H^1_{\Gamma_\varepsilon}(\mathsf{D}_\varepsilon)^d. \end{aligned} \tag{12.31}$$

Splitting the integral on the left hand side of (12.21), integrating by parts and using $\operatorname{div}(\mathbf{A}_2\epsilon(U^{(1)}))=0$ in $\bar{\omega}^{\mathsf{c}}$ yields

$$\begin{aligned} \int_{\mathsf{D}_\varepsilon} \mathbf{A}_\omega \epsilon(U^{(1)}) : \epsilon(\varphi)\, dx &= \int_\omega (\mathbf{A}_2 - \mathbf{A}_1)\epsilon(x_0) : \epsilon(\varphi)\, dx - \int_{\mathbf{R}^d\setminus \mathsf{D}_\varepsilon} \mathbf{A}_2 \epsilon(U^{(1)}) : \epsilon(\tilde{\varphi})\, dx \\ &= \int_\omega (\mathbf{A}_2 - \mathbf{A}_1)\epsilon(x_0) : \epsilon(\varphi)\, dx - \int_{\Gamma_\varepsilon^N} \mathbf{A}_2 \epsilon(U^{(1)})\tilde{n} \cdot \tilde{\varphi}\, dS \\ &\quad + \int_{\mathbf{R}^d\setminus \mathsf{D}_\varepsilon} \operatorname{div}(\mathbf{A}_2 \epsilon(U^{(1)})) \cdot \tilde{\varphi}\, dx \\ &= \int_\omega (\mathbf{A}_2 - \mathbf{A}_1)\epsilon(x_0) : \epsilon(\varphi)\, dx + \int_{\Gamma_\varepsilon^N} \mathbf{A}_2 \epsilon(U^{(1)}) n \cdot \varphi\, dS, \end{aligned} \tag{12.32}$$

where $\varphi \in H^1_{\Gamma_\varepsilon}(\mathsf{D}_\varepsilon)^d$, $\tilde{\varphi}$ denotes an extension to the whole domain and $\tilde{n}$ denotes the outer normal vector on the boundary of $\mathbf{R}^d \setminus \mathsf{D}_\varepsilon$. Subtracting (12.31) and (12.32) results in

$$\begin{aligned} \int_{\mathsf{D}_\varepsilon} \mathbf{A}_\omega \epsilon(U_\varepsilon^{(1)} - U^{(1)}) : \epsilon(\varphi)\, dx = & \int_\omega (\mathbf{A}_2 - \mathbf{A}_1)[\epsilon(u_0)\circ T_\varepsilon - \epsilon(u_0)(x_0)] : \epsilon(\varphi)\, dx \\ & + \varepsilon \int_\omega (f_1 - f_2)\circ T_\varepsilon \cdot \varphi\, dx \\ & - \int_{\Gamma_\varepsilon^N} \mathbf{A}_2 \epsilon(U^{(1)}) n \cdot \varphi\, dS, \end{aligned} \tag{12.33}$$

for all $\varphi \in H^1_{\Gamma_\varepsilon}(\mathrm{D}_\varepsilon)^d$. Next, we apply Lemma 12.4 to $V_\varepsilon := U^{(1)}_\varepsilon - U^{(1)}$, $g_\varepsilon := -U^{(1)}|_{\Gamma_\varepsilon}$ and F^1_ε defined as the right hand side of (12.33). Thus, we conclude that there exists a constant $C > 0$, such that

$$\|U^{(1)}_\varepsilon - U^{(1)}\|_\varepsilon \le C(\|F^1_\varepsilon\| + \varepsilon^{\frac{1}{2}}\|U^{(1)}\|_{L_2(\Gamma_\varepsilon)^d} + |U^{(1)}|_{H^{\frac{1}{2}}(\Gamma_\varepsilon)^d}). \tag{12.34}$$

To finish our proof, we need to estimate the norms of F^1_ε and $U^{(1)}$, which appear in (12.34). For the sake of clarity, we split the functional F^1_ε according to (12.33) and treat each term separately.
Let $\varphi \in H^1_{\Gamma_\varepsilon}(\mathrm{D}_\varepsilon)$. Throughout this proof, $C \in \mathbf{R}$ denotes a positive constant independent of ε.

- At first, we consider $\int_\omega (\mathbf{A}_2 - \mathbf{A}_1)[\epsilon(u_0) \circ T_\varepsilon - \epsilon(u_0)(x_0)] : \epsilon(\varphi)\, dx$. Since $u_0 \in C^3(B_\delta(x_0))$, we get

$$\epsilon(u_0)(x_0 + \varepsilon x) = \epsilon(u_0)(x_0) + \partial\epsilon(u_0)(x_0)\varepsilon x + o(\varepsilon x). \tag{12.35}$$

  Combined with an application of Hölder's inequality, we conclude

$$\begin{aligned}\left|\int_\omega [\epsilon(u_0) \circ T_\varepsilon - \epsilon(u_0)(x_0)] : \epsilon(\varphi)\, dx\right| &\le C\|\epsilon(u_0) \circ T_\varepsilon - \epsilon(u_0)(x_0)\|_{L_2(\omega)}\|\epsilon(\varphi)\|_{L_2(\omega)^{d\times d}} \\ &\le C\varepsilon\|\epsilon(\varphi)\|_{L_2(\omega)^{d\times d}} \le C\varepsilon\|\varphi\|_\varepsilon.\end{aligned} \tag{12.36}$$

- Next, we consider $\varepsilon \int_\omega (f_1 - f_2) \circ T_\varepsilon \cdot \varphi\, dx$. Since we want to apply the Gagliardo-Nirenberg inequality, we need to distinguish between dimensions $d = 2$ and $d = 3$.
  For $d = 3$ an application of Hölder's inequality with respect to $p = 2^*$ and Lemma 11.5, item (ii) yield

$$\left|\varepsilon \int_\omega (f_1 - f_2) \circ T_\varepsilon \cdot \varphi\, dx\right| \le C\varepsilon\|\varphi\|_\varepsilon. \tag{12.37}$$

  For $d = 2$ we apply Hölder's inequality with respect to $p = (2-\delta)^*$ for $\delta > 0$ sufficiently small and Lemma 11.5, item (iii) to obtain

$$\left|\varepsilon \int_\omega (f_1 - f_2) \circ T_\varepsilon \cdot \varphi\, dx\right| \le C\varepsilon^{1-\alpha}\|\varphi\|_\varepsilon. \tag{12.38}$$

  for a constant $C > 0$ and $\alpha > 0$ arbitrarily small.

- Finally, the last term can be estimated using Hölder's inequality and the scaled trace inequality (Lemma 11.5 item (iv)):

$$\left|\int_{\Gamma^N_\varepsilon} \mathbf{A}_2\epsilon(U^{(1)})n \cdot \varphi\, dS\right| \le C\|\epsilon(U^{(1)})\|_{L_2(\partial\mathrm{D}_\varepsilon)^{d\times d}}\|\varphi\|_{L_2(\partial\mathrm{D}_\varepsilon)^d} \tag{12.39}$$

$$\le C\varepsilon^{-\frac{1}{2}}\|\epsilon(U^{(1)})\|_{L_2(\partial\mathrm{D}_\varepsilon)^{d\times d}}\|\varphi\|_\varepsilon. \tag{12.40}$$

  Thus, Lemma 11.6, item (iii) with $m = d - 1$ yields

$$\left|\int_{\Gamma^N_\varepsilon} \mathbf{A}_2\epsilon(U^{(1)})n \cdot \varphi\, dS\right| \le C\varepsilon^{\frac{d}{2}}\|\varphi\|_\varepsilon. \tag{12.41}$$

Combining these estimates results in

$$\|F_\varepsilon^1\| \le \begin{cases} C\varepsilon^{1-\alpha} & \text{for } d=2,\\ C\varepsilon & \text{for } d=3, \end{cases} \tag{12.42}$$

for a constant $C>0$ and $\alpha>0$ small. Furthermore, Lemma 11.6 item (i) and (ii) with $m=d-1$ entail

$$\|U^{(1)}\|_{L_2(\Gamma_\varepsilon)^d} \le C\varepsilon^{\frac{d-1}{2}}, \quad |U^{(1)}|_{H^{\frac{1}{2}}(\Gamma_\varepsilon)^d} \le C\varepsilon^{\frac{d}{2}}. \tag{12.43}$$

Now plugging (12.42) and (12.43) into (12.34) finishes the proof. □

Note that for the first order approximation, boundary layer correctors are sufficient to achieve an appropriate approximation of the state variable. Yet, as it is visualised in the proof (cf. (12.43) and the last term in (12.33)), these introduce an error on the boundary. Even though this error is sufficiently small for the time being, it will reappear in the second order approximation, where two regular correctors are required.

Remark 12.7. At this point, we want to address some differences that occur, when the general case $\Omega \neq \emptyset$ is considered. Whilst the boundary layer corrector is defined identically in the general case, it introduces an additional error in the domain $\Omega^\varepsilon := T_\varepsilon^{-1}(\Omega)$. Since by our assumption $x_0 \notin \bar{\Omega}$, Ω^ε is shifted to the exterior as $\varepsilon \searrow 0$ (cf. Figure 11). Hence, remainder estimates for volume terms of $U^{(1)}$ in the exterior domain similarly to Lemma 11.5 enable an analogous analysis of the generalised problem.

Corollary 12.8. There holds

$$\lim_{\varepsilon \searrow 0} U_\varepsilon^{(1)} = U^{(1)} \quad \text{in } L_1(\omega)^d. \tag{12.44}$$

Proof. Let $\alpha \in (0,1)$ for $d=2$ and $\alpha = 0$ for $d=3$. Furthermore, for $p \in (1,\infty)$ let p' denote the Hölder conjugate, i.e. $p' = \frac{p}{1-p}$. Hölder's inequality and Lemma 11.5 item (ii), (iii) imply

$$\|U_\varepsilon^{(1)} - U^{(1)}\|_{L_1(\omega)^d} \le \|U_\varepsilon^{(1)} - U^{(1)}\|_{L_{(2-\alpha)^*}(\omega)^d} \|1\|_{L_{[(2-\alpha)^*]'}(\omega)^d} \le C\varepsilon^{-\alpha} \|U_\varepsilon^{(1)} - U^{(1)}\|_\varepsilon, \tag{12.45}$$

since ω is bounded. Choosing α sufficiently small, the result follows from Theorem 12.6. □

Remark 12.9. Reformulating the expression $U_\varepsilon^1 - U^1$ leaves us with the first order expansion

$$u_\varepsilon(x) \approx u_0(x) + \varepsilon U^1(T_\varepsilon^{-1}(x)),$$

where

$$\|u_\varepsilon - [u_0 + \varepsilon U^1 \circ T_\varepsilon^{-1}]\|_{H^1(\mathrm{D})^d} = \begin{cases} \mathcal{O}(\varepsilon^{\frac{d}{2}+1-\alpha}) & \text{for } d=2,\\ \mathcal{O}(\varepsilon^{\frac{d}{2}+1}) & \text{for } d=3. \end{cases} \tag{12.46}$$

We continue with the second order asymptotic expansion of u_ε. We therefore require a boundary layer corrector $U^{(2)}$, which acts similarly to $U^{(1)}$ but on a higher order. Furthermore, as we have just mentioned, we need to introduce two regular correctors. One for each boundary layer corrector, respectively. We specify their definition in the next lemma.

Lemma 12.10. We have the following existence results:

- There is a unique solution $u^{(1)} \in H^1(\mathsf{D})^d$ with $u^{(1)}(x) = -R^{(1)}(x - x_0)$ on Γ, such that

$$\int_{\mathsf{D}} \mathbf{A}_2 \epsilon(u^{(1)}) : \epsilon(\varphi)\, dx = -\int_{\Gamma^N} \mathbf{A}_2 \epsilon(R^{(1)})(x - x_0) n \cdot \varphi\, dS, \tag{12.47}$$

for all $\varphi \in H^1_\Gamma(\mathsf{D})^d$.

- There is a solution $[U] \in \dot{BL}_p(\mathbf{R}^d)^d$ to

$$\int_{\mathbf{R}^d} \mathbf{A}_\omega \epsilon([U]) : \epsilon(\varphi)\, dx = \int_\omega (\mathbf{A}_2 - \mathbf{A}_1)[\partial \epsilon(u_0)(x_0) x] : \epsilon(\varphi)\, dx, \tag{12.48}$$

for all $\varphi \in \dot{BL}_{p'}(\mathbf{R}^d)^d$, where

$$p = \begin{cases} 2 + \delta & \text{for } d = 2, \\ 2 & \text{for } d = 3, \end{cases}$$

and $\delta > 0$ small. Moreover, there exists a representative $\hat{U}^{(2)} \in [U]$, which satisfies pointwise for $|x| \to \infty$:

$$\hat{U}^{(2)}(x) = \hat{R}^{(2)}(x) + \mathcal{O}(|x|^{1-d}), \tag{12.49}$$

where $\hat{R}^{(2)} : \mathbf{R}^d \to \mathbf{R}^d$ satisfies

$$|\hat{R}^{(2)}(x)| = \begin{cases} \hat{c}_2 \ln(|x|) & \text{for } d = 2, \\ \hat{c}_3 |x|^{-1} & \text{for } d = 3, \end{cases} \tag{12.50}$$

for some constants $\hat{c}_2, \hat{c}_3 \in \mathbf{R}$.

- There exists a solution $[U] \in \dot{BL}_p(\mathbf{R}^d)^d$ to

$$\int_{\mathbf{R}^d} \mathbf{A}_\omega \epsilon([U]) : \epsilon(\varphi)\, dx = \int_\omega [(f_1(x_0) - f_2(x_0))] \cdot \varphi\, dx, \tag{12.51}$$

for all $\varphi \in C^1_c(\mathbf{R}^d)^d$, where

$$p = \begin{cases} 2 + \delta & \text{for } d = 2, \\ 2 & \text{for } d = 3, \end{cases}$$

and $\delta > 0$ small. Moreover, there exists a representative $\tilde{U}^{(2)} \in [U]$, which satisfies pointwise for $|x| \to \infty$:

$$\tilde{U}^{(2)}(x) = \tilde{R}^{(2)}(x) + \mathcal{O}(|x|^{1-d}), \tag{12.52}$$

where $\tilde{R}^{(2)} : \mathbf{R}^d \to \mathbf{R}^d$ satisfies

$$|\tilde{R}^{(2)}(x)| = \begin{cases} \tilde{c}_2 \ln(|x|) & \text{for } d = 2, \\ \tilde{c}_3 |x|^{-1} & \text{for } d = 3, \end{cases} \tag{12.53}$$

for some constants $\tilde{c}_2, \tilde{c}_3 \in \mathbf{R}$.

- There is a unique solution $u^{(2)} \in H^1(\mathsf{D})^d$ with $u^{(2)}(x) = -R^{(2)}(x-x_0)$ on Γ, such that

$$\int_{\mathsf{D}} \mathbf{A}_2 \epsilon(u^{(2)}) : \epsilon(\varphi)\, dx = -\int_{\Gamma^N} \mathbf{A}_2 \epsilon(R^{(2)})(x-x_0) n \cdot \varphi \, dS, \tag{12.54}$$

for all $\varphi \in H^1_\Gamma(\mathsf{D})^d$, where $R^{(2)} = \hat{R}^{(2)} + \tilde{R}^{(2)}$.

Proof. Unique solvability of (12.47) and (12.54) follows from the Lax-Milgram theorem. In order to show the existence and the desired representation formula of $\tilde{U}^{(2)}$, we use single layer potentials. Note that a solution $U \in BL_p(\mathbf{R}^d)^d$ of (12.51) can be characterised by the following set of equations:

$$-\operatorname{div}(\mathbf{A}_1 \epsilon(U)) = f_1(x_0) - f_2(x_0) \quad \text{in } \omega, \tag{12.55}$$

$$-\operatorname{div}(\mathbf{A}_2 \epsilon(U)) = 0 \quad \text{in } \bar{\omega}^c, \tag{12.56}$$

$$[U]^+ = [U]^- \quad \text{on } \partial\omega, \tag{12.57}$$

$$[\mathbf{A}_1 \epsilon(U) n]^+ = [\mathbf{A}_2 \epsilon(U) n]^- \quad \text{on } \partial\omega. \tag{12.58}$$

Now consider the volume potential $u(x) := \int_\omega \Gamma_1(x-y)[(f_1(x_0) - f_2(x_0))]\, dy$, for $x \in \omega$, which satisfies the inhomogeneous equation inside ω. By [9, p.76, Theorem 3.3.8] there are $f, g \in L_2(\partial\omega)^d$, such that

$$[\mathcal{S}^1_\omega f]^+ - [\mathcal{S}^2_\omega g]^- = -u|_{\partial\omega} \quad \text{on } \partial\omega, \tag{12.59}$$

$$[\mathbf{A}_1 \epsilon(\mathcal{S}^1_\omega f) n]^+ - [\mathbf{A}_2 \epsilon(\mathcal{S}^2_\omega g) n]^- = -(\mathbf{A}_1 \epsilon(u) n)|_{\partial\omega} \quad \text{on } \partial\omega. \tag{12.60}$$

Finally,

$$\tilde{U}^{(2)} := \begin{cases} u + \mathcal{S}^1_\omega f & \text{in } \omega, \\ \mathcal{S}^2_\omega g & \text{in } \bar{\omega}^c, \end{cases}$$

satisfies (12.55)-(12.58) and a Taylor expansion of $\mathcal{S}^2_\omega g$ shows the asymptotic representation of (12.52). The proof for $\hat{U}^{(2)}$ is similar and therefore omitted. □

Based on this lemma we introduce

$$U^{(2)} := \hat{U}^{(2)} + \tilde{U}^{(2)}, \quad R^{(2)} := \hat{R}^{(2)} + \tilde{R}^{(2)}. \tag{12.61}$$

Remark 12.11. Note that the requirement for p to be greater than 2 in dimension two is necessary to guarantee that the gradients of $\tilde{U}^{(2)}$ and $\hat{U}^{(2)}$ are in $L_p(\mathbf{R}^d)^{d\times d}$, which is not true for $p = 2$. In fact, there is a solution $[U] \in \dot{BL}(\mathbf{R}^2)^2$ of (12.48), but no representative $U \in [U]$ has the desired asymptotic representation. Furthermore, it is noteworthy that $\tilde{U}^{(2)}$ and $\hat{U}^{(2)}$ have a lower order asymptotic behaviour compared to $U^{(1)}$. This is a consequence of the vanishing average $\int_{\partial\omega} g\, dS = 0$ for the underlying function of the single layer potential corresponding to $U^{(1)}$. This in turn is directly linked to the fact that the right hand side in (12.27) is a constant. We will see in Part III of this thesis, which deals with higher order expansions, that indeed the first order expansion for transmission problems is a special case in this regard.

Remark 12.12. As a consequence of the equivalence relation defining the Beppo-Levi space, the function $U^{(2)}$ is defined up to a constant. Thus, we are allowed to add arbitrary constants to the boundary layer corrector $U^{(2)}$. As a result of the additive property of the leading term $R^{(2)}(x) = \ln(x)$, we need to add the ε dependent constant $c \ln(\varepsilon)$, with a suitable constant $c \in \mathbf{R}$ in dimension $d = 2$. In dimension $d = 3$ this problem does not appear since the leading term $|x|^{-1}$ is multiplicative and therefore can be compensated by the factor ε^{d-2} found in Definition 12.3.

Remark 12.13. A possible approach to approximate the solution $\tilde{U}^{(2)}$ of (12.51) numerically is to consider for each $\varepsilon > 0$ the unique solution $K_\varepsilon \in W_0^{1,p}(\mathsf{D})^d$ satisfying

$$\varepsilon^2 \int_{\mathsf{D}} \mathbf{A}_{\omega_\varepsilon} \epsilon(K_\varepsilon) : \epsilon(\varphi)\, dx = \int_{\omega_\varepsilon} [(f_1(x_0) - f_2(x_0))]\varphi\, dx, \tag{12.62}$$

for all $\varphi \in W_0^{1,p}(\mathsf{D})^d$. Applying Hölder's inequality and the Gagliardo-Nirenberg inequality for functions with vanishing trace (cf. [51, p. 279, Theorem 3]) entails

$$\left| \int_{\omega_\varepsilon} [(f_1(x_0) - f_2(x_0))]\varphi\, dx \right| \le |\omega_\varepsilon|^{\frac{1}{((p')^*)'}} \|\partial\varphi\|_{L_{p'}(\mathsf{D})^{d\times d}}. \tag{12.63}$$

Lemma 11.4 item (ii) yields

$$\varepsilon^2 \|\partial K_\varepsilon\|_{L_p(\mathsf{D})^{d\times d}} = \varepsilon^{\frac{d}{p}+1} \|\partial(K_\varepsilon \circ T_\varepsilon)\|_{L_p(\mathsf{D}_\varepsilon)^{d\times d}}.$$

Furthermore, a detailed computation shows

$$|\omega_\varepsilon|^{\frac{1}{((p')^*)'}} = C\varepsilon^{\frac{d+p}{p}},$$

for a constant $C > 0$. Hence, $K_\varepsilon \circ T_\varepsilon$ is bounded in $\dot{BL}_p$ and therefore has a weakly convergent subsequence with limit $[U]$ satisfying (12.51).

We are now able to state the main theorem covering the second order asymptotic expansion (cf. Theorem 12.6).

Theorem 12.14. Let $U_\varepsilon^{(2)}$ be as in Definition 12.3 and $\alpha \in (0,1)$.

(i) There is a constant $C > 0$ independent of ε such that

$$\|U_\varepsilon^{(2)} - U^{(2)} - \varepsilon^{d-2} u^{(2)} \circ T_\varepsilon - c\ln(\varepsilon)\|_\varepsilon \le C\varepsilon^{1-\alpha} \quad \text{for } d = 2, \tag{12.64}$$

$$\|U_\varepsilon^{(2)} - U^{(2)} - \varepsilon^{d-2} u^{(2)} \circ T_\varepsilon\|_\varepsilon \le C\varepsilon \quad \text{for } d = 3, \tag{12.65}$$

for $\varepsilon > 0$ sufficiently small and a suitable constant $c \in \mathbf{R}$.

(ii) There holds

$$\lim_{\varepsilon \searrow 0} \|\varepsilon^{-1}(\partial U_\varepsilon^{(1)} - \partial U^{(1)}) - \partial U^{(2)}\|_{L_2(\omega)^{d\times d}} = 0. \tag{12.66}$$

Proof. ad (i): Similarly to the estimation of the first order expansion, we aim to apply Lemma 12.4 in order to handle the inhomogeneous Dirichlet boundary condition on Γ_ε. Hence, we start by deriving an equation satisfied by $\varepsilon U_\varepsilon^{(3)} = U_\varepsilon^{(2)} - U^{(2)} - \varepsilon^{d-2} u^{(2)} \circ T_\varepsilon(x)$. Dividing (12.33) by $\varepsilon > 0$, changing variables in (12.47) and (12.54), and integrating by parts in the exterior domain of (12.48) and (12.51) yields

$$\int_{\mathsf{D}_\varepsilon} \mathbf{A}_\omega \epsilon(\varepsilon U_\varepsilon^{(3)}) : \epsilon(\varphi)\, dx = F_\varepsilon^2(\varphi) + F_\varepsilon^3(\varphi) \quad \text{for all } \varphi \in H^1_{\Gamma_\varepsilon}(\mathsf{D}_\varepsilon), \tag{12.67}$$

where

$$
\begin{aligned}
F_\varepsilon^2 :=& \int_\omega [(f_1 \circ T_\varepsilon - f_2 \circ T_\varepsilon) - (f_1(x_0) - f_2(x_0))] \cdot \varphi \, dx \\
&+ \int_\omega (\mathbf{A}_2 - \mathbf{A}_1)[\varepsilon^{-1}(\epsilon(u_0) \circ T_\varepsilon - \epsilon(u_0)(x_0)) - \partial\epsilon(u_0)(x_0)x] : \epsilon(\varphi) \, dx \\
&+ \varepsilon^{d-1} \int_\omega (\mathbf{A}_2 - \mathbf{A}_1)[\epsilon(u^{(1)} \circ T_\varepsilon) + \epsilon(u^{(2)} \circ T_\varepsilon)] : \epsilon(\varphi) \, dx,
\end{aligned} \tag{12.68}
$$

$$
\begin{aligned}
F_\varepsilon^3 :=& -\varepsilon^{-1} \int_{\Gamma^N e} [\mathbf{A}_2 \epsilon(U^{(1)}) - \varepsilon^d \mathbf{A}_2 \epsilon(R^{(1)})(\varepsilon x)] n \cdot \varphi \, dS \\
&- \int_{\Gamma^N e} [\mathbf{A}_2 \epsilon(U^{(2)}) - \varepsilon^{d-1} \mathbf{A}_2 \epsilon(R^{(2)})(\varepsilon x)] n \cdot \varphi \, dS.
\end{aligned} \tag{12.69}
$$

Since the bilinear form only depends on the symmetrised gradient of $U_\varepsilon^{(3)}$, one readily checks that $\varepsilon U_\varepsilon^{(3)} + c\ln(\varepsilon)$ satisfies

$$
\int_{\mathsf{D}_\varepsilon} \mathbf{A}_\omega \epsilon(\varepsilon U_\varepsilon^{(3)} + c\ln(\varepsilon)) : \epsilon(\varphi) \, dx = F_\varepsilon^2(\varphi) + F_\varepsilon^3(\varphi) \quad \text{for all } \varphi \in H^1_{\Gamma_\varepsilon}(\mathsf{D}_\varepsilon). \tag{12.70}
$$

Now we can apply Lemma 12.4 to

$$
V_\varepsilon := \begin{cases} \varepsilon U_\varepsilon^{(3)} + c\ln(\varepsilon) & \text{for } d = 2, \\ \varepsilon U_\varepsilon^{(3)} & \text{for } d = 3, \end{cases} \tag{12.71}
$$

$$
F_\varepsilon := F_\varepsilon^2 + F_\varepsilon^3, \tag{12.72}
$$

and

$$
g_\varepsilon := \begin{cases} (\varepsilon^{d-2} R^{(1)}(\varepsilon x) - \varepsilon^{-1} U^{(1)})|_{\Gamma_\varepsilon} + (\varepsilon^{d-2} R^{(2)}(\varepsilon x) - U^{(2)} + c\ln(\varepsilon))|_{\Gamma_\varepsilon} & \text{for } d = 2, \\ (\varepsilon^{d-2} R^{(1)}(\varepsilon x) - \varepsilon^{-1} U^{(1)})|_{\Gamma_\varepsilon} + (\varepsilon^{d-2} R^{(2)}(\varepsilon x) - U^{(2)})|_{\Gamma_\varepsilon} & \text{for } d = 3. \end{cases} \tag{12.73}
$$

Hence, we get the a priori estimate

$$
\|V_\varepsilon\|_\varepsilon \leq C(\|F_\varepsilon\| + \varepsilon^{\frac{1}{2}} \|g_\varepsilon\|_{L_2(\Gamma_\varepsilon)^d} + |g_\varepsilon|_{H^{\frac{1}{2}}(\Gamma_\varepsilon)^d}). \tag{12.74}
$$

Due to the similarity between $d = 2$ and $d = 3$, we will discuss both cases together and only highlight the terms that have to be treated separately. Thus, if not further specified, let $d \in \{2, 3\}$. Again, we start by estimating $\|F_\varepsilon\|$. Let $\varphi \in H^1_{\Gamma_\varepsilon}(\mathsf{D}_\varepsilon)$.

- A Taylor expansion of $(f_1(T_\varepsilon(x)) - f_2(T_\varepsilon(x)))$ at x_0, Hölder's inequality and Lemma 11.5, item (ii), (iii) entail

$$
\left| \int_\omega [(f_1 \circ T_\varepsilon - f_2 \circ T_\varepsilon) - (f_1(x_0) - f_2(x_0))] \cdot \varphi \, dx \right| \leq \begin{cases} C\varepsilon^{1-\alpha} \|\varphi\|_\varepsilon & \text{for } d = 2, \\ C\varepsilon \|\varphi\|_\varepsilon & \text{for } d = 3, \end{cases} \tag{12.75}
$$

for a constant $C > 0$ and $\alpha > 0$.

- Since u_0 is three times continuously differentiable in a neighbourhood of x_0, there is a constant $C > 0$, such that $|\varepsilon^{-1}(\epsilon(u_0)\circ T_\varepsilon - \epsilon(u_0)(x_0)) - \partial\epsilon(u_0)(x_0)x| \le C\varepsilon$, for $x \in \omega$. Hence, Hölder's inequality yields

$$\left|\int_\omega (\mathbf{A}_2-\mathbf{A}_1)[\varepsilon^{-1}(\epsilon(u_0)\circ T_\varepsilon - \epsilon(u_0)(x_0)) - \partial\varepsilon(u_0)(x_0)x] : \epsilon(\varphi)\,dx\right| \le C\varepsilon\|\varphi\|_\varepsilon. \tag{12.76}$$

- Furthermore, by Hölder's inequality we get

$$\left|\varepsilon^{d-1}\int_\omega (\mathbf{A}_2-\mathbf{A}_1)[\epsilon(u^{(1)}\circ T_\varepsilon)+\epsilon(u^{(2)}\circ T_\varepsilon)] : \epsilon(\varphi)\,dx\right| \le C\varepsilon\|\varphi\|_\varepsilon, \tag{12.77}$$

  for a constant $C > 0$.

Next we consider the boundary integral terms:

- We note that $\epsilon(U^{(1)})-\varepsilon^d\epsilon(R^{(1)})(\varepsilon x)$ cancels out the leading term of $U^{(1)}$ on ∂D. Thus we can apply Hölder's inequality, Lemma 11.6 item (iii) with $m = d$ and the scaled trace inequality (Lemma 11.5 item (v)) to conclude

$$\left|\varepsilon^{-1}\int_{\Gamma^N e} [\mathbf{A}_2\epsilon(U^{(1)}) - \varepsilon^d\mathbf{A}_2\epsilon(R^{(1)})(\varepsilon x)]n\cdot\varphi\,dS\right| \le C\varepsilon^{\frac{d}{2}}\|\varphi\|_\varepsilon, \tag{12.78}$$

  for a constant $C > 0$.

- Similarly, we deduce from Lemma 11.6, item (iii) with $m = d-1$ that there is a constant $C > 0$, such that

$$\left|\int_{\Gamma^N e} [\mathbf{A}_2\epsilon(U^{(2)}) - \varepsilon^{d-1}\mathbf{A}_2\epsilon(R^{(2)})(\varepsilon x)]n\cdot\varphi\,dS\right| \le C\varepsilon^{\frac{d}{2}}\|\varphi\|_\varepsilon. \tag{12.79}$$

Combining the previous estimates yields

$$\|F_\varepsilon\| \le \begin{cases} C\varepsilon^{1-\alpha} & \text{for } d=2,\\ C\varepsilon & \text{for } d=3,\end{cases} \tag{12.80}$$

for a constant $C > 0$ and $\alpha > 0$ small. In order to estimate the boundary term, we recall that g_ε is defined in (12.73). Therefore, we choose the constant $c \in \mathbf{R}$ such that

$$R^{(2)}(x) = R^{(2)}(\varepsilon x) + c\ln(\varepsilon) \quad \text{in } d=2.$$

Then, by Lemma 11.6, item (i), (ii) with $m = d$ and $m = d-1$ respectively, there is a constant $C > 0$, such that

$$\varepsilon^{\frac{1}{2}}\|g_\varepsilon\|_{L_2(\Gamma_\varepsilon)^d} + |g_\varepsilon|_{H^{\frac{1}{2}}(\Gamma_\varepsilon)^d} \le C\varepsilon^{\frac{d}{2}}. \tag{12.81}$$

Now we can plug (12.80) and (12.81) into the a priori estimate (12.74), which shows (12.64).
ad (ii): By the triangle inequality, we have

$$\begin{aligned}\|\varepsilon^{-1}(\partial(U_\varepsilon^{(1)}) - \partial(U^{(1)})) - \partial(U^{(2)})\|_{L_2(\omega)^{d\times d}} &\\ \le \|\partial(U_\varepsilon^{(2)} - U^{(2)} - \varepsilon^{d-2}u^{(2)}\circ T_\varepsilon)\|_{L_2(\omega)^{d\times d}}&\\ + \varepsilon^{d-1}\|\partial(u^{(1)})\circ T_\varepsilon\|_{L_2(\omega)^{d\times d}} + \varepsilon^{d-1}\|\partial(u^{(2)})\circ T_\varepsilon\|_{L_2(\omega)^{d\times d}}&\\ \le C\varepsilon^{1-\alpha},&\end{aligned} \tag{12.82}$$

for a positive constant C and $\alpha > 0$ small. This shows (ii) and thus finishes the proof. □

Corollary 12.15. In dimension $d=3$ there holds

$$\|\varepsilon^{-1}(U_\varepsilon^{(1)}-U^{(1)})-U^{(2)}\|_\varepsilon \le C\varepsilon^{\frac{1}{2}}, \tag{12.83}$$

for $\varepsilon>0$ sufficiently small.

Proof. The triangle inequality entails

$$\begin{aligned}\|\varepsilon^{-1}(U_\varepsilon^{(1)}-U^{(1)})-U^{(2)}\|_\varepsilon \le & \|U_\varepsilon^{(2)}-U^{(2)}-\varepsilon^{d-2}u^{(2)}\circ T_\varepsilon\|_\varepsilon+\|\varepsilon^{d-2}u^{(1)}\circ T_\varepsilon\|_\varepsilon \\ &+\|\varepsilon^{d-2}u^{(2)}\circ T_\varepsilon\|_\varepsilon.\end{aligned}$$

By Theorem 12.14 the first term on the right hand side can be bound by $C\varepsilon$. Furthermore, Lemma 11.4 item (iii) and Theorem 12.14 show

$$\|\varepsilon^{d-2}u^{(i)}\circ T_\varepsilon\|_\varepsilon=\varepsilon^{d-2-\frac{d}{2}+1}\|u^{(i)}\|_{H^1(\mathrm{D})^d} \quad \text{for } i\in\{1,2\}. \tag{12.84}$$

Now the result follows since $d-2-\frac{d}{2}+1=\frac{1}{2}$. □

Remark 12.16. Note that the result solely remains true in dimension 3. For $d=2$ the exponent vanishes and thus only yields uniform boundedness, but not convergence of the boundary layer correctors. Corollary 12.15 states that the correctors $u^{(1)}, u^{(2)}$ are not necessary to achieve convergence of $\varepsilon^{-1}(U_\varepsilon^{(1)}-U^{(1)})$ in dimension $d=3$. In fact, sparing the correctors results in a slower convergence of order $\varepsilon^{\frac{1}{2}}$ compared to the increased order ε. We are going to make use of this result in Section 14 to compute the topological derivatives following Amstutz' and Delfour's methods.

13 Analysis of the perturbed adjoint equations

In this section we examine the asymptotic behaviour of the adjoint variables. Since Delfour's method is based on the unperturbed adjoint equation, no further analysis is required in view of this approach. Hence, we only have to study the asymptotic expansion of the averaged adjoint variable (10.49) and Amstutz' adjoint variable (10.48). In what follows, we shall start with the latter.
Nonetheless, before we start we want to recast our problem formulation in the abstract setting (cf. Section 10). With the notations therein introduced, we have the following identifications of spaces: $\mathscr{X}=H^1(\mathrm{D})^d$, $\mathscr{W}=H^1_\Gamma(\mathrm{D})^d$, $\bar{u}\in\mathscr{X}$ such that $\bar{u}|_\Gamma=g_D$ is a fixed element that realises the inhomogeneous Dirichlet boundary conditions on Γ and thus

$$\mathscr{V}=\{u\in H^1(\mathrm{D})^d \,|\, u|_\Gamma=g_D\}. \tag{13.1}$$

Furthermore, we have for $\varepsilon>0$ small and $\Omega_\varepsilon=\Omega\cup T_\varepsilon(\omega)=T_\varepsilon(\omega)$

$$a_\varepsilon(u,v) = \int_D \mathbf{A}_{\Omega_\varepsilon}\epsilon(u) : \epsilon(v)\,dx \qquad \text{for all } u \in \mathscr{V}, v \in \mathscr{W}, \tag{13.2}$$

$$f_\varepsilon(v) = \int_D f_{\Omega_\varepsilon} \cdot v\,dx + \int_{\Gamma^N} g_N \cdot v\,dS \qquad \text{for all } v \in \mathscr{W}, \tag{13.3}$$

$$J_\varepsilon(u) = \gamma_f \int_D f_{\Omega_\varepsilon} \cdot u\,dx + \gamma_g \int_D |\partial u - \partial u_d|^2\,dx + \gamma_m \int_{\Gamma^m} |u - u_m|^2\,dS \qquad \text{for all } u \in \mathscr{V}. \tag{13.4}$$

13.1 Amstutz' adjoint equation

We now investigate Amstutz' adjoint variable. With the previous notations Amstutz' perturbed adjoint equation (10.48) reads: Find $p_\varepsilon \in H^1_\Gamma(\mathrm{D})^d$ such that

$$\begin{aligned}\int_D \mathbf{A}_{\omega_\varepsilon}\epsilon(\varphi) : \epsilon(p_\varepsilon)\,dx = &-\gamma_f \int_D f_{\omega_\varepsilon} \cdot \varphi\,dx - 2\gamma_m \int_{\Gamma_m} (u_0 - u_m) \cdot \varphi\,dS \\ &-2\gamma_g \int_D [\partial u_0 - \partial u_d] : \partial\varphi\,dx,\end{aligned} \tag{13.5}$$

for all $\varphi \in H^1_\Gamma(\mathrm{D})^d$ and $\varepsilon > 0$ sufficiently small. Similarly, Amstutz' unperturbed adjoint equation reads: Find $p_0 \in H^1_\Gamma(\mathrm{D})^d$ such that

$$\begin{aligned}\int_D \mathbf{A}_2\epsilon(\varphi) : \epsilon(p_0)\,dx = &-\gamma_f \int_D f_2 \cdot \varphi\,dx - 2\gamma_m \int_{\Gamma_m} (u_0 - u_m) \cdot \varphi\,dS \\ &-2\gamma_g \int_D [\partial u_0 - \partial u_d] : \partial\varphi\,dx,\end{aligned} \tag{13.6}$$

for all $\varphi \in H^1_\Gamma(\mathrm{D})^d$. Since the elastic tensors $\mathbf{A}_1, \mathbf{A}_2$ are symmetric, we have

$$\int_D \mathbf{A}_{\omega_\varepsilon}\epsilon(\varphi) : \epsilon(p_\varepsilon)\,dx = \int_D \mathbf{A}_{\omega_\varepsilon}\epsilon(p_\varepsilon) : \epsilon(\varphi)\,dx, \tag{13.7}$$

$$\int_D \mathbf{A}_2\epsilon(\varphi) : \epsilon(p_0)\,dx = \int_D \mathbf{A}_2\epsilon(p_0) : \epsilon(\varphi)\,dx. \tag{13.8}$$

Nevertheless, we will stick to the initial formulation. This allows an easier adaptation to nonsymmetric problems. We just observe that the elasticity tensors are self adjoint and thus $\mathbf{A}_i^\top = \mathbf{A}_i$, for $i \in \{1,2\}$.

Remark 13.1. It is noteworthy that the ε dependence of Amstutz' perturbed adjoint variable p_ε is solely given via the coefficients $\mathbf{A}_{\omega_\varepsilon}$ and f_{ω_ε}. This allows an asymptotic analysis similarly to the previous section. Indeed, the reduced ε dependence is a definite advantage over the averaged adjoint variable, which requires a more delicate asymptotic treatment.

We now compute an asymptotic expansion of p_ε in a similar fashion to the direct state u_ε. Therefore we define the variation of the adjoint state $P_\varepsilon^{(i)}$ for $i \geq 1$ in analogy to the definition of the variation of the direct state (Definition 12.3), where we replace the boundary layer correctors $U^{(i)}$ by similar correctors $P^{(i)}$ adapted to the new inhomogeneity and the regular correctors $u^{(i)}$ are replaced by correctors $p^{(i)}$ matching $P^{(i)}$.

Definition 13.2. For almost every $x \in \mathrm{D}$ and $\varepsilon > 0$ small we define the first variation of the state p_ε by

$$P_\varepsilon^{(1)}(x) := \left(\frac{p_\varepsilon - p_0}{\varepsilon}\right) \circ T_\varepsilon(x). \tag{13.9}$$

The second variation of p_ε is defined by

$$P_\varepsilon^{(2)}(x) := \frac{P_\varepsilon^{(1)}(x) - P^{(1)}(x) - \varepsilon^{d-1} p^{(1)} \circ T_\varepsilon}{\varepsilon} \qquad \text{for } \varepsilon > 0. \tag{13.10}$$

More generally, we define the $(i+1)$-th variation of p_ε for $i \geq 2$ by

$$P_\varepsilon^{(i+1)}(x) := \frac{P_\varepsilon^{(i)}(x) - P^{(i)}(x) - \varepsilon^{d-2} p^{(i)} \circ T_\varepsilon}{\varepsilon} \qquad \text{for } \varepsilon > 0. \tag{13.11}$$

Lemma 13.3. There is a solution $[P] \in \dot{BL}_2(\mathbf{R}^d)^d$ to

$$\int_{\mathbf{R}^d} \mathbf{A}_\omega \epsilon(\varphi) : \epsilon([P])\, dx = \int_\omega (\mathbf{A}_2 - \mathbf{A}_1)\epsilon(\varphi) : \epsilon(p_0)(x_0)\, dx, \tag{13.12}$$

for all $\varphi \in \dot{BL}_2(\mathbf{R}^d)^d$. Moreover, there exists a representative $P^{(1)} \in [P]$, which satisfies pointwise for $|x| \to \infty$:

$$P^{(1)}(x) = S^{(1)}(x) + \mathcal{O}(|x|^{-d}), \tag{13.13}$$

where $S^{(1)} : \mathbf{R}^d \to \mathbf{R}^d$ satisfies

$$|S^{(1)}(x)| = \begin{cases} b_2 |x|^{-1} & \text{for } d = 2, \\ b_3 |x|^{-2} & \text{for } d = 3, \end{cases} \tag{13.14}$$

for some constants $b_2, b_3 \in \mathbf{R}$.

Proof. Using the adjoint tensor $\mathbf{A}_\omega^\top : \mathbf{R}^{d\times d} \to \mathbf{R}^{d\times d}$, we can rewrite (13.12) to get

$$\int_{\mathbf{R}^d} \epsilon(\varphi) : \mathbf{A}_\omega^\top \epsilon([P])\, dx = \int_\omega \epsilon(\varphi) : (\mathbf{A}_2^\top - \mathbf{A}_1^\top)\epsilon(p_0)(x_0)\, dx. \tag{13.15}$$

Thus, using single layer potentials, the proof follows the lines of Lemma 12.5. □

Theorem 13.4. For $\alpha \in (0,1)$ and $\varepsilon > 0$ sufficiently small there is a constant $C > 0$ independent of ε such that

$$\|P_\varepsilon^{(1)} - P^{(1)}\|_\varepsilon \leq \begin{cases} C\varepsilon^{1-\alpha} & \text{for } d = 2, \\ C\varepsilon & \text{for } d = 3. \end{cases} \tag{13.16}$$

Proof. Similarly to the analysis of the state variable, we derive an equation of the form

$$\int_{\mathsf{D}_\varepsilon} \mathbf{A}_\omega \epsilon(\varphi) : \epsilon(P_\varepsilon^{(1)} - P^{(1)})\, dx = G_\varepsilon^1(\varphi) \quad \text{for all } \varphi \in H^1_{\Gamma_\varepsilon}(\mathsf{D}_\varepsilon)^d. \tag{13.17}$$

In order to compute G_ε^1, we subtract (13.5) and (13.6) to obtain

$$\begin{aligned} \int_{\mathsf{D}} \mathbf{A}_{\omega_\varepsilon} \epsilon(\varphi) : \epsilon(p_\varepsilon - p_0)\, dx = & \int_{\omega_\varepsilon} (\mathbf{A}_2 - \mathbf{A}_1)\epsilon(\varphi) : \epsilon(p_0)\, dx \\ & + \gamma_f \int_{\omega_\varepsilon} (f_2 - f_1) \cdot \varphi\, dx, \end{aligned} \tag{13.18}$$

for all $\varphi \in H^1_\Gamma(\mathsf{D})^d$. Next we change variables according to the transformation $y = T_\varepsilon(x)$, multiply with ε^{1-d} and subtract

$$\int_{\mathsf{D}_\varepsilon} \mathbf{A}_\omega \epsilon(\varphi) : \epsilon(P^{(1)})\, dx = \int_\omega (\mathbf{A}_2 - \mathbf{A}_1)\epsilon(\varphi) : \epsilon(p_0)(x_0)\, dx + \int_{\Gamma_\varepsilon^N} \mathbf{A}_2^\top \epsilon(P^{(1)}) n \cdot \varphi\, dS, \tag{13.19}$$

to conclude

$$\int_{\mathsf{D}_\varepsilon} \mathbf{A}_\omega \epsilon(\varphi) : \epsilon(P_\varepsilon^{(1)} - P^{(1)})\, dx = G_\varepsilon^1(\varphi), \tag{13.20}$$

for all $\varphi \in H^1_{\Gamma_\varepsilon}(\mathsf{D}_\varepsilon)^d$ with

$$\begin{aligned} G_\varepsilon^1(\varphi) = & \int_\omega (\mathbf{A}_2 - \mathbf{A}_1)\epsilon(\varphi) : [\epsilon(p_0) \circ T_\varepsilon - \epsilon(p_0)(x_0)]\, dx \\ & + \varepsilon\gamma_f \int_\omega (f_2 - f_1) \circ T_\varepsilon \cdot \varphi\, dx \\ & - \int_{\Gamma_\varepsilon^N} \mathbf{A}_2^\top \epsilon(P^{(1)}) n \cdot \varphi\, dS. \end{aligned} \tag{13.21}$$

Now we can find a constant $C > 0$, such that the following estimates hold:

$$\left| \int_\omega (\mathbf{A}_2 - \mathbf{A}_1)\epsilon(\varphi) : [\epsilon(p_0) \circ T_\varepsilon - \epsilon(p_0)(x_0)]\, dx \right| \leq C\varepsilon \|\varphi\|_\varepsilon, \tag{13.22}$$

which follows from a Taylor's expansion of $\epsilon(p_0) \circ T_\varepsilon$ in x_0 and Hölder's inequality.

$$\left| \varepsilon\gamma_f \int_\omega (f_2 - f_1) \circ T_\varepsilon \cdot \varphi\, dx \right| \leq \begin{cases} C\varepsilon^{1-\alpha}\|\varphi\|_\varepsilon & \text{for } d = 2, \\ C\varepsilon\|\varphi\|_\varepsilon & \text{for } d = 3, \end{cases} \tag{13.23}$$

which is a consequence of Hölder's inequality and Lemma 11.5 item (ii) and (iii), respectively.

$$\left| \int_{\Gamma_\varepsilon^N} \mathbf{A}_2^\top \epsilon(P^{(1)}) n \cdot \varphi\, dS \right| \leq C\varepsilon^{\frac{d}{2}} \|\varphi\|_\varepsilon, \tag{13.24}$$

which follows from Hölder's inequality, Lemma 11.5 item (iv) and Lemma 11.6, item (iii) with $m = d-1$. Combining the previous estimates entails

$$\|G_\varepsilon^1\| \leq \begin{cases} C\varepsilon^{1-\alpha} & \text{for } d = 2, \\ C\varepsilon & \text{for } d = 3. \end{cases} \tag{13.25}$$

In view of Lemma 12.4, we now estimate the boundary integral terms. Since $P_\varepsilon^{(1)}|_{\Gamma_\varepsilon} = 0$ we follow from Lemma 11.6 item (i), (ii) with $m = d-1$ that there is a constant $C > 0$, such that

$$\varepsilon^{\frac{1}{2}} \|P_\varepsilon^{(1)} - P^{(1)}\|_{L_2(\Gamma_\varepsilon)^d} + |P_\varepsilon^{(1)} - P^{(1)}|_{H^{\frac{1}{2}}(\Gamma_\varepsilon)^d} \leq C\varepsilon^{\frac{d}{2}}. \tag{13.26}$$

Thus, combining (13.25) and (13.26), an application of Lemma 12.4 shows (13.16), which finishes our proof. □

Corollary 13.5. There holds

$$\lim_{\varepsilon \searrow 0} P_\varepsilon^{(1)} = P^{(1)} \quad \text{in } L_1(\omega)^d. \tag{13.27}$$

Proof. The proof follows the lines of Corollary 12.8. □

It should be noted that again, the first boundary layer corrector $P^{(1)}$ admits a better asymptotic decline and thus did not necessitate a regular corrector in the previous result. We now continue with the second order expansion. Similarly to the asymptotic expansion of the state variable, we therefore introduce a number of correctors in the following Lemma, which approximate the first order expansion inside ω_ε and on the boundary $\partial \mathrm{D}$, respectively.

Lemma 13.6. The following results hold:

- There is a unique solution $p^{(1)} \in H^1(\mathrm{D})^d$ with $p^{(1)}(x) = -S^{(1)}(x - x_0)$ on Γ, such that

$$\int_{\mathrm{D}} \mathbf{A}_2 \epsilon(\varphi) : \epsilon(p^{(1)}) = -\int_{\Gamma^N} \mathbf{A}_2^\top \epsilon(S^{(1)})(x - x_0) n \cdot \varphi \, dS, \tag{13.28}$$

  for all $\varphi \in H_\Gamma^1(\mathrm{D})^d$.

- There is a solution $[P] \in \dot{BL}_p(\mathbf{R}^d)^d$ to

$$\int_{\mathbf{R}^d} \mathbf{A}_\omega \epsilon(\varphi) : \epsilon([P]) \, dx = \int_\omega (\mathbf{A}_2 - \mathbf{A}_1)\epsilon(\varphi) : [\partial \epsilon(p_0)(x_0) x] \, dx, \tag{13.29}$$

  for all $\varphi \in \dot{BL}_{p'}(\mathbf{R}^d)^d$, where

$$p = \begin{cases} 2 + \delta & \text{for } d = 2, \\ 2 & \text{for } d = 3, \end{cases}$$

  and $\delta > 0$ small. Moreover, there exists a representative $\hat{P}^{(2)} \in [P]$, which satisfies pointwise for $|x| \to \infty$:

$$\hat{P}^{(2)}(x) = \hat{S}^{(2)}(x) + \mathcal{O}(|x|^{1-d}), \tag{13.30}$$

where $\hat{S}^{(2)} : \mathbf{R}^d \to \mathbf{R}^d$ satisfies

$$|\hat{S}^{(2)}(x)| = \begin{cases} \hat{c}_2 \ln(|x|) & \text{for } d = 2, \\ \hat{c}_3 |x|^{-1} & \text{for } d = 3, \end{cases} \tag{13.31}$$

for some constants $\hat{c}_2, \hat{c}_3 \in \mathbf{R}$.

- There is a solution $[P] \in \dot{BL}_p(\mathbf{R}^d)^d$ to

$$\int_{\mathbf{R}^d} \mathbf{A}_\omega \epsilon(\varphi) : \epsilon([P]) \, dx = \gamma_f \int_\omega [f_2(x_0) - f_1(x_0)] \cdot \varphi \, dx, \tag{13.32}$$

for all $\varphi \in C_c^1(\mathbf{R}^d)^d$, where

$$p = \begin{cases} 2 + \delta & \text{for } d = 2, \\ 2 & \text{for } d = 3, \end{cases}$$

and $\delta > 0$ small. Moreover, there exists a representative $\tilde{P}^{(2)} \in [P]$, which satisfies pointwise for $|x| \to \infty$:

$$\tilde{P}^{(2)}(x) = \tilde{S}^{(2)}(x) + \mathcal{O}(|x|^{1-d}), \tag{13.33}$$

where $\tilde{S}^{(2)} : \mathbf{R}^d \to \mathbf{R}^d$ satisfies

$$|\tilde{S}^{(2)}(x)| = \begin{cases} \tilde{c}_2 \ln(|x|) & \text{for } d = 2, \\ \tilde{c}_3 |x|^{-1} & \text{for } d = 3, \end{cases} \tag{13.34}$$

for some constants $\tilde{c}_2, \tilde{c}_3 \in \mathbf{R}$.

- There is a unique solution $p^{(2)} \in H^1(\mathrm{D})^d$ with $p^{(2)}(x) = -S^{(2)}(x - x_0)$ on Γ, such that

$$\int_{\mathrm{D}} \mathbf{A}_2 \epsilon(\varphi) : \epsilon(p^{(2)}) = -\int_{\Gamma^N} \mathbf{A}_2^\top \varepsilon(S^{(2)})(x - x_0) n \cdot \varphi \, dS, \tag{13.35}$$

for all $\varphi \in H_\Gamma^1(\mathrm{D})^d$, where $S^{(2)} = \hat{S}^{(2)} + \tilde{S}^{(2)}$.

Proof. Rewriting these equations with the help of the adjoint operator $\mathbf{A}_\omega^\top$ leads to a proof similar to Lemma 12.10. □

We henceforth use the notation

$$P^{(2)} := \hat{P}^{(2)} + \tilde{P}^{(2)}, \quad S^{(2)} := \hat{S}^{(2)} + \tilde{S}^{(2)}. \tag{13.36}$$

Now we are able to state our main result regarding the second order expansion of Amstutz' adjoint variable p_ε.

Theorem 13.7. For $\varepsilon > 0$ sufficiently small let $P_\varepsilon^{(2)}$ as in Definition 13.2 and $\alpha \in (0,1)$.

(i) There is a constant $C > 0$ independent of ε such that

$$\|P_\varepsilon^{(2)} - P^{(2)} - \varepsilon^{d-2} p^{(2)} \circ T_\varepsilon - c\ln(\varepsilon)\|_\varepsilon \le C\varepsilon^{1-\alpha} \qquad \text{for } d = 2, \tag{13.37}$$

$$\|P_\varepsilon^{(2)} - P^{(2)} - \varepsilon^{d-2} p^{(2)} \circ T_\varepsilon\|_\varepsilon \le C\varepsilon \qquad \text{for } d = 3, \tag{13.38}$$

for a suitable constant $c \in \mathbf{R}$.

(ii) For $d \in \{2,3\}$, there holds

$$\lim_{\varepsilon \searrow 0} \|\varepsilon^{-1}(\partial(P_\varepsilon^{(1)}) - \partial(P^{(1)})) - \partial(P^{(2)})\|_{L_2(\omega)^{d\times d}} = 0. \tag{13.39}$$

Proof. ad (i): In view of the auxiliary result Lemma 12.4, we seek a governing equation for the quantity $\varepsilon P_\varepsilon^{(3)} = P_\varepsilon^{(2)} - P^{(2)} - \varepsilon^{d-2} p^{(2)} \circ T_\varepsilon$. Such an equation can be found using similar techniques to the analysis of the direct state. We start by dividing (13.20) by ε and subtract (13.28), (13.35), which can be formulated on the domain D_ε by a change of variables. Next we subtract (13.29) (13.32), whereas these equations can be restricted to the domain D_ε by splitting the integral over $\mathbf{R}^d$ and integrating by parts in the exterior domain. These operations leave us with

$$\int_{\mathsf{D}_\varepsilon} \mathbf{A}_\omega \epsilon(\varphi) : \epsilon(\varepsilon P_\varepsilon^{(3)})\, dx = G_\varepsilon^2(\varphi) + G_\varepsilon^3(\varphi), \tag{13.40}$$

for all $\varphi \in H^1_{\Gamma_\varepsilon}(\mathsf{D}_\varepsilon)^d$ where

$$\begin{aligned} G_\varepsilon^2(\varphi) = & \int_\omega (\mathbf{A}_2 - \mathbf{A}_1)\epsilon(\varphi) : [\varepsilon^{-1}(\epsilon(p_0)\circ T_\varepsilon - \epsilon(p_0)(x_0)) - \partial\varepsilon(p_0)(x_0)x]\, dx \\ & + \gamma_f \int_\omega [(f_2 - f_1)\circ T_\varepsilon - (f_2(x_0) - f_1(x_0))]\cdot \varphi\, dx \\ & + \varepsilon^{d-1} \int_\omega (\mathbf{A}_2 - \mathbf{A}_1)\epsilon(\varphi) : [\epsilon(p^{(1)})\circ T_\varepsilon + \epsilon(p^{(2)})\circ T_\varepsilon]\, dx, \\ G_\varepsilon^3(\varphi) = & -\varepsilon^{-1} \int_{\Gamma_\varepsilon^N} [\mathbf{A}_2^\top \epsilon(P^{(1)}) - \varepsilon^d \mathbf{A}_2^\top \epsilon(S^{(1)})(\varepsilon x)]n\cdot\varphi\, dS \\ & - \int_{\Gamma_\varepsilon^N} [\mathbf{A}_2^\top \epsilon(P^{(2)}) - \varepsilon^{d-1}\mathbf{A}_2^\top \epsilon(S^{(2)})(\varepsilon x)]n\cdot\varphi\, dS. \end{aligned} \tag{13.41}$$

One readily checks that, similarly to proof of the state variable, we can smuggle in a constant to adjust the boundary approximation in $d = 2$. This won't affect the interior estimates, as they depend on the gradient. Thus we aim to apply Lemma 12.4 to

$$V_\varepsilon := \begin{cases} \varepsilon P_\varepsilon^{(3)} + c\ln(\varepsilon) & \text{for } d = 2, \\ \varepsilon P_\varepsilon^{(3)} & \text{for } d = 3, \end{cases} \tag{13.42}$$

$$F_\varepsilon := G_\varepsilon^2 + G_\varepsilon^3, \tag{13.43}$$

and

$$g_\varepsilon := \begin{cases} (\varepsilon^{d-2}S^{(1)}(\varepsilon x) - \varepsilon^{-1}U^{(1)})|_{\Gamma_\varepsilon} + (\varepsilon^{d-2}S^{(2)}(\varepsilon x) - P^{(2)} + c\ln(\varepsilon))|_{\Gamma_\varepsilon} & \text{for } d = 2, \\ (\varepsilon^{d-2}S^{(1)}(\varepsilon x) - \varepsilon^{-1}P^{(1)})|_{\Gamma_\varepsilon} + (\varepsilon^{d-2}S^{(2)}(\varepsilon x) - P^{(2)})|_{\Gamma_\varepsilon} & \text{for } d = 3. \end{cases} \tag{13.44}$$

We start by estimating the norm $\|F_\varepsilon\|$. Therefore, let $\varphi \in H^1_\Gamma(\mathrm{D}_\varepsilon)^d$.

- Since p_0 is three times differentiable in a neighbourhood of x_0, there is a constant $C > 0$, such that $|\varepsilon^{-1}(\epsilon(p_0) \circ T_\varepsilon(x) - \epsilon(p_0)(x_0)) - \partial\epsilon(p_0)(x_0)x| \leq C\varepsilon$, for $x \in \omega$. Hence, Hölder's inequality yields

$$\left| \int_\omega (\mathbf{A}_2 - \mathbf{A}_1)\epsilon(\varphi) : [\varepsilon^{-1}(\epsilon(p_0) \circ T_\varepsilon - \epsilon(p_0)(x_0)) - \partial\epsilon(p_0)(x_0)x]\, dx \right| \leq C\varepsilon\|\varphi\|_\varepsilon. \tag{13.45}$$

- A Taylor expansion of $(f_2 - f_1) \circ T_\varepsilon$ at x_0, Hölder's inequality and Lemma 11.5 item (ii), item (iii) entail

$$\left| \gamma_f \int_\omega [(f_2 - f_1) \circ T_\varepsilon) - (f_2(x_0) - f_1(x_0))] \cdot \varphi\, dx \right| \leq \begin{cases} C\varepsilon^{1-\alpha}\|\varphi\|_\varepsilon & \text{for } d = 2, \\ C\varepsilon\|\varphi\|_\varepsilon & \text{for } d = 3, \end{cases} \tag{13.46}$$

  for a constant $C > 0$.

- Furthermore, by Hölder's inequality we conclude

$$\left| \varepsilon^{d-1} \int_\omega (\mathbf{A}_2 - \mathbf{A}_1)\epsilon(\varphi) : [\epsilon(p^{(1)}) \circ T_\varepsilon + \epsilon(p^{(2)}) \circ T_\varepsilon]\, dx \right| \leq C\varepsilon\|\varphi\|_\varepsilon, \tag{13.47}$$

  for a constant $C > 0$.

Combining the previous results leaves us with

$$\|G^2_\varepsilon\| \leq \begin{cases} C\varepsilon^{1-\alpha} & \text{for } d = 2, \\ C\varepsilon & \text{for } d = 3, \end{cases} \tag{13.48}$$

for a constant $C > 0$. Next we consider the boundary integral terms:

- Hölder's inequality, Lemma 11.6 item (iii) with $m = d$ and the scaled trace inequality entail

$$\left| \varepsilon^{-1} \int_{\Gamma^N_\varepsilon} [\mathbf{A}_2^\top \epsilon(P^{(1)}) - \varepsilon^d \mathbf{A}_2^\top \epsilon(S^{(1)})(\varepsilon x)] n \cdot \varphi\, dS \right| \leq C\varepsilon^{\frac{d}{2}}\|\varphi\|_\varepsilon, \tag{13.49}$$

  for a constant $C > 0$.

- Similarly, we deduce from Lemma 11.6 item (iii) with $m = d - 1$ that there is a constant $C > 0$, such that

$$\left| \int_{\Gamma^N_\varepsilon} [\mathbf{A}_2^\top \epsilon(P^{(2)}) - \varepsilon^{d-1} \mathbf{A}_2^\top \epsilon(S^{(2)})(\varepsilon x)] n \cdot \varphi\, dS \right| \leq C\varepsilon^{\frac{d}{2}}\|\varphi\|_\varepsilon. \tag{13.50}$$

These estimates show $\|G_\varepsilon^3\| \le C\varepsilon$ for a constant $C > 0$. Collecting the previous results entails

$$\|F_\varepsilon\| \le \begin{cases} C\varepsilon^{1-\alpha} & \text{for } d = 2, \\ C\varepsilon & \text{for } d = 3. \end{cases} \tag{13.51}$$

In view of Lemma 12.4 we now address the error on the Dirichlet boundary. Since

$$\varepsilon P_\varepsilon^{(3)}|_{\Gamma_\varepsilon} = (\varepsilon^{d-2} S^{(1)}(\varepsilon x) - \varepsilon^{-1} P^{(1)})|_{\Gamma_\varepsilon} + (\varepsilon^{d-2} S^{(2)}(\varepsilon x) - P^{(2)})|_{\Gamma_\varepsilon},$$

Lemma 11.6 item(i), (ii) with $m = d-1$ and $m = d$, respectively entail

$$\varepsilon^{\frac{1}{2}} \|\varepsilon P_\varepsilon^{(3)}\|_{L_2(\Gamma_\varepsilon)^d} + |\varepsilon P_\varepsilon^{(3)}|_{H^{\frac{1}{2}}(\Gamma_\varepsilon)^d} \le C\varepsilon^{\frac{d}{2}}. \tag{13.52}$$

Hence, considering (13.51) and (13.52), Lemma 12.4 shows (13.37).
ad (ii): By the triangle inequality we have

$$\begin{aligned} &\|\varepsilon^{-1}(\partial(P_\varepsilon^{(1)}) - \partial(P^{(1)})) - \partial(P^{(2)})\|_{L_2(\omega)^{d\times d}} \\ &\qquad \le \|\partial(P_\varepsilon^{(2)} - P^{(2)} - \varepsilon^{d-2} p^{(2)} \circ T_\varepsilon)\|_{L_2(\omega)^{d\times d}} \\ &\qquad\quad + \varepsilon^{d-1} \|\partial(p^{(1)}) \circ T_\varepsilon\|_{L_2(\omega)^{d\times d}} + \varepsilon^{d-1} \|\partial(p^{(2)}) \circ T_\varepsilon\|_{L_2(\omega)^{d\times d}} \\ &\qquad \le C\varepsilon^{1-\alpha}, \end{aligned} \tag{13.53}$$

for a positive constant C. This shows (ii) and therefore finishes the proof. □

13.2 Averaged adjoint equation

We now investigate the averaged adjoint variable. For the sake of simplicity we choose $\gamma_g = 0$ in this section. We will address this specific choice within the upcoming analysis. With the according formulations introduced in the beginning of Section 13, the perturbed averaged adjoint equation (10.49) reads: Find $q_\varepsilon \in H^1_\Gamma(\mathrm{D})^d$ such that

$$\int_{\mathrm{D}} \mathbf{A}_{\omega_\varepsilon} \epsilon(\varphi) : \epsilon(q_\varepsilon)\, dx = -\gamma_f \int_{\mathrm{D}} f_{\omega_\varepsilon} \cdot \varphi\, dx - \gamma_m \int_{\Gamma^m} (u_0 + u_\varepsilon - 2u_m) \cdot \varphi\, dS, \tag{13.54}$$

for all $\varphi \in H^1_\Gamma(\mathrm{D})^d$ and $\varepsilon > 0$ sufficiently small. Similarly, the unperturbed averaged adjoint equation reads: Find $q_0 \in H^1_\Gamma(\mathrm{D})^d$ such that

$$\int_{\mathrm{D}} \mathbf{A}_2 \epsilon(\varphi) : \epsilon(q_0)\, dx = -\gamma_f \int_{\mathrm{D}} f_2 \cdot \varphi\, dx - 2\gamma_m \int_{\Gamma_m} (u_0 - u_m) \cdot \varphi\, dS, \tag{13.55}$$

for all $\varphi \in H^1_\Gamma(\mathrm{D})^d$. One readily checks that (13.55) and (13.6) coincide. Since this equation admits a unique solution, it follows that $p_0 = q_0$ (cf. (10.51)). Furthermore, we want to highlight the occurrence of the perturbed state variable u_ε on the right hand side of (13.54). As we will see in the upcoming analysis, this term leads to some difficulties. As a result, we need more corrector terms in this asymptotic expansion. This is a definite disadvantage compared to Amstutz' adjoint variable. For the sake of completeness, we define the variation of the averaged adjoint variable:

Definition 13.8. For almost every $x \in \mathsf{D}$ and $\varepsilon > 0$ small we define the first variation of the state q_ε by

$$Q_\varepsilon^{(1)}(x) := \left(\frac{q_\varepsilon - q_0}{\varepsilon}\right) \circ T_\varepsilon(x). \tag{13.56}$$

The second variation of q_ε is defined by

$$Q_\varepsilon^{(2)}(x) := \frac{Q_\varepsilon^{(1)}(x) - Q^{(1)}(x) - \varepsilon^{d-1} q^{(1)} \circ T_\varepsilon}{\varepsilon} \quad \text{for } \varepsilon > 0. \tag{13.57}$$

More generally, we define the $(i+1)$-th variation of q_ε for $i \geq 2$ by

$$Q_\varepsilon^{(i+1)}(x) := \frac{Q_\varepsilon^{(i)}(x) - Q^{(i)}(x) - \varepsilon^{d-2} q^{(i)} \circ T_\varepsilon}{\varepsilon} \quad \text{for } \varepsilon > 0. \tag{13.58}$$

Lemma 13.9. There is a solution $[Q] \in \dot{BL}_2(\mathbf{R}^d)^d$ to

$$\int_{\mathbf{R}^d} \mathbf{A}_\omega \epsilon(\varphi) : \epsilon([Q])\, dx = \int_\omega (\mathbf{A}_2 - \mathbf{A}_1)\epsilon(\varphi) : \epsilon(q_0)(x_0)\, dx, \tag{13.59}$$

for all $\varphi \in \dot{BL}(\mathbf{R}^d)^d$. Moreover, there exists a representative $Q^{(1)} \in [Q]$, which satisfies pointwise for $|x| \to \infty$:

$$Q^{(1)}(x) = T^{(1)}(x) + \mathcal{O}(|x|^{-d}), \tag{13.60}$$

where $T^{(1)} : \mathbf{R}^d \to \mathbf{R}^d$ satisfies

$$|T^{(1)}(x)| = \begin{cases} b_2 |x|^{-1} & \text{for } d = 2, \\ b_3 |x|^{-2} & \text{for } d = 3, \end{cases} \tag{13.61}$$

for some constants $b_2, b_3 \in \mathbf{R}$.

Proof. Similarly to Lemma 12.5, a single-layer potential yields the result. □

Theorem 13.10. For $\alpha \in (0,1)$ and $\varepsilon > 0$ sufficiently small there is a constant $C > 0$ independent of ε, such that

$$\|Q_\varepsilon^{(1)} - Q^{(1)}\|_\varepsilon \leq \begin{cases} C\varepsilon^{1-\alpha} & \text{for } d = 2, \\ C\varepsilon & \text{for } d = 3. \end{cases} \tag{13.62}$$

Proof. We start by deriving an equation of the form

$$\int_{\mathsf{D}_\varepsilon} \mathbf{A}_\omega \epsilon(\varphi) : \epsilon(Q_\varepsilon^{(1)} - Q^{(1)})\, dx = G_\varepsilon^4(\varphi), \tag{13.63}$$

for all $\varphi \in H^1_{\Gamma_\varepsilon}(\mathrm{D}_\varepsilon)^d$. Therefore, subtracting (13.54), (13.55) and a change of variables with respect to T_ε entail

$$\begin{aligned} G^4_\varepsilon(\varphi) = &\int_\omega (\mathbf{A}_2 - \mathbf{A}_1)\epsilon(\varphi) : [\epsilon(q_0)\circ T_\varepsilon - \epsilon(q_0)(x_0)]\,dx \\ &+ \varepsilon\gamma_f \int_\omega (f_2 \circ T_\varepsilon - f_1 \circ T_\varepsilon)\cdot\varphi\,dx \\ &- \varepsilon\gamma_m \int_{\Gamma^m_\varepsilon} (U^{(1)}_\varepsilon)\cdot\varphi\,dS \\ &- \int_{\Gamma^N_\varepsilon} \mathbf{A}_2^\top \epsilon(Q^{(1)})n\cdot\varphi\,dS, \end{aligned} \tag{13.64}$$

where the last term stems from a partial integration of the exterior term $Q^{(1)}$ on $\mathbf{R}^d \setminus \mathrm{D}_\varepsilon$. In view of Lemma 12.4 we start with an estimation of $\|G^4_\varepsilon\|$. Therefore fix $\varphi \in H^1_{\Gamma_\varepsilon}(\mathrm{D}_\varepsilon)^d$. Then we have

- $\left|\int_\omega (\mathbf{A}_2 - \mathbf{A}_1)\epsilon(\varphi) : [\epsilon(q_0)\circ T_\varepsilon - \epsilon(q_0)(x_0)]\,dx\right| \le C\varepsilon\|\varphi\|_\varepsilon$, which can be seen by a Taylor's expansion of q_0 in x_0 and Hölder's inequality.
- Furthermore there holds
$$\left|\varepsilon\gamma_f \int_\omega (f_2\circ T_\varepsilon - f_1 \circ T_\varepsilon)\cdot\varphi\,dx\right| \le \begin{cases} C\varepsilon^{1-\alpha}\|\varphi\|_\varepsilon & \text{for } d=2, \\ C\varepsilon\|\varphi\|_\varepsilon & \text{for } d=3, \end{cases} \tag{13.65}$$
which is a consequence of Hölder's inequality and Lemma 11.5 item (ii) and item (iii), respectively.
- To estimate the third term, we introduce an intermediate term as follows
$$\varepsilon\gamma_m \int_{\Gamma^m_\varepsilon} (U^{(1)}_\varepsilon)\cdot\varphi\,dS = \varepsilon\gamma_m \int_{\Gamma^m_\varepsilon} (U^{(1)}_\varepsilon - U^{(1)})\cdot\varphi\,dS + \varepsilon\gamma_m \int_{\Gamma^m_\varepsilon} (U^{(1)})\cdot\varphi\,dS. \tag{13.66}$$
Now Hölder's inequality, the scaled trace inequality, Theorem 12.6 and Lemma 11.6 item (i) with $m = d-1$ entail
$$\begin{aligned} \left|\varepsilon\gamma_m \int_{\Gamma^m_\varepsilon} (U^{(1)}_\varepsilon)\cdot\varphi\,dS\right| \le & C\varepsilon\left(\|U^{(1)}_\varepsilon - U^{(1)}\|_{L_2(\Gamma_\varepsilon)^d} + \|U^{(1)}\|_{L_2(\Gamma_\varepsilon)^d}\right)\|\varphi\|_{L_2(\Gamma_\varepsilon)^d} \\ \le & C\left(\|U^{(1)}_\varepsilon - U^{(1)}\|_\varepsilon + \varepsilon^{\frac{1}{2}}\|U^{(1)}\|_{L_2(\Gamma_\varepsilon)^d}\right)\|\varphi\|_\varepsilon \\ \le & C\left(\varepsilon^{1-\alpha} + \varepsilon^{\frac{d}{2}}\right)\|\varphi\|_\varepsilon \\ \le & C\varepsilon^{1-\alpha}\|\varphi\|_\varepsilon, \end{aligned} \tag{13.67}$$
where $\alpha \in (0,1)$ for $d=2$ and $\alpha = 0$ for $d=3$. This is a consequence of Theorem 12.6.
- The last term can be addressed with the remainder estimate Lemma 11.6 item (iii) with $m = d-1$ to conclude
$$\left|\int_{\Gamma^N_\varepsilon} \mathbf{A}_2^\top \epsilon(Q^{(1)})n\cdot\varphi\,dS\right| \le C\|\epsilon(Q^{(1)})\|_{L_2(\Gamma^N_\varepsilon)^{d\times d}}\|\varphi\|_{L_2(\Gamma^N_\varepsilon)^{d\times d}} \le C\varepsilon^{\frac{d}{2}}\|\varphi\|_\varepsilon. \tag{13.68}$$

These estimates yield

$$\|G_\varepsilon^4\| \le \begin{cases} C\varepsilon^{1-\alpha} & \text{for } d=2, \\ C\varepsilon & \text{for } d=3. \end{cases} \tag{13.69}$$

Next, we deal with the error on the Dirichlet boundary. Since $Q_\varepsilon^{(1)}|_{\Gamma_\varepsilon} = 0$ we deduce from Lemma 11.6 item (i), (ii) with $m = d-1$ that there is a constant $C > 0$ satisfying

$$\varepsilon^{\frac{1}{2}}\|Q_\varepsilon^{(1)} - Q^{(1)}\|_{L_2(\Gamma_\varepsilon)^d} + |Q_\varepsilon^{(1)} - Q^{(1)}|_{H^{\frac{1}{2}}(\Gamma_\varepsilon)^d} \le C\varepsilon^{\frac{d}{2}}. \tag{13.70}$$

Thus, combining (13.69) and (13.70), an application of Lemma 12.4 shows (13.62). □

Corollary 13.11. There holds

$$\lim_{\varepsilon \searrow 0} Q_\varepsilon^{(1)} = Q^{(1)} \quad \text{in } L_1(\omega)^d. \tag{13.71}$$

Proof. The proof follows the lines of Corollary 12.8. □

It should be noted that the corrector term $Q^{(1)}$ used in the previous result coincides with the corrector $P^{(1)}$ introduced in the previous section. Nonetheless, the proof of Theorem 13.10 indicates that the analysis of both adjoint variables differs. Indeed, these differences will be highlighted in the second order expansion, where the regular correctors need to deal with the error on Γ_m as well.

Lemma 13.12. The following results hold:

- There is a unique solution $q^{(1)} \in H^1(\mathsf{D})^d$ with $q^{(1)}(x) = -T^{(1)}(x - x_0)$ on Γ, such that

$$\int_{\mathsf{D}} \mathbf{A}_2 \epsilon(\varphi) : \epsilon(q^{(1)})\, dx = -\int_{\Gamma^N} \mathbf{A}_2^\top \epsilon(T^{(1)})(x - x_0) n \cdot \varphi\, dS, \tag{13.72}$$

  for all $\varphi \in H_\Gamma^1(\mathsf{D})^d$.

- There is a solution $[Q] \in \dot{BL}_p(\mathbf{R}^d)^d$ to

$$\int_{\mathbf{R}^d} \mathbf{A}_\omega \epsilon(\varphi) : \epsilon([Q])\, dx = \int_\omega (\mathbf{A}_2 - \mathbf{A}_1)\epsilon(\varphi) : [\partial \epsilon(q_0)(x_0) x]\, dx, \tag{13.73}$$

  for all $\varphi \in \dot{BL}_{p'}(\mathbf{R}^d)^d$, where

$$p = \begin{cases} 2+\delta & \text{for } d=2, \\ 2 & \text{for } d=3, \end{cases}$$

  and $\delta > 0$ small. Moreover, there exists a representative $\hat{Q}^{(2)} \in [Q]$, which satisfies pointwise for $|x| \to \infty$:

$$\hat{Q}^{(2)}(x) = \hat{T}^{(2)}(x) + \mathcal{O}(|x|^{1-d}), \tag{13.74}$$

  where $\hat{T}^{(2)} : \mathbf{R}^d \to \mathbf{R}^d$ satisfies

$$|\hat{T}^{(2)}(x)| = \begin{cases} \hat{c}_2 \ln(|x|) & \text{for } d=2, \\ \hat{c}_3 |x|^{-1} & \text{for } d=3, \end{cases} \tag{13.75}$$

  for some constants $\hat{c}_2, \hat{c}_3 \in \mathbf{R}$.

- There is a solution $[Q] \in \dot{BL}_p(\mathbf{R}^d)^d$ to

$$\int_{\mathbf{R}^d} \mathbf{A}_\omega \epsilon(\varphi) : \epsilon([Q])\, dx = \gamma_f \int_\omega [f_2(x_0) - f_1(x_0)] \cdot \varphi\, dx, \tag{13.76}$$

for all $\varphi \in C_c^1(\mathbf{R}^d)^d$, where

$$p = \begin{cases} 2+\delta & \text{for } d = 2, \\ 2 & \text{for } d = 3, \end{cases}$$

and $\delta > 0$ small. Moreover, there exists a representative $\tilde{Q}^{(2)} \in [Q]$, which satisfies pointwise for $|x| \to \infty$:

$$\tilde{P}^{(2)}(x) = \tilde{T}^{(2)}(x) + \mathcal{O}(|x|^{1-d}), \tag{13.77}$$

where $\tilde{T}^{(2)} : \mathbf{R}^d \to \mathbf{R}^d$ satisfies

$$|\tilde{T}^{(2)}(x)| = \begin{cases} \tilde{c}_2 \ln(|x|) & \text{for } d = 2, \\ \tilde{c}_3 |x|^{-1} & \text{for } d = 3, \end{cases} \tag{13.78}$$

for some constants $\tilde{c}_2, \tilde{c}_3 \in \mathbf{R}$.

- There is a unique solution $q^{(2)} \in H^1(\mathrm{D})^d$ with $q^{(2)}(x) = -T^{(2)}(x - x_0)$ on Γ such that

$$\begin{aligned} \int_{\mathrm{D}} \mathbf{A}_2 \epsilon(\varphi) : \epsilon(q^{(2)})\, dx = &-\gamma_m \int_{\Gamma^m} R^{(1)}(x - x_0) \cdot \varphi\, dS - \gamma_m \int_{\Gamma^m} u^{(1)} \cdot \varphi\, dS \\ &-\gamma_m \int_{\Gamma^m} R^{(2)}(x - x_0) \cdot\, dS - \gamma_m \int_{\Gamma^m} u^{(2)} \cdot \varphi\, dS \\ &- \int_{\Gamma^N} \mathbf{A}_2^\top \epsilon(T^{(2)})(x - x_0) n \cdot \varphi\, dS, \end{aligned} \tag{13.79}$$

for all $\varphi \in H^1_\Gamma(\mathrm{D})^d$, where

$$T^{(2)} := \hat{T}^{(2)} + \tilde{T}^{(2)}.$$

Proof. The proof follows the lines of Lemma 12.10. □

We continue with the main result covering the second order asymptotic expansion of the adjoint variable q_ε.

Theorem 13.13. For $\varepsilon > 0$ sufficiently small let $Q_\varepsilon^{(2)}$ as in Definition 13.8 and $\alpha \in (0,1)$.

(i) There is a constant $C > 0$ independent of ε such that

$$\|Q_\varepsilon^{(2)} - Q^{(2)} - \varepsilon^{d-2} q^{(2)} \circ T_\varepsilon - c \ln(\varepsilon)\|_\varepsilon \le C \varepsilon^{1-\alpha} \quad \text{for } d = 2, \tag{13.80}$$

$$\|Q_\varepsilon^{(2)} - Q^{(2)} - \varepsilon^{d-2} q^{(2)} \circ T_\varepsilon\|_\varepsilon \le C \varepsilon \quad \text{for } d = 3, \tag{13.81}$$

for a suitable constant $c \in \mathbf{R}$.

(ii) There holds

$$\lim_{\varepsilon\searrow 0}\|\varepsilon^{-1}(\partial(Q_\varepsilon^{(1)})-\partial(Q^{(1)}))-\partial(Q^{(2)})\|_{L_2(\omega)^{d\times d}}=0. \tag{13.82}$$

Proof. ad (i): We first derive a governing equation for each term contained in

$$\varepsilon Q_\varepsilon^{(3)}=\varepsilon^{-1}\left(Q_\varepsilon^{(1)}-Q^{(1)}\right)-Q^{(2)}-\varepsilon^{d-2}q^{(1)}-\varepsilon^{d-2}q^{(2)}. \tag{13.83}$$

This can be achieved by a change of variables for the regular correctors $q^{(1)},q^{(2)}$. The boundary layer correctors can be reformulated on D_ε by splitting the integral and a partial integration. For a given $\varphi\in H^1_{\Gamma_\varepsilon}(\mathsf{D})^d$ we thus obtain the following set of equations

$$\begin{aligned}\int_{\mathsf{D}_\varepsilon}\mathbf{A}_\omega\epsilon(\varphi):\epsilon(\varepsilon^{-1}(Q_\varepsilon^{(1)}-Q^{(1)}))\,dx=&\int_\omega(\mathbf{A}_2-\mathbf{A}_1)\epsilon(\varphi):[\varepsilon^{-1}(\epsilon(q_0)\circ T_\varepsilon-\epsilon(q_0)(x_0))]\,dx\\&+\gamma_f\int_\omega(f_2\circ T_\varepsilon-f_1\circ T_\varepsilon)\cdot\varphi\,dx\\&-\gamma_m\int_{\Gamma_\varepsilon^m}(U_\varepsilon^{(1)})\cdot\varphi\,dS\\&-\int_{\Gamma_\varepsilon^N}\mathbf{A}_2^\top\varepsilon^{-1}\epsilon(Q^{(1)})n\cdot\varphi\,dS,\end{aligned} \tag{13.84}$$

$$\begin{aligned}\int_{\mathbf{R}^d}\mathbf{A}_\omega\epsilon(\varphi):\epsilon(Q^{(2)})\,dx=&\int_\omega(\mathbf{A}_2-\mathbf{A}_1)\epsilon(\varphi):[\partial\epsilon(q_0)(x_0)x]\,dx\\&+\gamma_f\int_\omega[f_2(x_0)-f_1(x_0)]\cdot\varphi\,dx,\\&+\int_{\Gamma_\varepsilon^N}\mathbf{A}_2^\top\epsilon(Q^{(2)})n\cdot\varphi\,dS,\end{aligned} \tag{13.85}$$

$$\int_{\mathsf{D}_\varepsilon}\mathbf{A}_2\epsilon(\varphi):\epsilon(\varepsilon^{d-2}q^{(1)}\circ T_\varepsilon)\,dx=-\varepsilon^{d-1}\int_{\Gamma_\varepsilon^N}\mathbf{A}_2^\top\epsilon(T^{(1)})(\varepsilon x)n\cdot\varphi\,dS, \tag{13.86}$$

$$\begin{aligned}\int_{\mathsf{D}_\varepsilon}\mathbf{A}_2\epsilon(\varphi):\epsilon(\varepsilon^{d-2}q^{(2)}\circ T_\varepsilon)\,dx=&-\varepsilon^{d-1}\gamma_m\int_{\Gamma_\varepsilon^m}R^{(1)}(\varepsilon x)\cdot\varphi\,dS-\varepsilon\gamma_m\int_{\Gamma_\varepsilon^m}(\varepsilon^{d-2}u^{(1)}\circ T_\varepsilon)\cdot\varphi\,dS\\&-\varepsilon^{d-1}\gamma_m\int_{\Gamma_\varepsilon^m}R^{(2)}(\varepsilon x)\cdot\,dS-\varepsilon\gamma_m\int_{\Gamma_\varepsilon^m}(\varepsilon^{d-2}u^{(2)}\circ T_\varepsilon)\cdot\varphi\,dS\\&-\varepsilon^{d-1}\int_{\Gamma_\varepsilon^N}\mathbf{A}_2^\top\epsilon(T^{(2)})(\varepsilon x)n\cdot\varphi\,dS.\end{aligned} \tag{13.87}$$

Recall the degrees of homogeneity

$$\begin{aligned} R^{(1)}(\varepsilon x) &= \varepsilon^{1-d} R^{(1)}(x), \\ \epsilon(T^{(1)})(\varepsilon x) &= \varepsilon^{-d} \epsilon(T^{(1)})(x), \\ \epsilon(T^{(2)})(\varepsilon x) &= \varepsilon^{1-d} \epsilon(T^{(2)})(x), \end{aligned} \tag{13.88}$$

and

$$R^{(2)}(\varepsilon x) = \begin{cases} R^{(2)}(x) + c\ln(\varepsilon) & \text{for } d = 2, \\ \varepsilon^{2-d} R^{(2)}(x) & \text{for } d = 3, \end{cases} \tag{13.89}$$

where we note that the constant $c \in \mathbf{R}$ occurring in (13.89) coincides with the constant introduced in Theorem 13.10. Combining the above equations entails

$$\int_{\mathsf{D}_\varepsilon} \mathbf{A}_\omega \epsilon(\varphi) : \epsilon(\varepsilon Q_\varepsilon^{(3)})\, dx = G_\varepsilon^5(\varphi), \tag{13.90}$$

with

$$\begin{aligned} G_\varepsilon^5(\varphi) = &\int_\omega (\mathbf{A}_2 - \mathbf{A}_1)\epsilon(\varphi) : [\varepsilon^{-1}(\epsilon(q_0)\circ T_\varepsilon - \epsilon(q_0)(x_0)) - \partial\epsilon(q_0)(x_0)x]\, dx \\ &+ \gamma_f \int_\omega [(f_2\circ T_\varepsilon - f_1 \circ T_\varepsilon) - (f_2(x_0) - f_1(x_0))]\cdot\varphi\, dx \\ &- \varepsilon\gamma_m \int_{\Gamma_\varepsilon^m} (\varepsilon^{-1}(U_\varepsilon^{(1)} - R^{(1)}) - \varepsilon^{d-2}u^{(1)}\circ T_\varepsilon - R^{(2)} - \varepsilon^{d-2}u^{(2)}\circ T_\varepsilon)\cdot\varphi\, dS \\ &- \int_{\Gamma_\varepsilon^N} \mathbf{A}_2^\top \varepsilon^{-1}\left[\epsilon(Q^{(1)}) - \epsilon(T^{(1)})\right] n\cdot\varphi\, dS \\ &- \int_{\Gamma_\varepsilon^N} \mathbf{A}_2^\top \left[\epsilon(Q^{(2)}) - \epsilon(T^{(2)})\right] n\cdot\varphi\, dS, \end{aligned} \tag{13.91}$$

for $d = 3$ and

$$\begin{aligned} G_\varepsilon^5(\varphi) = &\int_\omega (\mathbf{A}_2 - \mathbf{A}_1)\epsilon(\varphi) : [\varepsilon^{-1}(\epsilon(q_0)\circ T_\varepsilon - \epsilon(q_0)(x_0)) - \partial\epsilon(q_0)(x_0)x]\, dx \\ &+ \gamma_f \int_\omega [(f_2\circ T_\varepsilon - f_1 \circ T_\varepsilon) - (f_2(x_0) - f_1(x_0))]\cdot\varphi\, dx \\ &- \varepsilon\gamma_m \int_{\Gamma_\varepsilon^m} (\varepsilon^{-1}(U_\varepsilon^{(1)} - R^{(1)}) - \varepsilon^{d-2}u^{(1)}\circ T_\varepsilon - R^{(2)} - \varepsilon^{d-2}u^{(2)}\circ T_\varepsilon - c\ln(\varepsilon))\cdot\varphi\, dS \\ &- \int_{\Gamma_\varepsilon^N} \mathbf{A}_2^\top \varepsilon^{-1}\left[\epsilon(Q^{(1)}) - \epsilon(T^{(1)})\right] n\cdot\varphi\, dS \\ &- \int_{\Gamma_\varepsilon^N} \mathbf{A}_2^\top \left[\epsilon(Q^{(2)}) - \epsilon(T^{(2)})\right] n\cdot\varphi\, dS, \end{aligned} \tag{13.92}$$

for $d = 2$. In view of Lemma 12.4 we seek an estimate for $\|G_\varepsilon^5\|$. We only show the result for $d = 2$. The remaining case $d = 3$ can be proven employing the same methods.

- A Taylor's expansion and Hölder's inequality yield

$$|\int_{\omega}(\mathbf{A}_2-\mathbf{A}_1)\epsilon(\varphi):[\varepsilon^{-1}(\epsilon(q_0)\circ T_\varepsilon-\epsilon(q_0)(x_0))-\partial\epsilon(q_0)(x_0)x]\,dx|\leq C\varepsilon\|\varphi\|_\varepsilon, \tag{13.93}$$

  for a constant $C>0$.

- Similarly, Lemma 11.5 item (iii) yields

$$|\gamma_f\int_{\omega}[(f_2\circ T_\varepsilon-f_1\circ T_\varepsilon)-(f_2(x_0)-f_1(x_0))]\cdot\varphi\,dx|\leq C\varepsilon^{1-\alpha}\|\varphi\|_\varepsilon, \tag{13.94}$$

  for a constant $C>0$ and $\alpha\in(0,1)$.

- Smuggling in the missing terms $U^{(1)}$, $U^{(2)}$ further entails

$$\begin{aligned}
&|\varepsilon\gamma_m\int_{\Gamma_\varepsilon^m}(\varepsilon^{-1}(U_\varepsilon^{(1)}-R^{(1)})-\varepsilon^{d-2}u^{(1)}\circ T_\varepsilon-R^{(2)}-\varepsilon^{d-2}u^{(2)}\circ T_\varepsilon-c\ln(\varepsilon))\cdot\varphi\,dS|\\
&\quad\leq C\varepsilon\|\varepsilon^{-1}(U_\varepsilon^{(1)}-U^{(1)})-\varepsilon^{d-2}u^{(1)}\circ T_\varepsilon-U^{(2)}-\varepsilon^{d-2}u^{(2)}\circ T_\varepsilon-c\ln(\varepsilon)\|_{L_2(\Gamma_\varepsilon^m)^d}\|\varphi\|_{L_2(\Gamma_\varepsilon^m)^d}\\
&\qquad+C\left(\|U^{(1)}-R^{(1)}\|_{L_2(\Gamma_\varepsilon^m)^d}+\varepsilon\|U^{(2)}-R^{(2)}\|_{L_2(\Gamma_\varepsilon^m)^d}\right)\|\varphi\|_{L_2(\Gamma_\varepsilon^m)^d}\\
&\quad\leq C\|\varepsilon^{-1}(U_\varepsilon^{(1)}-U^{(1)})-\varepsilon^{d-2}u^{(1)}\circ T_\varepsilon-U^{(2)}-\varepsilon^{d-2}u^{(2)}\circ T_\varepsilon-c\ln(\varepsilon)\|_\varepsilon\|\varphi\|_\varepsilon\\
&\qquad+C\left(\|U^{(1)}-R^{(1)}\|_{L_2(\Gamma_\varepsilon^m)^d}+\varepsilon\|U^{(2)}-R^{(2)}\|_{L_2(\Gamma_\varepsilon^m)^d}\right)\varepsilon^{-\frac{1}{2}}\|\varphi\|_\varepsilon\\
&\quad\leq C\left(\varepsilon^{1-\alpha}+\varepsilon^{\frac{d}{2}}+\varepsilon^{\frac{d}{2}}\right)\|\varphi\|_\varepsilon,
\end{aligned} \tag{13.95}$$

  for a constant $C>0$ and $\alpha\in(0,1)$. Here, we used the scaled trace inequality (cf. Lemma 11.5 item (iv)), Theorem 12.14 and the remainder estimate Lemma 11.6 item (i) with $m=d$ and $m=d-1$, respectively.

- We employ the remainder estimates further to conclude

$$|\int_{\Gamma_\varepsilon^N}\mathbf{A}_2^\top\varepsilon^{-1}\left[\epsilon(Q^{(1)})-\epsilon(T^{(1)})\right]n\cdot\varphi\,dS+\int_{\Gamma_\varepsilon^N}\mathbf{A}_2^\top\left[\epsilon(Q^{(2)})-\epsilon(T^{(2)})\right]n\cdot\varphi\,dS|\leq C\varepsilon^{\frac{d}{2}}\|\varphi\|_\varepsilon, \tag{13.96}$$

  for a positive constant C.

Combining these estimates shows

$$\|G_\varepsilon^5\|\leq C\varepsilon^{1-\alpha}, \tag{13.97}$$

for $\alpha\in(0,1)$. With the same techniques employed in the proof of Theorem 13.7, one checks that

$$\varepsilon^{\frac{1}{2}}\|\varepsilon P_\varepsilon^{(3)}-\bar{c}\ln(\varepsilon)\|_{L_2(\Gamma_\varepsilon)^d}+|\varepsilon P_\varepsilon^{(3)}-\bar{c}\ln(\varepsilon)|_{H^{\frac{1}{2}}(\Gamma_\varepsilon)^d}\leq C\varepsilon^{\frac{d}{2}}, \tag{13.98}$$

for a suitable constant $\bar{c} \in \mathbf{R}$. Hence, taking into account (13.97), (13.98), Lemma 12.4 yields the result.
ad (ii): By the triangle inequality we have

$$\begin{aligned}\|\varepsilon^{-1}(\partial(Q_\varepsilon^{(1)}) - \partial(Q^{(1)})) - \partial(Q^{(2)})\|_{L_2(\omega)^{d\times d}} \\ \leq &\|\partial(Q_\varepsilon^{(2)} - Q^{(2)} - \varepsilon^{d-2} q^{(2)} \circ T_\varepsilon)\|_{L_2(\omega)^{d\times d}} \\ &+ \varepsilon^{d-1}\|\partial(q^{(1)}) \circ T_\varepsilon\|_{L_2(\omega)^{d\times d}} + \varepsilon^{d-1}\|\partial(q^{(2)}) \circ T_\varepsilon\|_{L_2(\omega)^{d\times d}} \\ \leq & C\varepsilon^{1-\alpha},\end{aligned} \tag{13.99}$$

for a positive constant C. This shows (ii) and therefore finishes the proof. □

Remark 13.14. Before we conclude this section, we want to address the simplification $\gamma_g = 0$. Similarly to the boundary term of the cost functional, this contributes to the right hand side of the variation of the adjoint state as follows:

$$\int_{\mathsf{D}_\varepsilon} \mathbf{A}_\omega \epsilon(\varphi) : \epsilon(Q_\varepsilon^{(1)})\, dx = \gamma_g \int_{\mathsf{D}_\varepsilon} \partial U_\varepsilon^{(1)} \cdot \partial \varphi \, dx \quad \text{for all } \varphi \in H^1_{\Gamma_\varepsilon}(\mathsf{D})^d. \tag{13.100}$$

Contrary to the previous analysis however, we cannot correct this error solely by regular correctors, since the error is attained on the whole domain D_ε and thus the asymptotic behaviour of $U^{(1)} - R^{(1)}$ is not sufficient to achieve convergence. Instead, one has to introduce a boundary layer corrector $\tilde{Q}^{(1)}$ with an appropriate right hand side. Unfortunately, this generalisation is not straight forward, since a similar asymptotic behaviour of $\tilde{Q}^{(1)}$ is not known. In fact, it has been shown in [25, Section 4.2] that a similar analysis can be carried out for $\gamma_g \neq 0$ in dimension $d = 3$, where a slower declining asymptotic behaviour of $\tilde{Q}^{(1)}$ is shown. Nonetheless, the special case $d = 2$ remains an open problem. This highlights the complexity of the asymptotic analysis of the averaged adjoint variable.

14 Computation of the topological derivatives

In this section we compute the first and second order topological derivative of the elasticity problem introduced in (9.6), namely,

$$\mathscr{J}(\Omega) = \gamma_f \int_{\mathsf{D}} f_{\omega_\varepsilon} \cdot u \, dx + \gamma_g \int_{\mathsf{D}} |\partial u - \partial u_d|^2 \, dx + \gamma_m \int_{\Gamma^m} |u - u_m|^2 \, dS, \tag{14.1}$$

subject to $u \in H^1(\mathsf{D})^d$ solves $u|_\Gamma = g_D$ and

$$\int_{\mathsf{D}} \mathbf{A}_\Omega \epsilon(u) : \epsilon(\varphi) = \int_{\mathsf{D}} f_\Omega \cdot \varphi \, dx + \int_{\Gamma^N} g_N \cdot \varphi \, dS \quad \text{for all } \varphi \in H^1_\Gamma(\mathsf{D})^d. \tag{14.2}$$

In view of Definition 9.1, we fix the following parameter throughout this section: $\Omega = \emptyset$, $\omega \subset \mathbf{R}^d$ and $x_0 \in \mathsf{D}$. Furthermore, we introduce for $\varepsilon > 0$ small the asymptotic orders (cf. Remark 9.2)

$$\ell_1(\varepsilon) = |\omega_\varepsilon| = \varepsilon^d |\omega|, \qquad \ell_2(\varepsilon) = \varepsilon |\omega_\varepsilon| = \varepsilon^{d+1}|\omega|. \tag{14.3}$$

Remark 14.1. Note that the more general case $\Omega \neq \emptyset$, $x_0 \in \mathsf{D} \setminus \bar{\Omega}$ and $\Omega_\varepsilon = \Omega \cup \omega_\varepsilon$ can be treated in a similar fashion. The main difference is that the unperturbed state equation and unperturbed adjoint state equation respectively depend on Ω and therefore u_0 and p_0 vary. Furthermore, as the boundary layer correctors coincide in both cases, a volume error is introduced in the exterior domain. This can be overcome by formulating remainder estimates for volume terms similar to Lemma 11.6. At last, the computation of the topological derivative for $x_0 \in \Omega$ and $\Omega_\varepsilon = \Omega \setminus \omega_\varepsilon$ can be done analogously to the presented one and only results in a change of sign.

Since each adjoint based method was introduced in the abstract Lagrangian framework, we want to recall the following notations:

$$a_\varepsilon(u,v) = \int_{\mathsf{D}} \mathbf{A}_{\Omega_\varepsilon} \epsilon(u) : \epsilon(v)\, dx \qquad \text{for all } u \in \mathscr{V}, v \in \mathscr{W}, \tag{14.4}$$

$$f_\varepsilon(v) = \int_{\mathsf{D}} f_{\Omega_\varepsilon} \cdot v\, dx + \int_{\Gamma^N} g_N \cdot v\, dS \qquad \text{for all } v \in \mathscr{W}, \tag{14.5}$$

$$J_\varepsilon(u) = \gamma_f \int_{\mathsf{D}} f_{\Omega_\varepsilon} \cdot u\, dx + \gamma_g \int_{\mathsf{D}} |\partial u - \partial u_d|^2\, dx + \gamma_m \int_{\Gamma^m} |u - u_m|^2\, dS \qquad \text{for all } u \in \mathscr{V}, \tag{14.6}$$

where the spaces $\mathscr{V}, \mathscr{W}$ are defined in (13.1).

14.1 Amstutz' method

We first follow Amstutz' approach. In view of Proposition 10.2 item (i), the first order topological derivative is given by

$$d\mathscr{J}(\Omega,\omega)(x_0) = \mathscr{R}^{(1)}(u_0,p_0) + \partial_\ell^{(1)} \mathscr{L}(0,u_0,p_0), \tag{14.7}$$

where

$$\mathscr{R}^{(1)}(u_0,p_0) = \lim_{\varepsilon \searrow 0} \frac{\mathscr{L}(\varepsilon,u_\varepsilon,p_\varepsilon) - \mathscr{L}(\varepsilon,u_0,p_\varepsilon)}{\ell_1(\varepsilon)}, \tag{14.8}$$

$$\partial_\ell^{(1)} \mathscr{L}(0,u_0,p_0) = \lim_{\varepsilon \searrow 0} \frac{\mathscr{L}(\varepsilon,u_0,p_\varepsilon) - \mathscr{L}(0,u_0,p_\varepsilon)}{\ell_1(\varepsilon)}, \tag{14.9}$$

if the above limits exist. Thus, we start with the first quotient $\mathscr{R}^{(1)}(u_0,p_0)$:

$$\begin{aligned}\frac{\mathscr{L}(\varepsilon,u_\varepsilon,p_\varepsilon)-\mathscr{L}(\varepsilon,u_0,p_\varepsilon)}{\ell_1(\varepsilon)} &= \frac{1}{|\omega_\varepsilon|}[J_\varepsilon(u_\varepsilon)+a_\varepsilon(u_\varepsilon,p_\varepsilon)-f_\varepsilon(p_\varepsilon)-J_\varepsilon(u_0)-a_\varepsilon(u_0,p_\varepsilon)+f_\varepsilon(p_\varepsilon)]\\ &= \frac{1}{|\omega_\varepsilon|}[J_\varepsilon(u_\varepsilon)-J_\varepsilon(u_0)+a_\varepsilon(u_\varepsilon-u_0,p_\varepsilon)]\\ &= \frac{1}{|\omega_\varepsilon|}\gamma_m\int_{\Gamma^m}[|u_\varepsilon-u_m|^2-|u_0-u_m|^2-2(u_0-u_m)(u_\varepsilon-u_0)]\,dS\\ &\quad+\frac{1}{|\omega_\varepsilon|}\gamma_g\int_{\mathsf{D}}\left[|\partial u_\varepsilon-\partial u_d|^2-|\partial u_0-\partial u_d|^2-2(\partial u_0-\partial u_d)(\partial u_\varepsilon-\partial u_0)\right]dx\\ &= \frac{1}{|\omega_\varepsilon|}\gamma_m\int_{\Gamma^m}|u_\varepsilon-u_0|^2\,dS+\frac{1}{|\omega_\varepsilon|}\gamma_g\int_{\mathsf{D}}|\partial u_\varepsilon-\partial u_0|^2\,dx,\end{aligned} \tag{14.10}$$

where we invoked (13.5). A change of variables with respect to T_ε entails

$$\frac{\mathscr{L}(\varepsilon,u_\varepsilon,p_\varepsilon)-\mathscr{L}(\varepsilon,u_0,p_\varepsilon)}{\ell_1(\varepsilon)} = \frac{\varepsilon}{|\omega|}\gamma_m\|U_\varepsilon^{(1)}\|^2_{L_2(\Gamma_\varepsilon^m)^d}+\frac{1}{|\omega|}\gamma_g\|\partial U_\varepsilon^{(1)}\|^2_{L_2(\mathsf{D}_\varepsilon)^{d\times d}}. \tag{14.11}$$

On the one hand, we have

$$\begin{aligned}\frac{\varepsilon}{|\omega|}\gamma_m\|U_\varepsilon^{(1)}\|^2_{L_2(\Gamma_\varepsilon^m)^d} &\le \frac{\gamma_m}{|\omega|}(\varepsilon\|U_\varepsilon^{(1)}-U^{(1)}\|^2_{L_2(\Gamma_\varepsilon^m)^d}+\varepsilon\|U^{(1)}\|^2_{L_2(\Gamma_\varepsilon^m)^d})\\ &\le C(\|U_\varepsilon^{(1)}-U^{(1)}\|_\varepsilon^2+\varepsilon^d)\le C\varepsilon^{2-\alpha},\end{aligned} \tag{14.12}$$

for $\alpha>0$ arbitrarily small and a constant $C>0$. Here, we used Lemma 11.5, item (iv), Lemma 11.6 item (i) with $m=d-1$ and Theorem 12.6. On the other hand, Theorem 12.6 and Lemma 11.6 item (iv) with $m=d-1$ entail

$$\begin{aligned}\|\partial U_\varepsilon^{(1)}-\partial U^{(1)}\|_{L_2(\mathbf{R}^d)^{d\times d}} &= \|\partial U_\varepsilon^{(1)}-\partial U^{(1)}\|_{L_2(\mathsf{D}_\varepsilon)^{d\times d}}+\|\partial U_\varepsilon^{(1)}-\partial U^{(1)}\|_{L_2(\mathbf{R}^d\setminus\mathsf{D}_\varepsilon)^{d\times d}}\\ &\le \|U_\varepsilon^{(1)}-U^{(1)}\|_\varepsilon+\|\partial U_\varepsilon^{(1)}\|_{L_2(\mathbf{R}^d\setminus\mathsf{D}_\varepsilon)^{d\times d}}+\|\partial U^{(1)}\|_{L_2(\mathbf{R}^d\setminus\mathsf{D}_\varepsilon)^{d\times d}}\\ &\le C\varepsilon^{1-\alpha}+\|\partial U_\varepsilon^{(1)}\|_{L_2(\mathbf{R}^d\setminus\mathsf{D}_\varepsilon)^{d\times d}}.\end{aligned} \tag{14.13}$$

for a positive constant $C\in\mathbf{R}$ and $\alpha\in(0,1)$. Since $U_\varepsilon^{(1)}\in\dot{B}L_2(\mathbf{R}^d)^d$ there holds

$$\lim_{\varepsilon\searrow 0}\|\partial U_\varepsilon^{(1)}\|_{L_2(\mathbf{R}^d\setminus\mathsf{D}_\varepsilon)^{d\times d}}=0.$$

This entails $\partial U_\varepsilon^{(1)}\to\partial U^{(1)}$ in $L_2(\mathbf{R}^d)^{d\times d}$ for $\varepsilon\searrow 0$. Now passing to the limit in (14.11) shows

$$\mathscr{R}^{(1)}(u_0,p_0)=\frac{1}{|\omega|}\gamma_g\int_{\mathbf{R}^d}|\partial U^{(1)}|^2\,dx. \tag{14.14}$$

Next, we consider $\partial_\ell^{(1)}\mathscr{L}(0,u_0,p_0)$. Splitting the quotient one observes

$$\begin{aligned}\frac{\mathscr{L}(\varepsilon,u_0,p_\varepsilon)-\mathscr{L}(0,u_0,p_\varepsilon)}{\ell_1(\varepsilon)} &= \frac{1}{|\omega_\varepsilon|}[J_\varepsilon(u_0)+a_\varepsilon(u_0,p_\varepsilon)-f_\varepsilon(p_\varepsilon)-J_0(u_0)-a_0(u_0,p_\varepsilon)+f_0(p_\varepsilon)]\\ &= \frac{1}{|\omega_\varepsilon|}\int_{\omega_\varepsilon}\left[\gamma_f(f_1-f_2)u_0+(\mathbf{A}_1-\mathbf{A}_2)\epsilon(u_0):\epsilon(p_\varepsilon)-(f_1-f_2)p_\varepsilon\right]dx\\ &= \frac{\gamma_f}{|\omega|}\int_\omega (f_1\circ T_\varepsilon - f_2\circ T_\varepsilon)\cdot u_0\circ T_\varepsilon\, dx\\ &\quad+\frac{1}{|\omega|}\int_\omega (\mathbf{A}_1-\mathbf{A}_2)\epsilon(u_0)\circ T_\varepsilon:\epsilon(P_\varepsilon^{(1)})\,dx\\ &\quad+\frac{1}{|\omega|}\int_\omega (\mathbf{A}_1-\mathbf{A}_2)\epsilon(u_0)\circ T_\varepsilon:\epsilon(p_0)\circ T_\varepsilon\,dx\\ &\quad-\frac{\varepsilon}{|\omega|}\int_\omega (f_1\circ T_\varepsilon - f_2\circ T_\varepsilon)\cdot(P_\varepsilon^{(1)})\,dx\\ &\quad-\frac{1}{|\omega|}\int_\omega (f_1\circ T_\varepsilon - f_2\circ T_\varepsilon)\cdot p_0\circ T_\varepsilon\,dx.\end{aligned} \tag{14.15}$$

Thus Theorem 13.4 and Corollary 13.5 entail

$$\begin{aligned}\partial_\ell^{(1)}\mathscr{L}(0,u_0,p_0) = &\frac{1}{|\omega|}\int_\omega (\mathbf{A}_1-\mathbf{A}_2)\epsilon(u_0)(x_0):\epsilon(P^{(1)})\,dx\\ &+\gamma_f(f_1(x_0)-f_2(x_0))\cdot u_0(x_0)\\ &+(\mathbf{A}_1-\mathbf{A}_2)\epsilon(u_0)(x_0):\epsilon(p_0)(x_0)\\ &-(f_1(x_0)-f_2(x_0))\cdot p_0(x_0).\end{aligned} \tag{14.16}$$

Therefore, the first order topological derivative is given by

$$\begin{aligned}d\mathscr{J}(\Omega,\omega)(x_0) = &\frac{1}{|\omega|}\int_\omega (\mathbf{A}_1-\mathbf{A}_2)\epsilon(u_0)(x_0):\epsilon(P^{(1)})\,dx + (\mathbf{A}_1-\mathbf{A}_2)\epsilon(u_0)(x_0):\epsilon(p_0)(x_0)\\ &+\gamma_f(f_1(x_0)-f_2(x_0))\cdot u_0(x_0)-(f_1(x_0)-f_2(x_0))\cdot p_0(x_0)\\ &+\frac{1}{|\omega|}\gamma_g\int_{\mathbf{R}^d}|\partial U^{(1)}|^2\,dx,\end{aligned} \tag{14.17}$$

with $P^{(1)}$ defined in (13.12) and $U^{(1)}$ defined in (12.21).
Next, we compute the second order topological derivative. By Proposition 10.2, item (ii), we have

$$d^2\mathscr{J}(\Omega,\omega)(x_0) = \mathscr{R}^{(2)}(u_0,p_0)+\partial_\ell^{(2)}\mathscr{L}(0,u_0,p_0), \tag{14.18}$$

where

$$\mathscr{R}^{(2)}(u_0,p_0) = \lim_{\varepsilon\searrow 0}\frac{\mathscr{L}(\varepsilon,u_\varepsilon,p_\varepsilon)-\mathscr{L}(\varepsilon,u_0,p_\varepsilon)-\ell_1(\varepsilon)\mathscr{R}^{(1)}(u_0,p_0)}{\ell_2(\varepsilon)},$$

$$\partial_\ell^{(2)}\mathscr{L}(0,u_0,p_0) = \lim_{\varepsilon\searrow 0}\frac{\mathscr{L}(\varepsilon,u_0,p_\varepsilon)-\mathscr{L}(0,u_0,p_\varepsilon)-\ell_1(\varepsilon)\partial_\ell^{(1)}\mathscr{L}(0,u_0,p_0)}{\ell_2(\varepsilon)},$$

if the above limits exist. Dividing (14.11) by ε and subtracting (14.14) it follows that

$$\begin{aligned}\mathscr{R}^{(2)}(u_0,p_0) &= \lim_{\varepsilon\searrow 0}\frac{\gamma_g}{\varepsilon|\omega|}\left[\int_{\mathrm{D}_\varepsilon}|\partial U_\varepsilon^{(1)}|^2-|\partial U^{(1)}|^2\,dx-\int_{\mathbf{R}^d\setminus \mathrm{D}_\varepsilon}|\partial U^{(1)}|^2\,dx\right]\\ &= \lim_{\varepsilon\searrow 0}\frac{\gamma_g}{|\omega|}\left[\int_{\mathrm{D}_\varepsilon}(\partial U_\varepsilon^{(1)}+\partial U^{(1)}):(\varepsilon^{-1}[\partial U_\varepsilon^{(1)}-\partial U^{(1)}])\,dx-\varepsilon^{-1}\int_{\mathbf{R}^d\setminus \mathrm{D}_\varepsilon}|\partial U^{(1)}|^2\,dx\right].\end{aligned} \tag{14.19}$$

In order to pass to the limit in (14.19), we need to assume $\gamma_g=0$ for $d=2$. This is necessary, since Corollary 12.15 is only applicable in dimension 3. Hence, with this assumption we obtain

$$\mathscr{R}^{(2)}(u_0,p_0)=\frac{2\gamma_g}{|\omega|}\int_{\mathbf{R}^d}\partial U^{(1)}:\partial U^{(2)}\,dx. \tag{14.20}$$

To conclude this section we need to investigate $\partial_\ell^{(2)}\mathscr{L}(0,u_0,p_0)$. Similarly to the previous computation, we obtain

$$\begin{aligned}&\frac{\mathscr{L}(\varepsilon,u_0,p_\varepsilon)-\mathscr{L}(0,u_0,p_\varepsilon)-\ell_1(\varepsilon)\partial_\ell^{(1)}\mathscr{L}(0,u_0,p_0)}{\ell_2(\varepsilon)}=\\ &\frac{\gamma_f}{|\omega|}\int_\omega \varepsilon^{-1}[(f_1\circ T_\varepsilon-f_2\circ T_\varepsilon)-(f_1(x_0)-f_2(x_0))]\cdot u_0\circ T_\varepsilon\,dx\\ &+\frac{\gamma_f}{|\omega|}\int_\omega (f_1(x_0)-f_2(x_0))\cdot\varepsilon^{-1}[u_0\circ T_\varepsilon-u_0(x_0)]\,dx\\ &+\frac{1}{|\omega|}\int_\omega(\mathbf{A}_1-\mathbf{A}_2)\epsilon(u_0)\circ T_\varepsilon:\epsilon(\varepsilon^{-1}[P_\varepsilon^{(1)}-P^{(1)}])\,dx\\ &+\frac{1}{|\omega|}\int_\omega(\mathbf{A}_1-\mathbf{A}_2)\varepsilon^{-1}[\epsilon(u_0)\circ T_\varepsilon-\epsilon(u_0)(x_0)]:\epsilon(P^{(1)})\,dx\\ &+\frac{1}{|\omega|}\int_\omega(\mathbf{A}_1-\mathbf{A}_2)\epsilon(u_0)\circ T_\varepsilon:\varepsilon^{-1}[\epsilon(p_0)\circ T_\varepsilon-\epsilon(p_0)(x_0)]\,dx\\ &+\frac{1}{|\omega|}\int_\omega(\mathbf{A}_1-\mathbf{A}_2)\varepsilon^{-1}[\epsilon(u_0)\circ T_\varepsilon-\epsilon(u_0)(x_0)]:\epsilon(p_0)(x_0)\,dx\\ &-\frac{1}{|\omega|}\int_\omega(f_1\circ T_\varepsilon-f_2\circ T_\varepsilon)\cdot(P_\varepsilon^{(1)})\,dx\\ &-\frac{1}{|\omega|}\int_\omega(f_1\circ T_\varepsilon-f_2\circ T_\varepsilon)\cdot\varepsilon^{-1}[p_0\circ T_\varepsilon-p_0(x_0)]\,dx\\ &-\frac{1}{|\omega|}\int_\omega\varepsilon^{-1}[(f_1\circ T_\varepsilon-f_2\circ T_\varepsilon)-(f_1(x_0)-f_2(x_0))]\cdot p_0(x_0)\,dx.\end{aligned} \tag{14.21}$$

Hence, invoking regularity of f_1, f_2, u_0, p_0, Theorem 13.7 item (ii) and Corollary 13.5, we can pass to the limit

$$
\begin{aligned}
\partial_\ell^{(2)}\mathscr{L}(0,u_0,p_0) = & \frac{\gamma_f}{|\omega|}\int_\omega [\partial f_1(x_0)-\partial f_2(x_0)]x\cdot u_0(x_0)\,dx + \frac{\gamma_f}{|\omega|}\int_\omega [f_1(x_0)-f_2(x_0)]\cdot \partial u_0(x_0)x\,dx \\
& + \frac{1}{|\omega|}\int_\omega (\mathbf{A}_1-\mathbf{A}_2)\epsilon(u_0)(x_0):\epsilon(P^{(2)})\,dx + \frac{1}{|\omega|}\int_\omega (\mathbf{A}_1-\mathbf{A}_2)[\partial(\epsilon(u_0))(x_0)x]:\epsilon(P^{(1)})\,dx \\
& + \frac{1}{|\omega|}\int_\omega (\mathbf{A}_1-\mathbf{A}_2)\epsilon(u_0)(x_0):[\partial(\epsilon(p_0))(x_0)x]\,dx \\
& + \frac{1}{|\omega|}\int_\omega (\mathbf{A}_1-\mathbf{A}_2)[\partial(\epsilon(u_0))(x_0)x]:\epsilon(p_0)(x_0)\,dx \\
& - \frac{1}{|\omega|}\int_\omega [f_1(x_0)-f_2(x_0)]\cdot\partial p_0(x_0)x\,dx - \frac{1}{|\omega|}\int_\omega [\partial f_1(x_0)-\partial f_2(x_0)]x\cdot p_0(x_0)\,dx \\
& - \frac{1}{|\omega|}\int_\omega (f_1(x_0)-f_2(x_0))\cdot(P^{(1)})\,dx.
\end{aligned}
\tag{14.22}
$$

Thus, the second order topological derivative is given by

$$
\begin{aligned}
d^2\mathscr{J}(\Omega,\omega)(x_0) = & \frac{2\gamma_g}{|\omega|}\int_{\mathbf{R}^d} \partial U^{(1)}:\partial U^{(2)}\,dx \\
& + \frac{\gamma_f}{|\omega|}\int_\omega [\partial f_1(x_0)-\partial f_2(x_0)]x\cdot u_0(x_0)\,dx + \frac{\gamma_f}{|\omega|}\int_\omega [f_1(x_0)-f_2(x_0)]\cdot \partial u_0(x_0)x\,dx \\
& + \frac{1}{|\omega|}\int_\omega (\mathbf{A}_1-\mathbf{A}_2)\epsilon(u_0)(x_0):\epsilon(P^{(2)})\,dx + \frac{1}{|\omega|}\int_\omega (\mathbf{A}_1-\mathbf{A}_2)[\partial(\epsilon(u_0))(x_0)x]:\epsilon(P^{(1)})\,dx \\
& + \frac{1}{|\omega|}\int_\omega (\mathbf{A}_1-\mathbf{A}_2)\epsilon(u_0)(x_0):[\partial(\epsilon(p_0))(x_0)x]\,dx \\
& + \frac{1}{|\omega|}\int_\omega (\mathbf{A}_1-\mathbf{A}_2)[\partial(\epsilon(u_0))(x_0)x]:\epsilon(p_0)(x_0)\,dx \\
& - \frac{1}{|\omega|}\int_\omega [f_1(x_0)-f_2(x_0)]\cdot\partial p_0(x_0)x\,dx - \frac{1}{|\omega|}\int_\omega [\partial f_1(x_0)-\partial f_2(x_0)]x\cdot p_0(x_0)\,dx \\
& - \frac{1}{|\omega|}\int_\omega (f_1(x_0)-f_2(x_0))\cdot(P^{(1)})\,dx,
\end{aligned}
\tag{14.23}
$$

with $P^{(1)}$ defined in (13.12), $U^{(1)}$ defined in (12.21), $P^{(2)}$ defined in (13.29),(13.32) and $U^{(2)}$ defined in (12.48),(12.51).

14.2 Averaged adjoint method

In this section we follow the averaged adjoint approach. In view of Proposition 10.4 item (i) we have

$$d\mathscr{J}(\Omega,\omega)(x_0) = \mathscr{R}^{(1)}(u_0,q_0) + \partial_\ell^{(1)}\mathscr{L}(0,u_0,q_0), \tag{14.24}$$

where

$$\begin{aligned}\mathscr{R}^{(1)}(u_0,q_0) &= \lim_{\varepsilon\searrow 0}\frac{\mathscr{L}(\varepsilon,u_0,q_\varepsilon)-\mathscr{L}(\varepsilon,u_0,q_0)}{\ell_1(\varepsilon)},\\ \partial_\ell^{(1)}\mathscr{L}(0,u_0,q_0) &= \lim_{\varepsilon\searrow 0}\frac{\mathscr{L}(\varepsilon,u_0,q_0)-\mathscr{L}(0,u_0,q_0)}{\ell_1(\varepsilon)},\end{aligned}$$

if the above limits exist. Thus, we start with the computation of $\mathscr{R}^{(1)}(u_0,q_0)$:

$$\begin{aligned}\frac{\mathscr{L}(\varepsilon,u_0,q_\varepsilon)-\mathscr{L}(\varepsilon,u_0,q_0)}{\ell_1(\varepsilon)} &= \frac{1}{|\omega_\varepsilon|}[J_\varepsilon(u_0)+a_\varepsilon(u_0,q_\varepsilon)-f_\varepsilon(q_\varepsilon)-J_\varepsilon(u_0)-a_\varepsilon(u_0,q_0)+f_\varepsilon(q_0)]\\ &= \frac{1}{|\omega_\varepsilon|}[a_\varepsilon(u_0,q_\varepsilon-q_0)-f_\varepsilon(q_\varepsilon-q_0)]\\ &= \frac{1}{|\omega_\varepsilon|}\left[\int_{\omega_\varepsilon}(\mathbf{A}_1-\mathbf{A}_2)\epsilon(u_0):\epsilon(q_\varepsilon-q_0)\,dx-\int_{\omega_\varepsilon}(f_1-f_2)\cdot(q_\varepsilon-q_0)\,dx\right]\\ &= \frac{1}{|\omega|}\int_\omega(\mathbf{A}_1-\mathbf{A}_2)\epsilon(u_0)\circ T_\varepsilon:\epsilon(Q_\varepsilon^{(1)})\,dx-\varepsilon\frac{1}{|\omega|}\int_\omega(f_1-f_2)\circ T_\varepsilon(Q_\varepsilon^{(1)})\,dx.\end{aligned} \tag{14.25}$$

Since $u_0\in C^3(B_\delta(x_0))^d$ for $\delta>0$ small and by Theorem 13.10 $\epsilon(Q_\varepsilon^{(1)})\to\epsilon(Q^{(1)})$ in $L_2(\omega)^{d\times d}$ as ε tends to zero, we have

$$\lim_{\varepsilon\searrow 0}\int_\omega(\mathbf{A}_1-\mathbf{A}_2)\epsilon(u_0)\circ T_\varepsilon:\epsilon(Q_\varepsilon^{(1)})\,dx = \int_\omega(\mathbf{A}_1-\mathbf{A}_2)\epsilon(u_0)(x_0):\epsilon(Q^{(1)})\,dx. \tag{14.26}$$

Furthermore, Corollary 12.8 entails

$$\lim_{\varepsilon\searrow 0}\varepsilon\int_\omega[(f_1-f_2)\circ T_\varepsilon]\cdot Q_\varepsilon^{(1)}\,dx = 0. \tag{14.27}$$

Hence, it follows that

$$\mathscr{R}^{(1)}(u_0,q_0) = \frac{1}{|\omega|}\int_\omega(\mathbf{A}_1-\mathbf{A}_2)\epsilon(u_0)(x_0):\epsilon(Q^{(1)})\,dx. \tag{14.28}$$

Next, we compute $\partial_\ell^{(1)}\mathscr{L}(0,u_0,q_0)$. We note for $\varepsilon>0$

$$\frac{\mathscr{L}(\varepsilon,u_0,q_0)-\mathscr{L}(0,u_0,q_0)}{\ell_1(\varepsilon)} = \frac{1}{|\omega_\varepsilon|}[(J_\varepsilon(u_0)-J_0(u_0))+(a_\varepsilon(u_0,q_0)-a_0(u_0,q_0))-(f_\varepsilon(q_0)-f_0(q_0))]$$
$$= \frac{1}{|\omega_\varepsilon|}\Big[\gamma_f\int_{\omega_\varepsilon}(f_1-f_2)\cdot u_0\,dx+\int_{\omega_\varepsilon}(\mathbf{A}_1-\mathbf{A}_2)\epsilon(u_0):\epsilon(q_0)\,dx - \int_{\omega_\varepsilon}(f_1-f_2)\cdot q_0\,dx\Big]$$
$$= \frac{\gamma_f}{|\omega|}\int_\omega (f_1-f_2)\circ T_\varepsilon\cdot u_0\circ T_\varepsilon\,dx - \int_\omega (f_1-f_2)\circ T_\varepsilon\cdot q_0\circ T_\varepsilon\,dx + \frac{1}{|\omega|}\int_\omega(\mathbf{A}_1-\mathbf{A}_2)\epsilon(u_0)\circ T_\varepsilon:\epsilon(q_0)\circ T_\varepsilon\,dx. \tag{14.29}$$

Passing to the limit yields

$$\partial_\ell^{(1)}\mathscr{L}(0,u_0,q_0) = \big[\gamma_f(f_1-f_2)\cdot u_0+(\mathbf{A}_1-\mathbf{A}_2)\epsilon(u_0):\epsilon(q_0)-(f_1-f_2)\cdot q_0\big](x_0), \tag{14.30}$$

where we employed regularity of f_1, f_2, u_0 and q_0. Combining (14.28) and (14.28) results in

$$d\mathscr{J}(\Omega,\omega)(x_0) = \frac{1}{|\omega|}\int_\omega(\mathbf{A}_1-\mathbf{A}_2)\epsilon(u_0)(x_0):\epsilon(Q^{(1)})\,dx+(\mathbf{A}_1-\mathbf{A}_2)\epsilon(u_0)(x_0):\epsilon(q_0)(x_0) + \gamma_f(f_1(x_0)-f_2(x_0))\cdot u_0(x_0)-(f_1(x_0)-f_2(x_0))\cdot q_0(x_0), \tag{14.31}$$

with $Q^{(1)}$ defined in (13.59).
Next we compute the second order topological derivative. By Proposition 10.4 item (ii) we have

$$d^2\mathscr{J}(\Omega,\omega)(x_0) = \mathscr{R}^{(2)}(u_0,q_0)+\partial_\ell^{(2)}\mathscr{L}(0,u_0,q_0), \tag{14.32}$$

where

$$\mathscr{R}^{(2)}(u_0,q_0) = \lim_{\varepsilon\searrow 0}\frac{\mathscr{L}(\varepsilon,u_0,q_\varepsilon)-\mathscr{L}(\varepsilon,u_0,q_0)-\ell_1(\varepsilon)\mathscr{R}^{(1)}(u_0,q_0)}{\ell_2(\varepsilon)},$$
$$\partial_\ell^{(2)}\mathscr{L}(0,u_0,q_0) = \lim_{\varepsilon\searrow 0}\frac{\mathscr{L}(\varepsilon,u_0,q_0)-\mathscr{L}(0,u_0,q_0)-\ell_1(\varepsilon)\partial_\ell^{(1)}\mathscr{L}(0,u_0,q_0)}{\ell_2(\varepsilon)},$$

if the above limits exist. We start by computing $\mathscr{R}^{(2)}(u_0,q_0)$. Using (14.25) we deduce

$$
\begin{aligned}
\mathcal{R}^{(2)}(u_0,q_0) = \lim_{\varepsilon\searrow 0}\Bigg[&\frac{1}{|\omega|}\int_\omega (\mathbf{A}_1-\mathbf{A}_2)[\varepsilon^{-1}(\epsilon(u_0)\circ T_\varepsilon - \epsilon(u_0)(x_0))] : \epsilon(Q_\varepsilon^{(1)})\,dx \\
&+ \frac{1}{|\omega|}\int_\omega (\mathbf{A}_1-\mathbf{A}_2)\epsilon(u_0)(x_0) : \epsilon(\varepsilon^{-1}(Q_\varepsilon^{(1)}-Q^{(1)}))\,dx \\
&- \frac{1}{|\omega|}\int_\omega (f_1-f_2)\circ T_\varepsilon \cdot (Q_\varepsilon^{(1)})\,dx \Bigg] \\
= \int_\omega (\mathbf{A}_1-\mathbf{A}_2)&[\partial(\epsilon(u_0))(x_0)x] : \epsilon(Q^{(1)})\,dx + \frac{1}{|\omega|}\int_\omega (\mathbf{A}_1-\mathbf{A}_2)\epsilon(u_0)(x_0) : \epsilon(Q^{(2)})\,dx \\
- \frac{1}{|\omega|}\int_\omega & (f_1(x_0)-f_2(x_0))\cdot(Q^{(1)})\,dx,
\end{aligned}
\tag{14.33}
$$

where we used $Q_\varepsilon^{(1)} \to Q^{(1)}$ in $L_1(\omega)^d$ by Corollary 13.11, $\epsilon(Q_\varepsilon^{(1)}) \to \epsilon(Q^{(1)})$ in $L_2(\omega)^d$ and by Theorem 13.13 $\varepsilon^{-1}(\epsilon(Q_\varepsilon^{(1)}) - \epsilon(Q^{(1)})) \to \epsilon(Q^{(2)})$ in $L_2(\omega)^d$. Next, we compute $\partial_\ell^{(2)}\mathcal{L}(0,u_0,q_0)$:

$$
\begin{aligned}
\partial_\ell^{(2)}\mathcal{L}(0,u_0,q_0) = \lim_{\varepsilon\searrow 0}\Bigg[&\frac{\gamma_f}{|\omega|}\int_\omega \varepsilon^{-1}[(f_1-f_2)\circ T_\varepsilon \cdot u_0\circ T_\varepsilon - (f_1(x_0)-f_2(x_0))\cdot u_0(x_0)]\,dx \\
&+ \frac{1}{|\omega|}\int_\omega \varepsilon^{-1}[(\mathbf{A}_1-\mathbf{A}_2)\epsilon(u_0)\circ T_\varepsilon : \epsilon(q_0)\circ T_\varepsilon - (\mathbf{A}_1-\mathbf{A}_2)\epsilon(u_0)(x_0) : \epsilon(q_0)(x_0)]\,dx \\
&- \frac{1}{|\omega|}\int_\omega \varepsilon^{-1}[(f_1-f_2)\circ T_\varepsilon \cdot q_0\circ T_\varepsilon - (f_1(x_0)-f_2(x_0))\cdot q_0(x_0)]\,dx \Bigg] \\
= &\frac{\gamma_f}{|\omega|}\int_\omega \partial[(f_1-f_2)](x_0)x\cdot u_0(x_0)\,dx + \frac{\gamma_f}{|\omega|}\int_\omega [f_1(x_0)-f_2(x_0)]\cdot \partial u_0(x_0)x\,dx \\
&+ \frac{1}{|\omega|}\int_\omega (\mathbf{A}_1-\mathbf{A}_2)[\partial(\epsilon(u_0))(x_0)x] : \epsilon(q_0)(x_0)\,dx \\
&+ \frac{1}{|\omega|}\int_\omega (\mathbf{A}_1-\mathbf{A}_2)\epsilon(u_0)(x_0) : [\partial(\epsilon(q_0))(x_0)x]\,dx \\
&- \frac{1}{|\omega|}\int_\omega [\partial(f_1-f_2)(x_0)]x\cdot q_0(x_0)\,dx - \frac{1}{|\omega|}\int_\omega [f_1(x_0)-f_2(x_0)]\cdot\partial q_0(x_0)x\,dx,
\end{aligned}
\tag{14.34}
$$

where again we used the smoothness of u_0, q_0, f_1, f_2 in the vicinity of x_0 in the last step. Furthermore, combining (14.33) and (14.34), we obtain the final formula for the second order topological derivative:

$$
\begin{aligned}
d^2\mathscr{J}(\Omega,\omega)(x_0) = &\int_\omega (\mathbf{A}_1-\mathbf{A}_2)[\partial(\epsilon(u_0))(x_0)x]:\epsilon(Q^{(1)})\,dx + \frac{1}{|\omega|}\int_\omega (\mathbf{A}_1-\mathbf{A}_2)\epsilon(u_0)(x_0):\epsilon(Q^{(2)})\,dx \\
&- \frac{1}{|\omega|}\int_\omega (f_1(x_0)-f_2(x_0))\cdot(Q^{(1)})\,dx \\
&+ \frac{\gamma_f}{|\omega|}\int_\omega \partial[(f_1-f_2)](x_0)x\cdot u_0(x_0)\,dx + \frac{\gamma_f}{|\omega|}\int_\omega [f_1(x_0)-f_2(x_0)]\cdot\partial u_0(x_0)x\,dx \\
&+ \frac{1}{|\omega|}\int_\omega (\mathbf{A}_1-\mathbf{A}_2)[\partial(\epsilon(u_0))(x_0)x]:\epsilon(q_0)(x_0)\,dx \\
&+ \frac{1}{|\omega|}\int_\omega (\mathbf{A}_1-\mathbf{A}_2)\epsilon(u_0)(x_0):[\partial(\epsilon(q_0))(x_0)x]\,dx \\
&- \frac{1}{|\omega|}\int_\omega [\partial(f_1-f_2)(x_0)]x\cdot q_0(x_0)\,dx - \frac{1}{|\omega|}\int_\omega [f_1(x_0)-f_2(x_0)]\cdot\partial q_0(x_0)x\,dx.
\end{aligned}
\tag{14.35}
$$

14.3 Delfour's method

At last, we consider Delfour's method to compute the topological derivative. Therefore, recall that by Proposition 10.6 item (i) we have

$$
d\mathscr{J}(\Omega,\omega)(x_0) = \mathscr{R}_1^{(1)}(u_0,p_0) + \mathscr{R}_2^{(1)}(u_0,p_0) + \partial_\ell^{(1)}\mathscr{L}(0,u_0,p_0), \tag{14.36}
$$

where

$$
\mathscr{R}_1^{(1)}(u_0,p_0) = \lim_{\varepsilon\searrow 0}\frac{\mathscr{L}(\varepsilon,u_\varepsilon,p_0)-\mathscr{L}(\varepsilon,u_0,p_0)-\partial_u\mathscr{L}(\varepsilon,u_0,p_0)(u_\varepsilon-u_0)}{\ell_1(\varepsilon)}, \tag{14.37}
$$

$$
\mathscr{R}_2^{(1)}(u_0,p_0) = \lim_{\varepsilon\searrow 0}\frac{(\partial_u\mathscr{L}(\varepsilon,u_0,p_0)-\partial_u\mathscr{L}(0,u_0,p_0))(u_\varepsilon-u_0)}{\ell_1(\varepsilon)}, \tag{14.38}
$$

$$
\partial_\ell^{(1)}\mathscr{L}(0,u_0,p_0) = \lim_{\varepsilon\searrow 0}\frac{\mathscr{L}(\varepsilon,u_0,p_0)-\mathscr{L}(0,u_0,p_0)}{\ell_1(\varepsilon)}. \tag{14.39}
$$

We now compute the limit of each term. Plugging in the definition of $\mathscr{L}(\varepsilon,u,v)$, we get for $\varepsilon>0$

$$
\begin{aligned}
\frac{\mathscr{L}(\varepsilon,u_\varepsilon,p_0)-\mathscr{L}(\varepsilon,u_0,p_0)-\partial_u\mathscr{L}(\varepsilon,u_0,p_0)(u_\varepsilon-u_0)}{\ell_1(\varepsilon)} &= \frac{1}{|\omega_\varepsilon|}(J_\varepsilon(u_\varepsilon)-J_\varepsilon(u_0)-\partial_u J_\varepsilon(u_0)(u_\varepsilon-u_0)) \\
&= \frac{\gamma_g}{|\omega_\varepsilon|}\int_{\mathsf{D}}|\partial u_\varepsilon-\partial u_0|^2\,dx + \frac{\gamma_m}{|\omega_\varepsilon|}\int_{\Gamma^m}|u_\varepsilon-u_0|^2\,dS \\
&= \frac{\gamma_g}{|\omega|}\int_{\mathsf{D}_\varepsilon}|\partial U_\varepsilon^{(1)}|^2\,dx + \varepsilon\frac{\gamma_m}{|\omega|}\int_{\Gamma_\varepsilon^m}|U_\varepsilon^{(1)}|^2\,dS.
\end{aligned}
\tag{14.40}
$$

Hence, passing to the limit $\varepsilon\searrow 0$ (cf. (14.11)) yields

$$
\mathscr{R}_1^{(1)}(u_0,p_0) = \frac{\gamma_g}{|\omega|}\|\partial U^{(1)}\|^2_{L_2(\mathbf{R}^d)^{d\times d}}. \tag{14.41}
$$

Furthermore, we have

$$
\begin{aligned}
\frac{1}{\ell_1(\varepsilon)}(\partial_u \mathcal{L}(\varepsilon,u_0,p_0)-\partial_u \mathcal{L}(0,u_0,p_0))(u_\varepsilon-u_0) =& \frac{1}{|\omega_\varepsilon|}\gamma_f \int_{\omega_\varepsilon}(f_1-f_2)\cdot(u_\varepsilon-u_0)\,dx \\
&+\frac{1}{|\omega_\varepsilon|}\int_{\omega_\varepsilon}(\mathbf{A}_1-\mathbf{A}_2)\epsilon(u_\varepsilon-u_0):\epsilon(p_0)\,dx \\
=&\varepsilon\frac{\gamma_f}{|\omega|}\int_\omega (f_1\circ T_\varepsilon-f_2\circ T_\varepsilon)\cdot(U_\varepsilon^{(1)})\,dx \\
&+\frac{1}{|\omega|}\int_\omega (\mathbf{A}_1-\mathbf{A}_2)\epsilon(U_\varepsilon^{(1)}):\epsilon(p_0)\circ T_\varepsilon\,dx.
\end{aligned}
\tag{14.42}
$$

Hence, Theorem 12.6 and Corollary 12.8 entail

$$
\mathcal{R}_2^{(1)}(u_0,p_0)=\frac{1}{|\omega|}\int_\omega (\mathbf{A}_1-\mathbf{A}_2)\epsilon(U^{(1)}):\epsilon(p_0)(x_0)\,dx. \tag{14.43}
$$

Similarly to the previous approaches, regularity of f_1, f_2, u_0 and p_0 yields

$$
\begin{aligned}
\partial_\ell^{(1)}\mathcal{L}(0,u_0,p_0)=&\lim_{\varepsilon\searrow 0}\frac{\mathcal{L}(\varepsilon,u_0,p_0)-\mathcal{L}(0,u_0,p_0)}{\ell_1(\varepsilon)} \\
=&\frac{1}{|\omega_\varepsilon|}\int_{\omega_\varepsilon}\left(\gamma_f(f_1-f_2)\cdot u_0+(\mathbf{A}_1-\mathbf{A}_2)\epsilon(u_0):\epsilon(p_0)-(f_1-f_2)\cdot p_0\right)\,dx \\
=&\frac{1}{|\omega|}\int_\omega \left(\gamma_f(f_1-f_2)\circ T_\varepsilon\cdot u_0\circ T_\varepsilon+(\mathbf{A}_1-\mathbf{A}_2)\epsilon(u_0)\circ T_\varepsilon:\epsilon(p_0)\circ T_\varepsilon\right)\,dx \\
&-\frac{1}{|\omega|}\int_\omega (f_1-f_2)\circ T_\varepsilon\cdot p_0\circ T_\varepsilon\,dx \\
=&\gamma_f(f_1(x_0)-f_2(x_0))\cdot u_0(x_0)+(\mathbf{A}_1-\mathbf{A}_2)\epsilon(u_0)(x_0):\epsilon(p_0)(x_0) \\
&-(f_1(x_0)-f_2(x_0))\cdot p_0(x_0).
\end{aligned}
\tag{14.44}
$$

Combining these limits results in

$$
\begin{aligned}
d\mathcal{J}(\Omega,\omega)(x_0)=&\frac{1}{|\omega|}\int_\omega (\mathbf{A}_1-\mathbf{A}_2)\epsilon(U^{(1)}):\epsilon(p_0)(x_0)\,dx+(\mathbf{A}_1-\mathbf{A}_2)\epsilon(u_0)(x_0):\epsilon(p_0)(x_0) \\
&+\gamma_f(f_1(x_0)-f_2(x_0))\cdot u_0(x_0)-(f_1(x_0)-f_2(x_0))\cdot p_0(x_0) \\
&+\frac{\gamma_g}{|\omega|}\int_{\mathbf{R}^d}|\partial U^{(1)}|^2\,dx,
\end{aligned}
\tag{14.45}
$$

with $U^{(1)}$ defined in (12.21).

Next, we compute the second order topological derivative. In view of Proposition 10.6, item (ii), we first show that the following limits exist:

$$\mathscr{R}_1^{(2)}(u_0,p_0) = \lim_{\varepsilon\searrow 0} \frac{\mathscr{L}(\varepsilon,u_\varepsilon,p_0) - \mathscr{L}(\varepsilon,u_0,p_0) - \partial_u\mathscr{L}(\varepsilon,u_0,p_0)(u_\varepsilon - u_0) - \ell_1(\varepsilon)\mathscr{R}_1^{(1)}(u_0,p_0)}{\ell_2(\varepsilon)}, \tag{14.46}$$

$$\mathscr{R}_2^{(2)}(u_0,p_0) = \lim_{\varepsilon\searrow 0} \frac{(\partial_u\mathscr{L}(\varepsilon,u_0,p_0) - \partial_u\mathscr{L}(0,u_0,p_0))(u_\varepsilon - u_0) - \ell_1(\varepsilon)\mathscr{R}_2^{(1)}(u_0,p_0)}{\ell_2(\varepsilon)}, \tag{14.47}$$

$$\partial_\ell^{(2)}\mathscr{L}(0,u_0,p_0) = \lim_{\varepsilon\searrow 0} \frac{\mathscr{L}(\varepsilon,u_0,p_0) - \mathscr{L}(0,u_0,p_0) - \ell_1(\varepsilon)\partial_\ell^{(1)}\mathscr{L}(0,u_0,p_0)}{\ell_2(\varepsilon)}. \tag{14.48}$$

Invoking the assumption $\gamma_g = 0$ in dimension $d = 2$, we can deduce

$$\mathscr{R}_1^{(2)}(u_0,p_0) = 2\frac{\gamma_g}{|\omega|}\int_{\mathbf{R}^d} \partial U^{(1)} : \partial U^{(2)}\,dx, \tag{14.49}$$

in a similar fashion to (14.19). Furthermore, we have

$$\begin{aligned}\frac{1}{\ell_2(\varepsilon)}&(\partial_u\mathscr{L}(\varepsilon,u_0,p_0) - \partial_u\mathscr{L}(0,u_0,p_0))(u_\varepsilon - u_0) - \ell_1(\varepsilon)\mathscr{R}_2^{(1)}(u_0,p_0)\\ &= \frac{\gamma_f}{|\omega|}\int_\omega (f_1\circ T_\varepsilon - f_2\circ T_\varepsilon)\cdot U_\varepsilon^{(1)}\,dx\\ &\quad + \frac{1}{|\omega|}\int_\omega (\mathbf{A}_1 - \mathbf{A}_2)\epsilon(\varepsilon^{-1}[U_\varepsilon^{(1)} - U^{(1)}]) : \epsilon(p_0)\circ T_\varepsilon\,dx\\ &\quad + \frac{1}{|\omega|}\int_\omega (\mathbf{A}_1 - \mathbf{A}_2)\epsilon(U^{(1)}) : [\varepsilon^{-1}(\epsilon(p_0)\circ T_\varepsilon - \epsilon(p_0)(x_0))]\,dx.\end{aligned} \tag{14.50}$$

Hence we obtain the limit

$$\begin{aligned}\mathscr{R}_2^{(2)}(u_0,p_0) =& \frac{\gamma_f}{|\omega|}\int_\omega (f_1(x_0) - f_2(x_0))\cdot U^{(1)}\,dx\\ &+ \frac{1}{|\omega|}\int_\omega (\mathbf{A}_1 - \mathbf{A}_2)\epsilon(U^{(2)}) : \epsilon(p_0)(x_0)\,dx\\ &+ \frac{1}{|\omega|}\int_\omega (\mathbf{A}_1 - \mathbf{A}_2)\epsilon(U^{(1)}) : \partial(\epsilon(p_0))(x_0)\,dx.\end{aligned} \tag{14.51}$$

To conclude the computation of the second order derivative we observe that, similarly to (14.44), (14.21), we get

$$
\begin{aligned}
\partial_\ell^{(2)}\mathscr{L}(0,u_0,p_0) =& \frac{\gamma_f}{|\omega|}\int_\omega \partial[f_1(x_0)-f_2(x_0)]x\cdot u_0(x_0)\,dx + \frac{\gamma_f}{|\omega|}\int_\omega [f_1(x_0)-f_2(x_0)]\cdot\partial u_0(x_0)x\,dx\\
&+\frac{1}{|\omega|}\int_\omega (\mathbf{A}_1-\mathbf{A}_2)[\partial(\epsilon(u_0))(x_0)x]:\epsilon(p_0)(x_0)\,dx\\
&+\frac{1}{|\omega|}\int_\omega (\mathbf{A}_1-\mathbf{A}_2)\epsilon(u_0)(x_0):[\partial(\epsilon(p_0))(x_0)x]\,dx\\
&-\frac{1}{|\omega|}\int_\omega \partial[f_1(x_0)-f_2(x_0)]x\cdot p_0(x_0)\,dx - \frac{1}{|\omega|}\int_\omega [f_1(x_0)-f_2(x_0)]\cdot\partial p_0(x_0)x\,dx.
\end{aligned}
\tag{14.52}
$$

Combining the limits (14.49), (14.51), (14.52) entails

$$
\begin{aligned}
d^2\mathscr{J}(\Omega,\omega)(x_0) =& 2\frac{\gamma_g}{|\omega|}\int_{\mathbf{R}^d}\partial U^{(1)}:\partial U^{(2)}\,dx + \frac{\gamma_f}{|\omega|}\int_\omega (f_1(x_0)-f_2(x_0))\cdot U^{(1)}\,dx\\
&+\frac{1}{|\omega|}\int_\omega (\mathbf{A}_1-\mathbf{A}_2)\epsilon(U^{(2)}):\epsilon(p_0)(x_0)\,dx + \frac{1}{|\omega|}\int_\omega (\mathbf{A}_1-\mathbf{A}_2)\epsilon(U^{(1)}):\partial(\epsilon(p_0))(x_0)\,dx\\
&+\frac{\gamma_f}{|\omega|}\int_\omega \partial[f_1(x_0)-f_2(x_0)]x\cdot u_0(x_0)\,dx + \frac{\gamma_f}{|\omega|}\int_\omega [f_1(x_0)-f_2(x_0)]\cdot\partial u_0(x_0)x\,dx\\
&+\frac{1}{|\omega|}\int_\omega (\mathbf{A}_1-\mathbf{A}_2)[\partial(\epsilon(u_0))(x_0)x]:\epsilon(p_0)(x_0)\,dx\\
&+\frac{1}{|\omega|}\int_\omega (\mathbf{A}_1-\mathbf{A}_2)\epsilon(u_0)(x_0):[\partial(\epsilon(p_0))(x_0)x]\,dx\\
&-\frac{1}{|\omega|}\int_\omega \partial[f_1(x_0)-f_2(x_0)]x\cdot p_0(x_0)\,dx - \frac{1}{|\omega|}\int_\omega [f_1(x_0)-f_2(x_0)]\cdot\partial p_0(x_0)x\,dx,
\end{aligned}
\tag{14.53}
$$

with $U^{(1)}$ defined in (12.21) and $U^{(2)}$ defined in (12.48),(12.51). This finishes the computation of the second order topological derivative using Delfour's method.

Remark 14.2. We would like to point out that, using the defining equations of the boundary layer correctors, one can show that all three expressions of the topological derivative coincide and therefore all methods lead to the same result. To get an idea, we show that the first order topological derivative of Amstutz' approach and Delfour's method are the same. Testing (12.21) with $\varphi = P^{(1)}$ yields

$$\int_\omega (\mathbf{A}_1-\mathbf{A}_2)\epsilon(u_0)(x_0):\epsilon(P^{(1)})\,dx = -\int_{\mathbf{R}^d}\mathbf{A}_\omega\epsilon(U^{(1)}):\epsilon(P^{(1)})\,dx.$$

Invoking symmetry of the elasticity tensors, we further deduce

$$\int_{\mathbf{R}^d}\mathbf{A}_\omega\epsilon(U^{(1)}):\epsilon(P^{(1)})\,dx = \int_\omega (\mathbf{A}_2-\mathbf{A}_1)\epsilon(U^{(1)}):\epsilon(p_0)(x_0)\,dx.$$

Hence, we conclude that both derivatives coincide. To obtain equivalence for the averaged adjoint method, one has to recall our assumption $\gamma_g = 0$ in Section 13.2.

15 Conclusion

In this part of the thesis we reviewed three different methods to compute the second order topological derivative and illustrated their methodologies by applying them to a linear elasticity model. To give a better insight into the differences of these methods, the cost functional consists of three terms: the compliance, a L_2 tracking-type over a part of the Neumann boundary and a gradient tracking-type over the whole domain, whereas the first one is linear and the latter two are quadratic. We observed that all three methods shared some similarities, as they rely on the asymptotic analysis of the state variable. Yet differences occur, whose magnitude is based on the specific cost functional.
Amstutz' method requires the asymptotic analysis of the adjoint state p_ε. Since p_ε depends on the unperturbed state variable u_ε, the ε dependence solely stems from the underlying cost functionals. This leads to a straight forward analysis of the adjoint state p_ε, which in our case resembled the analysis of the state variable u_ε closely. Hence we would like to point out that, even though an additional asymptotic expansion is required in this approach, this does not require a lot of extra work. Contrary, the averaged adjoint method requires the asymptotic analysis of the averaged adjoint state q_ε, which is more technically involved. These challenges arise, since q_ε additionally depends on the perturbed state variable u_ε. In this context Delfour's method is advantageous, as it only depends on the unperturbed adjoint state variable p_0 and thus does not necessitate an additional asymptotic analysis. This advantage seems to come with the shortcoming, that this method is only applicable to a selective set of cost functions.
The varying difficulties of each cost functional arise at different parts of the analysis. While the computation of the topological derivative for the linear compliance term is straight forward, the nonlinear nature of the tracking-type cost functionals introduces additional difficulties. Following Amstutz' and Delfour's approach, this leads to limits on the whole space $\mathbf{R}^d$ during the computation of the topological derivative. This is especially problematic for the second order topological derivative. Contrary, employing the averaged adjoint method, the computation of the topological derivative solely involves limits on the bounded domain ω. This comes at a cost of a strictly more involved analysis of the adjoint variable. In fact, the averaged adjoint method shifts the work from the computation of the topological derivative to the asymptotic analysis of the adjoint variable. Compared to Amstutz' and Delfour's method this leads to a slightly more challenging computation in total. Yet we want to highlight that, once the complete asymptotic expansion is known, this allows a straightforward schematic derivation of higher order topological derivatives. We will utilise this behaviour in the next part of this thesis.
To recapitulate, each method proposed in this work has some advantages and disadvantages over the others. The decision on which method fits the actual problem setting the best, greatly depends on the actual cost function as well as the properties of the underlying partial differential equation.

Part III

Complete topological asymptotic expansion

The content of this part stems from the following article, which is submitted for publication:

[23] P. Baumann, P. Gangl, and K. Sturm. Complete topological asymptotic expansion for L_2 and H^1 tracking-type cost functionals in dimension two and three. 2021. arXiv:2111.08418.

16 Introduction to higher order topological sensitivities

In this part of the thesis we are going to continue the investigation of topological derivatives. To specify, we are interested in the complete asymptotic expansion of a shape functional $\mathcal{J}$ subject to topological perturbations. This naturally involves the notion of higher order topological derivatives beyond the second order, which were introduced in the previous part. While the first order topological derivative can be used in gradient based methods (cf. [15,17,56] and further references found in the previous part), higher order topological derivatives give rise to higher order topology optimisation algorithms. Since these are noniterative, they are very robust with respect to noisy data.

For instance let us mention the work [86, Chapter 10] where the authors used second order topological derivatives to develop an one-shot Newton-type algorithm. The methodology of this algorithm is based on the idea to simultaneously consider m singular inclusions ω_ε^i and compute their topological expansion. This expansion is further used to solve a Newton-type equation leading to an efficient and robust way to detect geometric subsets (inhomogeneities, obstacles, anomalies). Hence, this algorithm has been extensively used to solve inverse reconstruction problems.

We refer to [71], where the authors utilised this one-shot approach to obtain a good initial shape, which they further improved in an iterative shape optimisation algorithm. Further applications of this algorithm to electrical impedance tomography can be found in [53] and [86, Chapter 11]. Furthermore, this idea was employed in an inverse potential reconstruction problem [35] and in an inverse source reconstruction problem [36]. In this context we would also like to mention obstacle reconstruction, which is addressed in [94]. For further applications, such as inverse conductivity and electromagnetic casting we refer to [86] and references therein.

In what follows we are going to target the foundation of these methodologies. That is, we study general formulas for higher order topological derivatives in two and three space dimensions for a simple PDE constrained model problem. This topic has already been considered in [10], where the authors investigated the higher order asymptotic expansion of a steady state voltage potential subject to singular perturbations of the conductivity. While their analysis addresses the case of a single perturbation, the authors argue that an analogous analysis can be carried out to deal with a finite number of simultaneous perturbations. In this regard, we also want to mention the recent work [52], where the authors studied the asymptotic expansion of the solution of Poisson's equation subject to a small perturbation attaining homogeneous Dirichlet boundary conditions.

In order to obtain an asymptotic expansion of the state variable, we employ the compound layer method (cf. [80,81]). Furthermore, we incorporate the cost functionals via the averaged adjoint method (cf. Section 14.2). This approach enables an iterative and systematic way to compute higher order topological derivatives with no additional effort as long as the complete asymptotic expansion of the averaged adjoint variable is known. We are going to study two kinds of tracking-type functionals, a gradient and an L_2 tracking-type functional. Similarly to the previous section, we observe a large gap in technical difficulties. In fact, we see that the analysis of the L_2 tracking-type functional is more involved and even includes the fundamental solution of the biharmonic equation. The content of this part stems from the article [23] in collaboration with Peter Gangl and Kevin Sturm. In this part of the thesis we investigate the following model problem:

Problem formulation

Let $\mathsf{D} \subset \mathbf{R}^d$ be an open and bounded Lipschitz domain, $\Gamma \subset \partial \mathsf{D}$ with $|\Gamma| > 0$, $\Gamma^N := \partial \mathsf{D} \setminus \Gamma$ and consider the minimisation problem

$$\text{minimise } \mathscr{J}(\Omega) := \alpha_1 \int_{\mathsf{D}} (u_\Omega - u_d)^2 \, dx + \alpha_2 \int_{\mathsf{D}} |\nabla(u_\Omega - u_d)|^2 \, dx, \quad \alpha_1, \alpha_2 \geq 0, \tag{16.1}$$

subject to $\Omega \subset \mathsf{D}$ and $u_\Omega \in H^1(\mathsf{D})$, $u_\Omega|_\Gamma = g_D$, such that

$$\int_{\mathsf{D}} \nabla u_\Omega \cdot \nabla \varphi \, dx = \int_{\mathsf{D}} f_\Omega \varphi \, dx + (g_N, \varphi)_{H^{-\frac{1}{2}}(\Gamma^N) \times H^{\frac{1}{2}}(\Gamma^N)} \quad \text{for all } \varphi \in H^1_\Gamma(\mathsf{D}), \tag{16.2}$$

where $f_\Omega(x) := f_1(x)\chi_\Omega(x) + f_2(x)\chi_{\Omega^c}(x)$ with $f_1, f_2 \in L_2(\mathsf{D}) \cap C^\infty(\mathsf{D})$, $g_D \in H^{\frac{1}{2}}(\Gamma)$, $g_N \in H^{-\frac{1}{2}}(\Gamma^N)$, $u_d \in H^1(\mathsf{D})$ and $(\cdot,\cdot)_{H^{-\frac{1}{2}}(\Gamma^N) \times H^{\frac{1}{2}}(\Gamma^N)}$ denotes the duality product.
For a given inclusion $\omega \subset \mathbf{R}^d$ open, bounded and connected, with C^1 boundary, such that $0 \in \omega$ and $x_0 \in \mathsf{D} \setminus \overline{\Omega}$, we derive for the cases $\alpha_1 = 0$ and $\alpha_2 = 0$ an arbitrary order topological derivative formula for this problem of the form

$$\mathscr{J}(\Omega \cup \omega_\varepsilon) = \mathscr{J}(\Omega) + \sum_{k=1}^{N} \ell_k(\varepsilon) d^k \mathscr{J}(\Omega, \omega)(x_0) + o(\ell_N(\varepsilon)), \quad N \geq 1,$$

where $\omega_\varepsilon = \{x_0 + \varepsilon y | \ y \in \omega\}$ (cf: (9.1)) denotes the domain perturbation and $\ell_k : \mathbf{R}^+ \to \mathbf{R}^+$ are continuous functions satisfying

$$\lim_{\varepsilon \searrow 0} \ell_k(\varepsilon) = 0 \quad \text{and} \quad \lim_{\varepsilon \searrow 0} \frac{\ell_{k+1}(\varepsilon)}{\ell_k(\varepsilon)} = 0 \quad \text{for } k \geq 1.$$

Here, $\mathbf{R}^+ := (0, \infty)$ denotes the set of positive real numbers. Furthermore, the real number $d^k \mathscr{J}(\Omega, \omega)(x_0)$ denotes the k-th order topological derivative at Ω evaluated for the inclusion shape ω and the point of perturbation x_0. The explicit form of the functions ℓ_k depends for our problem on the space dimension and will differ significantly in dimension $d = 2$ vs. $d = 3$.

Remark 16.1. Note that this is just a reformulation of Definition 9.1. Again, we want to highlight that our assumption $\Omega_\varepsilon = \Omega \cup \omega_\varepsilon$ is not a restriction. The other case, $x_0 \in \Omega$, $\Omega_\varepsilon = \Omega \setminus \omega_\varepsilon$ can be treated analogously and merely results in a change of sign of the final formulas. Additionally, we want to mention that the first order topological derivative is denoted by $d^1 \mathscr{J}(\Omega, \omega)(x_0)$. Even though this is a minor notational conflict in view of (9.3), we are going to employ this notation throughout this part. This allows a schematic representation of the results.

17 Analysis of the state equation

Let $\Omega \subset \mathsf{D}$ be an open and bounded Lipschitz set and $\omega \subset \mathbf{R}^d$ be an open, bounded and connected set with C^1 boundary $\partial \omega$. We assume that ω contains the origin $0 \in \omega$ and we let $x_0 \in \mathsf{D} \setminus \bar{\Omega}$ be a fixed spatial point. Furthermore, we recall the affine transformation $T_\varepsilon(x) = x_0 + \varepsilon x$ (cf. Definition 11.1) and set $\omega_\varepsilon := T_\varepsilon(\omega)$ for $\varepsilon \geq 0$. In the following we will derive an asymptotic expansion of the perturbed state variable u_ε, which is the unique solution to (16.2) subject to the perturbed domain $\Omega_\varepsilon := \Omega \cup \omega_\varepsilon$, for $\varepsilon > 0$. That is, $u_\varepsilon \in H^1(\mathsf{D})$ satisfies $u_\varepsilon|_\Gamma = g_D$ and

$$\int_{\mathsf{D}} \nabla u_\varepsilon \cdot \nabla \varphi \, dx = \int_{\mathsf{D}} f_{\Omega_\varepsilon} \varphi \, dx + (g_N, \varphi)_{H^{-\frac{1}{2}}(\Gamma^N) \times H^{\frac{1}{2}}(\Gamma^N)} \quad \text{for all } \varphi \in H^1_\Gamma(\mathsf{D}). \tag{17.1}$$

Similarly, the unperturbed state variable $u_0 \in H^1(\mathsf{D})$ satisfies $u_0|_\Gamma = g_D$ and

$$\int_{\mathsf{D}} \nabla u_0 \cdot \nabla \varphi \, dx = \int_{\mathsf{D}} f_{\Omega} \varphi \, dx + (g_N, \varphi)_{H^{-\frac{1}{2}}(\Gamma^N) \times H^{\frac{1}{2}}(\Gamma^N)} \quad \text{for all } \varphi \in H^1_\Gamma(\mathsf{D}). \tag{17.2}$$

Remark 17.1. Note that, contrary to the previous section, we do not consider a transmission problem here. That is, we do not introduce a perturbation to the differential operator of the partial differential equation. This improves the regularity of the solution, since transmission problems lack regularity on the boundary of Ω, i.e. where a jump occurs. Furthermore, this increases the first order approximation speed of the variation of the state $U_\varepsilon^{(1)}$. To obtain a cohesive definition nonetheless, we reformulate Definition 12.3 with some minor modifications.

Definition 17.2. For almost every $x \in \mathsf{D}_\varepsilon$ we define the first variation of the state u_ε by

$$U_\varepsilon^{(1)}(x) := \left(\frac{u_\varepsilon - u_0}{\varepsilon}\right) \circ T_\varepsilon(x) \quad \text{for } \varepsilon > 0. \tag{17.3}$$

More generally, we define the $(k+1)$-th variation of u_ε for $k \geq 1$ and $\varepsilon > 0$ by

$$U_\varepsilon^{(k+1)} := \begin{cases} \frac{U_\varepsilon^{(k)} - U^{(k)} - \varepsilon^{d-2} u^{(k)} \circ T_\varepsilon - \ln(\varepsilon) b^{(k)}}{\varepsilon} & \text{for } d = 2, \\ \frac{U_\varepsilon^{(k)} - U^{(k)} - \varepsilon^{d-2} u^{(k)} \circ T_\varepsilon}{\varepsilon} & \text{for } d = 3. \end{cases} \tag{17.4}$$

Remark 17.3. Note that, contrary to Definition 12.3, we introduce the first order scaling ε^{d-2} for the corrector $u^{(1)}$. In the previous part we obtained a faster decay of the first boundary layer corrector $U^{(1)}$ (cf. Remark 12.11), which allowed us to use a higher order ε^{d-1}. In our problem setting we do not have access to this special behaviour of the boundary layer corrector. Nonetheless, we will see that, due to the nature of our problem at hand, the corrector $U^{(1)}$ is not even necessary to achieve convergence. This is reflected by the property that (12.21) only depends on the operator perturbation.

In this part of the thesis we require similar scaling arguments and remainder estimates as in Part II. Even though the problem setting differs slightly, as we are working with scalar functions, we will not recast these result here. Instead we are going to keep this minor inaccuracy in mind whenever we employ Lemma 11.4, Lemma 11.5 and Lemma 11.6. For convenience we recall that the fundamental solution of the Laplace operator $(-\Delta)$ in dimension two and three is given for $x \neq 0$ by (cf. [90])

$$E(x) := \begin{cases} -\frac{1}{2\pi} \ln(|x|) & \text{for } d = 2, \\ \frac{1}{4\pi} \frac{1}{|x|} & \text{for } d = 3. \end{cases} \tag{17.5}$$

In order to allow a schematic representation and derivation of higher order derivatives, we introduce the compact notation of derivatives.

Definition 17.4. Let $f \in C^k(\Omega)$, $k \geq 0$ and $x_0 \in \Omega$. We define

$$\nabla^k f(x_0)[x]^k := \sum_{j_1=1}^{d} \cdots \sum_{j_k=1}^{d} \frac{\partial^k}{\partial x_{j_1} \cdots \partial x_{j_k}} f(x_0) x_{j_1} \cdots x_{j_k}, \tag{17.6}$$

with the convention $\nabla^0 f(x_0)[x]^0 := f(x_0)$.

Remark 17.5. Note that this definition captures the Taylor expansion of a sufficiently smooth function f. The first terms read as

$$\nabla^1 f(x_0)[x]^1 = \nabla f(x_0) \cdot x, \quad \nabla^2 f(x_0)[x]^2 = x^\top H(f)(x_0) x,$$

where $H(f)$ denotes the Hessian of f.

Remark 17.6. In the subsequent analysis we often omit the index $k = 1$. That is, we introduce

$$\nabla f(x_0)[x] := \nabla^1 f(x_0)[x]^1.$$

Yet, we need the notation including the first index to allow a uniform representation in terms of sequences.

In the following lemma we introduce the boundary layer correctors $U^{(k)}$ used in the definition of $U_\varepsilon^{(k)}$.

Lemma 17.7. Define for $k \geq 2$:

$$U^{(k)}(x) = \int_\omega E(x-y) F^{(k)}(y)\, dy, \tag{17.7}$$

where $F^{(k)}(y) := \frac{1}{(k-2)!} \nabla^{k-2}(f_1 - f_2)(x_0)[y]^{k-2}$. Then $U^{(k)}$ satisfies:

$$\int_{\mathbf{R}^d} \nabla U^{(k)} \cdot \nabla \varphi \, dx = \int_\omega F^{(k)} \varphi \, dx \quad \text{for all } \varphi \in C_c^1(\mathbf{R}^d), \tag{17.8}$$

and admits the following asymptotic expansion as $|x| \to \infty$

$$U^{(k)}(x) = R_1^{(k)}(x) + \cdots + R_N^{(k)}(x) + \mathcal{O}(|x|^{-(d-2+N)}), \tag{17.9}$$

where $R_{\ell+1}^{(k)} : \mathbf{R}^d \to \mathbf{R}$ are given for $k \geq 2$ and $\ell \geq 0$ by

$$R_{\ell+1}^{(k)}(x) = \frac{1}{\ell!} \int_\omega \partial_t^\ell E(x - ty)|_{t=0} F^{(k)}(y)\, dy. \tag{17.10}$$

Proof. It is clear that $U^{(k)}$ satisfies (17.8), since $U^{(k)}$ is given by the Newton potential. The asymptotic expansion (17.9) follows from a Taylor expansion of $y \mapsto E(x-y)$. □

Remark 17.8. The functions $F^{(k)}$ denote a Taylor's expansion of the error term $f_1 - f_2$. Thus, the sequence $U^{(k)}$ aims to approximate the error up to an increasing order. The functions $R_{\ell+1}^{(k)}$ in turn describe the different error-levels introduced by $U^{(k)}$ on the boundary. These will therefore guide the construction of the regular correctors $u^{(k)}$.

For the sake of completeness we give the following definition

Definition 17.9. For $k=1$ let

$$U^{(1)} \equiv 0, \quad u^{(1)} \equiv 0, \tag{17.11}$$

and for $\ell \geq 1$ let

$$R_\ell^{(1)} \equiv 0. \tag{17.12}$$

Furthermore we define $b^{(1)} := 0$ and more generally

$$b^{(k)} := -\frac{1}{2\pi} \int_\omega F^{(k)}(y)\, dy \quad \text{ for } k \geq 2, \tag{17.13}$$

where $F^{(k)}(y) := \frac{1}{(k-2)!} \nabla^{k-2}(f_1 - f_2)(x_0)[y]^{k-2}$.

Remark 17.10. In view of $R_1^{(k)}(x) = E(x) \int_\omega F^{(k)}(y)\, dy$ we have for $k \geq 2$

$$R_1^{(k)}(\varepsilon x) = \begin{cases} R_1^{(k)}(x) + \ln(\varepsilon) b^{(k)}, & \text{for } d = 2, \\ \frac{1}{\varepsilon} R_1^{(k)}(x), & \text{for } d = 3, \end{cases} \tag{17.14}$$

which explains the definition of $b^{(k)}$ in dimension two. Additionally, there holds

$$R_\ell^{(k)}(\varepsilon x) = \varepsilon^{-(d-2)} \varepsilon^{-(\ell-1)} R_\ell^{(k)}(x), \tag{17.15}$$

$$\partial_\nu R_\ell^{(k)}(\varepsilon x) = \varepsilon^{-(d-2)} \varepsilon^{-\ell} \partial_\nu R_\ell^{(k)}(x), \tag{17.16}$$

for $k \geq 1$, $\ell \geq 2$.

Example 17.11. We may compute the derivatives (17.10) explicitly for $\ell = 1,2,3,4$ and obtain for $d = 2$

$$R_1^{(k)}(x) = -\frac{1}{2\pi} \ln(|x|) \int_\omega F^{(k)}(y)\, dy, \tag{17.17}$$

$$R_2^{(k)}(x) = \frac{1}{2\pi} \frac{x}{|x|^2} \cdot \int_\omega y F^{(k)}(y)\, dy, \tag{17.18}$$

$$R_3^{(k)}(x) = -\frac{1}{4\pi} \frac{1}{|x|^2} \int_\omega \left(|y|^2 - 2\frac{(x \cdot y)^2}{|x|^2} \right) F^{(k)}(y)\, dy, \tag{17.19}$$

$$R_4^{(k)}(x) = -\frac{1}{12\pi} \frac{1}{|x|^4} \int_\omega \left(6|y|^2 (x \cdot y) - 8\frac{(x \cdot y)^3}{|x|^2} \right) F^{(k)}(y)\, dy, \tag{17.20}$$

and for $d = 3$

$$R_1^{(k)}(x) = \frac{1}{4\pi} \frac{1}{|x|} \int_\omega F^{(k)}(y)\, dy, \tag{17.21}$$

$$R_2^{(k)}(x) = \frac{1}{4\pi} \frac{x}{|x|^3} \cdot \int_\omega y F^{(k)}(y)\, dy, \tag{17.22}$$

$$R_3^{(k)}(x) = \frac{1}{8\pi} \frac{1}{|x|^3} \int_\omega \left(-|y|^2 + 3\frac{(x \cdot y)^2}{|x|^2} \right) F^{(k)}(y)\, dy. \tag{17.23}$$

(17.24)

We will also need remainder estimates for the expansion (17.9) of $U^{(k)}$ in various norms:

Lemma 17.12. Let $\Gamma_\varepsilon \subset \partial \mathsf{D}_\varepsilon$, $k \geq 2$ and $N \geq 1$. Then there is a constant $C > 0$, such that

- $\varepsilon^{\frac{1}{2}} \| U^{(k)} - \sum_{\ell=1}^N R_\ell^{(k)} \|_{L_2(\Gamma_\varepsilon)} \leq C \varepsilon^{\frac{d}{2}+N-1}$,
- $|U^{(k)} - \sum_{\ell=1}^N R_\ell^{(k)}|_{H^{\frac{1}{2}}(\Gamma_\varepsilon)} \leq C \varepsilon^{\frac{d}{2}+N-1}$,
- $\| \partial_\nu U^{(k)} - \sum_{\ell=1}^N \partial_\nu R_\ell^{(k)} \|_{L_2(\Gamma_\varepsilon)} \leq C \varepsilon^{\frac{d-1}{2}+N}$.

Proof. In view of (17.9) and (17.10) we have for $x \in \mathbf{R}^d$:

$$\left| U^{(k)}(x) - \sum_{\ell=1}^N R_\ell^{(k)}(x) \right| \leq C |x|^{-m} + \mathcal{O}(|x|^{-m-1}),$$

with $m = d - 2 + N$. Thus, an application of Lemma 11.6 yields the result. □

Next we introduce the regular corrector functions, which compensate the error introduced by the functions $U^{(k)}$.

Definition 17.13. We define for $k \geq 2$ the corrector $u^{(k)} \in H^1(\mathsf{D})$ as the unique solution to

$$u^{(k)}(x) = -\sum_{j=1}^k R_j^{(k-j+1)}(x - x_0) \quad \text{on } \Gamma, \tag{17.25}$$

$$\int_{\mathsf{D}} \nabla u^{(k)} \cdot \nabla \varphi \, dx = \int_{\Gamma^N} \left(\sum_{j=1}^k \partial_\nu R_j^{(k-j+1)}(x - x_0) \right) \varphi \, dS \quad \text{for all } \varphi \in H^1_\Gamma(\mathsf{D}). \tag{17.26}$$

Remark 17.14. Note that unique solvability of (17.25),(17.26) can be shown by the Lemma of Lax-Milgram, and therefore $u^{(k)}$ are well-defined. A change of variables entails that (17.26) can be equivalently written as $u^{(k)} \circ T_\varepsilon(x) = -\sum_{j=1}^k R_j^{(k-j+1)}(\varepsilon x)$ on Γ_ε and

$$\int_{\mathsf{D}_\varepsilon} \nabla(\varepsilon^{d-2} u^{(k)} \circ T_\varepsilon) \cdot \nabla \varphi \, dx = \varepsilon^{d-1} \int_{\Gamma_\varepsilon^N} \left(\sum_{j=1}^k \partial_\nu R_j^{(k-j+1)}(\varepsilon x) \right) \varphi \, dS \quad \text{for all } \varphi \in H^1_{\Gamma_\varepsilon}(\mathsf{D}_\varepsilon). \tag{17.27}$$

Later on we also need the following auxiliary result.

Lemma 17.15. Let $\varepsilon > 0$ be fixed. We have for all $k \geq 2$ and $d = 2$:

$$U_\varepsilon^{(1)} - \varepsilon^{k-1} U_\varepsilon^{(k)} = \sum_{\ell=1}^{k-1} \varepsilon^{\ell-1} \left(U^{(\ell)} + \varepsilon^{d-2} u^{(\ell)} \circ T_\varepsilon + \ln(\varepsilon) b^{(\ell)} \right) \quad \text{on } \mathsf{D}_\varepsilon, \tag{17.28}$$

with $b^{(\ell)}$ defined in (17.13). Furthermore, we have for all $k \geq 2$ and $d = 3$:

$$U_\varepsilon^{(1)} - \varepsilon^{k-1} U_\varepsilon^{(k)} = \sum_{\ell=1}^{k-1} \varepsilon^{\ell-1} \left(U^{(\ell)} + \varepsilon^{d-2} u^{(\ell)} \circ T_\varepsilon \right) \quad \text{on } \mathsf{D}_\varepsilon. \tag{17.29}$$

Proof. This follows from Definition 17.2 and an induction proof. □

Similarly to Lemma 12.4, the next lemma helps us to compactly handle the inhomogeneous Dirichlet boundary conditions on Γ_ε:

Lemma 17.16. Let $F_\varepsilon : H^1_{\Gamma_\varepsilon}(\mathsf{D}_\varepsilon) \to \mathbf{R}$ be a linear and continuous functional with respect to $\|\cdot\|_\varepsilon$ and $g_\varepsilon \in H^{\frac{1}{2}}(\Gamma_\varepsilon)$. Then there exists a unique $V_\varepsilon \in H^1(\mathsf{D}_\varepsilon)$, such that

$$\int_{\mathsf{D}_\varepsilon} \nabla V_\varepsilon \cdot \nabla \varphi \, dx = F_\varepsilon(\varphi) \quad \text{for all } \varphi \in H^1_{\Gamma_\varepsilon}(\mathsf{D}_\varepsilon), \tag{17.30}$$

$$V_\varepsilon|_{\Gamma_\varepsilon} = g_\varepsilon. \tag{17.31}$$

Furthermore, there is a constant $C > 0$ independent of ε such that

$$\|V_\varepsilon\|_\varepsilon \leq C(\|F_\varepsilon\|_\varepsilon + \varepsilon^{\frac{1}{2}}\|g_\varepsilon\|_{L_2(\Gamma_\varepsilon)} + |g_\varepsilon|_{H^{\frac{1}{2}}(\Gamma_\varepsilon)}). \tag{17.32}$$

Proof. The proof follows the lines of Lemma 12.4. □

We first address the boundary term g_ε in the previous lemma.

Corollary 17.17. Let $k \geq 2$ and $d = 2$. There is a constant $C > 0$ such that for all $\varepsilon > 0$ small enough:

$$\varepsilon^{\frac{1}{2}}\|U_\varepsilon^{(k)} - U^{(k)} - \varepsilon^{d-2}u^{(k)} \circ T_\varepsilon - \ln(\varepsilon)b^{(k)}\|_{L_2(\Gamma_\varepsilon)} \leq C\varepsilon^{\frac{d}{2}}, \tag{17.33}$$

$$|U_\varepsilon^{(k)} - U^{(k)} - \varepsilon^{d-2}u^{(k)} \circ T_\varepsilon - \ln(\varepsilon)b^{(k)}|_{H^{\frac{1}{2}}(\Gamma_\varepsilon)} \leq C\varepsilon^{\frac{d}{2}}. \tag{17.34}$$

Let $k \geq 2$ and $d = 3$. There is a constant $C > 0$ such that for all $\varepsilon > 0$ small enough:

$$\varepsilon^{\frac{1}{2}}\|U_\varepsilon^{(k)} - U^{(k)} - \varepsilon^{d-2}u^{(k)} \circ T_\varepsilon\|_{L_2(\Gamma_\varepsilon)} \leq C\varepsilon^{\frac{d}{2}}, \tag{17.35}$$

$$|U_\varepsilon^{(k)} - U^{(k)} - \varepsilon^{d-2}u^{(k)} \circ T_\varepsilon|_{H^{\frac{1}{2}}(\Gamma_\varepsilon)} \leq C\varepsilon^{\frac{d}{2}}. \tag{17.36}$$

Proof. Let $\varepsilon > 0$ be sufficiently small. For the sake of simplicity we restrict ourselves to the proof for $d = 3$. Employing the additive property of the logarithm (17.14), the proof for $d = 2$ follows the same lines. First note that by definition $U_\varepsilon^{(k)} - U^{(k)} - \varepsilon^{d-2}u^{(k)} \circ T_\varepsilon = \varepsilon U_\varepsilon^{(k+1)}$ and that we have in view of Lemma 17.15

$$\varepsilon U_\varepsilon^{(k+1)} = \varepsilon^{-(k-1)}U_\varepsilon^{(1)} + \sum_{\ell=1}^{k} \varepsilon^{\ell-k}(U^{(\ell)} + \varepsilon^{(d-2)}u^{(\ell)} \circ T_\varepsilon) \quad \text{on } \mathsf{D}_\varepsilon. \tag{17.37}$$

Moreover, since $R_j^{(k-j+1)}(\varepsilon x) = \varepsilon^{-(d-2)}\varepsilon^{-(j-1)}R_j^{(k-j+1)}(x)$ for $1 \leq j \leq k$ (cf. (17.15)), we have for $x \in \Gamma_\varepsilon$

$$u^{(\ell)} \circ T_\varepsilon(x) = -\varepsilon^{-(d-2)} \sum_{j=1}^{\ell} \varepsilon^{-(j-1)} R_j^{(\ell-j+1)}(x), \tag{17.38}$$

and thus

$$\sum_{\ell=1}^{k}\varepsilon^{\ell-k}\varepsilon^{(d-2)}u^{(\ell)}\circ T_\varepsilon(x) \overset{(17.38)}{=} -\varepsilon^{-k}\sum_{\ell=1}^{k}\sum_{j=1}^{\ell}\varepsilon^{\ell-j+1}R_j^{(\ell-j+1)}(x) \tag{17.39}$$

$$= -\sum_{\ell=1}^{k}\varepsilon^{\ell-k}\sum_{j=1}^{k-\ell+1}R_j^{(\ell)}(x), \tag{17.40}$$

where in the last step we reordered the sum as illustrated in Figure 12 with $a_{ij} = R_i^{(j)}$. Therefore, plugging this into (17.37) yields

$$\varepsilon U_\varepsilon^{(k+1)} = \varepsilon^{-(k-1)}U_\varepsilon^{(1)} + \sum_{\ell=1}^{k}\varepsilon^{\ell-k}\left(U^{(\ell)} - \sum_{j=1}^{k-\ell+1}R_j^{(\ell)}\right) \quad \text{on } \mathrm{D}_\varepsilon, \tag{17.41}$$

and since $U_\varepsilon^{(1)} = 0$ on Γ_ε, it follows that there is a constant $C > 0$, such that

$$\varepsilon^{\frac{1}{2}}\|\varepsilon U_\varepsilon^{(k+1)}\|_{L_2(\Gamma_\varepsilon)} \le \sum_{\ell=1}^{k}\varepsilon^{\ell-k}\underbrace{\varepsilon^{\frac{1}{2}}\left\|U^{(\ell)} - \sum_{j=1}^{k-\ell+1}R_j^{(\ell)}\right\|_{L_2(\Gamma_\varepsilon)}}_{\le C\varepsilon^{\frac{d}{2}+k-\ell},\ \text{Lemma 17.12}} \le C\varepsilon^{\frac{d}{2}}. \tag{17.42}$$

In the same way, using the $H^{\frac{1}{2}}$ estimate of Lemma 17.12, one can show $|\varepsilon U_\varepsilon^{(k+1)}|_{H^{\frac{1}{2}}(\Gamma_\varepsilon)} \le C\varepsilon^{\frac{d}{2}}$. □

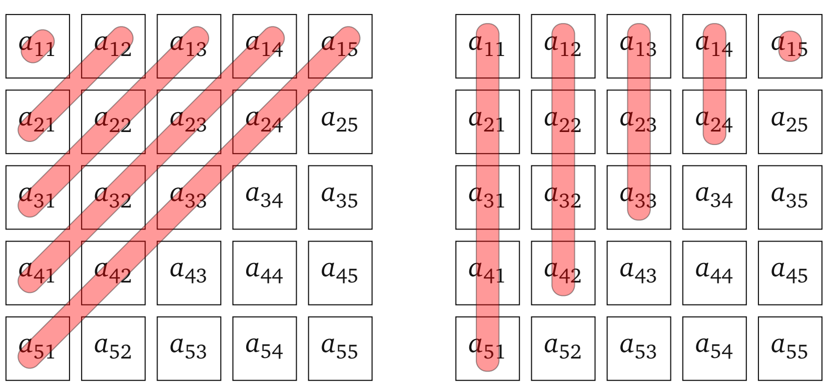

Figure 12: Visualisation of the reordering of the sums in (17.39),(17.40) [23].

We are now able to state the main result regarding the asymptotic expansion of the state u_ε (cf. Theorem 12.14).

Theorem 17.18. Let $k \ge 1$ and $\alpha \in (0,1)$. There is a constant $C > 0$, such that

$$\|U_\varepsilon^{(k)} - U^{(k)} - \varepsilon^{d-2}u^{(k)}\circ T_\varepsilon - \ln(\varepsilon)b^{(k)}\|_\varepsilon \le C\varepsilon^{1-\alpha} \qquad \text{for } d = 2, \tag{17.43}$$

$$\|U_\varepsilon^{(k)} - U^{(k)} - \varepsilon^{d-2}u^{(k)}\circ T_\varepsilon\|_\varepsilon \le C\varepsilon \qquad \text{for } d = 3. \tag{17.44}$$

Proof. Again, we are only going to provide a proof for the estimate in dimension $d = 3$. The proof for $d = 2$ follows the same lines. Subtracting (17.1), (17.2) we obtain

$$\int_{\mathsf{D}} \nabla(u_\varepsilon - u_0)\cdot\nabla\varphi\, dx = \int_{\mathsf{D}} (f_{\Omega_\varepsilon} - f_\Omega)\varphi\, dx \quad \text{for all } \varphi \in H^1_\Gamma(\mathsf{D}), \tag{17.45}$$

and thus, a change of variables with respect to T_ε entails

$$\int_{\mathsf{D}_\varepsilon} \nabla U_\varepsilon^{(1)}\cdot\nabla\varphi\, dx = \varepsilon\int_\omega (f_1 - f_2)\circ T_\varepsilon\varphi\, dx =: F_\varepsilon^{(1)}(\varphi), \tag{17.46}$$

for all $\varphi \in H^1_{\Gamma_\varepsilon}(\mathsf{D}_\varepsilon)$. An application of Lemma 11.5, item (ii) shows $\|F_\varepsilon^{(1)}\|_\varepsilon \le C\varepsilon$. Since $U_\varepsilon^{(1)}$ vanishes on the boundary Γ_ε, $U^{(1)} = 0$ and $u^{(1)} = 0$, Lemma 17.16 yields the desired estimate (17.44) for $k = 1$. Next we divide by ε and subtract the equation for $U^{(2)}$, that is, equation (17.8) for $k = 2$ and the rescaled equation for $\varepsilon^{d-2}u^{(2)}\circ T_\varepsilon$, that is, equation (17.27) for $k = 2$ from (17.46) to obtain

$$\int_{\mathsf{D}_\varepsilon} \nabla(U_\varepsilon^{(2)} - U^{(2)} - \varepsilon^{d-2}u^{(2)}\circ T_\varepsilon)\cdot\nabla\varphi\, dx = \int_\omega \Big((f_1 - f_2)\circ T_\varepsilon - (f_1(x_0) - f_2(x_0))\Big)\varphi\, dx \tag{17.47}$$

$$+ \int_{\Gamma_\varepsilon^N} \Big(\partial_\nu U^{(2)} - \varepsilon^{d-1}\partial_\nu R_1^{(2)}(\varepsilon x)\Big)\varphi\, dS, \tag{17.48}$$

for $\varphi \in H^1_{\Gamma_\varepsilon}(\mathsf{D}_\varepsilon)$. Recalling $\varepsilon U_\varepsilon^{(k+1)} = U_\varepsilon^{(k)} - U^{(k)} - \varepsilon^{d-2}u^{(k)}\circ T_\varepsilon$ and continuing this process we obtain more generally for $k \ge 3$:

$$\begin{aligned}\int_{\mathsf{D}_\varepsilon} \nabla(\varepsilon U_\varepsilon^{(k+1)})\cdot\nabla\varphi\, dx &= \int_\omega \varepsilon^{-(k-2)}\Big((f_1 - f_2)\circ T_\varepsilon - (f_1(x_0) - f_2(x_0))\Big)\varphi\, dx\\ &- \int_\omega \sum_{\ell=1}^{k-2} \varepsilon^{-(k-2)+\ell}\frac{\nabla^\ell\big(f_1 - f_2\big)(x_0)[x]^\ell}{\ell!}\varphi\, dx\\ &+ \int_{\Gamma_\varepsilon^N} \sum_{\ell=2}^{k} \varepsilon^{\ell-k}\left(\partial_\nu U^{(\ell)} - \sum_{j=1}^{k-\ell+1} \varepsilon^{d-1+j-1}\partial_\nu R_j^{(\ell)}(\varepsilon x)\right)\varphi\, dS =: F_\varepsilon^{(k)}(\varphi),\end{aligned} \tag{17.49}$$

for $\varphi \in H^1_{\Gamma_\varepsilon}(\mathsf{D}_\varepsilon)$. A Taylor expansion of $(f_1 - f_2)\circ T_\varepsilon$ at $\varepsilon = 0$ shows for all ε small enough:

$$\left|\int_\omega \varepsilon^{-(k-2)}\Big((f_1 - f_2)\circ T_\varepsilon - (f_1(x_0) - f_2(x_0))\Big)\varphi\, dx - \int_\omega \sum_{\ell=1}^{k-2} \varepsilon^{-(k-2)+\ell}\frac{\nabla^\ell\big(f_1 - f_2\big)(x_0)[x]^\ell}{\ell!}\varphi\, dx\right| \le C\varepsilon\|\varphi\|_\varepsilon, \tag{17.50}$$

for a constant $C > 0$. Furthermore, taking into account that

$$\partial_\nu R_j^{(\ell)}(\varepsilon x) = \varepsilon^{-(d-2+j)}\partial_\nu R_j^{(\ell)}(x) \quad \text{for all } \ell, j \ge 1,$$

(cf. (17.16),(17.14)) it follows from Lemma 17.12 and Hölder's inequality that

$$\begin{aligned}\left|\int_{\Gamma_\varepsilon^N}\sum_{\ell=2}^{k}\varepsilon^{\ell-k}\left(\partial_\nu U^{(\ell)}-\sum_{j=1}^{k-\ell+1}\varepsilon^{d-1+j-1}\partial_\nu R_j^{(\ell)}(\varepsilon x)\right)\varphi\, dS\right| &\le \sum_{\ell=2}^{k}\varepsilon^{\ell-k}\left\|\partial_\nu U^{(\ell)}-\sum_{j=1}^{k-\ell+1}\partial_\nu R_j^{(\ell)}(x)\right\|_{L_2(\Gamma_\varepsilon^N)}\|\varphi\|_{L_2(\Gamma_\varepsilon^N)}\\ &\le C\varepsilon^{\frac{d+1}{2}}\|\varphi\|_{L_2(\Gamma_\varepsilon^N)}\\ &\le C\varepsilon^{\frac{d}{2}}\|\varphi\|_{\varepsilon},\end{aligned} \tag{17.51}$$

for a constant $C > 0$, where in the last step we used the continuity of the trace operator (cf. Lemma 11.5, item (iv)). Combining (17.50) and (17.51) we get $\|F_\varepsilon^{(k)}\|_\varepsilon \le C\varepsilon$ for a constant $C > 0$ and $k \ge 2$. Additionally, we deduce from Corollary 17.17 that

$$\varepsilon^{\frac{1}{2}}\|\varepsilon U_\varepsilon^{(k+1)}\|_{L_2(\Gamma_\varepsilon)}+|\varepsilon U_\varepsilon^{(k+1)}|_{H^{\frac{1}{2}}(\Gamma_\varepsilon)}\le C\varepsilon^{\frac{d}{2}},$$

for a positive constant $C > 0$. Thus, Lemma 17.16 yields (17.44) and therefore finishes the proof. □

Example 17.19 (Spherical inclusion)**.** We now assume that the inclusion $\omega = B_1(0)$ is the unit ball in $\mathbf{R}^d$ centered at the origin and $f_1, f_2 \in \mathbf{R}$ are constant. In this case we see that $U^{(2)} \neq 0$ and $U^{(k)} = 0$ for all $k \ge 3$. Moreover, we have

$$U^{(2)}(x) = (f_1 - f_2)\int_{B_1(0)} E(x-y)\, dy. \tag{17.52}$$

Now we note that $y \mapsto E(x-y)$ is harmonic for all $x \in \mathbf{R}^d \setminus \overline{B_1(0)}$ and thus by the mean value theorem for harmonic functions

$$U^{(2)}(x) = (f_1 - f_2)|B_1(0)|E(x) \quad \text{for } x \in \mathbf{R}^d \setminus \overline{B_1(0)}. \tag{17.53}$$

This means that $R_1^{(2)}(x) = (f_1 - f_2)|B_1(0)|E(x)$ and $R_\ell^{(2)}(x) = 0$ for all $\ell \ge 2$. Moreover, as mentioned before, we have $U^{(k)} = 0$ for all $k \ge 3$, which implies that $R_\ell^{(k)}(x) = 0$ for all $\ell \ge 1$ and $k \ge 3$. Therefore

$$\sum_{j=1}^{k} R_j^{(k-j+1)}(x) = \begin{cases} R_1^{(2)}(x), & \text{for } k = 2,\\ 0, & \text{for } k \ge 3.\end{cases} \tag{17.54}$$

This implies in particular that $u^{(k)} = 0$ for all $k \ge 3$. Hence it follows from (17.18) that

$$U_\varepsilon^{(2)} - U^{(2)} - u^{(2)}\circ T_\varepsilon - \ln(\varepsilon)b^{(2)} = 0 \quad \text{for } d = 2, \tag{17.55}$$

$$U_\varepsilon^{(2)} - U^{(2)} - \varepsilon u^{(2)}\circ T_\varepsilon = 0 \quad \text{for } d = 3, \tag{17.56}$$

or equivalently

$$u_\varepsilon = u_0 + \varepsilon^2\left(U^{(2)}\circ T_\varepsilon^{-1} + u^{(2)} + \ln(\varepsilon)b^{(2)}\right), \quad \text{for } d = 2, \tag{17.57}$$

$$u_\varepsilon = u_0 + \varepsilon^3\left(\varepsilon^{-1}U^{(2)}\circ T_\varepsilon^{-1} + u^{(2)}\right), \quad \text{for } d = 3. \tag{17.58}$$

We finally show that $U^{(2)}$ can be explicitly computed. In fact, $U^{(2)}$ solves

$$-\Delta U^{(2)} = (f_1 - f_2)\chi_{B_1(0)} \quad \text{in } \mathbf{R}^d. \tag{17.59}$$

But since $U^{(2)}(x) = (f_1 - f_2)|B_1(0)|E(x)$ for all $x \in \mathbf{R}^d \setminus \overline{B_1(0)}$ and since $U^{(2)}$ is continuous it follows that $U^{(2)}(x) = (f_1 - f_2)|B_1(0)|E(x)$ on $\partial B_1(0)$ and thus $U^{(2)}$ must be a solution to the inhomogeneous Dirichlet problem: find $U^{(2)} \in H^1(B_1(0))$, such that $U^{(2)}(x) = (f_1 - f_2)|B_1(0)|E(x)$ on $\partial B_1(0)$ and

$$-\Delta U^{(2)} = (f_1 - f_2) \quad \text{in } B_1(0). \tag{17.60}$$

Employing polar coordinates, it is readily checked that the solution is given for $d = 2$ by

$$U^{(2)}(x) = \begin{cases} -(f_1 - f_2)\frac{1}{4}(|x|^2 - 1) & \text{for } x \in B_1(0), \\ -(f_1 - f_2)\frac{1}{2}\ln(|x|) & \text{for } x \in \mathbf{R}^2 \setminus \overline{B_1(0)}, \end{cases} \tag{17.61}$$

and in dimension $d = 3$ using spherical coordinates leads to:

$$U^{(2)}(x) = \begin{cases} -(f_1 - f_2)\frac{1}{6}(|x|^2 - 3) & \text{for } x \in B_1(0), \\ (f_1 - f_2)\frac{1}{3}\frac{1}{|x|} & \text{for } x \in \mathbf{R}^3 \setminus \overline{B_1(0)}. \end{cases} \tag{17.62}$$

Note that, according to Example 17.11 and the fact that $F^{(2)}(x) = f_1 - f_2$ and $|B_1(x_0)|$ is equal to π for $d = 2$ and equal to $\frac{4\pi}{3}$ for $d = 3$, we have

$$R_1^{(2)}(x) = \begin{cases} -\frac{f_1 - f_2}{2}\ln(|x|), & \text{for } d = 2, \\ \frac{f_1 - f_2}{3|x|}, & \text{for } d = 3. \end{cases} \tag{17.63}$$

Furthermore, the function $u^{(2)}$ was defined in (17.26) and is given by

$$-\Delta u^{(2)} = 0 \qquad \text{in D}, \tag{17.64}$$

$$u^{(2)} = -R_1^{(2)}(x - x_0) \qquad \text{on } \Gamma, \tag{17.65}$$

$$-\partial_\nu u^{(2)} = R_1^{(2)}(x - x_0) \qquad \text{on } \Sigma. \tag{17.66}$$

For a general domain D its solution cannot be explicitly computed. However, we know $U^{(2)}$ explicitly and thus can write the expansion of u_ε as follows

$$u_\varepsilon = u_0 + \varepsilon^2 \begin{cases} \left(-\frac{f_1 - f_2}{4}(\varepsilon^{-2}|x - x_0|^2 - 1) + u^{(2)} - \frac{f_1 - f_2}{2}\ln(\varepsilon)\right) & \text{for } x \in B_\varepsilon(x_0), \\ \left(-\frac{f_1 - f_2}{2}\ln(|x - x_0|) + u^{(2)}\right) & \text{for } x \in \mathrm{D} \setminus \overline{B_\varepsilon(x_0)}, \end{cases} \tag{17.67}$$

and in dimension $d = 3$:

$$u_\varepsilon = u_0 + \varepsilon^3 \begin{cases} \left(-(f_1 - f_2)\frac{1}{6}(\varepsilon^{-3}|x - x_0|^2 - 3) + u^{(2)}\right) & \text{for } x \in B_\varepsilon(x_0), \\ \left(\frac{f_1 - f_2}{3}\frac{1}{|x - x_0|} + u^{(2)}\right) & \text{for } x \in \mathrm{D} \setminus \overline{B_\varepsilon(x_0)}. \end{cases} \tag{17.68}$$

Note that the $\ln(\varepsilon)$ term in $d = 2$ disappears outside of $B_\varepsilon(0)$ and that indeed $u_\varepsilon - u_0 = 0$ on ∂D.

18 Analysis of the averaged adjoint equation for the H^1 tracking-type cost function

Since the analysis of the averaged adjoint variable for the L_2 tracking-type cost functional differs significantly from the analysis of the H^1 tracking-type cost functional, we split the cost functional $\mathscr{J}$ defined in (16.1) into two parts and treat each one separately. Thus, in this section we derive the asymptotics of the averaged adjoint state q_ε for the H^1 tracking-type part of (16.1). The L_2 tracking-type part of (9.6) is treated in Section 20.

Hence, in this section we are interested in the cost function

$$\mathscr{J}_2(\Omega) := \alpha_2 \int_{\mathsf{D}} |\nabla(u_\Omega - u_d)|^2 \, dx, \tag{18.1}$$

where $\alpha_2 \geq 0$ and $u_\Omega \in H^1(\mathsf{D})$ satisfies $u_\Omega|_\Gamma = g_D$ and

$$\int_{\mathsf{D}} \nabla u_\Omega \cdot \nabla \varphi \, dx = \int_{\mathsf{D}} f_\Omega \varphi \, dx + (g_N, \varphi)_{H^{-\frac{1}{2}}(\Gamma^N) \times H^{\frac{1}{2}}(\Gamma^N)} \quad \text{for all } \varphi \in H^1_\Gamma(\mathsf{D}). \tag{18.2}$$

The associated Lagrangian is given by

$$\mathscr{L}(\varepsilon, u, v) := \alpha_2 \int_{\mathsf{D}} |\nabla(u - u_d)|^2 \, dx + \int_{\mathsf{D}} \nabla u \cdot \nabla v - f_{\Omega_\varepsilon} v \, dx - (g_N, v)_{H^{-\frac{1}{2}}(\Gamma^N) \times H^{\frac{1}{2}}(\Gamma^N)} \quad \text{for all } u \in \mathscr{V}, v \in \mathscr{W}, \tag{18.3}$$

where $\mathscr{W} = H^1_\Gamma(\mathsf{D})$ and $\mathscr{V} = \bar{u} + \mathscr{W}$ with an element $\bar{u} \in H^1(\mathsf{D})$ satisfying the boundary condition $\bar{u}|_\Gamma = g_D$. For more details regarding such an affine setting we refer to Section 10. In view of (10.49) we deduce the perturbed averaged adjoint equation: for $\varepsilon > 0$ small find $q_\varepsilon \in H^1_\Gamma(\mathsf{D})$, such that

$$\int_0^1 \partial_u \mathscr{L}(\varepsilon, s u_\varepsilon + (1-s) u_0, q_\varepsilon)(\varphi) \, ds = 0 \quad \text{for all } \varphi \in H^1_\Gamma(\mathsf{D}). \tag{18.4}$$

Or explicitly, evaluating the ds-integral, the perturbed averaged adjoint equation reads: find $q_\varepsilon \in H^1_\Gamma(\mathsf{D})$, such that

$$\int_{\mathsf{D}} \nabla \varphi \cdot \nabla q_\varepsilon \, dx = -\alpha_2 \int_{\mathsf{D}} \nabla(u_\varepsilon + u_0 - 2u_d) \cdot \nabla \varphi \, dx \quad \text{for all } \varphi \in H^1_\Gamma(\mathsf{D}). \tag{18.5}$$

Similarly, we deduce the unperturbed adjoint equation: find $q_0 \in H^1_\Gamma(\mathsf{D})$, such that

$$\int_{\mathsf{D}} \nabla \varphi \cdot \nabla q_0 \, dx = -2\alpha_2 \int_{\mathsf{D}} \nabla(u_0 - u_d) \cdot \nabla \varphi \, dx \quad \text{for all } \varphi \in H^1_\Gamma(\mathsf{D}). \tag{18.6}$$

Analogously to the definition of the variation of the state, we introduce the variation of the averaged adjoint state.

Definition 18.1. For almost every $x \in \mathsf{D}_\varepsilon$ we define the first variation of the averaged adjoint state q_ε by

$$Q^{(1)}_\varepsilon(x) := \left(\frac{q_\varepsilon - q_0}{\varepsilon} \right) \circ T_\varepsilon(x) \quad \text{for } \varepsilon > 0. \tag{18.7}$$

More generally, we define the $(k+1)$-th variation of q_ε for $k \geq 1$ and $\varepsilon > 0$ by

$$Q_\varepsilon^{(k+1)} := \begin{cases} \frac{Q_\varepsilon^{(k)} - Q^{(k)} - \varepsilon^{d-2} q^{(k)} \circ T_\varepsilon - \ln(\varepsilon) c^{(k)}}{\varepsilon} & \text{for } d = 2, \\ \frac{Q_\varepsilon^{(k)} - Q^{(k)} - \varepsilon^{d-2} q^{(k)} \circ T_\varepsilon}{\varepsilon} & \text{for } d = 3. \end{cases} \tag{18.8}$$

Subtracting (18.5), (18.6) changing variables with respect to T_ε and dividing the results by $\varepsilon > 0$ shows that the first variation of the averaged adjoint state satisfies

$$\int_{\mathsf{D}_\varepsilon} \nabla Q_\varepsilon^{(1)} \cdot \nabla \varphi \, dx = -\alpha_2 \int_{\mathsf{D}_\varepsilon} \nabla U_\varepsilon^{(1)} \cdot \nabla \varphi \, dx \quad \text{for all } \varphi \in H^1_{\Gamma_\varepsilon}(\mathsf{D}_\varepsilon). \tag{18.9}$$

Since $Q_\varepsilon^{(1)} \in H^1_\Gamma(\mathsf{D})$, it follows that $Q_\varepsilon^{(1)} = -\alpha_2 U_\varepsilon^{(1)}$. Hence, one readily checks that we have the following asymptotic expansion.

Theorem 18.2. For $k \geq 1$ let $Q^{(k)} := -\alpha_2 U^{(k)}$, $q^{(k)} := -\alpha_2 u^{(k)}$ and $c^{(k)} := -\alpha_2 b^{(k)}$, with $U^{(k)}$ defined in Lemma 17.7, $u^{(k)}$ defined in (17.26) and $b^{(k)}$ defined in (17.13). Additionally, let $k \geq 1$ and $\alpha \in (0,1)$. Then there is a constant $C > 0$, such that for all $\varepsilon > 0$ sufficiently small:

$$\|Q_\varepsilon^{(k)} - Q^{(k)} - \varepsilon^{d-2} q^{(k)} \circ T_\varepsilon - \ln(\varepsilon) c^{(k)}\|_\varepsilon \leq C \varepsilon^{1-\alpha} \qquad \text{for } d = 2, \tag{18.10}$$

$$\|Q_\varepsilon^{(k)} - Q^{(k)} - \varepsilon^{d-2} q^{(k)} \circ T_\varepsilon\|_\varepsilon \leq C \varepsilon \qquad \text{for } d = 3. \tag{18.11}$$

Proof. Since $Q_\varepsilon^{(1)} = -\alpha_2 U_\varepsilon^{(1)}$ the result follows from Theorem 17.18. □

Analogously to Lemma 17.15 we deduce the following recursion:

Lemma 18.3. Let $\varepsilon > 0$ be fixed. We have for all $k \geq 2$ and $d = 2$:

$$Q_\varepsilon^{(1)} - \varepsilon^{k-1} Q_\varepsilon^{(k)} = \sum_{\ell=1}^{k-1} \varepsilon^{\ell-1} \left(Q^{(\ell)} + \varepsilon^{d-2} q^{(\ell)} \circ T_\varepsilon + \ln(\varepsilon) c^{(\ell)} \right) \quad \text{on } \mathsf{D}_\varepsilon, \tag{18.12}$$

with $c^{(\ell)}$ defined in Theorem 18.2. Furthermore, we have for all $k \geq 2$ and $d = 3$:

$$Q_\varepsilon^{(1)} - \varepsilon^{k-1} Q_\varepsilon^{(k)} = \sum_{\ell=1}^{k-1} \varepsilon^{\ell-1} \left(Q^{(\ell)} + \varepsilon^{d-2} q^{(\ell)} \circ T_\varepsilon \right), \quad \text{on } \mathsf{D}_\varepsilon. \tag{18.13}$$

19 Complete topological expansion - H^1 tracking-type

In this section we compute the n-th topological derivative of the H^1 tracking-type part of the cost function defined in (18.1). That is, we are deriving an asymptotic expansion of the form

$$\mathcal{J}_2(\Omega_\varepsilon) = \mathcal{J}_2(\Omega) + \sum_{k=1}^{n} \ell_k(\varepsilon) d^k \mathcal{J}_2(\Omega, \omega)(x_0) + o(\ell_n(\varepsilon)), \tag{19.1}$$

with $\mathscr{J}_2(\Omega)$ defined as in (18.1). Here $d^k\mathscr{J}_2(\Omega,\omega)(x_0)$ denotes the k-th topological derivative with respect to the initial domain Ω for the perturbation shape ω at the point x_0 and $\ell_k : \mathbf{R}^+ \to \mathbf{R}^+$ are continuous functions satisfying

$$\lim_{\varepsilon\searrow 0} \ell_k(\varepsilon) = 0 \quad \text{and} \quad \lim_{\varepsilon\searrow 0} \frac{\ell_{k+1}(\varepsilon)}{\ell_k(\varepsilon)} = 0 \quad \text{for } k \geq 1.$$

As we will see, the logarithmic term $\ln(\varepsilon)c^{(k)}$ in the asymptotic expansion of the adjoint state variable in $d = 2$ leads to a differing topological derivative compared to dimension $d = 3$. Thus, we will distinguish between both scenarios and derive a general formula of the topological derivative for both cases separately.

The following lemma helps us compute the product of two finite sums in view of the asymptotic behaviour with respect to $\varepsilon > 0$.

Lemma 19.1. For $N \geq 0$, $x \in \omega$ and $\varepsilon > 0$ small let

$$f_\varepsilon(x) := \sum_{n=0}^{N} \varepsilon^n a_n(x) + \mathcal{O}(\varepsilon^{N+1}; x), \quad g_\varepsilon(x) := \sum_{n=0}^{N} \varepsilon^n b_n(x) + \mathcal{O}(\varepsilon^{N+1}; x),$$

where $a_n, b_n : \omega \to \mathbf{R}$, $n \geq 0$ are functions independent of ε. Then

$$f_\varepsilon(x) g_\varepsilon(x) = \sum_{n=0}^{N} \varepsilon^n \sum_{j=0}^{n} a_j(x) b_{n-j}(x) + \mathcal{O}(\varepsilon^{N+1}; x). \tag{19.2}$$

Proof. Let $a_n(x) = b_n(x) = 0$ for $n > N$. The Cauchy product yields

$$\left(\sum_{n=0}^{\infty} \varepsilon^n a_n(x)\right)\left(\sum_{n=0}^{\infty} \varepsilon^n b_n(x)\right) = \sum_{n=0}^{\infty} \varepsilon^n \sum_{j=0}^{n} a_j(x) b_{n-j}(x),$$

which finishes the proof. □

19.1 General formula for higher order topological derivatives in dimension two

In this section we address the topological derivatives in dimension $d = 2$. The next theorem states the main result of this section:

Theorem 19.2. Let $\ell_1(\varepsilon) := |\omega_\varepsilon|$, $\ell_{2n}(\varepsilon) = \varepsilon^n \ln(\varepsilon)|\omega_\varepsilon|$ and $\ell_{2n+1}(\varepsilon) = \varepsilon^n |\omega_\varepsilon|$, for $n \geq 1$. The topological derivative of $\mathscr{J}_2$ at $x_0 \in \mathrm{D} \setminus \bar{\Omega}$ and $\omega \subset \mathbf{R}^2$ with $0 \in \omega$ in dimension $d = 2$ is given by

$$d^1\mathscr{J}_2(\Omega,\omega)(x_0) = \big((f_2 - f_1)q_0\big)(x_0), \tag{19.3}$$

$$d^{2n}\mathscr{J}_2(\Omega,\omega)(x_0) = \frac{1}{|\omega|}\left(\sum_{j=0}^{n-2} \frac{1}{j!} \int_\omega \nabla^j\big(f_2 - f_1\big)(x_0)[x]^j c^{(n-j)}\, dx\right), \tag{19.4}$$

$$
\begin{aligned}
d^{2n+1}\mathscr{J}_2(\Omega,\omega)(x_0) = & \frac{1}{|\omega|}\frac{1}{n!}\int_\omega \nabla^n\big((f_2-f_1)q_0\big)(x_0)[x]^n\,dx \\
& + \frac{1}{|\omega|}\left(\sum_{j=0}^{n-2}\frac{1}{j!}\int_\omega \nabla^j\big(f_2-f_1\big)(x_0)[x]^j Q^{(n-j)}(x)\,dx\right) \\
& + \frac{1}{|\omega|}\left(\sum_{j=0}^{n-2}\frac{1}{j!}\int_\omega \nabla^j\big((f_2-f_1)q^{(n-j)}\big)(x_0)[x]^j\,dx\right),
\end{aligned} \tag{19.5}
$$

for $n \geq 1$, where for $\ell \geq 1$ $q^{(\ell)}, Q^{(\ell)}$ and $c^{(\ell)}$ are defined in Theorem 18.2.

Proof. Recall the Lagrangian introduced in (18.3). Let $\varepsilon \geq 0$. In view of (10.27) we have

$$
\mathscr{J}_2(\Omega_\varepsilon) = \mathscr{L}(\varepsilon, u_\varepsilon, q_\varepsilon) = \mathscr{L}(\varepsilon, u_0, q_\varepsilon), \tag{19.6}
$$

so that the cost function can be written only in terms of the averaged adjoint variable. Therefore, we deduce

$$
\mathscr{J}_2(\Omega_\varepsilon) - \mathscr{J}(\Omega) = \mathscr{L}(\varepsilon, u_0, q_\varepsilon) - \mathscr{L}(\varepsilon, u_0, q_0) + \mathscr{L}(\varepsilon, u_0, q_0) - \mathscr{L}(0, u_0, q_0). \tag{19.7}
$$

Using Theorem 18.2, we now derive an expansion for both differences on the right hand side. Note that this splitting resembles the methodology of the proof of Proposition 10.4.

Expansion of $\mathscr{L}(\varepsilon, u_0, q_0) - \mathscr{L}(0, u_0, q_0)$: We have

$$
\begin{aligned}
\mathscr{L}(\varepsilon, u_0, q_0) - \mathscr{L}(0, u_0, q_0) &= -\int_{\omega_\varepsilon} (f_1 - f_2) q_0\,dx \\
&= \varepsilon^d \int_\omega \underbrace{\big((f_2 - f_1)q_0\big)\circ T_\varepsilon}_{=:\hat{q}_0 \circ T_\varepsilon}\,dx,
\end{aligned} \tag{19.8}
$$

where we used a change of variables in the last step. Hence, a Taylor expansion of $\varepsilon \mapsto \hat{q}_0 \circ T_\varepsilon$ in $\varepsilon = 0$ yields

$$
\hat{q}_0 \circ T_\varepsilon(x) = \hat{q}_0(x_0) + \sum_{k=1}^{N} \varepsilon^k \frac{\nabla^k \hat{q}_0(x_0)[x]^k}{k!} + \mathscr{O}(\varepsilon^{N+1}). \tag{19.9}
$$

Now plugging the Taylor expansion (19.9) into (19.8) we get

$$
\frac{\mathscr{L}(\varepsilon, u_0, q_0) - \mathscr{L}(0, u_0, q_0)}{|\omega_\varepsilon|} = \hat{q}_0(x_0) + \sum_{k=1}^{N} \varepsilon^k \frac{1}{|\omega|}\frac{1}{k!}\int_\omega \nabla^k \hat{q}_0(x_0)[x]^k\,dx + \mathscr{O}(\varepsilon^{N+1}), \tag{19.10}
$$

where $|\omega_\varepsilon|$ denotes the volume of ω_ε. Thus, we have discovered one part of the n-th order topological derivative.

Expansion of $\mathscr{L}(\varepsilon,u_0,q_\varepsilon)-\mathscr{L}(\varepsilon,u_0,q_0)$: We proceed in several steps. First, we compute

$$\begin{aligned}\mathscr{L}(\varepsilon,u_0,q_\varepsilon)-\mathscr{L}(\varepsilon,u_0,q_0)=&\int_D \nabla u_0\cdot\nabla(q_\varepsilon-q_0)-f_{\Omega_\varepsilon}(q_\varepsilon-q_0)\,dx-(g_N,q_\varepsilon-q_0)_{H^{-\frac{1}{2}}(\Gamma^N)\times H^{\frac{1}{2}}(\Gamma^N)}\\ =&\underbrace{\int_D \nabla u_0\cdot\nabla(q_\varepsilon-q_0)-f_\Omega(q_\varepsilon-q_0)\,dx-(g_N,q_\varepsilon-q_0)_{H^{-\frac{1}{2}}(\Gamma^N)\times H^{\frac{1}{2}}(\Gamma^N)}}_{=0,\text{ in view of (17.2)}}\\ &-\int_D (f_{\Omega_\varepsilon}-f_\Omega)(q_\varepsilon-q_0)\,dx\\ =&\varepsilon^d\int_\omega (f_2-f_1)\circ T_\varepsilon \varepsilon Q_\varepsilon^{(1)}\,dx,\end{aligned}\tag{19.11}$$

where in the last step we used a change of variables with respect to the transformation T_ε and the definition $\varepsilon Q_\varepsilon^{(1)}=(q_\varepsilon-q_0)\circ T_\varepsilon$. We now substitute $\varepsilon Q_\varepsilon^{(1)}$ by the recursion formula of Lemma 18.3 and obtain

$$\int_\omega (f_2-f_1)\circ T_\varepsilon \varepsilon Q_\varepsilon^{(1)}\,dx=\sum_{n=1}^N\int_\omega (f_2-f_1)\circ T_\varepsilon \varepsilon^n Q^{(n)}\,dx \tag{19.12}$$

$$+\sum_{n=1}^N\int_\omega (f_2-f_1)\circ T_\varepsilon \varepsilon^n q^{(n)}\circ T_\varepsilon\,dx \tag{19.13}$$

$$+\sum_{n=1}^N\int_\omega (f_2-f_1)\circ T_\varepsilon \varepsilon^n \ln(\varepsilon)c^{(n)}\,dx \tag{19.14}$$

$$+\int_\omega (f_2-f_1)\circ T_\varepsilon \varepsilon^{N+1}Q_\varepsilon^{(N+1)}\,dx. \tag{19.15}$$

Next we can expand all four terms:

- First term (19.12): We use Taylor's expansion to write:

$$(f_2-f_1)\circ T_\varepsilon(x)=\sum_{j=0}^N \varepsilon^j a_j(x)+\mathscr{O}(\varepsilon^{N+1};x),\qquad a_j(x):=\frac{\nabla^j\big(f_2-f_1\big)(x_0)[x]^j}{j!}. \tag{19.16}$$

  For the proof we set $Q^{(0)}:=0$. Then, by Lemma 19.1 we have

$$(f_2-f_1)\circ T_\varepsilon(x)\left(\sum_{n=1}^N\varepsilon^n Q^{(n)}(x)\right)=\sum_{n=0}^N\varepsilon^n\left(\sum_{j=0}^n a_j(x)Q^{(n-j)}(x)\right)+\mathscr{O}(\varepsilon^{N+1};x) \tag{19.17}$$

  and further, taking into account that $Q^{(0)}=Q^{(1)}=0$,

$$\sum_{n=1}^N\int_\omega (f_2-f_1)\circ T_\varepsilon \varepsilon^n Q^{(n)}\,dx=\sum_{n=2}^N\varepsilon^n\int_\omega\left(\sum_{j=0}^{n-2}a_j(x)Q^{(n-j)}(x)\right)dx+\mathscr{O}(\varepsilon^{N+1}). \tag{19.18}$$

- Second term (19.13): Again we use Taylor's formula to expand the functions $\varepsilon \mapsto \hat{q}^{(n)} \circ T_\varepsilon$ at $\varepsilon = 0$ with $\hat{q}^{(n)} := (f_2 - f_1) q^{(n)}$, $n \geq 1$ to deduce

$$\hat{q}^{(n)}(x) = \sum_{j=0}^{N} \varepsilon^j b_j^{(n)}(x) + \mathcal{O}(\varepsilon^{N+1}; x), \qquad b_j^{(n)}(x) := \frac{\nabla^j \hat{q}^{(n)}(x_0)[x]^j}{j!}. \tag{19.19}$$

Hence, a similar computation as in the first bullet point and an application of Lemma 19.1 yield

$$\begin{aligned}\sum_{n=1}^{N} \int_\omega \varepsilon^n \left((f_2 - f_1) q^{(n)} \right) \circ T_\varepsilon \, dx &= \sum_{n=1}^{N} \varepsilon^n \left(\sum_{j=0}^{N} \varepsilon^j \int_\omega b_j^{(n)}(x) \, dx \right) + \mathcal{O}(\varepsilon^{N+1}), \\ &= \sum_{n=2}^{N} \varepsilon^n \left(\sum_{j=0}^{n-2} \int_\omega b_j^{(n-j)}(x) \, dx \right) + \mathcal{O}(\varepsilon^{N+1}),\end{aligned} \tag{19.20}$$

where we took into account $q^{(1)} = 0$ and therefore $b_j^{(1)} = 0$ for $j \geq 0$ as well.

- Third term (19.14): In view of the terms $a_j(x)$, $j \geq 0$ introduced above in (19.16) we have

$$\begin{aligned}\sum_{n=1}^{N} \int_\omega \varepsilon^n \ln(\varepsilon)(f_2 - f_1) \circ T_\varepsilon c^{(n)} \, dx &= \left(\sum_{j=0}^{N} \varepsilon^j \ln(\varepsilon) \int_\omega a_j(x) \, dx \right) \left(\sum_{n=1}^{N} \varepsilon^n c^{(n)} \right) + o(\varepsilon^{N+1}) \\ &= \sum_{n=2}^{N} \varepsilon^n \ln(\varepsilon) \left(\sum_{j=0}^{n-2} \int_\omega a_j(x) c^{(n-j)} \, dx \right) + o(\varepsilon^N),\end{aligned} \tag{19.21}$$

where we took into account that $c^{(1)} = 0$.

- Fourth term (19.15): Applying Lemma 11.5, item (iii), to the last term and using the asymptotics derived in Theorem 18.2 entails

$$\left| \int_\omega (f_1 - f_2) \circ T_\varepsilon \varepsilon^{N+1} Q_\varepsilon^{(N+1)} \, dx \right| \leq C \varepsilon^{N-\alpha} \| \varepsilon Q_\varepsilon^{(N+1)} \|_\varepsilon \leq C \varepsilon^{N+1-2\alpha}, \tag{19.22}$$

for a constant $C > 0$ and $\alpha \in (0,1)$ sufficiently small.

Combining (19.18) - (19.22) leaves us with the expansion

$$\frac{\mathfrak{L}(\varepsilon, u_0, q_\varepsilon) - \mathfrak{L}(\varepsilon, u_0, q_0)}{|\omega_\varepsilon|} = \frac{1}{|\omega|} \sum_{k=2}^{N} \varepsilon^k \left(\sum_{j=0}^{k-2} \int_\omega a_j(x) Q^{(k-j)}(x) \, dx \right) \tag{19.23}$$

$$+ \frac{1}{|\omega|} \sum_{k=2}^{N} \varepsilon^k \left(\sum_{j=0}^{k-2} \int_\omega b_j^{(k-j)}(x) \, dx \right) \tag{19.24}$$

$$+ \frac{1}{|\omega|} \sum_{k=2}^{N} \varepsilon^k \ln(\varepsilon) \left(\sum_{j=0}^{k-2} \int_\omega a_j(x) c^{(k-j)} \, dx \right) + o(\varepsilon^N). \tag{19.25}$$

From this formula, together with (19.10), we see that the n-th topological derivative is given by (19.3)-(19.5). □

Remark 19.3. In the context of the previous part of this thesis (cf. Section 14.2), the first expansion we considered in the proof correlates to the terms $\partial_\ell^{(1)}\mathscr{L}(0,u_0,q_0), \partial_\ell^{(2)}\mathscr{L}(0,u_0,q_0)$. Similarly, the second part matches the terms $\mathscr{R}^{(1)}(u_0,q_0), \mathscr{R}^{(2)}(u_0,q_0)$. We observe that in both cases the latter require a more involved analysis.

Corollary 19.4. The first five topological derivatives in dimension $d=2$ read as follows:

$$d^1\mathscr{J}_2(\Omega,\omega)(x_0) = \big((f_2-f_1)q_0\big)(x_0), \qquad \ell_1(\varepsilon)=|\omega|\varepsilon^2, \tag{19.26}$$

$$d^2\mathscr{J}_2(\Omega,\omega)(x_0) = 0, \qquad \ell_2(\varepsilon)=|\omega|\varepsilon^2(\varepsilon\ln(\varepsilon)), \tag{19.27}$$

$$d^3\mathscr{J}_2(\Omega,\omega)(x_0) = \frac{1}{|\omega|}\int_\omega \nabla\big((f_2-f_1)q_0\big)(x_0)[x]\,dx, \qquad \ell_3(\varepsilon)=|\omega|\varepsilon^3, \tag{19.28}$$

$$d^4\mathscr{J}_2(\Omega,\omega)(x_0) = \alpha_2[f_1-f_2](x_0)b^{(2)}, \qquad \ell_4(\varepsilon)=|\omega|\varepsilon^3(\varepsilon\ln(\varepsilon)), \tag{19.29}$$

$$d^5\mathscr{J}_2(\Omega,\omega)(x_0) = \frac{1}{2|\omega|}\int_\omega \nabla^2\big((f_2-f_1)q_0\big)(x_0)[x]^2\,dx \qquad \ell_5(\varepsilon)=|\omega|\varepsilon^4, \tag{19.30}$$

$$+\frac{\alpha_2\big(f_1-f_2\big)(x_0)}{|\omega|}\int_\omega U^{(2)}\,dx \tag{19.31}$$

$$+\alpha_2\big((f_1-f_2)u^{(2)}\big)(x_0). \tag{19.32}$$

19.1.1 Special cases

In this section we consider some special cases for our input data in dimension $d=2$ and discuss how this influences the topological derivative. At first, let the inhomogeneity be piecewise constant, that is, assume $f_1, f_2 \in \mathbf{R}$. Thus, it follows from (17.8) that $U^{(k)}=0$ for $k\neq 2$. Additionally, we have $Q^{(k)}=0$ and $b^{(k)}=c^{(k)}=0$, for $k\neq 2$. Since $a_j(x)$ denotes the j-th term of the Taylor's expansion of $(f_2-f_1)\circ T_\varepsilon$, we further deduce that $a_j(x)=0$ for $j>0$. These observations yield the following result:

Corollary 19.5. Assume that $f_1, f_2 \in \mathbf{R}$. Let $\ell_1(\varepsilon):=|\omega_\varepsilon|$, $\ell_{2n}(\varepsilon):=\varepsilon^n\ln(\varepsilon)|\omega_\varepsilon|$ and $\ell_{2n+1}(\varepsilon)=\varepsilon^n|\omega_\varepsilon|$, for $n\geq 1$. The topological derivative of $\mathscr{J}_2$ at $x_0\in \mathsf{D}\setminus\bar{\Omega}$ and $\omega\subset\mathbf{R}^d$ with $0\in\omega$ in dimension $d=2$ is given by

$$d^1\mathscr{J}_2(\Omega,\omega)(x_0) = (f_2-f_1)q_0(x_0), \quad d^2\mathscr{J}_2(\Omega,\omega)(x_0)=0, \tag{19.33}$$

$$d^3\mathscr{J}_2(\Omega,\omega)(x_0) = \frac{f_2-f_1}{|\omega|}\int_\omega \nabla q_0(x_0)[x]\,dx, \quad d^4\mathscr{J}_2(\Omega,\omega)(x_0)=(f_2-f_1)c^{(2)}, \tag{19.34}$$

$$\begin{aligned} d^5\mathscr{J}_2(\Omega,\omega)(x_0) =& \frac{1}{|\omega|}\frac{f_2-f_1}{2}\int_\omega \nabla^2 q_0(x_0)[x]^2\,dx \\ &+\frac{f_2-f_1}{|\omega|}\int_\omega Q^{(2)}(x)\,dx \\ &+(f_2-f_1)q^{(2)}(x_0), \end{aligned} \tag{19.35}$$

$$d^{2n}\mathscr{J}_2(\Omega,\omega)(x_0)=0, \tag{19.36}$$

$$
\begin{aligned}
d^{2n+1}\mathscr{J}_2(\Omega,\omega)(x_0) =& \frac{f_2-f_1}{|\omega|}\frac{1}{n!}\int_\omega \nabla^n q_0(x_0)[x]^n\,dx \\
&+ \frac{f_2-f_1}{|\omega|}\left(\sum_{j=0}^{n-2}\frac{1}{j!}\int_\omega \nabla^j q^{(n-j)}(x_0)[x]^j\,dx\right),
\end{aligned}
\tag{19.37}
$$

for $n \geq 3$, where $q^{(\ell)}, Q^{(\ell)}$ and $c^{(\ell)}$, $\ell \geq 1$ are defined in Theorem 18.2.

Next we consider a symmetric inclusion $\omega \subset \mathbf{R}^2$. To be precise, we assume that ω can be written as the union $\omega^+ \cup (-\omega^+)$, where ω^+ is a subset of ω. Additionally, we require this union to overlap only on a set of zero measure, i.e. $|\omega^+ \cap (-\omega^+)| = 0$. For example the square $(-1,1)\times(-1,1)$ and the unit sphere satisfy this property. One readily checks that

$$
\int_\omega \nabla^k h(x_0)[x]^k\,dx = 0 \quad \text{for } k \text{ odd}, \tag{19.38}
$$

for a sufficiently smooth function h, since the integrand is an odd function. As a result, the odd numbered boundary layer correctors and the corresponding logarithmic terms vanish. That is,

$$
U^{(k)} = Q^{(k)} = 0 \quad \text{for } k \text{ odd},
$$

$$
b^{(k)} = c^{(k)} = 0 \quad \text{for } k \text{ odd}.
$$

Additionally, since we derived the topological derivative by expanding q_0, $f_2 - f_1$ and $q^{(k)}$, $k \geq 2$ with the help of Taylor's expansion, some terms in the general formula can be skipped by the same argument. These considerations yield the following corollary:

Corollary 19.6. Assume that $f_1, f_2 \in \mathbf{R}$ and the perturbation shape ω is symmetric. Let $\ell_1(\varepsilon) := |\omega_\varepsilon|$, $\ell_{2n}(\varepsilon) = \varepsilon^n \ln(\varepsilon)|\omega_\varepsilon|$ and $\ell_{2n+1}(\varepsilon) = \varepsilon^n|\omega_\varepsilon|$, for $n \geq 1$. The topological derivative of $\mathscr{J}_2$ at $x_0 \in \mathrm{D}\setminus\bar{\Omega}$ and $\omega \subset \mathbf{R}^2$ with $0 \in \omega$ in dimension $d = 2$ is given by

$$
d^1\mathscr{J}_2(\Omega,\omega)(x_0) = (f_2-f_1)q_0(x_0), \quad d^2\mathscr{J}_2(\Omega,\omega)(x_0) = 0, \tag{19.39}
$$

$$
d^3\mathscr{J}_2(\Omega,\omega)(x_0) = 0, \quad d^4\mathscr{J}_2(\Omega,\omega)(x_0) = (f_2-f_1)c^{(2)}, \tag{19.40}
$$

$$
\begin{aligned}
d^5\mathscr{J}_2(\Omega,\omega)(x_0) =& \frac{1}{|\omega|}\frac{f_2-f_1}{2}\int_\omega \nabla^2 q_0(x_0)[x]^2\,dx \\
&+ \frac{f_2-f_1}{|\omega|}\int_\omega Q^{(2)}(x)\,dx \\
&+ (f_2-f_1)q^{(2)}(x_0),
\end{aligned}
\tag{19.41}
$$

$$
d^{2n}\mathscr{J}_2(\Omega,\omega)(x_0) = 0, \tag{19.42}
$$

$$
\begin{aligned}
d^{2n+1}\mathscr{J}_2(\Omega,\omega)(x_0) =& \frac{f_2-f_1}{|\omega|}\frac{1}{n!}\int_\omega \nabla^n q_0(x_0)[x]^n\,dx \\
&+ \frac{f_2-f_1}{|\omega|}\left(\sum_{j=0}^{\frac{n-2}{2}}\frac{1}{(2j)!}\int_\omega \nabla^{2j} q^{(n-2j)}(x_0)[x]^{2j}\,dx\right) \quad \text{for } n \text{ even},
\end{aligned}
\tag{19.43}
$$

$$d^{2n+1}\mathscr{J}_2(\Omega,\omega)(x_0) = \frac{f_2-f_1}{|\omega|}\left(\sum_{j=0}^{\frac{n-3}{2}} \frac{1}{(2j)!}\int_\omega \nabla^{2j} q^{(n-2j)}(x_0)[x]^{2j}\,dx\right) \quad \text{for } n \text{ odd,} \tag{19.44}$$

for $n \geq 3$, where $q^{(\ell)}, Q^{(\ell)}$ and $c^{(\ell)}$, $\ell \geq 1$ are defined in Theorem 18.2.

Let us finish this section by computing the first five topological derivatives for the unit ball perturbation shape and constant functions $f_1, f_2 \in \mathbf{R}$. Note that, in view of Example 17.19, we have an explicit formulation of the corrector $U^{(2)}$.

Corollary 19.7. For the inclusion $\omega := B_1(0)$ the unit ball in $\mathbf{R}^2$ centered at the origin and $f_1, f_2 \in \mathbf{R}$, the first five topological derivatives in dimension $d = 2$ read:

$$\begin{aligned}
d^1\mathscr{J}_2(\Omega,\omega)(x_0) &= (f_2-f_1)q_0(x_0), && \ell_1(\varepsilon) = |\omega|\varepsilon^2,\\
d^2\mathscr{J}_2(\Omega,\omega)(x_0) &= 0, && \ell_2(\varepsilon) = |\omega|\varepsilon^2(\varepsilon\ln(\varepsilon)),\\
d^3\mathscr{J}_2(\Omega,\omega)(x_0) &= 0, && \ell_3(\varepsilon) = |\omega|\varepsilon^3,\\
d^4\mathscr{J}_2(\Omega,\omega)(x_0) &= -\frac{\alpha_2(f_1-f_2)^2}{2}, && \ell_4(\varepsilon) = |\omega|\varepsilon^3(\varepsilon\ln(\varepsilon)),\\
d^5\mathscr{J}_2(\Omega,\omega)(x_0) &= \frac{(f_2-f_1)}{2\pi}\int_\omega \nabla^2 q_0(x_0)[x]^2\,dx && \ell_5(\varepsilon) = |\omega|\varepsilon^4.\\
&\quad + \frac{\alpha_2(f_1-f_2)^2}{8}\\
&\quad + \alpha_2(f_1-f_2)u^{(2)}(x_0),
\end{aligned}$$

Proof. Following Example 17.19, we have $U^{(2)} = -(f_1-f_2)\frac{1}{4}(1-|x|)$ for $x \in B_1(0)$. Hence, we can compute the integral of $U^{(2)}$ explicitly and obtain

$$\int_\omega U^{(2)}\,dx = (f_1-f_2)\frac{\pi}{8}.$$

Taking into account vanishing terms due to the symmetry of the inclusion, the result follows from Corollary 19.4. □

19.2 General formula for higher order topological derivatives in dimension three

Similarly to the previous section one can derive the following result regarding the topological derivative of the H^1 tracking-type part of the cost functional in dimension $d = 3$.

Theorem 19.8. Let $\ell_1(\varepsilon) := |\omega_\varepsilon|$ and $\ell_n(\varepsilon) = \varepsilon^{n-1}|\omega_\varepsilon|$, for $n \geq 2$. The topological derivative of $\mathscr{J}_2$ at $x_0 \in \mathrm{D}\setminus\bar{\Omega}$ and $\omega \subset \mathbf{R}^3$ with $0 \in \omega$ in dimension $d = 3$ is given by

$$d^1\mathscr{J}_2(\Omega,\omega)(x_0) = \big((f_2-f_1)q_0\big)(x_0), \quad d^2\mathscr{J}_2(\Omega,\omega)(x_0) = \frac{1}{|\omega|}\int_\omega \nabla\big((f_2-f_1)q_0\big)(x_0)[x]\,dx, \tag{19.45}$$

$$
\begin{aligned}
d^{n+1}\mathscr{J}_2(\Omega,\omega)(x_0) = &\frac{1}{|\omega|}\frac{1}{n!}\int_\omega \nabla^n\big((f_2-f_1)q_0\big)(x_0)[x]^n\,dx \\
&+\frac{1}{|\omega|}\left(\sum_{j=0}^{n-2}\frac{1}{j!}\int_\omega \nabla^j\big(f_2-f_1\big)(x_0)[x]^j Q^{(n-j)}(x)\,dx\right) \\
&+\frac{1}{|\omega|}\left(\sum_{j=0}^{n-3}\frac{1}{j!}\int_\omega \nabla^j\big((f_2-f_1)q^{(n-1-j)}\big)(x_0)[x]^j\,dx\right).
\end{aligned}
\tag{19.46}
$$

for $n \geq 2$, where $q^{(\ell)}, Q^{(\ell)}$ and $c^{(\ell)}$, $\ell \geq 1$ are defined in Theorem 18.2.

Proof. This can be shown similarly to the proof in dimension $d = 2$. The main difference is the shift in the third term of (19.46), which is a result of the factor $\varepsilon^{d-2} = \varepsilon^1$ in Lemma 18.3. Additionally, the absence of the logarithmic terms leads to a clearer representation of the general formula of the topological derivative compared to the two dimensional case. □

Similarly to Corollary 19.4, we deduce the following result.

Corollary 19.9. The first five topological derivatives in terms of the correctors of $U_\varepsilon^{(1)}$ in dimension $d = 3$ read

$$
\begin{aligned}
d^1\mathscr{J}_2(\Omega,\omega)(x_0) = &\big((f_2-f_1)q_0\big)(x_0), && \ell_1(\varepsilon)=|\omega|\varepsilon^3,\\
d^2\mathscr{J}_2(\Omega,\omega)(x_0) = &\frac{1}{|\omega|}\int_\omega \nabla\big((f_2-f_1)q_0\big)(x_0)[x]\,dx, && \ell_2(\varepsilon)=|\omega|\varepsilon^4,\\
d^3\mathscr{J}_2(\Omega,\omega)(x_0) = &\frac{1}{2|\omega|}\int_\omega \nabla^2\big((f_2-f_1)q_0\big)(x_0)[x]^2\,dx && \ell_3(\varepsilon)=|\omega|\varepsilon^5,\\
&+\frac{\alpha_2\big(f_1-f_2\big)(x_0)}{|\omega|}\int_\omega U^{(2)}\,dx,\\
d^4\mathscr{J}_2(\Omega,\omega)(x_0) = &\frac{1}{6|\omega|}\int_\omega \nabla^3\big((f_2-f_1)q_0\big)(x_0)[x]^3\,dx && \ell_4(\varepsilon)=|\omega|\varepsilon^6,\\
&+\frac{\alpha_2\big(f_1-f_2\big)(x_0)}{|\omega|}\int_\omega U^{(3)}\,dx\\
&+\frac{\alpha_2}{|\omega|}\left(\int_\omega \nabla\big(f_1-f_2\big)(x_0)[x]U^{(2)}(x)\,dx\right)\\
&+\frac{\alpha_2}{|\omega|}\left(\int_\omega \big((f_1-f_2)u^{(2)}\big)(x_0)\,dx\right),
\end{aligned}
$$

$$
\begin{aligned}
d^5 \mathscr{J}_2(\Omega,\omega)(x_0) = & \frac{1}{24|\omega|}\int_\omega \nabla^4\big((f_2-f_1)q_0\big)(x_0)[x]^4\, dx \qquad\qquad \ell_5(\varepsilon) = |\omega|\varepsilon^7.\\
&+ \frac{\alpha_2\big(f_1-f_2\big)(x_0)}{|\omega|}\int_\omega U^{(4)}\, dx\\
&+ \frac{\alpha_2}{|\omega|}\left(\int_\omega \nabla\big(f_1-f_2\big)(x_0)[x]U^{(3)}(x)\, dx\right)\\
&+ \frac{\alpha_2}{2|\omega|}\left(\int_\omega \nabla^2\big(f_1-f_2\big)(x_0)[x]^2U^{(2)}(x)\, dx\right)\\
&+ \frac{\alpha_2}{|\omega|}\left(\int_\omega \big((f_1-f_2)u^{(3)}\big)(x_0)\, dx\right)\\
&+ \frac{\alpha_2}{|\omega|}\left(\int_\omega \nabla\big((f_1-f_2)u^{(2)}\big)(x_0)[x]\, dx\right),
\end{aligned}
$$

20 Analysis of the averaged adjoint equation for the L_2 tracking-type cost function

In this section we derive the asymptotic expansion of the averaged adjoint state q_ε for the L_2 tracking-type part of (16.1). The analysis differs significantly from the H^1 tracking-type cost function and involves the fundamental solution of the biharmonic equation. Since the fundamental solution is not homogeneous in dimension $d=2$, the analysis in this case is more complicated and requires the introduction of several regular corrector equations. In this section, our objective function is

$$
\mathscr{J}_1(\Omega) := \alpha_1 \int_{\mathsf{D}} (u_\Omega - u_d)^2\, dx, \tag{20.1}
$$

where $\alpha_1 \geq 0$ and $u_\Omega \in H^1(\mathsf{D})$ satisfies $u_\Omega|_\Gamma = g_D$ and

$$
\int_{\mathsf{D}} \nabla u_\Omega \cdot \nabla \varphi\, dx = \int_{\mathsf{D}} f_\Omega \varphi\, dx + (g_N,\varphi)_{H^{-\frac{1}{2}}(\Gamma^N)\times H^{\frac{1}{2}}(\Gamma^N)} \quad \text{for all } \varphi \in H^1_\Gamma(\mathsf{D}). \tag{20.2}
$$

In analogy to (18.3) the associated Lagrangian is given by

$$
\mathscr{L}(\varepsilon,u,v) := \alpha_1 \int_{\mathsf{D}} (\varphi - u_d)^2\, dx + \int_{\mathsf{D}} \nabla u\cdot\nabla v - f_{\Omega_\varepsilon} v\, dx - (g_N, v)_{H^{-\frac{1}{2}}(\Gamma^N)\times H^{\frac{1}{2}}(\Gamma^N)} \quad \text{for all } u\in\mathscr{V}, v\in\mathscr{W}, \tag{20.3}
$$

where $\mathscr{W} = H^1_\Gamma(\mathsf{D})$ and $\mathscr{V} = \bar{u} + \mathscr{W}$ with an element $\bar{u}\in H^1(\mathsf{D})$ satisfying the boundary condition $\bar{u}|_\Gamma = g_D$. Now, the averaged adjoint equation reads: for $\varepsilon > 0$ find $q_\varepsilon \in H^1_\Gamma(\mathsf{D})$, such that

$$
\int_0^1 \partial_u \mathscr{L}(\varepsilon, su_\varepsilon + (1-s)u_0, q_\varepsilon)(\varphi)\, ds = 0 \quad \text{for all } \varphi \in H^1_\Gamma(\mathsf{D}). \tag{20.4}
$$

Or explicitly, evaluating the ds-integral, the perturbed averaged adjoint equation reads: find $q_\varepsilon \in H^1_\Gamma(\mathrm{D})$, such that

$$\int_{\mathrm{D}} \nabla\varphi \cdot \nabla q_\varepsilon \, dx = -\alpha_1 \int_{\mathrm{D}} (u_\varepsilon + u_0 - 2u_d)\varphi \, dx \quad \text{for all } \varphi \in H^1_\Gamma(\mathrm{D}). \tag{20.5}$$

Similarly, the unperturbed averaged adjoint equation reads: find $q_0 \in H^1_\Gamma(\mathrm{D})$, such that

$$\int_{\mathrm{D}} \nabla\varphi \cdot \nabla q_0 \, dx = -\alpha_1 \int_{\mathrm{D}} (2u_0 - 2u_d)\varphi \, dx \quad \text{for all } \varphi \in H^1_\Gamma(\mathrm{D}). \tag{20.6}$$

Due to the differing boundary layer correctors occurring in the analysis of the averaged adjoint state variable associated with this specific cost functional, some modifications of the variation of the averaged adjoint state compared to the direct state have to be considered. We will introduce them in the following:

Definition 20.1. For almost every $x \in \mathrm{D}_\varepsilon$ we define the first variation of the averaged adjoint state q_ε by

$$Q^{(1)}_\varepsilon(x) := \left(\frac{q_\varepsilon - q_0}{\varepsilon}\right) \circ T_\varepsilon(x) \quad \text{for } \varepsilon > 0. \tag{20.7}$$

More generally, we define the $(k+1)$-th variation of q_ε for $k \geq 1$ and $\varepsilon > 0$ by

$$Q^{(k+1)}_\varepsilon := \begin{cases} \frac{Q^{(k)}_\varepsilon - \varepsilon^2 Q^{(k)} - \varepsilon^{d-2} L^{(k)}_\varepsilon \circ T_\varepsilon - \varepsilon^d q^{(k)} \circ T_\varepsilon - \varepsilon^{d-2} m^{(k)} \circ T_\varepsilon - \ln(\varepsilon) n^{(k)} \circ T_\varepsilon}{\varepsilon} & \text{for } d = 2, \\ \frac{Q^{(k)}_\varepsilon - \varepsilon^2 Q^{(k)} - \varepsilon^{d-2} L^{(k)}_\varepsilon \circ T_\varepsilon - \varepsilon^d q^{(k)} \circ T_\varepsilon - \varepsilon^{d-2} m^{(k)} \circ T_\varepsilon}{\varepsilon} & \text{for } d = 3. \end{cases} \tag{20.8}$$

Here, $Q^{(k)}$, $m^{(k)}$ and $n^{(k)}$ aim to approximate $U^{(k)}$, $u^{(k)}$ and $b^{(k)}$, respectively, whereas $L^{(k)}$ and $q^{(k)}$ correct the error on the boundary, which is introduced by $Q^{(k)}$.

As a result of Definition 20.1, we get the following analogue to Lemma 17.15.

Lemma 20.2. We have for $k \geq 2$ and $d = 2$

$$Q^{(1)}_\varepsilon - \varepsilon^{k-1} Q^{(k)}_\varepsilon = \sum_{\ell=1}^{k-1} \varepsilon^{\ell-1} \left(\varepsilon^2 Q^{(\ell)} + \varepsilon^{d-2} L^{(\ell)}_\varepsilon \circ T_\varepsilon + \varepsilon^d q^{(\ell)} \circ T_\varepsilon + \varepsilon^{d-2} m^{(\ell)} \circ T_\varepsilon + \ln(\varepsilon) n^{(\ell)} \circ T_\varepsilon \right), \tag{20.9}$$

and for $k \geq 2$ and $d = 3$

$$Q^{(1)}_\varepsilon - \varepsilon^{k-1} Q^{(k)}_\varepsilon = \sum_{\ell=1}^{k-1} \varepsilon^{\ell-1} \left(\varepsilon^2 Q^{(\ell)} + \varepsilon^{d-2} L^{(\ell)}_\varepsilon \circ T_\varepsilon + \varepsilon^d q^{(\ell)} \circ T_\varepsilon + \varepsilon^{d-2} m^{(\ell)} \circ T_\varepsilon \right). \tag{20.10}$$

Proof. Similarly to Lemma 17.15, this follows from induction arguments. □

In the following we introduce the corrector variables appearing in Definition 20.1. The methodology resembles our approaches utilised in the previous sections of this thesis covering asymptotic expansions. Nonetheless, we will proceed with more detailed steps, since the number of correctors is significantly larger.

Lemma 20.3. For $k \geq 2$ let $Q^{(k)}(x) := -\alpha_1 \int_\omega \phi(x-y) F^{(k)}(y)\,dy$, where

$$\phi(x) := \begin{cases} \frac{1}{8\pi}\left(|x|^2 \ln(|x|) - |x|^2\right) & \text{for } d = 2, \\ -\frac{1}{8\pi}|x| & \text{for } d = 3, \end{cases} \tag{20.11}$$

denotes the fundamental solution of the biharmonic equation (see [65, Section 4.2, pp. 201]) and $F^{(k)}$ is defined in Lemma 17.7. Then $Q^{(k)}$ satisfies

$$\int_{\mathbf{R}^d} \nabla Q^{(k)} \cdot \nabla \varphi \, dx = -\alpha_1 \int_{\mathbf{R}^d} U^{(k)} \varphi \, dx \quad \text{for all } \varphi \in C_c^1(\mathbf{R}^d). \tag{20.12}$$

Moreover, in dimension $d = 2$, $Q^{(k)}$ has the asymptotic behaviour

$$\begin{aligned} Q^{(k)}(x) =& A_2^{(k)}(x)\ln(|x|) + A_1^{(k)}(x)\ln(|x|) + A_0^{(k)}(x)\ln(|x|) \\ &+ B_2^{(k)}(x) + B_1^{(k)}(x) + B_0^{(k)}(x) + \sum_{\ell=1}^{N} S_\ell^{(k)}(x) + \mathcal{O}(|x|^{-(d-2+N+1)}), \end{aligned} \tag{20.13}$$

and in dimension $d = 3$, we have

$$Q^{(k)}(x) = A_1^{(k)}(x) + A_0^{(k)}(x) + A_{-1}^{(k)}(x) + \sum_{\ell=1}^{N} S_\ell^{(k)}(x) + \mathcal{O}(|x|^{-(d-2+N+1)}), \tag{20.14}$$

for $|x| \to \infty$, where $N \geq 1$, $A_i^{(k)}, B_i^{(k)}$ are homogeneous of degree i and $S_i^{(k)}$ are homogeneous of degree $-(d-2+i)$.

Proof. Similarly to [67, Lemma 4.1, pp. 54], one can show that $Q^{(k)} \in C^2(\mathbf{R}^d)$ and

$$\frac{\partial^2}{\partial x_i \partial x_j} Q^{(k)} = -\alpha_1 \int_\omega \frac{\partial^2}{\partial x_i \partial x_j} \phi(x-y) F^{(k)}(y)\,dy.$$

Since $-\Delta\phi = E$, where E denotes the fundamental solution of the Laplace equation introduced in (17.5), one readily follows

$$-\Delta Q^{(k)} = \alpha_1 \int_\omega \Delta\phi(x-y) F^{(k)}(y)\,dy = -\alpha_1 \int_\omega E(x-y) F^{(k)}(y)\,dy = -\alpha_1 U^{(k)} \quad \text{on } \mathbf{R}^d,$$

where in the last step we used (17.7). This shows (20.12). Now, the asymptotic behaviour (20.13),(20.14) follows from a Taylor's expansion of ϕ. □

Example 20.4. The terms $S_\ell^{(k)} : \mathbf{R}^d \to \mathbf{R}$ are given for $k \geq 2$ and $\ell \geq 1$ by

$$S_\ell^{(k)}(x) = \frac{1}{(\ell+2)!} \int_\omega \partial_t^{\ell+2} \phi(x - ty)|_{t=0} F^{(k)}(y)\,dy, \tag{20.15}$$

with $F^{(k)}(y) := \frac{1}{(k-2)!}\nabla^{k-2}(f_1 - f_2)(x_0)[y]^{k-2}$. Additionally, the leading terms can be explicitly computed for $d = 2$ as

$$A_2^{(k)}(x) = -\frac{\alpha_1}{8\pi}|x|^2 \int_\omega F^{(k)}(y)\,dy, \tag{20.16}$$

$$A_1^{(k)}(x) = \frac{\alpha_1}{4\pi}\int_\omega x \cdot y F^{(k)}(y)\,dy, \tag{20.17}$$

$$A_0^{(k)}(x) = -\frac{\alpha_1}{8\pi}\int_\omega |y|^2 F^{(k)}(y)\,dy, \tag{20.18}$$

$$B_2^{(k)}(x) = \frac{\alpha_1}{8\pi}|x|^2 \int_\omega F^{(k)}(y)\,dy, \tag{20.19}$$

$$B_1^{(k)}(x) = -\frac{\alpha_1}{8\pi}\int_\omega x \cdot y F^{(k)}(y)\,dy, \tag{20.20}$$

$$B_0^{(k)}(x) = -\frac{\alpha_1}{8\pi}\int_\omega \left(\frac{(x\cdot y)^2}{|x|^2} - \frac{|y|^2}{2}\right) F^{(k)}(y)\,dy, \tag{20.21}$$

and similarly for $d = 3$ the leading terms are given as

$$A_1^{(k)}(x) = \frac{\alpha_1}{8\pi}|x| \int_\omega F^{(k)}(y)\,dy, \tag{20.22}$$

$$A_0^{(k)}(x) = -\frac{\alpha_1}{8\pi}\int_\omega \frac{x\cdot y}{|x|} F^{(k)}(y)\,dy, \tag{20.23}$$

$$A_{-1}^{(k)}(x) = \frac{\alpha_1}{16\pi}\int_\omega \left(\frac{|x|^2|y|^2 - (x\cdot y)^2}{|x|^3}\right) F^{(k)}(y)\,dy. \tag{20.24}$$

Next we will look at the remaining components of (20.8).

Definition 20.5. For $k \geq 3$ we define the corrector $q^{(k)} \in H^1(\mathrm{D})$ as the unique solution to

$$q^{(k)} = -\sum_{\ell=1}^{k} S_\ell^{(k-\ell)}(x - x_0) \quad \text{on } \Gamma, \tag{20.25}$$

$$\int_{\mathrm{D}} \nabla q^{(k)} \cdot \nabla\varphi\,dx = \int_{\Gamma^N}\left(\sum_{\ell=1}^{k} \partial_\nu S_\ell^{(k-\ell)}(x - x_0)\right)\varphi\,dS \quad \text{for all } \varphi \in H^1_\Gamma(\mathrm{D}), \tag{20.26}$$

where we introduce $S_\ell^{(0)} = S_\ell^{(1)} = 0$ for $\ell \geq 1$. Additionally, we define for $k \geq 2$ the corrector $m^{(k)} \in H^1_\Gamma(\mathrm{D})$ as the unique solution to

$$\int_{\mathrm{D}} \nabla m^{(k)} \cdot \nabla\varphi\,dx = -\alpha_1 \int_{\mathrm{D}} u^{(k)}\varphi\,dx \quad \text{for all } \varphi \in H^1_\Gamma(\mathrm{D}), \tag{20.27}$$

and $n^{(k)} \in H^1_\Gamma(\mathrm{D})$ as the unique solution to

$$\int_{\mathrm{D}} \nabla n^{(k)} \cdot \nabla\varphi\,dx = -\alpha_1 b^{(k)} \int_{\mathrm{D}} \varphi\,dx \quad \text{for all } \varphi \in H^1_\Gamma(\mathrm{D}). \tag{20.28}$$

For the sake of completeness we introduce the remaining correctors.

Definition 20.6. We define

$$Q^{(1)} \equiv 0,$$

as well as

$$q^{(1)} \equiv 0, \quad q^{(2)} \equiv 0, \quad m^{(1)} \equiv 0, \quad n^{(1)} \equiv 0.$$

The function $Q^{(k)}$ approximates $Q_\varepsilon^{(k)}$ inside ω but introduces an error on the boundary $\partial \mathsf{D}_\varepsilon$ in analogy to the approximation of the variation of the state $U_\varepsilon^{(k)}$ by the boundary layer correctors $U^{(k)}$. The main difference now is that the asymptotic behaviour of $Q^{(k)}$ (see (20.13), (20.14)) requires the first six terms in dimension $d = 2$ and the first three terms in dimension $d = 3$ to be corrected during each step. This can readily be done for homogeneous terms, whereas the logarithm occurring in dimension two causes some issues that require special attention. We illustrate the procedure for the Dirichlet boundary Γ_ε in the following. In view of the expansion (20.13) of $Q^{(k)}$ in dimension $d = 2$, we can correct the error produced by $Q^{(k)}$ on the boundary part Γ_ε, by correcting the terms $\ln(|\cdot|)A_i^{(k)}(\cdot), B_i^{(k)}(\cdot)$, $i = 0,1,2$ individually.
In order to correct a term $f(x)$ (e.g. $f(x) = B_1^{(k)}(x)$) on the boundary Γ_ε, which we assume is homogeneous of degree r, we introduce a regular corrector $s \in H^1(\mathsf{D})$ defined on the fixed domain D, such that $s|_\Gamma = -f(x - x_0)$. Now rescaling s to the domain D_ε yields $s \circ T_\varepsilon|_{\Gamma_\varepsilon} = -f(\varepsilon x)$. Hence, since f is homogeneous of degree r, we just need to scale s by the factor ε^{-r} to obtain

$$\varepsilon^{-r} s \circ T_\varepsilon|_{\Gamma_\varepsilon} = -\varepsilon^{-r} f(\varepsilon x) = -f(x).$$

Utilising this method, we can correct the terms $B_i^{(k)}$, $i = 0,1,2$. Unfortunately, the terms $\ln(|x|)A_i^{(k)}(x)$, $i = 0,1,2$ are not homogeneous, since the natural logarithm admits the additive property

$$\ln(|\varepsilon x|) = \ln(\varepsilon) + \ln(|x|) \quad \text{for all } \varepsilon > 0.$$

Thus, correcting a term $f(x)\ln(|x|)$ (e.g. $f(x) = A_1^{(k)}(x)$), where f is homogeneous of degree r, with a function s defined on the fixed domain and boundary values $s|_\Gamma = -f(x - x_0)\ln(|x - x_0|)$ yields

$$\varepsilon^{-r} s \circ T_\varepsilon|_{\Gamma_\varepsilon} = -f(x)\ln(|x|) - f(x)\ln(\varepsilon). \tag{20.29}$$

Hence, the scaled function s corrects $f(x)\ln(|x|)$, but also introduces the new error $-f(x)\ln(\varepsilon)$ on the boundary Γ_ε. Fortunately, this term can be corrected by another function $s' \in H^1(\mathsf{D})$ with boundary values $s'|_\Gamma = f(x - x_0)$ scaled by the factor $\varepsilon^{-r}\ln(\varepsilon)$:

$$\varepsilon^{-r} s \circ T_\varepsilon|_{\Gamma_\varepsilon} + \ln(\varepsilon)\varepsilon^{-r} s' \circ T_\varepsilon|_{\Gamma_\varepsilon} = -f(x)\ln(|x|).$$

In this way we can correct every function $A_i^{(k)}, B_i^{(k)}$ appearing in (20.13), (20.14). Summarising, for $d = 2$, we need to introduce one corrector equation for each function $B_0^{(k)}, B_1^{(k)}, B_2^{(k)}$ and two corrector equations for each function $\ln(|\cdot|)A_0^{(k)}(\cdot), \ln(|\cdot|)A_1^{(k)}(\cdot), \ln(|\cdot|)A_2^{(k)}(\cdot)$, which makes a total of 9 corrector equations. This motivates the following definition.

Definition 20.7. For $k \geq 2$ and $d = 2$ let

$$L_\varepsilon^{(k)} := s_1^{(k)} + \ln(\varepsilon)s_2^{(k)} + \varepsilon s_3^{(k)} + \varepsilon\ln(\varepsilon)s_4^{(k)} + \varepsilon^2 s_5^{(k)} + \varepsilon^2\ln(\varepsilon)s_6^{(k)} + s_7^{(k)} + \varepsilon s_8^{(k)} + \varepsilon^2 s_9^{(k)}, \tag{20.30}$$

where $s_i^{(k)} \in H^1(\mathsf{D})$, $i \in \{1,\dots,9\}$ are the unique solutions to the following set of equations:

(i) corrector equations for $A_2^{(k)}(x)\ln(|x|)$

▹ $s_1^{(k)} = -A_2^{(k)}(x-x_0)\ln(|x-x_0|)$ on Γ and

$$\int_{\mathrm{D}} \nabla s_1^{(k)} \cdot \nabla \varphi \, dx = \int_{\Gamma^N} \partial_\nu \left(A_2^{(k)}(x-x_0)\ln(|x-x_0|) \right) \varphi \, dS \quad \text{for all } \varphi \in H^1_\Gamma(\mathrm{D}). \tag{20.31}$$

▹ $s_2^{(k)} = A_2^{(k)}(x-x_0)$ on Γ and

$$\int_{\mathrm{D}} \nabla s_2^{(k)} \cdot \nabla \varphi \, dx = -\int_{\Gamma^N} \partial_\nu \left(A_2^{(k)}(x-x_0) \right) \varphi \, dS \quad \text{for all } \varphi \in H^1_\Gamma(\mathrm{D}). \tag{20.32}$$

(ii) corrector equations for $A_1^{(k)}(x)\ln(|x|)$

▹ $s_3^{(k)} = -A_1^{(k)}(x-x_0)\ln(|x-x_0|)$ on Γ and

$$\int_{\mathrm{D}} \nabla s_3^{(k)} \cdot \nabla \varphi \, dx = \int_{\Gamma^N} \partial_\nu \left(A_1^{(k)}(x-x_0)\ln(|x-x_0|) \right) \varphi \, dS \quad \text{for all } \varphi \in H^1_\Gamma(\mathrm{D}). \tag{20.33}$$

▹ $s_4^{(k)} = A_1^{(k)}(x-x_0)$ on Γ and

$$\int_{\mathrm{D}} \nabla s_4^{(k)} \cdot \nabla \varphi \, dx = -\int_{\Gamma^N} \partial_\nu \left(A_1^{(k)}(x-x_0) \right) \varphi \, dS \quad \text{for all } \varphi \in H^1_\Gamma(\mathrm{D}). \tag{20.34}$$

(iii) corrector equations for $A_0^{(k)}(x)\ln(|x|)$

▹ $s_5^{(k)} = -A_0^{(k)}(x-x_0)\ln(|x-x_0|)$ on Γ and

$$\int_{\mathrm{D}} \nabla s_5^{(k)} \cdot \nabla \varphi \, dx = \int_{\Gamma^N} \partial_\nu \left(A_0^{(k)}(x-x_0)\ln(|x-x_0|) \right) \varphi \, dS \quad \text{for all } \varphi \in H^1_\Gamma(\mathrm{D}). \tag{20.35}$$

▹ $s_6^{(k)} = A_0^{(k)}(x-x_0)$ on Γ and

$$\int_{\mathrm{D}} \nabla s_6^{(k)} \cdot \nabla \varphi \, dx = -\int_{\Gamma^N} \partial_\nu \left(A_0^{(k)}(x-x_0) \right) \varphi \, dS \quad \text{for all } \varphi \in H^1_\Gamma(\mathrm{D}). \tag{20.36}$$

(iv) corrector equation for $B_2^{(k)}(x)$

▹ $s_7^{(k)} = -B_2^{(k)}(x-x_0)$ on Γ and

$$\int_{\mathrm{D}} \nabla s_7^{(k)} \cdot \nabla \varphi \, dx = \int_{\Gamma^N} \partial_\nu \left(B_2^{(k)}(x-x_0) \right) \varphi \, dS \quad \text{for all } \varphi \in H^1_\Gamma(\mathrm{D}). \tag{20.37}$$

(v) corrector equation for $B_1^{(k)}(x)$

▷ $s_8^{(k)} = -B_1^{(k)}(x - x_0)$ on Γ and

$$\int_{\mathsf{D}} \nabla s_8^{(k)} \cdot \nabla \varphi \, dx = \int_{\Gamma^N} \partial_\nu \left(B_1^{(k)}(x - x_0) \right) \varphi \, dS \quad \text{for all } \varphi \in H^1_\Gamma(\mathsf{D}). \tag{20.38}$$

(vi) corrector equation for $B_0^{(k)}(x)$

▷ $s_9^{(k)} = -B_0^{(k)}(x - x_0)$ on Γ and

$$\int_{\mathsf{D}} \nabla s_9^{(k)} \cdot \nabla \varphi \, dx = \int_{\Gamma^N} \partial_\nu \left(B_0^{(k)}(x - x_0) \right) \varphi \, dS \quad \text{for all } \varphi \in H^1_\Gamma(\mathsf{D}). \tag{20.39}$$

Since the three leading terms of $Q^{(k)}$, $k \geq 2$ in dimension $d = 3$ are homogeneous functions, we deduce that each one can be treated by a single corrector equation. This makes a total of three corrector equations, which we introduce in the following definition.

Definition 20.8. For $k \geq 2$ and $d = 3$ let

$$L_\varepsilon^{(k)} := s_1^{(k)} + \varepsilon s_2^{(k)} + \varepsilon^2 s_3^{(k)}, \tag{20.40}$$

where $s_i^{(k)} \in H^1(\mathsf{D})$, $i \in \{1, 2, 3\}$ are the unique solutions to the following set of equations:

(i) corrector equation for $A_1^{(k)}(x)$

▷ $s_1^{(k)} = -A_1^{(k)}(x - x_0)$ on Γ and

$$\int_{\mathsf{D}} \nabla s_1^{(k)} \cdot \nabla \varphi \, dx = \int_{\Gamma^N} \partial_\nu A_1^{(k)}(x - x_0) \varphi \, dS \quad \text{for all } \varphi \in H^1_\Gamma(\mathsf{D}). \tag{20.41}$$

(ii) corrector equation for $A_0^{(k)}(x)$

▷ $s_2^{(k)} = -A_0^{(k)}(x - x_0)$ on Γ and

$$\int_{\mathsf{D}} \nabla s_2^{(k)} \cdot \nabla \varphi \, dx = \int_{\Gamma^N} \partial_\nu A_0^{(k)}(x - x_0) \varphi \, dS \quad \text{for all } \varphi \in H^1_\Gamma(\mathsf{D}). \tag{20.42}$$

(iii) corrector equation for $A_{-1}^{(k)}(x)$

▷ $s_3^{(k)} = -A_{-1}^{(k)}(x - x_0)$ on Γ and

$$\int_{\mathsf{D}} \nabla s_3^{(k)} \cdot \nabla \varphi \, dx = \int_{\Gamma^N} \partial_\nu A_{-1}^{(k)}(x - x_0) \varphi \, dS \quad \text{for all } \varphi \in H^1_\Gamma(\mathsf{D}). \tag{20.43}$$

Remark 20.9. Note that contrary to the asymptotic expansion of the state variable, where $u^{(2)} \neq 0$, the corresponding corrector $q^{(2)}$ vanishes in our expansion (cf. Definition 20.6). This is possible, since the additional corrector $L_\varepsilon^{(2)}$ addresses the leading order terms of $Q^{(2)}$. This behaviour can also be observed for $k \geq 3$, where the correctors $L_\varepsilon^{(k)}$ allow a shift in the sum of the leading terms $S_\ell^{(k)}$ (cf. (20.25) vs. (17.25)).

Lemma 20.10. Let $k \geq 2$ and $\varepsilon > 0$ small. Then there holds

$$\varepsilon^2 Q^{(k)} + \varepsilon^{d-2} L_\varepsilon^{(k)} \circ T_\varepsilon = \varepsilon^2 \left(\sum_{\ell=1}^{N} S_\ell^{(k)} + \mathcal{O}(|x|^{-(d-2+N+1)}) \right) \quad \text{on } \Gamma_\varepsilon, \tag{20.44}$$

for $N \geq 1$.

Proof. We restrict our proof to dimension $d = 2$. The three dimensional case follows from similar arguments. Since $A_i^{(k)}, B_i^{(k)}$, $i \in \{0,1,2\}$ are homogeneous of degree i, Definition 20.7 entails that

$$L_\varepsilon^{(k)} \circ T_\varepsilon = -\varepsilon^2 \left(A_2^{(k)}(x)\ln(|x|) + A_1^{(k)}(x)\ln(|x|) + A_0^{(k)}(x)\ln(|x|) + B_2^{(k)}(x) + B_1^{(k)}(x) + B_0^{(k)}(x) \right), \tag{20.45}$$

on Γ_ε. Hence, the asymptotic behaviour (20.13) of $Q^{(k)}$ yields the desired result. □

As a result of this pointwise behaviour of $Q^{(k)}$, we get the following boundary estimates in the L_2 norm and $H^{\frac{1}{2}}$ semi-norm:

Corollary 20.11. For $k \geq 2$ and $d = 2$ we have

$$\varepsilon^{\frac{1}{2}} \|Q_\varepsilon^{(k)} - \varepsilon^2 Q^{(k)} - \varepsilon^{d-2} L_\varepsilon^{(k)} \circ T_\varepsilon - \varepsilon^d q^{(k)} \circ T_\varepsilon - \varepsilon^{d-2} m^{(k)} \circ T_\varepsilon - \ln(\varepsilon) n^{(k)} \circ T_\varepsilon\|_{L_2(\Gamma_\varepsilon)} \leq C\varepsilon^{\frac{d}{2}+2}, \tag{20.46}$$

$$|Q_\varepsilon^{(k)} - \varepsilon^2 Q^{(k)} - \varepsilon^{d-2} L_\varepsilon^{(k)} \circ T_\varepsilon - \varepsilon^d q^{(k)} \circ T_\varepsilon - \varepsilon^{d-2} m^{(k)} \circ T_\varepsilon - \ln(\varepsilon) n^{(k)} \circ T_\varepsilon|_{H^{\frac{1}{2}}(\Gamma_\varepsilon)} \leq C\varepsilon^{\frac{d}{2}+2}, \tag{20.47}$$

$$\|\varepsilon^2 \partial_\nu Q^{(k)} + \varepsilon^{d-2} \partial_\nu L_\varepsilon^{(k)} \circ T_\varepsilon\|_{L_2(\Gamma_\varepsilon^N)} \leq C\varepsilon^{\frac{d+1}{2}+2}. \tag{20.48}$$

Similarly, we have for $k \geq 2$ and $d = 3$

$$\varepsilon^{\frac{1}{2}} \|Q_\varepsilon^{(k)} - \varepsilon^2 Q^{(k)} - \varepsilon^{d-2} L_\varepsilon^{(k)} \circ T_\varepsilon - \varepsilon^d q^{(k)} \circ T_\varepsilon - \varepsilon^{d-2} m^{(k)} \circ T_\varepsilon\|_{L_2(\Gamma_\varepsilon)} \leq C\varepsilon^{\frac{d}{2}+2}, \tag{20.49}$$

$$|Q_\varepsilon^{(k)} - \varepsilon^2 Q^{(k)} - \varepsilon^{d-2} L_\varepsilon^{(k)} \circ T_\varepsilon - \varepsilon^d q^{(k)} \circ T_\varepsilon - \varepsilon^{d-2} m^{(k)} \circ T_\varepsilon|_{H^{\frac{1}{2}}(\Gamma_\varepsilon)} \leq C\varepsilon^{\frac{d}{2}+2}, \tag{20.50}$$

$$\|\varepsilon^2 \partial_\nu Q^{(k)} + \varepsilon^{d-2} \partial_\nu L_\varepsilon^{(k)} \circ T_\varepsilon\|_{L_2(\Gamma_\varepsilon^N)} \leq C\varepsilon^{\frac{d+1}{2}+2}. \tag{20.51}$$

Proof. First, we observe that $m^{(k)} = n^{(k)} = 0$ on Γ. Hence, employing the recursion in Lemma 20.10 and (20.25), we can follow the steps of the proof of Corollary 17.17 to obtain the desired boundary estimates. The increased order of ε^2 stems from the occurrence of the corresponding factor in front of each contributing corrector in the asymptotic expansion. □

We have now gathered all ingredients to prove the following main result establishing the remainder estimate for the asymptotic behaviour of $Q_\varepsilon^{(k)}$.

Theorem 20.12. Let $k \geq 1$, $\varepsilon > 0$ small and $\alpha \in (0,1)$. There is a constant $C > 0$, such that

$$\|Q_\varepsilon^{(k)} - \varepsilon^2 Q^{(k)} - \varepsilon^{d-2} L_\varepsilon^{(k)} \circ T_\varepsilon - \varepsilon^d q^{(k)} \circ T_\varepsilon - \varepsilon^{d-2} m^{(k)} \circ T_\varepsilon - \ln(\varepsilon) n^{(k)} \circ T_\varepsilon\|_\varepsilon \leq C\varepsilon^{1-\alpha} \quad \text{for } d = 2, \tag{20.52}$$

$$\|Q_\varepsilon^{(k)} - \varepsilon^2 Q^{(k)} - \varepsilon^{d-2} L_\varepsilon^{(k)} \circ T_\varepsilon - \varepsilon^d q^{(k)} \circ T_\varepsilon - \varepsilon^{d-2} m^{(k)} \circ T_\varepsilon\|_\varepsilon \leq C\varepsilon \quad \text{for } d = 3, \tag{20.53}$$

where we further introduce $L_\varepsilon^{(1)} \equiv 0$.

Proof. We shall only give a sketch of the proof for $d = 2$, as the idea is similar to the proof of Theorem 17.18. At first, we note that there holds

$$\int_{\mathsf{D}_\varepsilon} \nabla Q_\varepsilon^{(1)} \cdot \nabla \varphi \, dx = -\varepsilon^2 \alpha_1 \int_{\mathsf{D}_\varepsilon} U_\varepsilon^{(1)} \varphi \, dx \quad \text{for all } \varphi \in H^1_{\Gamma_\varepsilon}(\mathsf{D}_\varepsilon). \tag{20.54}$$

Thus, an application of Hölder's inequality and the estimate $\|U_\varepsilon^{(1)}\|_\varepsilon \le C\varepsilon^{1-\alpha}$ yield

$$\|Q_\varepsilon^{(1)}\|_\varepsilon \le C\varepsilon^{1-\alpha}, \tag{20.55}$$

for a positive constant $C > 0$. Here, we additionally used that $Q_\varepsilon^{(1)}$ has homogeneous boundary values on Γ_ε. Next, we seek a governing equation for $V_\varepsilon^{(2)} := Q_\varepsilon^{(2)} - \varepsilon^2 Q^{(2)} - \varepsilon^{d-2} L_\varepsilon^{(2)} \circ T_\varepsilon - \varepsilon^{d-2} m^{(2)} \circ T_\varepsilon - \ln(\varepsilon) n^{(2)} \circ T_\varepsilon$. Reformulating the respective equations on the scaled domain D_ε entails

$$\int_{\mathsf{D}_\varepsilon} \nabla V_\varepsilon^{(2)} \cdot \nabla \varphi \, dx = -\varepsilon^2 \alpha_1 \int_{\mathsf{D}_\varepsilon} \left(U_\varepsilon^{(2)} - U^{(2)} - \varepsilon^{d-2} u^{(2)} \circ T_\varepsilon - \ln(\varepsilon) b^{(2)} \right) \varphi \, dx \tag{20.56}$$

$$+ \int_{\Gamma_\varepsilon^N} \partial_\nu \left(\varepsilon^2 Q^{(2)} + \varepsilon^{d-2} L^{(2)} \circ T_\varepsilon \right) \varphi \, dS, \tag{20.57}$$

for all $\varphi \in H^1_{\Gamma_\varepsilon}(\mathsf{D}_\varepsilon)$. Now we can deduce from Lemma 17.16, Corollary 20.11 and Theorem 17.18 that there is a positive constant $C > 0$, such that

$$\|V_\varepsilon^{(2)}\|_\varepsilon \le C\varepsilon^{1-\alpha}, \tag{20.58}$$

which shows the estimate (20.52) for $k = 2$. Now successively dividing by $\varepsilon > 0$ and subtracting the respective terms, one can check that the estimate holds for $k \ge 3$. □

21 Complete topological expansion - L_2 tracking-type

In this section we compute the n-th topological derivative of the L_2 tracking-type part of the cost function defined in (18.1). That is, we are deriving an asymptotic expansion of the form

$$\mathscr{J}_1(\Omega_\varepsilon) = \mathscr{J}_1(\Omega) + \sum_{k=1}^{n} \ell_k(\varepsilon) d^k \mathscr{J}_1(\Omega, \omega)(x_0) + o(\ell_n(\varepsilon)), \tag{21.1}$$

with $\mathscr{J}_1(\Omega)$ defined in (20.1). Here $d^k \mathscr{J}_1(\Omega, \omega)(x_0)$ denotes the k-th topological derivative with respect to the initial domain Ω and perturbation shape ω at the point x_0 and $\ell_k : \mathbf{R}^+ \to \mathbf{R}^+$ are continuous functions satisfying

$$\lim_{\varepsilon \searrow 0} \ell_k(\varepsilon) = 0 \quad \text{and} \quad \lim_{\varepsilon \searrow 0} \frac{\ell_{k+1}(\varepsilon)}{\ell_k(\varepsilon)} = 0 \quad \text{for } k \ge 1.$$

As we will see, the terms of logarithmic order, which occur in the asymptotic expansion of the adjoint state variable in $d = 2$, lead to a differing topological derivative compared to dimension $d = 3$. Thus, we will distinguish between both scenarios and derive a general formula of the topological derivative for both cases separately.

21.1 General formula for higher order topological derivatives in dimension two

In this section we restrict ourselves to dimension $d = 2$ and present the following result:

Theorem 21.1. Let $\ell_1(\varepsilon) := |\omega_\varepsilon|$, $\ell_{2n}(\varepsilon) = \varepsilon^n \ln(\varepsilon)|\omega_\varepsilon|$ and $\ell_{2n+1}(\varepsilon) = \varepsilon^n|\omega_\varepsilon|$, for $n \geq 1$. The topological derivative of $\mathscr{J}_2$ at $x_0 \in \mathsf{D} \setminus \bar{\Omega}$ and $\omega \subset \mathbf{R}^2$ with $0 \in \omega$ in dimension $d = 2$ is given by

$$d^1\mathscr{J}_1(\Omega,\omega)(x_0) = \big((f_2 - f_1)q_0\big)(x_0), \quad d^2\mathscr{J}_1(\Omega,\omega)(x_0) = 0, \tag{21.2}$$

$$\begin{aligned}
d^{2n+1}\mathscr{J}_1(\Omega,\omega)(x_0) = &\frac{1}{|\omega|}\frac{1}{n!}\int_\omega \nabla^n\big((f_2-f_1)p_0\big)(x_0)[x]^n\,dx \\
&+ \frac{1}{|\omega|}\left(\sum_{j=0}^{n-4}\frac{1}{j!}\int_\omega \nabla^j\big(f_2-f_1\big)(x_0)[x]^j Q^{(n-2-j)}(x)\,dx\right) \\
&+ \frac{1}{|\omega|}\left(\sum_{j=0}^{n-2}\frac{1}{j!}\int_\omega \nabla^j\big((f_2-f_1)s_1^{(n-j)}\big)(x_0)[x]^j\,dx\right) \\
&+ \frac{1}{|\omega|}\left(\sum_{j=0}^{n-3}\frac{1}{j!}\int_\omega \nabla^j\big((f_2-f_1)s_3^{(n-1-j)}\big)(x_0)[x]^j\,dx\right) \\
&+ \frac{1}{|\omega|}\left(\sum_{j=0}^{n-4}\frac{1}{j!}\int_\omega \nabla^j\big((f_2-f_1)s_5^{(n-2-j)}\big)(x_0)[x]^j\,dx\right) \\
&+ \frac{1}{|\omega|}\left(\sum_{j=0}^{n-2}\frac{1}{j!}\int_\omega \nabla^j\big((f_2-f_1)s_7^{(n-j)}\big)(x_0)[x]^j\,dx\right) \\
&+ \frac{1}{|\omega|}\left(\sum_{j=0}^{n-3}\frac{1}{j!}\int_\omega \nabla^j\big((f_2-f_1)s_8^{(n-1-j)}\big)(x_0)[x]^j\,dx\right) \\
&+ \frac{1}{|\omega|}\left(\sum_{j=0}^{n-4}\frac{1}{j!}\int_\omega \nabla^j\big((f_2-f_1)s_9^{(n-2-j)}\big)(x_0)[x]^j\,dx\right) \\
&+ \frac{1}{|\omega|}\left(\sum_{j=0}^{n-5}\frac{1}{j!}\int_\omega \nabla^j\big((f_2-f_1)q^{(n-2-j)}\big)(x_0)[x]^j\,dx\right) \\
&+ \frac{1}{|\omega|}\left(\sum_{j=0}^{n-2}\frac{1}{j!}\int_\omega \nabla^j\big((f_2-f_1)m^{(n-j)}\big)(x_0)[x]^j\,dx\right),
\end{aligned} \tag{21.3}$$

$$\begin{aligned}d^{2n}\mathscr{J}_1(\Omega,\omega)(x_0) = &\frac{1}{|\omega|}\left(\sum_{j=0}^{n-2}\frac{1}{j!}\int_\omega \nabla^j\big((f_2-f_1)s_2^{(n-j)}\big)(x_0)[x]^j\,dx\right)\\ &+\frac{1}{|\omega|}\left(\sum_{j=0}^{n-3}\frac{1}{j!}\int_\omega \nabla^j\big((f_2-f_1)s_4^{(n-1-j)}\big)(x_0)[x]^j\,dx\right)\\ &+\frac{1}{|\omega|}\left(\sum_{j=0}^{n-4}\frac{1}{j!}\int_\omega \nabla^j\big((f_2-f_1)s_6^{(n-2-j)}\big)(x_0)[x]^j\,dx\right)\\ &+\frac{1}{|\omega|}\left(\sum_{j=0}^{n-2}\frac{1}{j!}\int_\omega \nabla^j\big((f_2-f_1)n^{(n-j)}\big)(x_0)[x]^j\,dx\right),\end{aligned} \tag{21.4}$$

for $n \geq 1$, where for $\ell \geq 1$, $i \in \{1,...,9\}$, $Q^{(\ell)}$ are defined in Lemma 20.3, $s_i^{(\ell)}$ in Definition 20.7 and $q^{(\ell)}, m^{(\ell)}, n^{(\ell)}$ are defined in (20.26), (20.27) and (20.28), respectively.

Proof. We follow a similar approach to the proof of Theorem 19.2. Therefore, recall the Lagrangian introduced in (20.3). Let $\varepsilon \geq 0$. We first observe by testing (20.4) with $\varphi = u_\varepsilon - u_0$ that

$$\mathscr{J}_1(\Omega_\varepsilon) = \mathscr{L}(\varepsilon, u_\varepsilon, q_\varepsilon) = \mathscr{L}(\varepsilon, u_0, q_\varepsilon), \tag{21.5}$$

so that the cost function can be written only in terms of the averaged adjoint variable. Thus, we have

$$\mathscr{J}_1(\Omega_\varepsilon) - \mathscr{J}_1(\Omega) = \mathscr{L}(\varepsilon, u_0, q_\varepsilon) - \mathscr{L}(\varepsilon, u_0, q_0) + \mathscr{L}(\varepsilon, u_0, q_0) - \mathscr{L}(0, u_0, q_0). \tag{21.6}$$

Employing Theorem 20.12, we now derive an expansion for both differences on the right hand side.

Expansion of $\mathscr{L}(\varepsilon, u_0, q_0) - \mathscr{L}(0, u_0, q_0)$: The expansion of this difference is obtained by a Taylor expansion as shown in (19.8)-(19.10):

$$\frac{\mathscr{L}(\varepsilon, u_0, q_0) - \mathscr{L}(0, u_0, q_0)}{|\omega_\varepsilon|} = \hat{q}_0(x_0) + \sum_{n=1}^{N} \varepsilon^n \frac{1}{|\omega|}\frac{1}{n!}\int_\omega \nabla^n \hat{q}_0(x_0)[x]^n\,dx + \mathscr{O}(\varepsilon^{N+1}), \quad N \geq 1, \tag{21.7}$$

where $\hat{q}_0 = (f_2 - f_1)q_0$.

Expansion of $\mathscr{L}(\varepsilon, u_0, q_\varepsilon) - \mathscr{L}(\varepsilon, u_0, q_0)$: We proceed as in (19.11) and obtain with the definition $\varepsilon Q_\varepsilon^{(1)}(x) = (q_\varepsilon - q_0) \circ T_\varepsilon$ and a change of variables:

$$\mathscr{L}(\varepsilon, u_0, q_\varepsilon) - \mathscr{L}(\varepsilon, u_0, q_0) = \varepsilon^d \int_\omega (f_2 - f_1) \circ T_\varepsilon \varepsilon Q_\varepsilon^{(1)}\,dx. \tag{21.8}$$

Substituting $\varepsilon Q_\varepsilon^{(1)}$ by the recursion formula of Lemma 20.2 leads to

$$\int_\omega (f_2 - f_1)\circ T_\varepsilon \varepsilon Q_\varepsilon^{(1)}\,dx = \sum_{n=1}^N \int_\omega (f_2-f_1)\circ T_\varepsilon \varepsilon^{n+2} Q^{(n)}\,dx \tag{21.9}$$

$$+\sum_{n=1}^N \int_\omega (f_2-f_1)\circ T_\varepsilon \varepsilon^n L_\varepsilon^{(n)}\circ T_\varepsilon\,dx \tag{21.10}$$

$$+\sum_{n=1}^N \int_\omega (f_2-f_1)\circ T_\varepsilon \varepsilon^{n+2} q^{(n)}\circ T_\varepsilon\,dx \tag{21.11}$$

$$+\sum_{n=1}^N \int_\omega (f_2-f_1)\circ T_\varepsilon \varepsilon^n m^{(n)}\circ T_\varepsilon\,dx \tag{21.12}$$

$$+\sum_{n=1}^N \int_\omega (f_2-f_1)\circ T_\varepsilon \varepsilon^n \ln(\varepsilon) n^{(n)}\circ T_\varepsilon\,dx \tag{21.13}$$

$$+\int_\omega (f_2-f_1)\circ T_\varepsilon \varepsilon^{N+1} Q_\varepsilon^{(N+1)}\,dx. \tag{21.14}$$

Now we can expand all six terms:

- First term (21.9): We use a Taylor's expansion to write:

$$(f_2-f_1)\circ T_\varepsilon = \sum_{j=0}^N \varepsilon^j a_j(x) + \mathcal{O}(\varepsilon^{N+1};x), \qquad a_j(x) := \frac{\nabla^j\big(f_2-f_1\big)(x_0)[x]^j}{j!}. \tag{21.15}$$

  For the proof we let $Q^{(0)} := 0$, and $Q^{(j)} := 0$ and $a_j := 0$ for all $j > N$. Then, by Lemma 19.1 we have

$$(f_2-f_1)\circ T_\varepsilon \left(\sum_{n=1}^N \varepsilon^{n+2}Q^{(n)}\right) = \sum_{n=0}^{N-2} \varepsilon^{n+2}\left(\sum_{j=0}^n a_j(x)Q^{(n-j)}(x)\right) + \mathcal{O}(\varepsilon^{N+1};x), \tag{21.16}$$

  and therefore

$$\sum_{n=1}^N \int_\omega (f_2-f_1)\,\varepsilon^{n+2}Q^{(n)}\,dx = \sum_{n=4}^N \varepsilon^n \int_\omega \left(\sum_{j=0}^{n-4} a_j(x)Q^{(n-2-j)}(x)\right)dx + \mathcal{O}(\varepsilon^{N+1}), \tag{21.17}$$

  where we took into account $Q^{(0)} = Q^{(1)} = 0$.

- Second term (21.10): In order to derive the correct formula, we first need to split the corrector $L_\varepsilon^{(\ell)}$ into its components. That is, we have

$$L_\varepsilon^{(k)} := s_1^{(\ell)} + \ln(\varepsilon)s_2^{(\ell)} + \varepsilon s_3^{(\ell)} + \varepsilon\ln(\varepsilon)s_4^{(\ell)} + \varepsilon^2 s_5^{(\ell)} + \varepsilon^2\ln(\varepsilon)s_6^{(\ell)} + s_7^{(\ell)} + \varepsilon s_8^{(\ell)} + \varepsilon^2 s_9^{(\ell)}. \tag{21.18}$$

  Next, we use Taylor's formula to expand the functions $\varepsilon \mapsto \hat{s}_\ell^{(n)}\circ T_\varepsilon$ with $\hat{s}_\ell^{(n)} := \big((f_2-f_1)s_\ell^{(n)}\big)$, $n \geq 1$ and $\ell \in \{1,\dots,9\}$ to deduce

$$\hat{s}_\ell^{(n)}\circ T_\varepsilon(x) = \sum_{j=0}^N \varepsilon^j b_{\ell,j}^{(n)}(x) + \mathcal{O}(\varepsilon^{N+1};x), \qquad b_{\ell,j}^{(n)}(x) := \frac{\nabla^j \hat{s}_\ell^{(n)}(x_0)[x]^j}{j!}. \tag{21.19}$$

Hence, a similar computation to the previous one yields

$$\begin{aligned}\sum_{n=1}^{N}\int_\omega \varepsilon^n\left((f_2-f_1)s_1^{(n)}\right)\circ T_\varepsilon(x)\,dx &= \sum_{n=1}^{N}\varepsilon^n\left(\sum_{j=0}^{N}\varepsilon^j\int_\omega b_{1,j}^{(n)}(x)\,dx\right)+\mathcal{O}(\varepsilon^{N+1}) \\ &= \sum_{n=2}^{N}\varepsilon^n\left(\sum_{j=0}^{n-2}\int_\omega b_{1,j}^{(n-j)}(x)\,dx\right)+\mathcal{O}(\varepsilon^{N+1}),\end{aligned} \tag{21.20}$$

where we took into account that $s_1^{(1)}=0$ and therefore $b_{1,j}^{(1)}=0$ for $j\geq 0$ as well. With the same arguments we get

$$\sum_{n=1}^{N}\int_\omega \ln(\varepsilon)\varepsilon^n\left((f_2-f_1)s_2^{(n)}\right)\circ T_\varepsilon\,dx = \sum_{n=2}^{N}\ln(\varepsilon)\varepsilon^n\left(\sum_{j=0}^{n-2}\int_\omega b_{2,j}^{(n-j)}(x)\,dx\right)+o(\varepsilon^N), \tag{21.21}$$

$$\sum_{n=1}^{N}\int_\omega \varepsilon^{n+1}\left((f_2-f_1)s_3^{(n)}\right)\circ T_\varepsilon\,dx = \sum_{n=3}^{N}\varepsilon^n\left(\sum_{j=0}^{n-3}\int_\omega b_{3,j}^{(n-1-j)}(x)\,dx\right)+\mathcal{O}(\varepsilon^{N+1}), \tag{21.22}$$

$$\sum_{n=1}^{N}\int_\omega \ln(\varepsilon)\varepsilon^{n+1}\left((f_2-f_1)s_4^{(n)}\right)\circ T_\varepsilon\,dx = \sum_{n=3}^{N}\ln(\varepsilon)\varepsilon^n\left(\sum_{j=0}^{n-3}\int_\omega b_{4,j}^{(n-1-j)}(x)\,dx\right)+o(\varepsilon^N), \tag{21.23}$$

$$\sum_{n=1}^{N}\int_\omega \varepsilon^{n+2}\left((f_2-f_1)s_5^{(n)}\right)\circ T_\varepsilon\,dx = \sum_{n=4}^{N}\varepsilon^n\left(\sum_{j=0}^{n-4}\int_\omega b_{5,j}^{(n-2-j)}(x)\,dx\right)+\mathcal{O}(\varepsilon^{N+1}), \tag{21.24}$$

$$\sum_{n=1}^{N}\int_\omega \ln(\varepsilon)\varepsilon^{n+2}\left((f_2-f_1)s_6^{(n)}\right)\circ T_\varepsilon\,dx = \sum_{n=4}^{N}\ln(\varepsilon)\varepsilon^n\left(\sum_{j=0}^{n-4}\int_\omega b_{6,j}^{(n-2-j)}(x)\,dx\right)+o(\varepsilon^N), \tag{21.25}$$

$$\sum_{n=1}^{N}\int_\omega \varepsilon^{n}\left((f_2-f_1)s_7^{(n)}\right)\circ T_\varepsilon\,dx = \sum_{n=2}^{N}\varepsilon^n\left(\sum_{j=0}^{n-2}\int_\omega b_{7,j}^{(n-j)}(x)\,dx\right)+\mathcal{O}(\varepsilon^{N+1}), \tag{21.26}$$

$$\sum_{n=1}^{N}\int_\omega \varepsilon^{n+1}\left((f_2-f_1)s_8^{(n)}\right)\circ T_\varepsilon\,dx = \sum_{n=3}^{N}\varepsilon^n\left(\sum_{j=0}^{n-3}\int_\omega b_{8,j}^{(n-1-j)}(x)\,dx\right)+\mathcal{O}(\varepsilon^{N+1}), \tag{21.27}$$

$$\sum_{n=1}^{N}\int_\omega \varepsilon^{n+2}\left((f_2-f_1)s_9^{(n)}\right)\circ T_\varepsilon\,dx = \sum_{n=4}^{N}\varepsilon^n\left(\sum_{j=0}^{n-4}\int_\omega b_{9,j}^{(n-2-j)}(x)\,dx\right)+\mathcal{O}(\varepsilon^{N+1}). \tag{21.28}$$

- Third term (21.11): Employing a Taylor's expansion of $\varepsilon\mapsto\hat{q}^{(n)}\circ T_\varepsilon$ at $\varepsilon=0$ where we denote $\hat{q}^{(n)}:=(f_2-f_1)q^{(n)}$ entails

$$\hat{q}^{(n)}\circ T_\varepsilon(x)=\sum_{j=0}^{N}\varepsilon^j\hat{q}_j^{(n)}(x)+\mathcal{O}(\varepsilon^{N+1};x),\qquad \hat{q}_j^{(n)}(x):=\frac{\nabla^j\hat{q}^{(n)}(x_0)[x]^j}{j!}, \tag{21.29}$$

for $n \geq 1$. Hence, one analogously computes

$$\sum_{n=1}^{N} \int_{\omega} \varepsilon^{n+2} \left((f_2 - f_1) q^{(n)} \right) \circ T_\varepsilon \, dx = \sum_{n=5}^{N} \varepsilon^n \left(\sum_{j=0}^{n-5} \int_{\omega} \hat{q}_j^{(n-2-j)}(x) \, dx \right) + \mathcal{O}(\varepsilon^{N+1}), \tag{21.30}$$

where we took into account that $q^{(1)} = q^{(2)} = 0$, which explains the index shift.

- Fourth term (21.12): Similarly, the expansion of $\varepsilon \mapsto \hat{m}^{(n)} \circ T_\varepsilon$ at $\varepsilon = 0$ with $\hat{m}^{(n)} := (f_2 - f_1) m^{(n)}$ reads

$$\hat{m}^{(n)} \circ T_\varepsilon(x) = \sum_{j=0}^{N} \varepsilon^j \hat{m}_j^{(n)}(x) + \mathcal{O}(\varepsilon^{N+1}; x), \qquad \hat{m}_j^{(n)}(x) := \frac{\nabla^j \hat{m}^{(n)}(x_0)[x]^j}{j!}, \tag{21.31}$$

for $n \geq 1$ and yields

$$\sum_{n=1}^{N} \int_{\omega} \varepsilon^n \left((f_2 - f_1) m^{(n)} \right) \circ T_\varepsilon \, dx = \sum_{n=2}^{N} \varepsilon^n \left(\sum_{j=0}^{n-2} \int_{\omega} \hat{m}_j^{(n-j)}(x) \, dx \right) + \mathcal{O}(\varepsilon^{N+1}). \tag{21.32}$$

- Fifth term (21.13): Again, we have by a Taylor's expansion of $\varepsilon \mapsto \hat{n}^{(n)} \circ T_\varepsilon$ at $\varepsilon = 0$ with the notation $\hat{n}^{(n)} := (f_2 - f_1) n^{(n)}$ that

$$\hat{n}^{(n)} \circ T_\varepsilon(x) = \sum_{j=0}^{N} \varepsilon^j \hat{n}_j^{(n)}(x) + \mathcal{O}(\varepsilon^{N+1}; x), \qquad \hat{n}_j^{(n)}(x) := \frac{\nabla^j \hat{n}^{(n)}(x_0)[x]^j}{j!}, \tag{21.33}$$

for $n \geq 1$ and therefore it follows that

$$\sum_{n=1}^{N} \int_{\omega} \ln(\varepsilon) \varepsilon^n \left((f_2 - f_1) n^{(n)} \right) \circ T_\varepsilon \, dx = \sum_{n=2}^{N} \ln(\varepsilon) \varepsilon^n \left(\sum_{j=0}^{n-2} \int_{\omega} \hat{n}_j^{(n-j)}(x) \, dx \right) + o(\varepsilon^N). \tag{21.34}$$

- Sixth term (21.14): Applying Lemma 11.5 item (iii) to the last term and using the asymptotics derived in Theorem 20.12, gives

$$\left| \int_{\omega} (f_1 - f_2) \circ T_\varepsilon \varepsilon^{N+1} Q_\varepsilon^{(N+1)} \, dx \right| \leq C \varepsilon^{N-\alpha} \| \varepsilon Q_\varepsilon^{(N+1)} \|_\varepsilon \leq C \varepsilon^{N+1-2\alpha}, \tag{21.35}$$

for a constant $C > 0$ and $\alpha \in (0, 1)$ sufficiently small.

Now combining (21.17) - (21.35) shows the formula given in Theorem 21.1. □

We finish the section by stating the first five topological derivatives.

Corollary 21.2. The first five terms of the topological expansion in dimension $d = 2$ read:

$$\begin{aligned}
d^1\mathscr{J}_1(\Omega,\omega)(x_0) &= \big((f_2-f_1)q_0\big)(x_0), & \ell_1(\varepsilon) &= |\omega|\varepsilon^2,\\
d^2\mathscr{J}_1(\Omega,\omega)(x_0) &= 0, & \ell_2(\varepsilon) &= |\omega|\varepsilon^2(\varepsilon\ln(\varepsilon)),\\
d^3\mathscr{J}_1(\Omega,\omega)(x_0) &= \frac{1}{|\omega|}\int_\omega \nabla\big((f_2-f_1)q_0\big)(x_0)[x]\,dx, & \ell_3(\varepsilon) &= |\omega|\varepsilon^3,\\
d^4\mathscr{J}_1(\Omega,\omega)(x_0) &= \big((f_1-f_2)s_2^{(2)}\big)(x_0) + \big((f_1-f_2)n^{(2)}\big)(x_0), & \ell_4(\varepsilon) &= |\omega|\varepsilon^3(\varepsilon\ln(\varepsilon)),\\
d^5\mathscr{J}_1(\Omega,\omega)(x_0) &= \frac{1}{2|\omega|}\int_\omega \nabla^2\big((f_2-f_1)q_0\big)(x_0)[x]^2\,dx & \ell_5(\varepsilon) &= |\omega|\varepsilon^4.\\
&\quad + \big((f_1-f_2)s_1^{(2)}\big)(x_0) + \big((f_1-f_2)s_7^{(2)}\big)(x_0)\\
&\quad + \big((f_1-f_2)m^{(2)}\big)(x_0),
\end{aligned}$$

21.2 General formula for higher order topological derivatives in dimension three

In this section we give an analogous result to Theorem 21.1 in three space dimensions.

Theorem 21.3. For $n \geq 1$ let $\ell_n(\varepsilon) := \varepsilon^{n-1}|\omega_\varepsilon|$. The topological derivative of $\mathscr{J}_1$ at $x_0 \in \mathsf{D}\setminus\bar{\Omega}$ and $\omega \subset \mathbf{R}^3$ with $0 \in \omega$ in dimension $d = 3$ is given by

$$\begin{aligned}
d^{n+1}\mathscr{J}_1(\Omega,\omega)(x_0) =& \frac{1}{|\omega|}\frac{1}{n!}\int_\omega \nabla^n\big((f_2-f_1)q_0\big)(x_0)[x]^n\,dx\\
&+ \frac{1}{|\omega|}\left(\sum_{j=0}^{n-4}\frac{1}{j!}\int_\omega \nabla^j\big(f_2-f_1\big)(x_0)[x]^j Q^{(n-2-j)}(x)\,dx\right)\\
&+ \frac{1}{|\omega|}\left(\sum_{j=0}^{n-3}\frac{1}{j!}\int_\omega \nabla^j\big((f_2-f_1)s_1^{(n-1-j)}\big)(x_0)[x]^j\,dx\right)\\
&+ \frac{1}{|\omega|}\left(\sum_{j=0}^{n-4}\frac{1}{j!}\int_\omega \nabla^j\big((f_2-f_1)s_2^{(n-2-j)}\big)(x_0)[x]^j\,dx\right)\\
&+ \frac{1}{|\omega|}\left(\sum_{j=0}^{n-5}\frac{1}{j!}\int_\omega \nabla^j\big((f_2-f_1)s_3^{(n-3-j)}\big)(x_0)[x]^j\,dx\right)\\
&+ \frac{1}{|\omega|}\left(\sum_{j=0}^{n-6}\frac{1}{j!}\int_\omega \nabla^j\big((f_2-f_1)q^{(n-3-j)}\big)(x_0)[x]^j\,dx\right)\\
&+ \frac{1}{|\omega|}\left(\sum_{j=0}^{n-3}\frac{1}{j!}\int_\omega \nabla^j\big((f_2-f_1)m^{(n-1-j)}\big)(x_0)[x]^j\,dx\right),
\end{aligned} \tag{21.36}$$

for $n \geq 0$, where for $\ell \geq 1$, $i \in \{1,\dots,3\}$, $Q^{(\ell)}$ are defined in Lemma 20.3, $s_i^{(\ell)}$ in Definition 20.8 and $q^{(\ell)}, m^{(\ell)}$ are defined in (20.26) and (20.27), respectively.

Similarly to Corollary 21.2, we deduce the following result.

Corollary 21.4. The first five terms of the topological derivative of the L_2 cost functional for dimension $d = 3$ are given as

$$
\begin{aligned}
d^1\mathscr{J}_1(\Omega,\omega)(x_0) &= \big((f_2-f_1)q_0\big)(x_0), && \ell_1(\varepsilon) = |\omega|\varepsilon^3,\\
d^2\mathscr{J}_1(\Omega,\omega)(x_0) &= \frac{1}{|\omega|}\int_\omega \nabla\big((f_2-f_1)q_0\big)(x_0)[x]\,dx, && \ell_2(\varepsilon) = |\omega|\varepsilon^4,\\
d^3\mathscr{J}_1(\Omega,\omega)(x_0) &= \frac{1}{2|\omega|}\int_\omega \nabla^2\big((f_2-f_1)q_0\big)(x_0)[x]^2\,dx, && \ell_3(\varepsilon) = |\omega|\varepsilon^5,\\
d^4\mathscr{J}_1(\Omega,\omega)(x_0) &= \frac{1}{6|\omega|}\int_\omega \nabla^3\big((f_2-f_1)q_0\big)(x_0)[x]^3\,dx, && \ell_4(\varepsilon) = |\omega|\varepsilon^6,\\
&\quad + \big((f_1-f_2)s_1^{(2)}\big)(x_0) + \big((f_1-f_2)m^{(2)}\big)(x_0),\\
d^5\mathscr{J}_1(\Omega,\omega)(x_0) &= \frac{1}{24|\omega|}\int_\omega \nabla^4\big((f_2-f_1)q_0\big)(x_0)[x]^4\,dx && \ell_5(\varepsilon) = |\omega|\varepsilon^7.\\
&\quad + \big((f_1-f_2)s_2^{(2)}\big)(x_0) + \frac{(f_2-f_1)(x_0)}{|\omega|}\int_\omega Q^{(2)}\,dx\\
&\quad + \big((f_1-f_2)s_1^{(3)}\big)(x_0) + \big((f_1-f_2)m^{(3)}\big)(x_0)\\
&\quad + \frac{1}{|\omega|}\int_\omega \nabla\big((f_2-f_1)s_1^{(2)}\big)(x_0)[x]\,dx\\
&\quad + \frac{1}{|\omega|}\int_\omega \nabla\big((f_2-f_1)m^{(2)}\big)(x_0)[x]\,dx,
\end{aligned}
$$

22 Conclusion

In this part of the thesis we investigated the complete topological expansion of two kinds of tracking-type cost functionals, a gradient tracking and a L_2 tracking cost functional, subject to a PDE constraint in terms of Poisson's equation. We observed that the averaged adjoint approach presented in the previous part entailed beneficial properties in view of a schematic derivation of arbitrary order topological derivatives. Contrary to the observations gathered in the previous part, the analysis of the averaged adjoint variable associated with the gradient cost functional did not lead to any complications. In fact, the corresponding averaged adjoint equation entailed a linear correlation between the state variable u_ε and the averaged adjoint state q_ε. Thus, the asymptotic expansion was a direct consequence of the according results for the state variable. On the other hand, the analysis of the averaged adjoint variable for the L_2 tracking-type cost functional was more involved, as it included the fundamental solution of the biharmonic equation. This complexity was further extended by the non-homogeneity of the first few terms of the fundamental solution in dimension $d = 2$, which necessitated 9 different corrector equations. Nonetheless, we obtained a schematic formula for both cost functionals which allowed further simplification by assumptions on the right hand side of the state equation and the inclusion shape.
For future research it would be interesting to study the complete topological asymptotic expansion of a PDE constrained cost functional, where a perturbation of the principal operator is considered. Since the topological expansion mainly depends on the knowledge of the asymptotics of the averaged adjoint

variable q_ε, we assume that a similar analysis can be carried out as long as the dependence of q_ε on the state variable u_ε is well understood.

Part IV

Numerical results in the context of topology optimisation

23 Topological state derivative

To conclude this thesis, we want to address the numerical aspects of topology optimisation. We therefore follow a novel approach introduced in [42], which involves generalised singular perturbations - so-called dilatations. In contrast to the previously discussed point perturbations, these allow to consider "higher order" perturbations, e.g. a curve or a closed surface. This methodology was further addressed on an analytical level in [24]. Based on the notion of the **topological state derivative** the authors investigated the first order asymptotic expansion of a PDE constrained shape functional subject to such higher order dilatations. In this context, the topological state derivative acts as the "interior" derivative of the state variable and can be utilised in a chain rule approach to compute the first order expansion for various shape functionals.
In what follows we are going to employ the topological state derivative in two different numerical schemes. On the one hand, we are going to utilise this method in an approximated level-set approach and compare its efficiency to the original level-set method introduced in [17]. Furthermore, we employ the shape derivative discussed in Part I to mimic a steepest descend approach for the topological derivative in the context of generalised dilatations. Since we put our focus on the numerical aspects in this section, we are going to state the main results revolving around the topological state derivative without proofs. For more insights on this topic, we refer to the article [24]. We are interested in the following problem setting:

Problem formulation

Let $\mathsf{D} \subset \mathbf{R}^d$ denote an open and bounded Lipschitz domain. Furthermore we define the admissible set

$$\mathscr{U}_{\text{ad}} := \{\Omega \subset \mathsf{D} |\ \Omega \text{ is Lipschitz } \}.$$

Our goal is

$$\min_{\Omega \in \mathscr{U}_{\text{ad}}} \mathscr{J}(\Omega) = \int_{\mathsf{D}} |u_\Omega - u_d|^2 \, dx, \tag{23.1}$$

where u_d is a given target and $u_\Omega \in H^1_0(\mathsf{D})$ solves

$$\int_{\mathsf{D}} \nabla u_\Omega \cdot \nabla \varphi + \rho_\Omega(x, u_\Omega)\varphi \, dx = \int_{\mathsf{D}} f_\Omega \varphi \, dx \quad \text{for all } \varphi \in H^1_0(\mathsf{D}). \tag{23.2}$$

Here, $f_\Omega = f_1 \chi_\Omega + f_2 \chi_{\mathsf{D}\setminus\bar{\Omega}}$ with $f_1, f_2 \in \mathbf{R}$ and the nonlinearity ρ_Ω satisfies

$$\rho_\Omega(x, u) := g_1(u)\chi_\Omega(x) + g_2(u)\chi_{\mathsf{D}\setminus\bar{\Omega}}(x),$$

where g_1, g_2 are C^1, increasing and globally bounded in $\mathbf{R}^+$. For the sake of simplicity we introduce the shape-to-state operator

$$S : \mathscr{A} \to H^1_0(\mathsf{D}), \quad \Omega \mapsto u_\Omega.$$

Note that by our assumptions (23.2) admits a unique solution and thus S is well defined. We are interested in the sensitivity analysis with respect to the following perturbations:

Definition 23.1. Let $\Omega \in \mathscr{A}(\mathrm{D})$ and $E \subset \mathrm{D}$ be a compact set such that $\partial\Omega \cap E = \emptyset$. Furthermore, denote by $E_\varepsilon := \{x \in \mathbf{R}^d : d_E(x) < \varepsilon\}$ the tubular neighbourhood of E of width $\varepsilon > 0$. We define the perturbed set $\Omega(E_\varepsilon) \subset \mathrm{D}$ by

$$\Omega(E_\varepsilon) := \begin{cases} \Omega \cup E_\varepsilon & E \subset \mathrm{D} \setminus \overline{\Omega}, \\ \Omega \setminus \overline{E}_\varepsilon & E \subset \Omega. \end{cases} \tag{23.3}$$

Definition 23.2 (Topological state derivative)**.** Let $\Omega \in \mathscr{A}(\mathrm{D})$ and consider a compact set $E \subset \mathrm{D} \setminus \overline{\Omega}$ or $E \subset \Omega$. For $\varepsilon > 0$ we introduce

$$U_\varepsilon := U_{\Omega(E_\varepsilon)} := \frac{u_{\Omega(E_\varepsilon)} - u_\Omega}{|E_\varepsilon|}, \tag{23.4}$$

where $u_{\Omega(E_\varepsilon)}, u_\Omega$ solve (23.2) on their respective sets. The *topological state derivative* of the shape-to-state operator S at Ω in direction E is defined by

$$S'(\Omega)(E) := U_0 := U_{E,0} := \lim_{\varepsilon \searrow 0} U_\varepsilon, \tag{23.5}$$

where the limit has to be understood in an appropriate function space.

We have the following result covering the topological state derivative:

Theorem 23.3. Let $E \subset \Omega$ or $E \subset \mathrm{D}\setminus\overline{\Omega}$ be either a point, a $d-1$-dimensional Lipschitz surface with finite perimeter or a $1 < k < d-1$ dimensional compact and smooth submanifold without boundary. Then, for every $q \in [1, \frac{d}{d-1})$,

$$U_\varepsilon \underset{\varepsilon \searrow 0}{\rightarrow} U_0 \quad \text{in } W_0^{1,q}(\mathrm{D}),$$

where U_0 is the unique solution to $U_0 = 0$ on $\partial\mathrm{D}$ and

$$-\Delta U_0 + \partial_u \rho_\Omega(x, u_\Omega) U_0 = \mathrm{sgn}_\Omega(E) \{(g_2(u_\Omega) - g_1(u_\Omega)) + (f_1 - f_2)\} \mu_E \quad \text{in D},$$

and

$$\mu_E := \begin{cases} \delta_{x_0} & \text{if } E = \{x_0\}, \\ \frac{1}{\mathrm{Per}(E)}(\mathscr{H}^{d-1} \lfloor E) & \text{if } E \text{ is a } d-1 \text{ dimensional Lipschitz surface }, \\ \frac{1}{\mathscr{H}^k(E)}(\mathscr{H}^k \lfloor E) & \text{else.} \end{cases}$$

Here, $\mathscr{H}^n$ denotes the n-dimensional Hausdorff measure.

Proof. A proof can be found in [24, Theorem 2.7]. □

Note that the PDE governing U_0 involves a measure on the right hand side. This topic is addressed in [24, Section 2] in more detail.

Remark 23.4. A similar analysis can be carried out for linear PDEs including a point perturbation of the operator (cf. [24, Section 3]). The limitation to point perturbations is a result of the first variation of the state occurring in the analysis. This has not yet been studied with respect to generalised perturbations. Furthermore, the topological state derivative of these transmission problems necessitates the introduction of very-weak solutions and leads to a weaker convergence in $L_q(\mathrm{D})$, $q \in [1, \frac{d}{d-1})$.

Definition 23.5. In analogy to Definition 9.1 we define the (generalised) first order topological derivative of $\mathscr{J}$ at $\Omega \in \mathscr{A}$ in direction $E \subset \Omega$ or $E \subset \mathsf{D} \setminus \overline{\Omega}$ by

$$D^{\text{top}}\mathscr{J}(\Omega)(E) := \lim_{\varepsilon \searrow 0} \frac{\mathscr{J}(\Omega(E_\varepsilon)) - \mathscr{J}(\Omega)}{|E_\varepsilon|}.$$

Remark 23.6. Note that this definition assumes that the first order of the topological expansion is of order $|E_\varepsilon|$. In view of the results obtained in Part II and Part III of this thesis, this assumption seems reasonable. Yet we want to highlight that this does not constitute a general rule. In fact there are problem formulations, which involve lower order terms. Such an example is given in the article [16], where Dirichlet conditions are enforced on the boundary of the inclusion.

Remark 23.7. In order to avoid any notational conflict, we denoted the derivative $D^{\text{top}}\mathscr{J}$ compared to the previously introduced notation $d\mathscr{J}$. In fact, one readily checks that for $E = \{x_0\}$ we have

$$D^{\text{top}}\mathscr{J}(\Omega)(E) = d\mathscr{J}(\Omega, \omega)(x_0),$$

with the first order $\ell_1 = |\omega_\varepsilon|$ and the special deformation shape $\omega = B_1(0)$.

Employing Theorem 23.3 we can readily compute the first order topological derivative of the cost functional introduced in (23.1).

Theorem 23.8. Let $\Omega \in \mathscr{A}$ and $E \subset \Omega$ or $E \subset \mathsf{D}\setminus\overline{\Omega}$ be either a point, a $d-1$-dimensional Lipschitz surface with finite perimeter or a $1 < k < d-1$ dimensional compact and smooth submanifold without boundary. Then there holds

$$D^{\text{top}}\mathscr{J}(\Omega)(E) = \int_{\mathsf{D}} 2U_0(u_\Omega - u_d)\, dx.$$

Proof. The Sobolev embedding entails $W^{1,q}(\mathsf{D}) \hookrightarrow L_2(\mathsf{D})$ for $q < \frac{d}{d-1}$ sufficiently large (cf. [82]). Thus we obtain

$$D^{\text{top}}\mathscr{J}(\Omega)(E) = \lim_{\varepsilon \searrow 0} \int_{\mathsf{D}} U_\varepsilon(u_{\Omega(E_\varepsilon)} + u_\Omega - 2u_d)\, dx = \int_{\mathsf{D}} 2U_0(u_\Omega - u_d)\, dx,$$

where in the last step we utilised the convergence $u_{\Omega(E_\varepsilon)} \to u_\Omega$ in $L_2(\mathsf{D})$. □

We now have gathered all necessary tools to continue with the numerical investigation.

24 Approximated level-set approach

For the first application of the the topological state derivative we want to address the well established level-set method introduced in [17]. Therefore, we consider the following model problem. Let the hold-all domain denote a square, i.e. $\mathsf{D} = (-2,2) \times (-2,2) \subset \mathbf{R}^2$, $g_1 \equiv g_2 \equiv 0$, $f_1 = 10$ and $f_2 = 1$. Furthermore, we define the target function u_d as the solution of (23.2) with respect to the target shape Ω^*, i.e. $u_d = u_{\Omega^*}$. Here, Ω^* denotes the clover shape defined as the sub level-set of a specific function [57]. That is

$$\Omega^* = \{(x,y) \in \mathsf{D} |\ \Psi(x,y) \le 0\}, \tag{24.1}$$

where

$$\Psi(x,y)=c_1((\sqrt{(x-a)^2+by^2}-1)(\sqrt{(x+a)^2+by^2}-1)(\sqrt{bx^2+(y-a)^2}-1)(\sqrt{bx^2+(y+a)^2}-1)-c_2),$$

with $a=\frac{5}{4}$, $b=2$, $c_1=10^{-1}$ and $c_2=10^{-3}$. The shape is depicted in Figure 13.

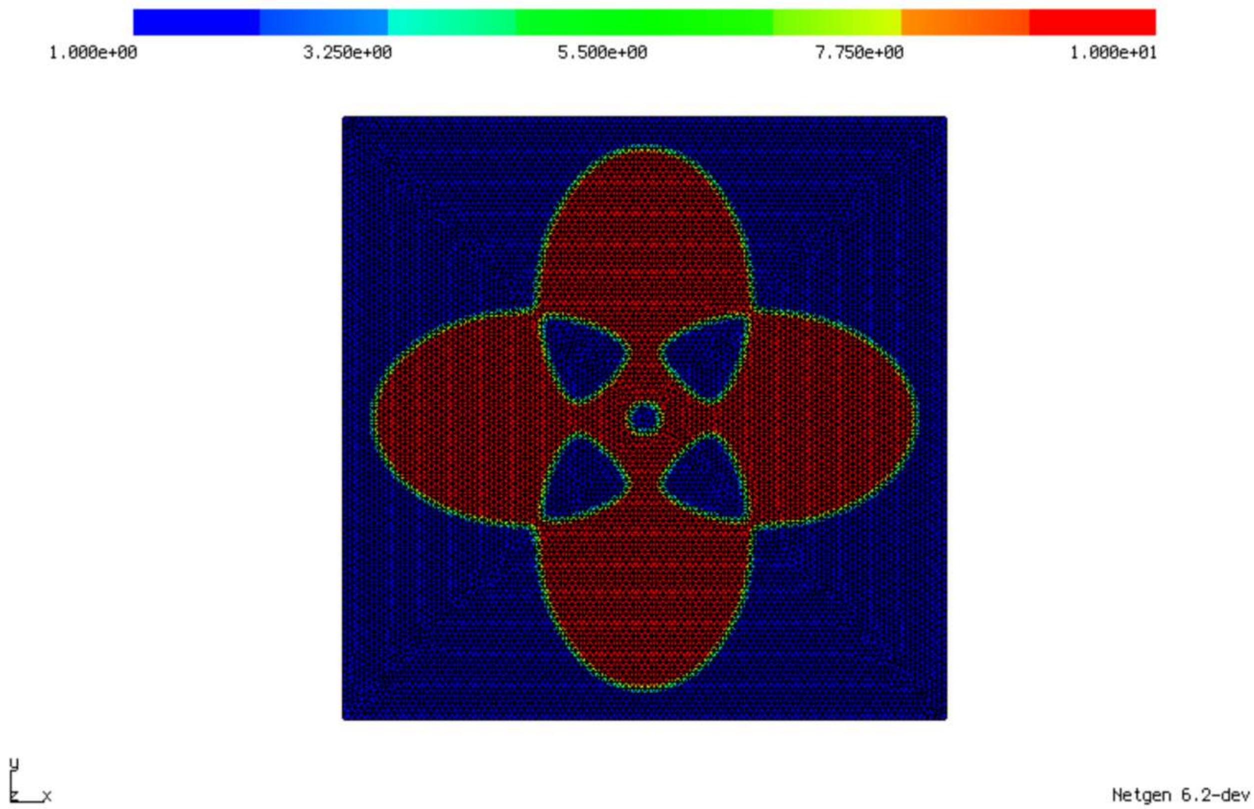

Figure 13: Visualisation of the target shape Ω^* (red).

24.1 Standard level-set algorithm

We first employ the classical level-set approach (cf. [17]). Since this algorithm employs the usual topological derivative introduced in Part II we recall the following result.

Lemma 24.1. For $\Omega\subset \mathsf{D}$ open and Lipschitz let $\mathscr{J}(\Omega)=\int_{\mathsf{D}}|u_\Omega-u_d|^2\,dx$, where $u_\Omega\in H_0^1(\mathsf{D})$ solves

$$\int_{\mathsf{D}}\nabla u_\Omega\cdot\nabla\varphi\,dx=\int_{\mathsf{D}}f_\Omega\varphi\,dx\quad\text{ for all }\varphi\in H_0^1(\mathsf{D}). \tag{24.2}$$

Then there holds

$$d\mathscr{J}(\Omega,\omega)(x_0)=\begin{cases}(f_2-f_1)q_\Omega(x_0) & \text{if } x_0\in\mathsf{D}\setminus\bar{\Omega},\\ -(f_2-f_1)q_\Omega(x_0), & \text{if } x_0\in\Omega,\end{cases}$$

where the unperturbed adjoint variable $q_0 \in H_0^1(\mathrm{D})$ satisfies

$$\int_{\mathrm{D}} \nabla\varphi \cdot \nabla q_\Omega \, dx = -\int_{\mathrm{D}} 2(u_\Omega - u_d)\varphi \, dx \quad \text{for all } \varphi \in H_0^1(\mathrm{D}). \tag{24.3}$$

Proof. This follows from Theorem 21.1. □

We further define the quantity

$$g_\Omega(x) = \chi_\Omega(x)(-d\mathcal{J}(\Omega,\omega)(x)) + \chi_{\mathrm{D}\setminus\bar{\Omega}}(x)d\mathcal{J}(\Omega,\omega)(x) = (f_2 - f_1)q_0(x), \tag{24.4}$$

which measures the sign affected sensitivity of the functional $\mathcal{J}$ with respect to singular changes of the constant force. This definition entails the sufficient local minimality condition (cf. [17, Section 3.1]).

$$\begin{cases} g_\Omega(x) > 0 & \text{in } \mathrm{D}\setminus\bar{\Omega}, \\ g_\Omega(x) < 0 & \text{in } \Omega. \end{cases} \tag{24.5}$$

Based on the ideas of [17], we introduce the following level-set algorithm.

Algorithm 3 Level-set algorithm

Require: initial level-set function Ψ_0, $N_{\max} \in \mathbf{N}$, $N_{\text{fix}} \in \mathbf{N}$, $\kappa, \beta \in (0,1)$
 while $n \leq N_{\max}$ **do**
  identify set $\Omega_n = \{x \in \mathbf{R}^2 | \ \Psi_n(x) < 0\}$.
  compute state u_{Ω_n} as the solution of (24.2).
  compute adjoint state q_{Ω_n} by solving the adjoint state equation (24.3).
  compute the generalised topological gradient g_{Ω_n}.
  initialise iteration count $k = 0$.
  while $k \leq N_{\text{fix}}$ **do**
   compute new level-set function $\Psi_{\text{new}} = (1-\kappa)\frac{\Psi_n}{\|\Psi_n\|_{L_2(\mathrm{D})}} + \kappa\frac{g_{\Omega_n}}{\|g_{\Omega_n}\|_{L_2(\mathrm{D})}}$.
   identify shape $\Omega_{\text{new}} = \{x \in \mathbf{R}^2 | \ \Psi_{\text{new}}(x) < 0\}$.
   if $\mathcal{J}(\Omega_{\text{new}}) > \mathcal{J}(\Omega_n)$ **then**
    set $\kappa = \beta\kappa$ and $k += 1$.
   else
    step size accepted, exit inner while loop.
   end if
  end while
  $\Psi_{n+1} = \Psi_{\text{new}}$.
  $\kappa = \min\{1, \frac{6}{5}\kappa\}$.
  $n += 1$.
 end while

We want to highlight that this setting allowed us to use continuous P1 elements for the function space containing the level-set functions Ψ_n and the topological gradients g_{Ω_n}. This enables a smooth representation of the level-set and this is definitely a preferable choice. Nonetheless we are going to exclude this property on purpose in the next approach.

24.2 Averaged level-set algorithm

In this section we aim to utilise the topological state derivative as follows. Instead of working with a continuous topological gradient, we seek $g_\Omega \in L_2^{\mathrm{pwc}}(\mathrm{D})$, where $L_2^{\mathrm{pwc}}(\mathrm{D})$ denotes the set of piecewise constant functions on D. Therefore, we define for each triangular element $E \subset \mathrm{D}$ in analogy to (24.4)

$$\bar{g}_\Omega(E) = \chi_\Omega(x)\big(-D^{\mathrm{top}}\mathcal{J}(\Omega)(\partial E)\big) + \chi_{\mathrm{D}\setminus\bar{\Omega}}(x)D^{\mathrm{top}}\mathcal{J}(\Omega)(\partial E). \tag{24.6}$$

Remark 24.2. Note that the boundary ∂E intersects the boundary of Ω for a selected number of elements. This contradicts the assumptions of Theorem 23.3. On an analytical level this can be overcome by splitting the boundary of an element E into three separate edges. For each edge e that intersects $\partial\Omega$ and $\varepsilon > 0$ sufficiently small we define $e_\varepsilon^- = \{x \in e|\ x \in \Omega, d_{\partial\Omega} > \varepsilon\}$, $e_\varepsilon^+ = \{x \in e|\ x \in \mathrm{D}\setminus\bar{\Omega}, d_{\partial\Omega} > \varepsilon\}$ and $e_\varepsilon^0 = \{x \in e|\ d_{\partial\Omega} \le \varepsilon\}$ and treat those parts accordingly. Nonetheless, in the numerical realm we can neglect the problematic part e_ε^0 as it only contributes a small portion.

In view of (24.3) and Theorem 23.8, sufficient regularity of the variables entails

$$\bar{g}_\Omega(E) = \frac{1}{|\partial E|}\int_{\partial E}(f_2 - f_1)q_\Omega\, dS. \tag{24.7}$$

Hence, the piecewise constant topological gradient indeed denotes an averaging of the topological gradient defined in (24.4). This result gives rise to the following algorithm.

Algorithm 4 Approximated level-set algorithm

Require: initial level-set function Ψ_0, $N_{\max} \in \mathbf{N}$, $N_{\mathrm{fix}} \in \mathbf{N}$, $\kappa, \beta \in (0,1)$
 while $n \le N_{\max}$ **do**
  identify set $\Omega_n = \{x \in \mathbf{R}^2|\ \Psi_n(x) < 0\}$.
  compute state u_{Ω_n} as the solution of (24.2).
  compute adjoint state q_{Ω_n} by solving the adjoint state equation (24.3).
  compute the averaged topological gradient $\bar{g}_{\Omega_n}$.
  initialise iteration count $k = 0$.
  while $k \le N_{\mathrm{fix}}$ **do**
   compute new level-set function $\Psi_{\mathrm{new}} = (1-\kappa)\frac{\Psi_n}{\|\Psi_n\|_{L_2(\mathrm{D})}} + \kappa\frac{\bar{g}_{\Omega_n}}{\|\bar{g}_{\Omega_n}\|_{L_2(\mathrm{D})}}$.
   identify shape $\Omega_{\mathrm{new}} = \{x \in \mathbf{R}^2|\ \Psi_{\mathrm{new}}(x) < 0\}$.
   if $\mathcal{J}(\Omega_{\mathrm{new}}) > \mathcal{J}(\Omega_n)$ **then**
    set $\kappa = \beta\kappa$ and $k+=1$.
   else
    step size accepted, exit inner while loop.
   end if
  end while
  $\Psi_{n+1} = \Psi_{\mathrm{new}}$.
  $\kappa = \min\{1, \frac{6}{5}\kappa\}$.
  $n+=1$.
 end while

In order to compare our results to the classical level-set approach, we projected the final level-set $\Psi_{N_{\max}}$ into the continuous finite element space $P1$.

24.3 Results

For our example we used the following set of parameters. Number of iterations $N_{\max} = 100$, maximal number of linesearch $N_{\text{fix}} = 10$, linesearch control parameter $\kappa = 0.05$, $\beta = 0.8$ and the initial level-set function

$$\Psi_0(x, y) = x^2 + y^2 - \frac{1}{16}.$$

Hence, the initial guess Ω_0 denotes a ball with radius $\frac{1}{4}$ centered at the origin. The resulting shapes and level-set functions are depicted in the following figures. Note that we additionally used a continuous version of the piecewise constant function f_Ω to achieve a clearer visualisation.

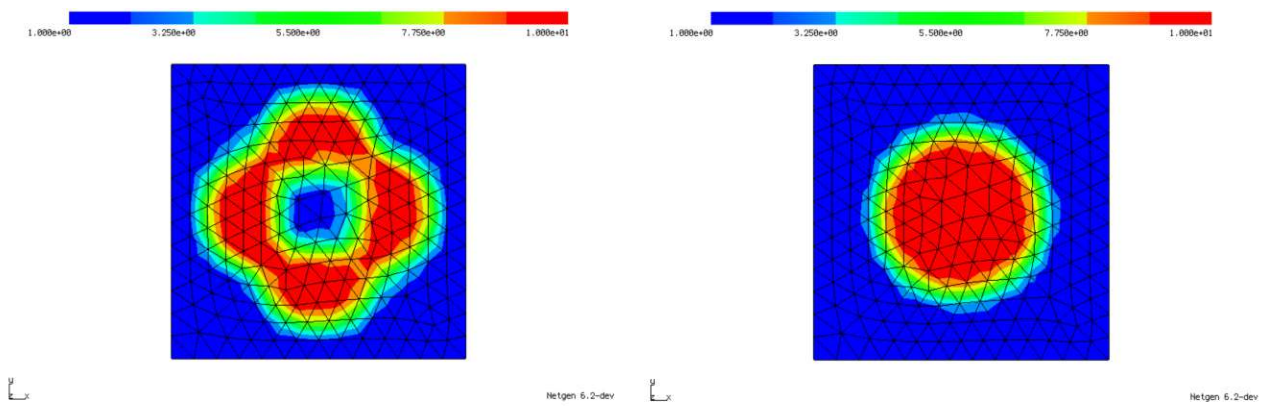

(a) Standard level-set algorithm

(b) Averaged level-set algorithm

Figure 14: Visualisation of f_Ω for the final shape Ω and mesh size $m = 0.3$.

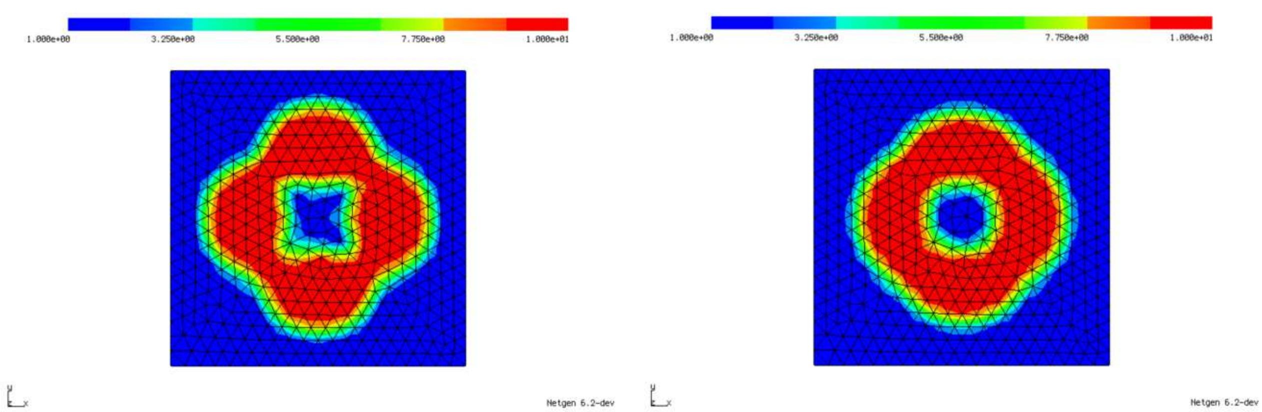

(a) Standard level-set algorithm

(b) Averaged level-set algorithm

Figure 15: Visualisation of f_Ω for the final shape Ω and mesh size $m = 0.2$.

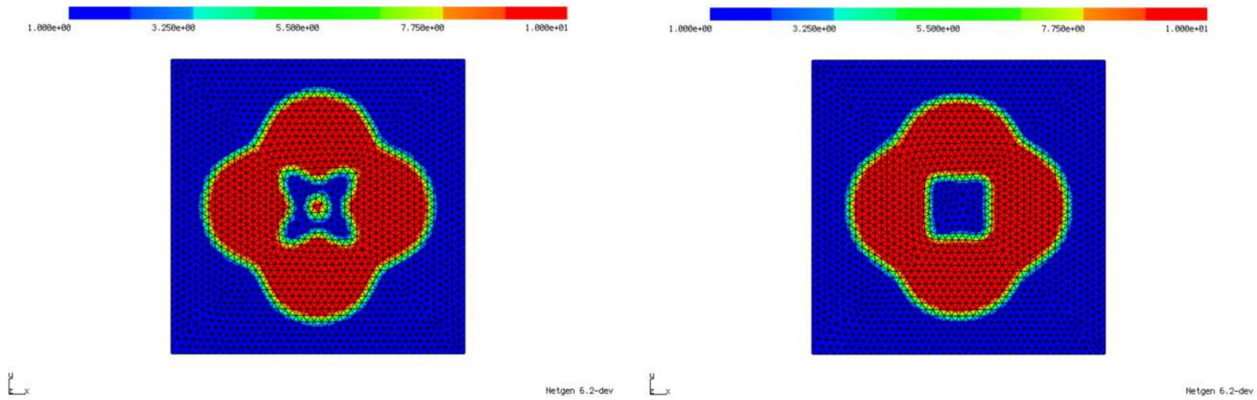

(a) Standard level-set algorithm (b) Averaged level-set algorithm

Figure 16: Visualisation of f_{Ω} for the final shape Ω and mesh size $m = 0.1$.

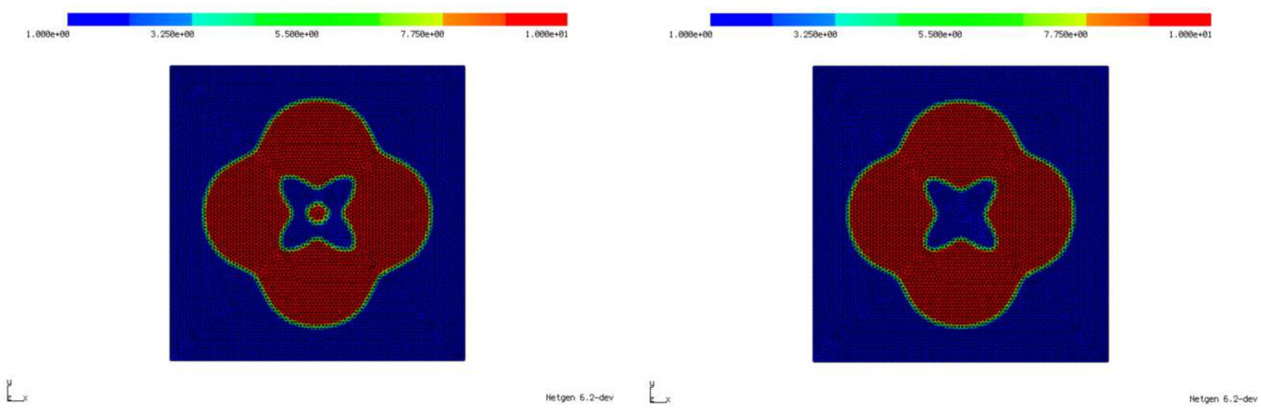

(a) Standard level-set algorithm (b) Averaged level-set algorithm

Figure 17: Visualisation of f_{Ω} for the final shape Ω and mesh size $m = 0.05$.

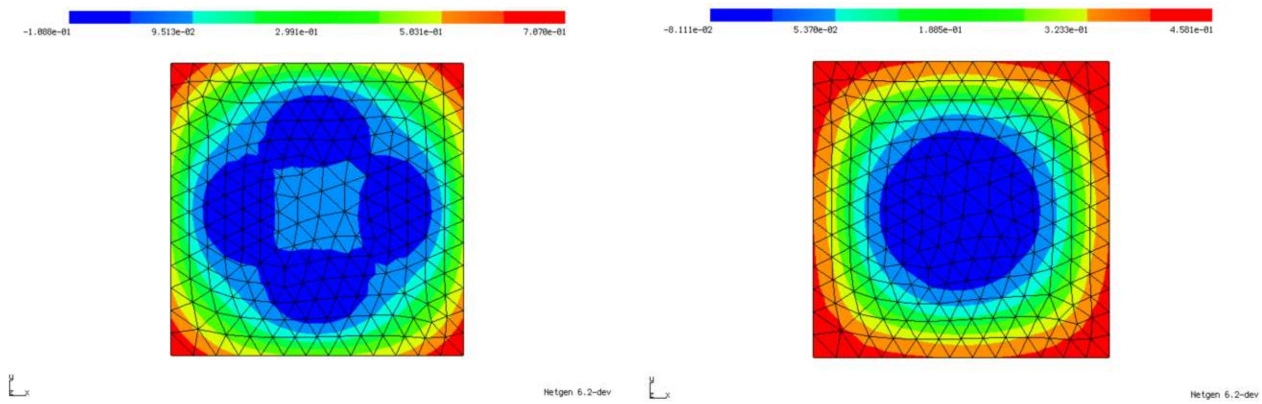

(a) Standard level-set algorithm (b) Averaged level-set algorithm

Figure 18: Visualisation of the final level-set function $\Psi_{N_{\max}}$ for the mesh size $m = 0.3$.

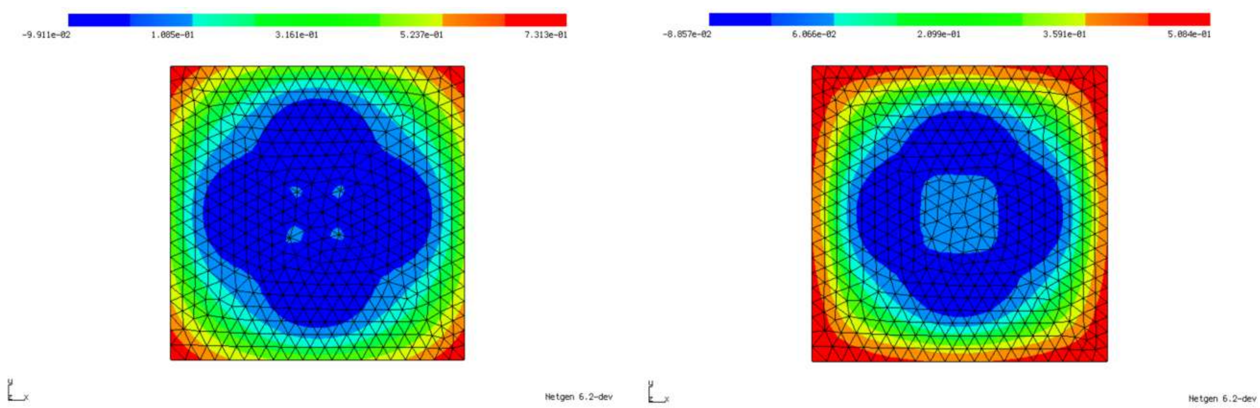

(a) Standard level-set algorithm (b) Averaged level-set algorithm

Figure 19: Visualisation of the final level-set function $\Psi_{N_{\max}}$ for the mesh size $m = 0.2$.

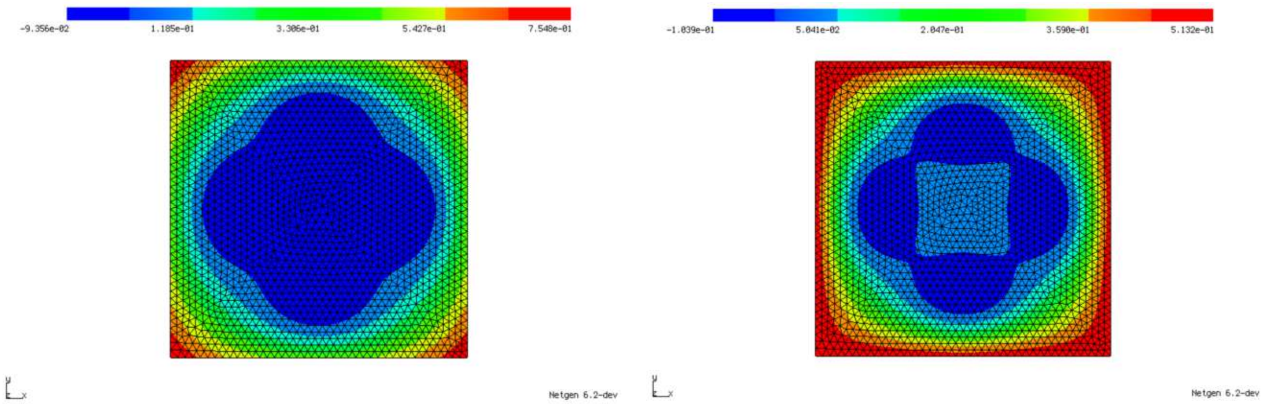

(a) Standard level-set algorithm

(b) Averaged level-set algorithm

Figure 20: Visualisation of the final level-set function $\Psi_{N_{\max}}$ for the mesh size $m = 0.1$.

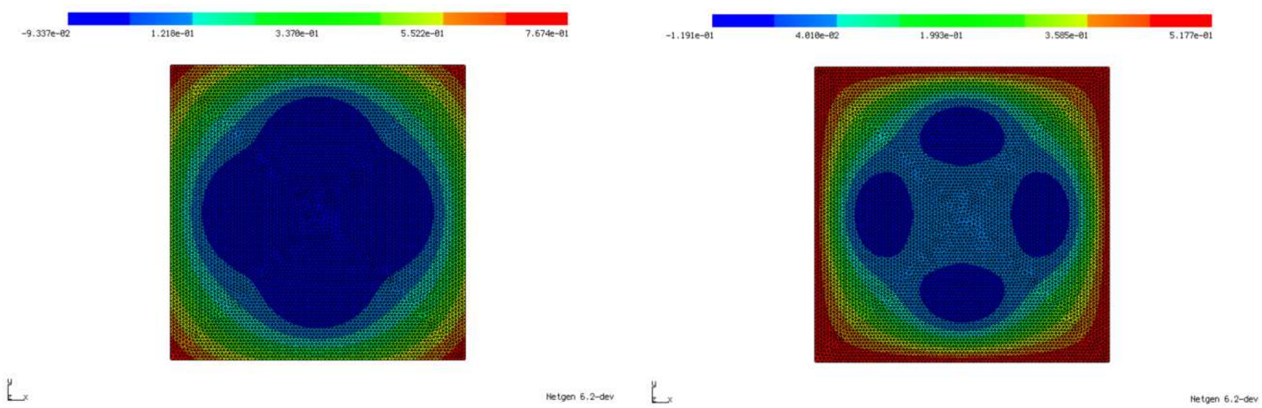

(a) Standard level-set algorithm

(b) Averaged level-set algorithm

Figure 21: Visualisation of the final level-set function $\Psi_{N_{\max}}$ for the mesh size $m = 0.05$.

We observe that both algorithms achieve an increasingly accurate result with respect to a declining mesh size (cf. Figures 14a-17a and Figures 14b-17b, respectively). Nonetheless, the standard level-set algorithm outperforms the approximated one in some aspects. On the one hand, the classical level-set algorithm yields a rough guess of the optimal shape even for a very coarse discretisation (cf. Figure 14a), which the approximated level-set algorithm fails to do (cf. Figure 14b). On the other hand, the standard level-set algorithm yields a closer guess of the target shape (cf. Figure 13) than the approximated level-set algorithm (cf. Figure 17a vs. Figure 17b) even subject to a fine discretisation. Furthermore, another deficit of the averaged algorithm can be observed in view of its runtime. That is, the difference of the respective runtimes increases significantly as the mesh size declines (cf. Table 4). However, we want to point out that the large gap of the according runtimes is a result of a very simplistic implementation approach involving loops in python. Hence improvements in this regard are plausible.
Furthermore, we want to emphasize that the averaged level-set algorithm yields appropriate results for a sufficiently small mesh size. Additionally, the algorithm does not necessitate point evaluation of the

topological gradient. This could be advantageous in cases, where low regularity issues occur.

	standard	averaged
mesh size = 0.3	5 s	10 s
mesh size = 0.2	10 s	20 s
mesh size = 0.1	33 s	110 s
mesh size = 0.05	137 s	1054 s

Table 4: Comparison of the runtime for the classical level-set algorithm and the averaged level-set algorithm.

25 Steepest descent approach

In this section we want to address another application of the topological state derivative, which combines methods of Part I and Part IV. The main observation that motivates the upcoming algorithm is as follows. Given a fixed hold-all domain $\mathsf{D} \subset \mathbf{R}^2$, $\Omega \subset \mathsf{D}$ open and Lipschitz and w.l.o.g. $E \subset \mathsf{D}\setminus\bar{\Omega}$ a smooth curve. By definition $D\mathscr{J}(\Omega)(E)$ captures the sensitivity of the cost functional with respect to a E-shaped inclusion. One way to incorporate this information in an algorithm would be to compute the quantity $D\mathscr{J}(\Omega)(E)$ for various shapes, e.g. a number of line segments and use this information in a one-shot type approach. We want to follow a different route. To specify, we consider $D\mathscr{J}(\Omega)(E)$ as a directional derivative and seek a deepest descend direction $\bar{E}$. To achieve this goal we view E as a design variable for the objective functional $D\mathscr{J}(\Omega)(\cdot)$. Therefore, we choose an initial direction E and perform a shape optimisation of the functional $E \mapsto D\mathscr{J}(\Omega)(E)$ with the tools developed in Part I of this thesis. Therefore, we need the following result.

Lemma 25.1. Let $\mathsf{D} \subset \mathbf{R}^2$ be an open and bounded Lipschitz domain and $E \subset \mathsf{D}$ a piecewise smooth curve. Furthermore, fix $X \in C^1_c(\mathsf{D})^2$ and recall the notation $F_t = \mathrm{Id} + tX$, for $t > 0$. For $f \in H^2(\mathsf{D})$ there holds

$$\lim_{t\searrow 0} \frac{1}{t}\left(\frac{1}{|F_t(E)|}\int_{F_t(E)} f\; dS - \frac{1}{|E|}\int_E f\; dS\right) = |E|^{-1}\int_E (\mathrm{div}(X) - \partial X n\cdot n) f\; dS + |E|^{-1}\int_E \nabla f\cdot X\; dS \\ - |E|^{-2}\left(\int_E f\; dS\right)\left(\int_E \mathrm{div}(X) - \partial X n\cdot n\; dS\right),$$

Proof. To abbreviate the notation let $E_t := F_t(E)$ for $t > 0$ small. We can expand the difference quotient as follows:

$$\left(\frac{1}{|F_t(E)|}\int_{F_t(E)} f\; dS - \frac{1}{|E|}\int_E f\; dS\right) = \frac{1}{|E_t||E|}\left[|E|\left(\int_{E_t} f\; dS - \int_E f\; dS\right) - (|E_t| - |E|)\int_E f\; dS\right]. \tag{25.1}$$

In view of $|E_t| = \int_{E_t} dS$ we observe that both quantities

$$\frac{\int_{E_t} f\; dS - \int_E f\; dS}{t}, \quad \frac{|E_t| - |E|}{t},$$

can be handled by Lemma 3.3 and Lemma 3.4. Thus, dividing (25.1) by $t > 0$ and passing to the limit $t \searrow 0$ entails

$$\lim_{t \searrow 0} \frac{1}{t}\left(\frac{1}{|F_t(E)|}\int_{F_t(E)} f\, dS - \frac{1}{|E|}\int_E f\, dS\right) = \frac{|E|}{|E|^2}\int_E (\mathrm{div}(X) - \partial X n\cdot n) f\, dS + \frac{|E|}{|E|^2}\int_E \nabla f \cdot X\, dS$$
$$- \frac{1}{|E|^2}\left(\int_E f\, dS\right)\left(\int_E \mathrm{div}(X) - \partial X n \cdot n\, dS\right),$$

which finishes the proof. □

In order to visualise these ideas, we consider the following model problem. Let

$$\mathsf{D} = (-2,2)\times(-2,2) \subset \mathbf{R}^2,$$

$g_1(u) = 10u$, $g_2(u) = u^3$, $f_1 = 10$ and $f_2 = 1$. Furthermore, we define the target function u_d as the solution of (23.2) with respect to the target shape $\Omega^* := \{x \in \mathsf{D} |\ 0.8 \leq |x| \leq 1.2\}$. For the sake of simplicity we consider the initial shape $\Omega = \emptyset$. The optimal shape is depicted in Figure 22.

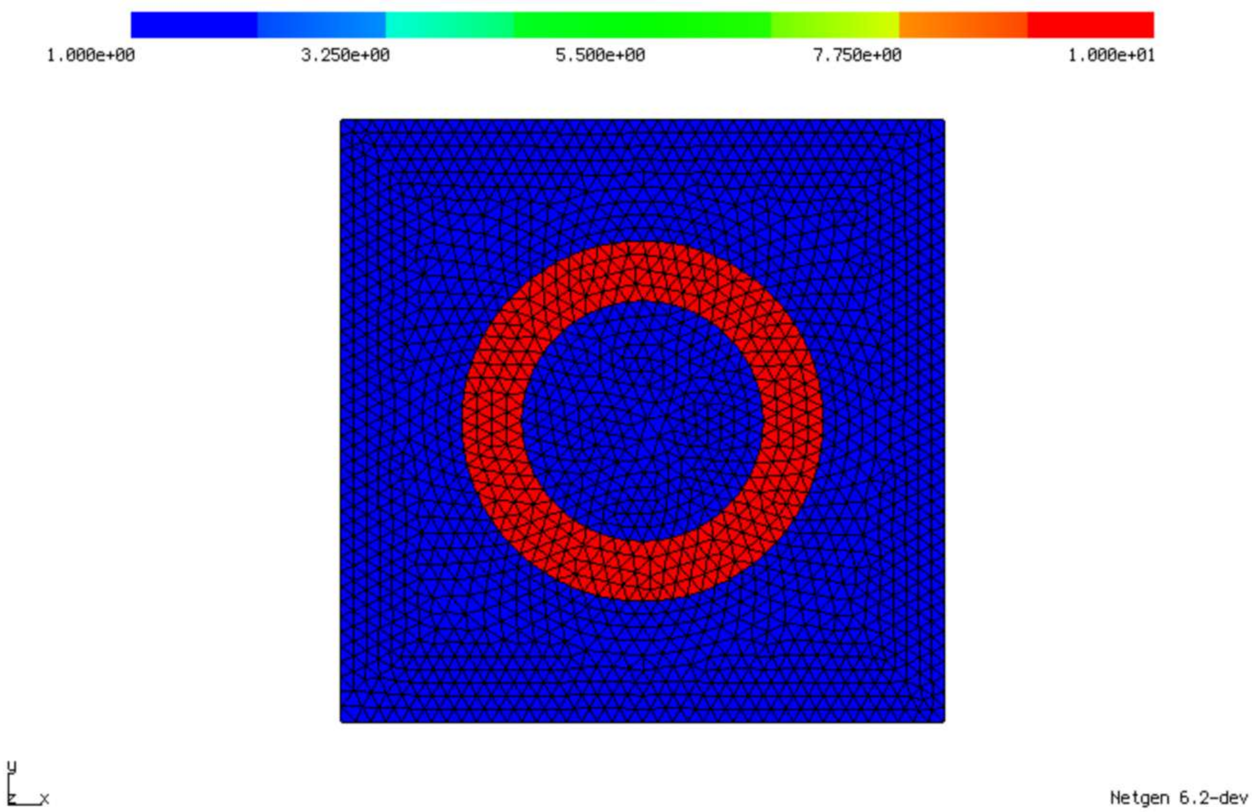

Figure 22: Visualisation of the target shape Ω^* (red).

This setting entails the state equation: Find $u_0 \in H_0^1(\mathsf{D})$ such that

$$\int_{\mathsf{D}} \nabla u_0 \cdot \nabla \varphi + u_0^3 \varphi\, dx = \int_{\mathsf{D}} f_2 \varphi\, dx \quad \text{for all } \varphi \in H_0^1(\mathsf{D}). \tag{25.2}$$

Furthermore, we deduce the unperturbed adjoint equation: Find $q_0 \in H_0^1(\mathsf{D})$ such that

$$\int_{\mathsf{D}} \nabla\varphi \cdot \nabla q_0 + 3u_\Omega^2 q_0 \varphi \, dx = -\int_{\mathsf{D}} 2(u_0 - u_d)\varphi \, dx \quad \text{for all } \varphi \in H_0^1(\mathsf{D}). \tag{25.3}$$

Note that, similarly to the averaged topological gradient (cf. (24.7)), we deduce

$$D^{\text{top}} \mathscr{J}(\emptyset)(E) = \frac{1}{|E|} \int_E [(f_2 - f_1) + (g_1(u_0) - g_2(u_0))] q_0 \, dS \quad \text{for each admissible set } E.$$

Corollary 25.2. For a smooth curve $E \subset \mathsf{D}$ in $\mathbf{R}^2$ let $\mathscr{G}(E) = \frac{1}{|E|}\int_E [(f_2 - f_1) + (g_1(u_0) - g_2(u_0))] q_0 \, dS$. Then there holds for $X \in C_c^1(\mathsf{D})$

$$\begin{aligned} D\mathscr{G}(E)(X) = & |E|^{-1} \int_E (\operatorname{div}(X) - \partial X n \cdot n)[(f_2 - f_1) + (g_1(u_0) - g_2(u_0))] q_0 \, dS \\ & + |E|^{-1} \int_E \nabla([(f_2 - f_1) + (g_1(u_0) - g_2(u_0))] q_0) \cdot X \, dS \\ & - |E|^{-2} \left(\int_E [(f_2 - f_1) + (g_1(u_0) - g_2(u_0))] q_0 \, dS \right) \left(\int_E \operatorname{div}(X) - \partial X n \cdot n \, dS \right), \end{aligned}$$

where the left hand side denotes the shape derivative introduced in Definition 4.1.

Proof. This follows from an application of Lemma 25.1. □

Note that we can expand the function $\mathscr{G}$ introduced in the previous corollary to obtain

$$\begin{aligned} D\left(D^{\text{top}} \mathscr{J}(\emptyset)(E)\right)(X) = & |E|^{-1} \int_E (\operatorname{div}(X) - \partial X n \cdot n)[(f_2 - f_1) + (g_1(u_0) - g_2(u_0))] q_0 \, dS \\ & + |E|^{-1} \int_E \nabla([(f_2 - f_1) + (g_1(u_0) - g_2(u_0))] q_0) \cdot X \, dS \\ & - |E|^{-2} \left(\int_E [(f_2 - f_1) + (g_1(u_0) - g_2(u_0))] q_0 \, dS \right) \left(\int_E \operatorname{div}(X) - \partial X n \cdot n \, dS \right). \end{aligned}$$

Similarly to the methodology presented in Section 7, the deformation of the shape is based on the moving-mesh approach. Hence, during each iteration, we move the nodes according to a specific vector field. Additionally, we use a bilinear form to identify shape gradients. That is, for each linear and continuous shape derivative $D\tilde{\mathscr{J}}$ we define the shape gradient $\nabla\tilde{\mathscr{J}} \in H_0^1(\mathsf{D})^2$ as the solution to the sub-problem

$$\int_\Omega \partial(\nabla\tilde{\mathscr{J}}) : \partial(X) + \alpha B\nabla\tilde{\mathscr{J}} \cdot BX + \nabla\tilde{\mathscr{J}} \cdot X \, dx = D\tilde{\mathscr{J}}(\Omega)(X) \quad \text{for all } X \in H_0^1(\mathsf{D})^2. \tag{25.4}$$

Here, $\alpha \in \{0, 1\}$ and

$$B = \begin{pmatrix} -\partial_x & \partial_y \\ \partial_y & \partial_x \end{pmatrix}, \tag{25.5}$$

accounts for the Cauchy-Riemann conditions, which encourage conformal deformation fields. Since we do not integrate a remeshing process into our algorithm, we observe that the specific choice of the bilinear greatly impacts the result. To visualise this behaviour, we compare our results for the bilinear form with $\alpha = 1$ and $\alpha = 0$. Based on these ideas we present the following algorithm

Algorithm 5 Steepest descend algorithm

Require: initial curve function E_0, $N_{\max} \in \mathbf{N}$, $N_{\text{fix}} \in \mathbf{N}$, step size $s_0 \in \mathbf{R}^+$, line search parameter $\beta \in (0,1)$
  Hilbert space $\mathscr{H} = H_0^1(\mathrm{D})$
  compute state u_0 as the solution of (25.2).
  compute adjoint state q_0 by solving the adjoint state equation (25.3).
  define $\mathscr{G}$ (cf. Corollary 25.2).
  while $n \leq N_{\max}$ **do**
    compute shape derivative $D\mathscr{G}(E_n)(\cdot)$.
    compute associated shape gradient $\nabla\mathscr{G}$.
    compute the averaged topological gradient $\bar{g}_{\Omega_n}$.
    initialise iteration count $k = 0$ and $s = s_0$.
    while $k \leq N_{\text{fix}}$ **do**
      choose descend direction $X_n = -s\nabla\mathscr{G}$.
      if $\mathscr{G}((\mathrm{Id} + X_n)(E)) > \mathscr{G}(E_n)$ **then**
        set $s = \beta s$ and $k+ = 1$.
      else
        step size accepted, exit inner while loop.
      end if
    end while
    update shape $E_{n+1} = (\mathrm{Id} + sX_n)(E_n)$.
    $n+ = 1$.
  end while

25.1 Results

For the initialisation of the algorithm we used the following set of parameters: maximal number of iterations $N_{\max} = 600$, maximal number of linesearches $N_{\text{fix}} = 15$, $s = 10^{-1}$, $\beta = \frac{1}{2}$ and the initial curve E_0 denotes the boundary of the rectangle $[-\frac{3}{2}, \frac{3}{2}] \times [-\frac{3}{2}, \frac{3}{2}]$. The initial shape E_0 is depicted in Figure 23b. Furthermore, we visualised the function $f := [(f_2 - f_1) + (g_1(u_0) - g_2(u_0))]\, q_0$ in Figure 23a.

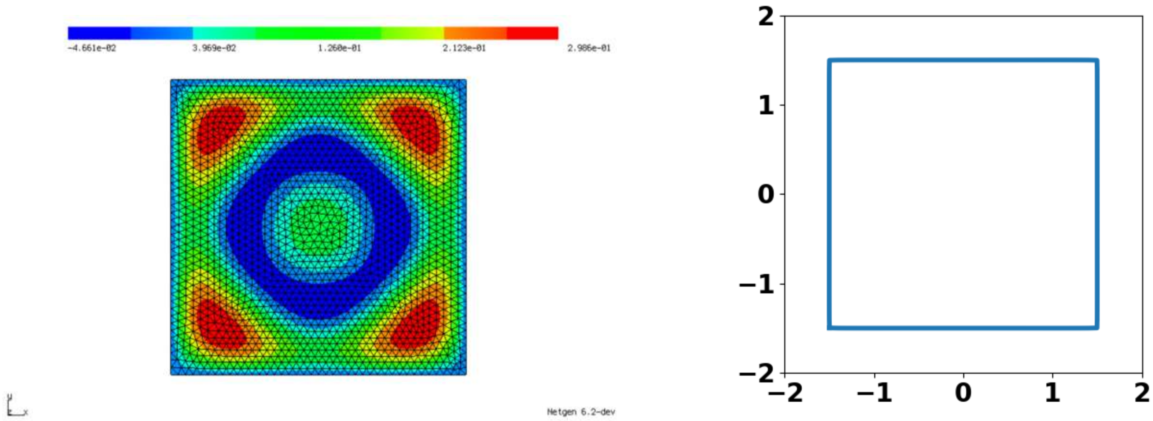

(a) Visualisation of the function f. (b) Initial shape E_0.

Figure 23: Initial conditions.

The initial shape (cf. Figure 22) and the function f (cf. Figure 23a) both suggest that the optimal shape E^* is attained approximately as the boundary of the unit ball $B_1(0)$. The results of the algorithm agree with this idea (cf. Figure 24)

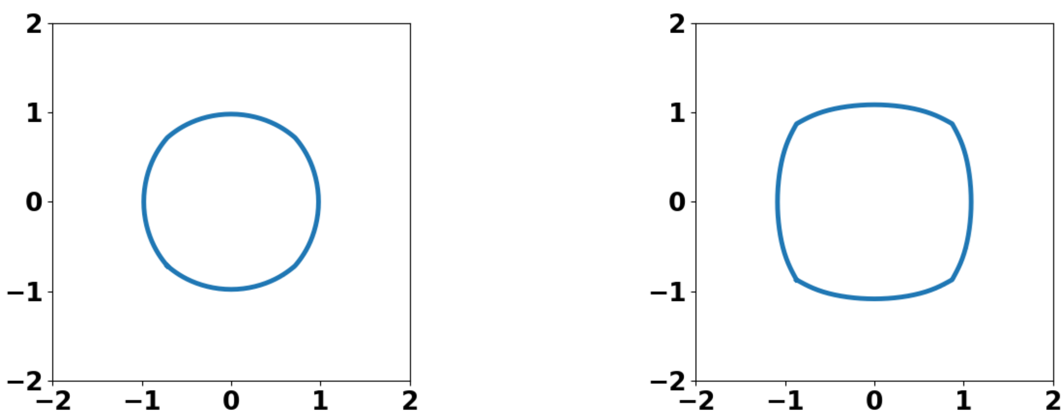

(a) Optimised shape $E_{N_{\max}}$ for $\alpha = 0$. (b) Optimised shape $E_{N_{\max}}$ for $\alpha = 1$.

Figure 24: Visualisation of the optimised shape.

We observe that the algorithm without the Cauchy-Riemann condition (i.e. $\alpha = 0$) manages to attain a circular shape (cf. Figure 24a), which was anticipated. Contrary, the algorithm including the Cauchy-Riemann condition behaves similarly but fails to completely smoothen the corners (cf. Figure 24b). This is a result of the elements close to the corners of the initial rectangle being stretched in the optimisation process. Without any remeshing in the optimisation algorithm, this stretching is necessary to achieve a circular shape. Yet, the Cauchy-Riemann condition aims to prevent extensive stretching of the elements and thus fails to achieve the task. To visualise the behaviour, we depicted the according deformed meshes in Figure 25a, Figure 25b.

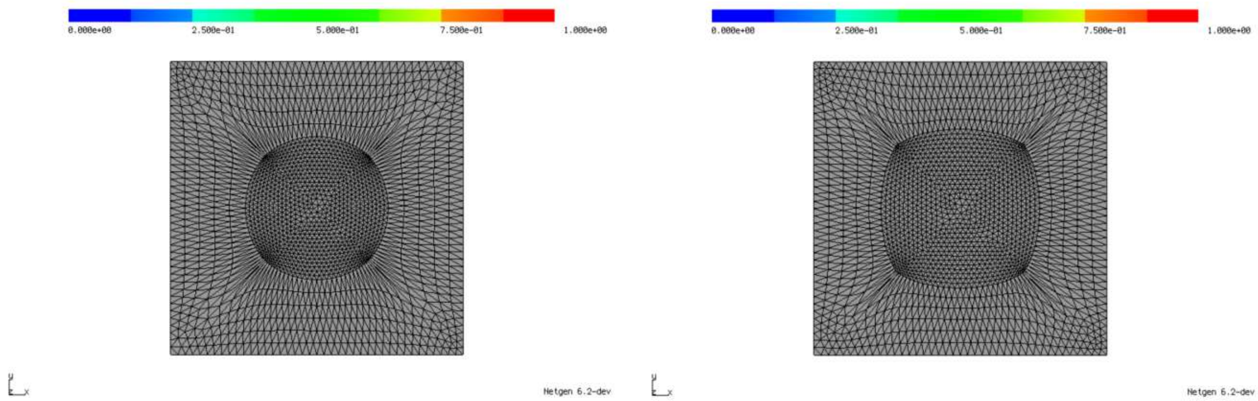

(a) Deformed mesh for $\alpha = 0$. (b) Deformed mesh for $\alpha = 1$.

Figure 25: Deformation of the mesh.

This issue is also reflected in terms of the value of the cost functional $\mathscr{G}(E)$, which decreases when Cauchy-Riemann conditions are not prescribed (cf. Figure 26).

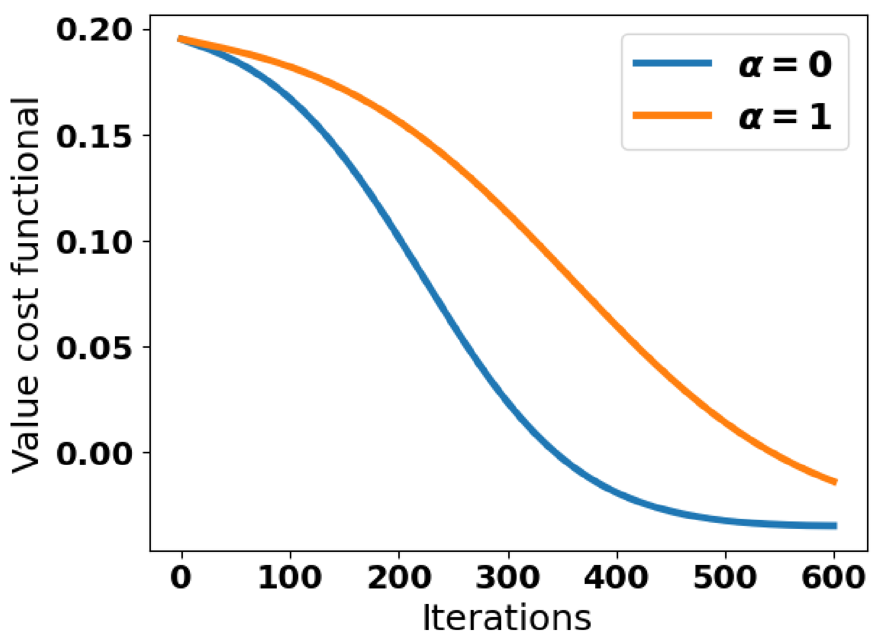

Figure 26: Visualisation of the function value $\mathscr{G}(E)$.

References

[1] G. Allaire. *Shape optimization by the homogenization method*, volume 146 of *Applied Mathematical Sciences*. Springer-Verlag, New York, 2002.

[2] G. Allaire, C. Dapogny, R. Estevez, A. Faure, and G. Michailidis. Structural optimization under overhang constraints imposed by additive manufacturing technologies. *J. Comput. Phys.*, 351:295–328, 2017.

[3] G. Allaire, C. Dapogny, A. Faure, and Georgios Michailidis. Shape optimization of a layer by layer mechanical constraint for additive manufacturing. *C. R. Math. Acad. Sci. Paris*, 355, 2017.

[4] G. Allaire, C. Dapogny, and F. Jouve. Shape and topology optimization. 22:1–132, [2021] ©2021.

[5] G. Allaire and F. Jouve. Minimum stress optimal design with the level set method. *Engineering Analysis with Boundary Elements*, 32(11):909–918, 2008. Shape and Topological Sensitivity Analysis: Theory and Applications.

[6] G. Allaire, F. Jouve, and H. Maillot. Topology optimization for minimum stress design with the homogenization method. *Struct. Multidiscip. Optim.*, 28(2-3):87–98, 2004.

[7] G. Allaire, F. Jouve, and A.-M. Toader. A level-set method for shape optimization. *C. R. Math. Acad. Sci. Paris*, 334(12):1125–1130, 2002.

[8] C. J. S. Alves and N. F. M. Martins. The direct method of fundamental solutions and the inverse Kirsch-Kress method for the reconstruction of elastic inclusions or cavities. *J. Integral Equations Appl.*, 21(2):153–178, 2009.

[9] H. Ammari. *An introduction to mathematics of emerging biomedical imaging*. Springer, Berlin New York, 2008.

[10] H. Ammari and H. Kang. High-order terms in the asymptotic expansions of the steady-state voltage potentials in the presence of conductivity inhomogeneities of small diameter. *SIAM J. Math. Anal.*, 34(5):1152–1166, 2003.

[11] H. Ammari, H. Kang, G. Nakamura, and K. Tanuma. Complete asymptotic expansions of solutions of the system of elastostatics in the presence of an inclusion of small diameter and detection of an inclusion. *Journal of elasticity and the physical science of solids*, 67(2):97–129, 2002.

[12] S. Amstutz. *Aspects théoriques et numériques en optimisation de forme topologique*. PhD thesis, L'institut National des Sciences Appliquées de Toulouse, 2003.

[13] S. Amstutz. Sensitivity analysis with respect to a local perturbation of the material property. *Asym. Analysis*, 49(1,2):87–108, 2006.

[14] S. Amstutz. Topological sensitivity analysis for some nonlinear pde systems. *Journal de Mathématiques Pures et Appliquées*, 85(4):540–557, apr 2006.

[15] S. Amstutz. Analysis of a level set method for topology optimization. *Optim. Methods Softw.*, 26(4-5):555–573, 2011.

[16] S. Amstutz. An introduction to the topological derivative. *Engineering Computations*, September 2021.

[17] S. Amstutz and H. Andrä. A new algorithm for topology optimization using a level-set method. *J. Comput. Phys.*, 216(2):573–588, 2006.

[18] S. Amstutz and A. A. Novotny. Topological asymptotic analysis of the Kirchhoff plate bending problem. *ESAIM: Control, Optimisation and Calculus of Variations*, 17(3):705–721, mar 2010.

[19] S. Amstutz and A. A. Novotny. Topological optimization of structures subject to von Mises stress constraints. *Struct. Multidiscip. Optim.*, 41(3):407–420, 2010.

[20] S. Amstutz, A. A. Novotny, and E. A. de Souza Neto. Topological derivative-based topology optimization of structures subject to Drucker-Prager stress constraints. *Comput. Methods Appl. Mech. Engrg.*, 233/236:123–136, 2012.

[21] S. Amstutz, A. A. Novotny, and N. Van Goethem. Topological sensitivity analysis for elliptic differential operators of order $2m$. *J. Differential Equations*, 256(4):1735–1770, 2014.

[22] M. Aurada, J. M. Melenk, and D. Praetorius. FEM–BEM coupling for the large-body limit in micromagnetics. *Journal of Computational and Applied Mathematics*, 281:10–31, 2015.

[23] P. Baumann, P. Gangl, and K. Sturm. Complete topological asymptotic expansion for L_2 and H^1 tracking-type cost functionals in dimension two and three, 2021. arXiv:2111.08418.

[24] P. Baumann, I. Mazari-Fouquer, and K. Sturm. The topological state derivative: an optimal control perspective on topology optimisation. *J. Geom. Anal.*, 33(8):Paper No. 243, 49, 2023.

[25] P. Baumann and K. Sturm. Adjoint based methods for the computation of higher order topological derivatives with an application to linear elasticity. *Engineering Computations*, 39(1), 2021.

[26] P. Baumann and K. Sturm. Minimisation of peak stresses with the shape derivative, 2024. arXiv:2402.12978.

[27] M. P. Bendsø e. *Optimal shape design as a material distribution problem*, volume 1 of *Structural optimization*. Springer-Verlag, New York, 1989.

[28] M. P. Bendsø e and N. Kikuchi. Generating optimal topologies in structural design using a homogenization method. *Comput. Methods Appl. Mech. Engrg.*, 71(2):197–224, 1988.

[29] E. Beretta, A. Manzoni, and L. Ratti. A reconstruction algorithm based on topological gradient for an inverse problem related to a semilinear elliptic boundary value problem. *Inverse Problems*, 33(3):035010, feb 2017.

[30] L. Blank, H. Garcke, L. Sarbu, T. Srisupattarawanit, V. Styles, and A. Voigt. Phase-field approaches to structural topology optimization. In *Constrained optimization and optimal control for partial differential equations*, volume 160 of *Internat. Ser. Numer. Math.*, pages 245–256. Birkhäuser/Springer Basel AG, Basel, 2012.

[31] S. Blauth and K. Sturm. Quasi-Newton methods for topology optimization using a level-set method. *Struct. Multidiscip. Optim.*, 66(9):Paper No. 203, 21, 2023.

[32] M. Bonnet and R. Cornaggia. Higher order topological derivatives for three-dimensional anisotropic elasticity. *ESAIM: Mathematical Modelling and Numerical Analysis*, 51(6):2069–2092, nov 2017.

[33] M. Bruggi. On an alternative approach to stress constraints relaxation in topology optimization. *Struct. Multidiscip. Optim.*, 36(2):125–141, 2008.

[34] M. Burger and R. Stainko. Phase-field relaxation of topology optimization with local stress constraints. *SIAM J. Control Optim.*, 45(4):1447–1466, 2006.

[35] A. Canelas, A. Laurain, and A. A. Novotny. A new reconstruction method for the inverse potential problem. *J. Comput. Phys.*, 268:417–431, 2014.

[36] A. Canelas, A. Laurain, and A. A. Novotny. A new reconstruction method for the inverse source problem from partial boundary measurements. *Inverse Problems*, 31(7):075009, 24, 2015.

[37] P. W. Christensen and A. Klarbring. *An introduction to structural optimization*, volume 153 of *Solid Mechanics and its Applications*. Springer, New York, 2009.

[38] P. G. Ciarlet. *Mathematical elasticity. Volume I. Three-dimensional elasticity*, volume 84 of *Classics in Applied Mathematics*. Society for Industrial and Applied Mathematics (SIAM), Philadelphia, PA, [2022] ©2022. Reprint of the 1988 edition [0936420].

[39] F. H. Clarke. *Optimization and nonsmooth analysis*. Canadian Mathematical Society Series of Monographs and Advanced Texts. John Wiley & Sons, Inc., New York, 1983. A Wiley-Interscience Publication.

[40] C. Dapogny, A. Faure, G. Michailidis, G. Allaire, A. Couvelas, and R. Estevez. Geometric constraints for shape and topology optimization in architectural design. *Comput. Mech.*, 59, 2017.

[41] M. C. Delfour. Control, shape, and topological derivatives via minimax differentiability of Lagrangians. In *Springer INdAM Series*, pages 137–164. Springer International Publishing, 2018.

[42] M. C. Delfour. Topological derivative of state-constrained objective functions: A direct method. *SIAM Journal on Control and Optimization*, 60(1):22–47, 2022.

[43] M. C. Delfour and J.-P. Zolésio. Structure of shape derivatives for nonsmooth domains. *J. Funct. Anal.*, 104(1):1–33, 1992.

[44] M. C. Delfour and J.-P. Zolésio. *Shapes and geometries*, volume 22 of *Advances in Design and Control*. Society for Industrial and Applied Mathematics (SIAM), Philadelphia, PA, second edition, 2011. Metrics, analysis, differential calculus, and optimization.

[45] V. F. Demyanov and V. N. Malozemov. *Introduction to minimax*. Dover Publications, Inc., New York, 1990. Translated from the Russian by D. Louvish, Reprint of the 1974 edition.

[46] J. Deny and J. L. Lions. Les espaces du type de Beppo Levi. *Ann. Inst. Fourier, Grenoble*, 5:305–370 (1955), 1953–54.

[47] C. Dev, G. Stankiewicz, and P. Steinmann. Sequential topology and shape optimization framework to design compliant mechanisms with boundary stress constraints. *Struct. Multidiscip. Optim.*, 65(6):Paper No. 180, 16, 2022.

[48] M. Eigel and K. Sturm. Reproducing kernel Hilbert spaces and variable metric algorithms in pde-constrained shape optimization. *Optimization Methods and Software*, 33(2):268–296, may 2017.

[49] K. Eppler, S. Schmidt, V. Schulz, and C. Ilic. Preconditioning the pressure tracking in fluid dynamics by shape Hessian information. *Journal of Optimization Theory and Applications*, 141(3):513–531, jan 2009.

[50] H. A. Eschenauer, V. V. Kobelev, and A. Schumacher. Bubble method for topology and shape optimization of structures. *Structural Optimization*, 8(1):42–51, 1994.

[51] L. C. Evans. *Partial differential equations*. Graduate studies in mathematics. American Mathematical Society, 2010.

[52] F. Feppon and H. Ammari. High order topological asymptotics: reconciling layer potentials and compound asymptotic expansions. *Multiscale Model. Simul.*, 20(3):957–1001, 2022.

[53] A. D. Ferreira and A. A. Novotny. A new non-iterative reconstruction method for the electrical impedance tomography problem. *Inverse Problems*, 33(3):035005, 27, 2017.

[54] B. Führ, V. Schulz, and K. Welker. Shape optimization for interface identification with obstacle problems. *Vietnam Journal of Mathematics*, oct 2018.

[55] P. Gangl. *Sensitivity-Based Topology and Shape Optimization with Application to Electrical Machines*. PhD thesis, Johannes Keppler Universität, 2017.

[56] P. Gangl. A multi-material topology optimization algorithm based on the topological derivative. *Comput. Methods Appl. Mech. Engrg.*, 366:113090, 23, 2020.

[57] P. Gangl, J. Schöberl, and K. Sturm. Ngsolve documentation. https://docu.ngsolve.org/latest/i-tutorials/unit-7-optimization/04_Topological_Derivative_Levelset.html, 1999. Accessed: 2024-04-30.

[58] P. Gangl and K. Sturm. A simplified derivation technique of topological derivatives for quasi-linear transmission problems. *ESAIM Control Optim. Calc. Var.*, 26:Paper No. 106, 20, 2020.

[59] P. Gangl and K. Sturm. Topological derivative for PDEs on surfaces. *preprint*, 2020.

[60] P. Gangl and K. Sturm. Asymptotic analysis and topological derivative for 3d quasi-linear magnetostatics. *ESAIM Math. Model. Numer. Anal.*, 55(suppl.):S853–S875, 2021.

[61] P. Gangl, K. Sturm, M. Neunteufel, and J. Schöberl. Fully and semi-automated shape differentiation in `ngsolve`. *Struct. Multidiscip. Optim.*, 63(3):1579–1607, 2021.

[62] Z. Gao, Y. Ma, and H. Zhuang. Shape optimization for stokes flow. *Applied Numerical Mathematics*, 58(6):827–844, jun 2008.

[63] S. Garreau, P. Guillaume, and M. Masmoudi. The topological asymptotic for pde systems: The elasticity case. *SIAM Journal on Control and Optimization*, 39(6):1756–1778, jan 2001.

[64] C. Geiger and C. Kanzow. *Theorie und Numerik restringierter Optimierungsaufgaben : [mit 140 Übungsaufgaben*. Springer, Berlin, 2002.

[65] I. M. Gelfand and G. E. Shilov. *Generalized functions. Vol. 1*. AMS Chelsea Publishing, Providence, RI, 2016. Properties and operations, Translated from the 1958 Russian original [MR0097715] by Eugene Saletan, Reprint of the 1964 English translation [MR0166596].

[66] M. Giacomini, O. Pantz, and K. Trabelsi. An a posteriori error estimator for shape optimization: application to EIT. *Journal of Physics: Conference Series*, 657:012004, nov 2015.

[67] D. Gilbarg and N. Trudinger. *Elliptic partial differential equations of second order*. Springer, Berlin New York, 2001.

[68] M. Hassine and M. Masmoudi. The topological asymptotic expansion for the quasi-Stokes problem. *ESAIM Control Optim. Calc. Var.*, 10(4):478–504, 2004.

[69] A. Henrot and M. Pierre. *Shape variation and optimization*, volume 28 of *EMS Tracts in Mathematics*. European Mathematical Society (EMS), Zürich, 2018. A geometrical analysis, English version of the French publication [MR2512810] with additions and updates.

[70] M. Hintermüller and A. Laurain. Electrical impedance tomography: from topology to shape. *Control Cybernet.*, 37(4):913–933, 2008.

[71] M. Hintermüller, A. Laurain, and A. A. Novotny. Second-order topological expansion for electrical impedance tomography. *Adv. Comput. Math.*, 36(2):235–265, 2012.

[72] M. Hintermüller, A. Laurain, and I. Yousept. Shape sensitivities for an inverse problem in magnetic induction tomography based on the eddy current model. *Inverse Problems*, 31(6):065006, may 2015.

[73] M. Hinze, R. Pinnau, M. Ulbrich, and S. Ulbrich. *Optimization with PDE constraints*. Springer, New York, 2009.

[74] E. Holmberg, B. Torstenfelt, and A. Klarbring. Stress constrained topology optimization. *Struct. Multidiscip. Optim.*, 48(1):33–47, 2013.

[75] M. Iguernane, S. Nazarov, J.-R. Roche, J. Sokolowski, and K. Szulc. Topological derivatives for semilinear elliptic equations. *International Journal of Applied Mathematics and Computer Science*, 19(2), jan 2009.

[76] K. Ito and K. Kunisch. *Lagrange multiplier approach to variational problems and applications*. Society for Industrial and Applied Mathematics, Philadelphia, PA, 2008.

[77] C. Jong and W. Springer. Teaching von Mises stress: From principal axes to nonprincipal axes. (10.18260/1-2–5353), June 2009. https://peer.asee.org/5353.

[78] C. Le, J. Norato, T. Bruns, C. Ha, and D. Tortorelli. Stress-based topology optimization for continua. *Structural and Multidisciplinary Optimization*, 41:605–620, 2010.

[79] M. Masmoudi, J. Pommier, and B. Samet. The topological asymptotic expansion for the Maxwell equations and some applications. *Inverse Problems*, 21(2):547–564, 2005.

[80] V. Mazya, S. Nazarov, and B. Plamenevskij. *Asymptotic theory of elliptic boundary value problems in singularly perturbed domains. Vol. I*, volume 111 of *Operator Theory: Advances and Applications*. Birkhäuser Verlag, Basel, 2000.

[81] V. Mazya, S. Nazarov, and B. Plamenevskij. *Asymptotic theory of elliptic boundary value problems in singularly perturbed domains. Vol. II*, volume 112 of *Operator Theory: Advances and Applications*. Birkhäuser Verlag, Basel, 2000.

[82] J. Nečas. *Introduction to the theory of nonlinear elliptic equations*. A Wiley-Interscience Publication. John Wiley & Sons, Ltd., Chichester, 1986. Reprint of the 1983 edition.

[83] S. H. Nguyen and H.-G. Kim. Level set based shape optimization using trimmed hexahedral meshes. *Comput. Methods Appl. Mech. Engrg.*, 345:555–583, 2019.

[84] S. H. Nguyen and H.-G. Kim. Stress-constrained shape and topology optimization with the level set method using trimmed hexahedral meshes. *Comput. Methods Appl. Mech. Engrg.*, 366:113061, 24, 2020.

[85] A. A. Novotny, R. A. Feijóo, E. Taroco, and C. Padra. Topological sensitivity analysis. *Comput. Methods Appl. Mech. Engrg.*, 192(7-8):803–829, 2003.

[86] A. A. Novotny and A. Żochowski J. Sokołowski. *Applications of the topological derivative method*. Springer, Cham, Switzerland, 2019.

[87] A. A. Novotny and J. Sokolowski. *Topological derivatives in shape optimization*. Interaction of Mechanics and Mathematics. Springer, Heidelberg, 2013.

[88] O. A. Oleĭnik, A. S. Shamaev, and G. A. Yosifian. *Mathematical problems in elasticity and homogenization*, volume 26 of *Studies in Mathematics and its Applications*. North-Holland Publishing Co., Amsterdam, 1992.

[89] C. Ortner and E. Süli. A note on linear elliptic systems on $\mathbf{R}^d$. *ArXiv e-prints*, 1202.3970, 2012.

[90] N. Ortner and P. Wagner. *Fundamental solutions of linear partial differential operators*. Springer, Cham, 2015. Theory and practice.

[91] O. Pantz and K. Trabelsi. A post-treatment of the homogenization method for shape optimization. *SIAM J. Control Optim.*, 47(3):1380–1398, 2008.

[92] R. Picelli, S. Townsend, C. Brampton, J. Norato, and H. A. Kim. Stress-based shape and topology optimization with the level set method. *Comput. Methods Appl. Mech. Engrg.*, 329:1–23, 2018.

[93] R. Picelli, S. Townsend, and H. A. Kim. Stress and strain control via level set topology optimization. *Struct. Multidiscip. Optim.*, 58(5):2037–2051, 2018.

[94] S. S. Rocha and A. A. Novotny. Obstacles reconstruction from partial boundary measurements based on the topological derivative concept. *Struct. Multidiscip. Optim.*, 55(6):2131–2141, 2017.

[95] M. A. Salazar de Troya and D. A. Tortorelli. Adaptive mesh refinement in stress-constrained topology optimization. *Struct. Multidiscip. Optim.*, 58(6):2369–2386, 2018.

[96] J. Schöberl. C++11 implementation of finite elements in ngsolve. 09 2014.

[97] M. Silva, M. Matalon, and D. A. Tortorelli. Higher order topological derivatives in elasticity. *International Journal of Solids and Structures*, 47(22):3053–3066, 2010.

[98] J. Simon and F. Murat. Sur le contrôle par un domaine géométrique. *Laboratoire d'Analyse Numérique de l'Université de Paris VI*, 01 1976.

[99] J. Sokolowski and A. Zochowski. On the topological derivative in shape optimization. *SIAM Journal on Control and Optimization*, 37(4):1251–1272, 1999.

[100] J. Sokolowski and J.-P. Zolésio. *Introduction to Shape Optimization*. Springer Berlin Heidelberg, 1992.

[101] K. Sturm. *On shape optimization with non-linear partial differential equations*. PhD thesis, Technische Universität Berlin, 2014.

[102] K. Sturm. Shape differentiability under non-linear pde constraints. In *New trends in shape optimization*, volume 166 of *Internat. Ser. Numer. Math.*, pages 271–300. Birkhäuser/Springer, Cham, 2015.

[103] K. Sturm. Convergence of Newton's method in shape optimisation via approximate normal functions, 2016. arXiv:1608.02699.

[104] K. Sturm. Shape optimization with nonsmooth cost functions: from theory to numerics. *SIAM J. Control Optim.*, 54(6):3319–3346, 2016.

[105] K. Sturm. Topological sensitivities via a Lagrangian approach for semilinear problems. *Nonlinearity*, 33(9):4310–4337, jul 2020.

[106] K. Suresh and M. Takalloozadeh. Stress-constrained topology optimization: a topological level-set approach. *Struct. Multidiscip. Optim.*, 48(2):295–309, 2013.

[107] A. Verbart, M. Langelaar, and F. van Keulen. A unified aggregation and relaxation approach for stress-constrained topology optimization. *Struct. Multidiscip. Optim.*, 55(2):663–679, 2017.

[108] C. Wang and X. Qian. Heaviside projection-based aggregation in stress-constrained topology optimization. *Internat. J. Numer. Methods Engrg.*, 115(7):849–871, 2018.

[109] J. Wloka. *Partial differential equations*. Cambridge University Press, Cambridge Cambridgeshire New York, 1987.

[110] W. P. Ziemer. *Weakly differentiable functions*, volume 120 of *Graduate Texts in Mathematics*. Springer-Verlag, New York, 1989. Sobolev spaces and functions of bounded variation.

Curriculum Vitae

Persönliche Daten

Name	**Phillip Baumann**
Geburtsdatum	[redacted]
Geburtsort	[redacted]
Nationalität	[redacted]
Email	[redacted]

Ausbildung

seit 10/2020	Doktoratsstudent unter der Betreuung von Associate Prof. Dr. Kevin Sturm, TU Wien, Österreich.
10/2017-09/2020	Masterstudium Technische Mathematik, TU Wien, Österreich.
10/2013-09/2017	Bachelorstudium Technische Mathematik, TU Wien, Österreich.
06/2012	Matura, BGBRG Perchtoldsdorf, Österreich.

Wissenschaftliche Publikationen

1. P. Baumann and K. Sturm. Adjoint based methods for the computation of higher order topological derivatives with an application to linear elasticity. *Engineering Computations*, 39(1), 2021.

2. P. Baumann, P. Gangl, and K. Sturm. Complete topological asymptotic expansion for L_2 and H^1 tracking-type cost functionals in dimension two and three. 2021. arXiv:2111.08418.

3. P. Baumann, I. Mazari-Fouquer, K. Sturm. The topological state derivative: an optimal control perspective on topology optimisation. *J. Geom. Anal.*, 33(8): Paper No. 243, 49, 2023.

4. P. Baumann and K. Sturm. Minimsation of peak stresses with the shape derivative. 2024. arXiv:2402.12978.

Wien, am 13. Mai 2024

Phillip Baumann